PB84-169275

Burner Criteria for NOx Control. Volume 3 Heavy-Oil and Coal-Fired Furnaces and Further Furnace Investigations

International Flame Research Foundation
Ijmuiden (Netherlands)

Prepared for

Industrial Environmental Research Lab.
Research Triangle Park, NC

Feb 84

U.S. Department of Commerce
National Technical Information Service
NTIS

PB84-169275

EPA-600/7-84-015b
February 1984

BURNER CRITERIA FOR NO_X CONTROL
Volume III.
Heavy-oil and Coal-fired Furnaces and Further Furnace Investigations

by

M. P. Heap, T. M. Lowes, R. Walmsley,
H. Bartelds, and P. LeVaguerese

International Flame Research Foundation
IJmuiden, Holland

Contract No. 68-02-0202

EPA Project Officer: G. Blair Martin

Industrial Environmental Research Laboratory
Office of Environmental Engineering and Technology
Research Triangle Park, NC 27711

INDUSTRIAL ENVIRONMENTAL RESEARCH LABORATORY
OFFICE OF RESEARCH AND DEVELOPMENT
U.S. ENVIRONMENTAL PROTECTION AGENCY
RESEARCH TRIANGLE PARK, NC 27711

REPRODUCED BY
NATIONAL TECHNICAL
INFORMATION SERVICE
U.S. DEPARTMENT OF COMMERCE
SPRINGFIELD, VA 22161

TECHNICAL REPORT DATA
(Please read Instructions on the reverse before completing)

1. REPORT NO.
EPA-600/7-84-015b

2.

3. RECIPIENT'S ACCESSION NO.
PB84 169275

4. TITLE AND SUBTITLE
Burner Criteria for NO_x Control: Volume III. Heavy-oil and Coal-fired Furnaces and Further Furnace Investigations

5. REPORT DATE
February 1984

6. PERFORMING ORGANIZATION CODE

7. AUTHOR(S)
M. P. Heap, T. M. Lowes, R. Walmsley, H. Bartelds, and P. LeVaguerese

8. PERFORMING ORGANIZATION REPORT NO.

9. PERFORMING ORGANIZATION NAME AND ADDRESS
International Flame Research Foundation
c/o Hoogovens
IJmuiden, The Netherlands

10. PROGRAM ELEMENT NO.

11. CONTRACT/GRANT NO.
68-02-0202

12. SPONSORING AGENCY NAME AND ADDRESS
EPA, Office of Research and Development
Industrial Environmental Research Laboratory
Research Triangle Park, NC 27711

13. TYPE OF REPORT AND PERIOD COVERED
Final; 7/75 - 7/76

14. SPONSORING AGENCY CODE
EPA/600/13

15. SUPPLEMENTARY NOTES IERL-RTP project officer is G. Blair Martin, Mail Drop 62-B, 919/541-7504. EPA-600/2-76-061a is Volume I of this series. EPA-600/7-84-015a is Volume II.

16. ABSTRACT
The report describes the third phase of a research program with the overall objective of specifying burner design criteria for minimum pollutant emissions from both pulverized-coal- and residual-fuel-oil-fired combustors. A distributed mixing burner was developed, and its potential for NOx control was evaluated for different fuels. The burner produces a fuel-rich zone that reduces the conversion of fuel nitrogen species to NOx. Injecting additional air from outboard ports completes fuel oxidation. It was postulated that achievable NOx control depended on nitrogen volatility and oxygen content. This was confirmed by burning coal, a low volatile petroleum coke, heavy fuel oil, and a heavy fuel oil/water emulsion. A television pyrometer flame diagnostic technique that was evaluated gave promising results.

17. KEY WORDS AND DOCUMENT ANALYSIS

a. DESCRIPTORS		b. IDENTIFIERS/OPEN ENDED TERMS	c. COSATI Field/Group	
Pollution	Coal	Pollution Control	13B	
Nitrogen Oxides	Coke	Stationary Sources	07B	
Combustion	Residual Oils	Oil/Water Emulsions	21B	
Burners	Emulsions	Distributed Mixing Burners	13A	07D
Design Criteria			14G	
Fuel Oil			21D	

18. DISTRIBUTION STATEMENT
Release to Public

19. SECURITY CLASS *(This Report)*
Unclassified

20. SECURITY CLASS *(This page)*
Unclassified

21. NO. OF PAGES
219

22. PRICE

EPA Form 2220-1 (9-73)

NOTICE

This document has been reviewed in accordance with U.S. Environmental Protection Agency policy and approved for publication. Mention of trade names or commercial products does not constitute endorsement or recommendation for use.

ABSTRACT

This report describes the third phase of a research program whose overall objective is the specification of burner design criteria for minimum pollutant emissions from both pulverized-coal- and residual-fuel-oil-fired combustors. A distributed mixing burner was developed and its potential for NO_x control was evaluated for different fuels. The burner produces a fuel-rich zone that reduces the conversion of fuel nitrogen species to NO_x. Injection of additional air from outboard ports completes fuel oxidation. It was postulated that the achievable NO_x control was dependent on nitrogen volatility and local oxygen content. This was confirmed by burning coal, a low volatile petroleum coke, heavy fuel oil, and a heavy fuel oil/water emulsion. A television pyrometer flame diagnostic technique that was evaluated gave promising results.

TABLE OF CONTENTS

Section Page

List of Figures vi

List of Tables xii

1.0 SUMMARY 1-1

1.1 Program Overview 1-1
1.2 Results 1-3

2.0 POLLUTANT GENERATION AND CONTROL DURING PULVERIZED COAL COMBUSTION 2-1

2.1 The Problem 2-1
2.2 The State-of-the-Art of NO_x Control 2-3

2.2.1 Overall Excess Air 2-3
2.2.2 Flue Gas Recirculation 2-6
2.2.3 Staged Heat Release 2-6
2.2.4 Burner Modifications 2-6

2.3 Pollutant Formation in Pulverized Coal Flames 2-11

2.3.1 Coal Chemistry 2-14
2.3.2 Homogeneous Gas Phase Reactions 2-21
2.3.3 Heterogeneous Reactions 2-22

3.0 BURNER DESIGN TO CONTROL NO_x FORMATION IN TURBULENT DIFFUSION FLAMES 3-1

3.1 The Characteristics of Swirling Flames 3-1
3.2 Phase I and Phase II Efforts 3-8
3.3 Purpose of the Phase III Investigations 3-14

4.0 EXPERIMENTAL RESULTS 4-1

4.1 Evaluation of the Distributed Mixing Burner Concept . . 4-1

4.1.1 Delayed Mixing Burner Design 4-2
4.1.2 Investigations Involving Pulverized Coal 4-6
4.1.3 Investigations Involving Pulverized Coke 4-15
4.1.4 The Influence of Fuel Oil-Water Emulsions on Nitrogen Oxide and Particulate Formation 4-19

Section Page

4.1.5 NO Formation and Fuel Oil Injector Design . . . 4-33

4.2 Pollutant Measurements in Multi-Burner Systems 4-36

4.2.1 Experimental Systems 4-36
4.2.2 Results 4-38
4.2.3 Discussion 4-57

4.3 An Investigation to Assess the Use of a Television Pyrometer to Control Low Emission Burners 4-59

4.3.1 Description of the Television Pyrometer (TVP) . 4-61
4.3.2 Connection Between the Videosignal and the Intensity Distributions and Flame Properties . . 4-63
4.3.3 Experimental Arrangements and Flames Investigated 4-69
4.3.4 Experimental Results 4-70
4.3.5 Conclusion 4-83

4.4 Detailed Measurements in Natural Gas and Coal Flames . 4-84

4.4.1 Flame Conditions and Measurement Systems 4-84
4.4.2 Results 4-87

5.0 DISCUSSION AND CONCLUSION 5-1

5.1 Natural Gas Flames 5-1
5.2 Pulverized Coal Flames 5-3
5.3 Heavy Oil Flames 5-8
5.4 The Importance of Volatile and Char Nitrogen 5-11
5.5 Burner Parameters and NO_x Control 5-12

APPENDIX A-1

LIST OF FIGURES

Number	Title	Page
1-1	Effects of Swirl, Cooling Rate and Burner Zone Stoichiometry on NO_x Emissions for a Pilot Scale Distributed Mixing Burner	1-4
1-2	The Influence of Burner Spacing, Type and Configuration on NO Formation in Natural Gas Flames	1-7
1-3	The Influence of Burner Spacing, Type and Configuration on NO Formation in Fuel Oil Flames	1-8
1-4	Schematic Setup of the Composite Units of the Television Pyrometer (TVP)	1-9
2-1	ppm NO_x vs % Stoichiometric Air for Coal Fired Boilers	2-4
2-2	CO Emissions as a Function of NO_x Emissions for Coal-Fired Boilers as the Excess Air is Changed	2-5
2-3	NO Dependence on Gas Recirculation During Normal (Air-Rich) Operation	2-7
2-4	Effect of Excess Air on NO_x Emissions Under Modified Firing Conditions	2-8
2-5	Burner Arrangement - Opposed Fired	2-9
2-6	Boiler Baseline Performance with Unmodified Burners	2-10
2-7	NO Production in Pulverized Coal Flames	2-12
2-8	Phenomerological Model of NO Production in Coal Flames	2-13
2-9	Fractional Coal Mass and Coal Nitrogen Loss as Functions of Pyrolysis Temperature	2-15
2-10	Retention of Nitrogen in Devolatilized Lignite and Bituminous Coal Chars	2-17
2-11	Conversion of Coal Nitrogen as a Function of Fuel Equivalence Ratio in a 1500 Furnace	2-18
2-12	Conversion of Nitrogen vs Fuel Equivalence Ratio in a 1500 K Furnace for a Lignite Char Previously Devolatilized at 1500 K for One Second	2-19
2-13	Conversion of Coal Nitrogen as a Function of Fuel Equivalence Ratio in a 1750 K Furnace	2-20

Number Title Page

3-1 Sketches of Four Typical Flame Types 3-4

3-2 Axial Temperature Distribution Showing the Characteristics of Different Flame Types 3-5

3-3 The Influence of Swirl on the Characteristics of Anthracite Flames 3-7

3-4 Emission Characteristics of Pulverized Coal Flames Produced with Radial Fuel Injection (5% Excess Air, 300 C Preheat) . 3-11

3-5 Emission Characteristics of Pulverized Coal Flames Produced with Axial Fuel Injection (300 C Preheat, 5% Excess Air, and 1.1% Nitrogen Coal) 3-12

4-1 Sketch Showing the Refractory Tunnel Furnace and the Cooling Loop Arrangements 4-3

4-2 Versatile Test Burner Showing the Position of Tertiary Air Injection and a Scaled Down Version of a Practical Type Coal Injector 4-4

4-3a The Relationship Between Relative Swirl Index, R_s, and Swirl Number, S 4-5

4-3b Double Concentric Burner System 4-5

4-4 The Effect of Tertiary Air Injection on NO_x Emissions . . . 4-9

4-5 The Effect of Tertiary Air Injection on NO_x Emissions . . . 4-10

4-6 The Influence of Primary Air Percentage on NO Emissions . . 4-11

4-7 The Influence of Secondary Swirl Level 4-12

4-8 The Influence of Primary Air Percentage and Swirl Level . . 4-13

4-9 Effects of Swirl, Cooling Rate and Burner Zone Stoichiometry on NO_x Emissions 4-14

4-10 The Influence of Fuel Injector Type on NO Formation from Petroleum Coke (2.5% Excess Oxygen, 340 C Preheat) 4-17

4-11 The Influence of Preheat on NO Emission from Petroleum Coke Flames 4-18

4-12 Comparison of NO Emissions from Coal and Petroleum Coke Using a Coal Spreaker 4-20

Number Title Page

4-13 Comparison of NO Emission from Coal and Petroleum Coke with Axial Fuel Injection 4-21

4-14 Relative Increase in NO Emissions with Increased Fuel Flow . 4-22

4-15 The Influence of Burner Stoichiometry on Emissions from Pulverized Coal and Petroleum Coke 4-23

4-16 Installation of TOTAL Emulsifier in the IFRF Oil Delivery System 4-25

4-17 The Influence of Emulsion Water Content on Particulate Mass Emissions (Steam Atomization, 5% Excess Air, 300 C Preheat). 4-26

4-18 The Influence of Emulsion Water Content on NO Emissions . . 4-28

4-19 The Influence of Atomizing Air Flow Rate on NO Emissions (5% Excess Air, 300 C Preheat, $S_I = 9$) 4-29

4-20 The Influence of Atomizing Air Flow Rate on Particulate Emissions (5% Excess Air, 300 C Preheat, $S_I = 9$) 4-30

4-21 The Influence of Tertiary Air Flow on NO Emissions (Air Atomized, 5% Excess $S_I = 9$, Preheat 300 C) 4-31

4-22 The Influence of Tertiary Air Flow on Particulate Emissions (Air Atomized, 5% Excess $S_I = 9$, Preheat 300 C) 4-32

4-23 Modification of the Distributed Mixing Burner Showing Primary Swirl Vanes and Oil Injector Cup 4-34

4-24 Comparison of NO Emissions from Standard Y Jets and Y Jets Fitted with Distributor Caps 4-35

4-25 Multiple Burner System 4-37

4-26 Triangular Multiple Burner Array 4-39

4-27 CO Concentration on Axis of the Central Burner of Three-In-Line, Configuration (Type A), and Larger Burner 4-40

4-28 Heat Transferred to Cooling Pipes. Natural Gas Flames in a Triangular Array 4-42

4-29 Heat Transferred to the Cooling Pipes. Oil Flames in a Triangular Array 4-43

4-30 Axial Distribution of Heat Flux to the Cooling Pipes. Type A Oil Flames in a Triangular Array 4-44

Number	Title	Page
4-31	The Influence of Burner Spacing, Type, and Orientation on Noise Generation in Natural Gas Flames	4-46
4-32	The Influence of Burner Type, Spacing, and Orientation on Noise Generation in Oil Flames	4-47
4-33	The Influence of Burner Spacing, Type, and Configuration on NO Formation in Natural Gas Flames	4-49
4-34	The Effect of the Primary Secondary Mass Ratio on NO and CO Formation	4-50
4-35	The Influence of Burner Spacing, Type, and Configuration on NO Formation in Natural Gas Flames Supported by Oxygen Enriched Air	4-51
4-36	Carbon Monoxide Formation as a Function of Burner Configuration and Excess Air with Non-Uniform Air Distribution	4-54
4-37	Effect of Load on NO Emissions from Type A Gas Flames Produced with a Single Burner and a 3 Burner In Line System.	4-55
4-38	The Influence of Burner Spacing, Type, and Configuration on NO Formation in Fuel Oil Flames	4-56
4-39	The Influence of Primary Air Rate on NO and CO Emissions from the Large Single Type Oil Burner (Oxygen Flue Gas Cone 0.5%)	4-58
4-40	The Influence of Burner Spacing on Temperature Profiles Measured Along a Flame Axis	4-60
4-41	Schematic Setup of the Composite Units of the Television Pyrometer (TVP)	4-62
4-42	Approximation of the Transmittance of the Optical Filter (λ = 0.58 - 0.78 μ) and the TV Camera by a Hat Function	4-65
4-43	Comparison Between Calculated (Eqn. 3) and Measured Video Signal	4-66
4-44	Transmittance Characteristic of the Optical Blue Filter Used in Front of the TV Camera	4-68
4-45	Construction and Positioning of the Natural Gas Injectors as Used for the TVP-Test	4-71
4-46a	Intensity Distribution Within the Range of the Total Video Signal from the TVP for Run 7.1, 7.2, and 7.3	4-74

Number Title Page

4-46b NO Flue Gas Concentrations as Measured for Run 7.1, 7.2, and 7.3 4-74

4-47a Intensity Distribution with the Range of the Total Video Signal from the TVP for Run 9.1, 9.2, and 9.3 4-75

4-47b NO Flue Gas Concentrations as Measured for Run 9.1, 9.2, and 9.3 4-75

4-48a Intensity Distribution Within the Range of Total Video Signal from the TVP for Run 8.1, 8.2, and 8.3 4-76

4-48b NO Flue Gas Concentrations as Measured for Run 8.1, 8.2, and 8.3 4-76

4-49 Correlation of TVP Intensity Data with Flue Gas Nitric Oxide (NO) Concentrations for Two Intensity Ranges; 40-100% and 60-100% of Total Video Signal 4-77

4-50 The Burner Quarl as Viewed by the TV Camera (Shadow Effect). 4-79

4-51 Isotherms (C) in the Flames of Run 7 as Measured by a Suction Pyrometer 4-80

4-52 Isotherms (C) in the Flames of Run 8 as Measured by a Suction Pyrometer 4-81

4-53 Isotherms (C) in the Flames of Run 9 as Measured by a Suction Pyrometer 4-82

4-54 Suction Pyrometer with Replaceable Refractory Shields . . . 4-86

4-55 Water Cooled Quartz Lines Probe for Sampling from Gas Flames 4-88

4-56 Water Quench Probe for NC Measurement 4-89

4-57 Solid Sampling Probe (High Loadings) 4-90

4-58 Solid Concentration Sampling Probe (Low Loadings) 4-91

4-59 Radial NO, O_2 and Temperature Distribution in Natural Gas Flame 4-92

4-60 Isotherms Measured in Natural Gas Flames 4-93

4-61 Radial NO, O_2 and Temperature Distribution in Pulverized Coal Flames 4-94

4-62 Isotherms Measured in Pulverized Coal Flames 4-95

Number	Title	Page
4-63	Radial NO, O_2 and Temperature Distribution in Pulverized Coal Flames	4-96
4-64	Axial Temperature and Concentration Profiles for Flames 123 and 124	4-98
5-1	NO Emission Characteristics of the Various Natural Gas Flame Types	5-4
5-2	Flame Characteristics	5-5
5-3	Measurements Within a Burner Stabilized Flame	5-6
5-4	Measurements Within a High Fineness Ratio Diffusion Flame .	5-7
5-5	Effects of Primary Stoichiometry on Gases Within a Swirl Stabilized Flame	5-9
5-6a	Spray Trajectory Passes Through the Internal Recirculation Zone	5-10
5-6b	Concept of Fuel Air Contacting at the Base of a Residual Oil Flame	5-10
5-7	Effects of Air Swirl and Coal Injection on NO Emissions from Versatile Pilotscale Burner	5-13
5-8	Effects of Primary Stoichiometry, Air Swirl, and Coal Injection on NO_x Emissions	5-15
5-9	NO Emissions from IFRF Burner Operating with Tertiary Air .	5-16
5-10	Effects of Swirl, Cooling Rate, and Burner Zone Stoichiometry on NO_x Emissions	5-18

LIST OF TABLES

Number	Title	Page
2-1	New System Goals--Average NO_x (ppm at 3% O_2)	2-3
4-1	Flame Conditions	4-7
4-2	Ultimate Analysis (Dry)	4-16
4-3	The Influence of Non-Uniform Air Distribution on NO Formation in Type A Natural Gas-Oxygen-Air Flames (Flue Gas O_2 Concentration 0.5%) for Three In-Line Configuration	4-53
4-4	Selected Ranges of Intensity Distributions	4-61
4-5	Input Conditions in the Flames Investigated and Nitric Oxide Concentrations Measured in the Fluegas	4-72
4-6	Conditions for Detailed Flame Measurements	4-85

1.0 SUMMARY

1.1 Program Overview

This report describes the third phase of a research program whose overall objective is the specification of burner design criteria for minimum pollutant emissions from both pulverized coal and residual fuel oil-fired combustors. The first phase of the program was concerned with the definition of the effect of various burner design parameters upon the formation of nitrogen oxides (NO_x) in both pulverized coal and natural gas flames. Furnace trials were carried out which evaluated both input/output investigations and detailed flame mapping in an attempt to establish those flow and mixing patterns which yielded the most promise for controlling NO_x emissions by burner redesign. The major accomplishment of the first series of furnace investigations(1.1) was the finding that under subscale conditions, NO_x emissions from pulverized coal flames could be varied by a factor of four by changes in furnace design and operating conditions. This variation was achieved mainly by the selection of three burner design parameters:

- The method of fuel injection. Any tendency to rapidly mix the coal with all the combustion air resulted in higher emissions. The lowest emissions were achieved with a high velocity axial fuel injector which maintained a coherent fuel jet of high coal density.
- Optimum level of swirl to provide a stable ignition source at the fuel injector without mixing the fuel too rapidly with the secondary air. Swirl refers to the fact that the secondary air stream has both a tangential and axial velocity component.
- The amount of primary air. Primary air refers to that air which is mixed with the pulverized coal prior to delivery into the furnace. NO_x emissions were lowest when the minimum amount of primary air was used consistent with maintaining slow mixing of the fuel jet with the secondary air.

Although burner conditions had been identified which gave low NO_x emissions, it was readily recognized that such a burner design would be unsuitable for use in existing wall-fired utility boilers.

The second series of furnace trials(1.2) were carried out in order to:

- provide further information on the formation of NO_x in pulverized coal flames to aid in interpretation of the results;
- extend the investigation to include residual fuel oil firing in order to define those parameters which give minimum emissions; and
- investigate methods of satisfying process requirements and produce minimum emissions. This involves the definition of the combustion requirements of practical systems as well as an attempt to reduce emissions via burner design.

Results were obtained which defined the emission characteristics of a subscale practical pulverized coal burner and the development of a tertiary air injection system to minimize NO_x formation via the use of outboard staged air ports. Emissions from dual fuel firing were investigated by firing both natural gas and coal simultaneously. Emissions were not additive and were dependent upon burner parameters such as the type of fuel injector. Emissions from heavy fuel oil were found to be most dependent upon the method of atomization and, in general, the lowest emissions were produced from the narrowest spray angles. In addition to the furnace investigations, the predictive capabilities of several radiative heat transfer models were evaluated against experimental data and hypothetical test cases.

The third and final phase of the program included a furnace trial which was planned to answer several specific questions as follows:

1. What is the potential of tertiary air injection as a method of NO_x control for coal flames?
2. What is the impact of char nitrogen?
3. How are pollutant emissions affected by multiple burner arrays?
4. Is the use of emulsions beneficial?
5. Can a control system be developed for low NO_x burners based upon a TV pyrometer?
6. Does an evaluation of detailed flame measurements made in earlier

reports indicate the controlling mechanisms of NO formation in flames?

1.2 Results

Initial Development of a Delayed Mixing Burner

In the second phase of this program, a pulverized coal burner design was identified (1.2) for pulverized coal which produced low NO_x emissions and a flame type suitable for use in wall fired boilers. In this burner the total combustion air supply was divided into three streams. The fuel rich primary zone was supplied with the primary air used to transport the coal and secondary air through the burner throat. The third air stream was injected from the periphery of the burner exit in order to mix the partially oxidized products of the fuel rich zone some distance downstream and thereby complete combustion. Experiments were conducted to investigate the effect of the following parameters:

- air delivery system variables;
- fuel injector design;
- air preheat level;
- furnace heat extraction.

Figure 1-1 summarizes the data obtained at different furnace heat extraction rates for two swirl levels (of the secondary air). It can be seen that for both furnace conditions an increase in burner equivalence ratio (equivalence ratio is the air supplied divided by the amount necessary for complete combustion) causes a dramatic reduction in NO_x emissions. The level of swirl has a significant impact upon emissions close to an equivalence ratio of 1.0 but emissions are almost independent of swirl level at high burner equivalence ratios.

Nitric Oxide Formation from Petroleum Coke

Petroleum coke is a high nitrogen, low volatile solid produced by thermally cracking petroleum residuals. Investigations were carried out with pulverized petroleum coke to assess the impact of volatile fuel nitrogen fragments on NO_x formation. Emissions from petroleum coke were found to be relatively insensitive to burner parameters. With fuel injectors that produced rapid mixing between the fuel and air, emissions from

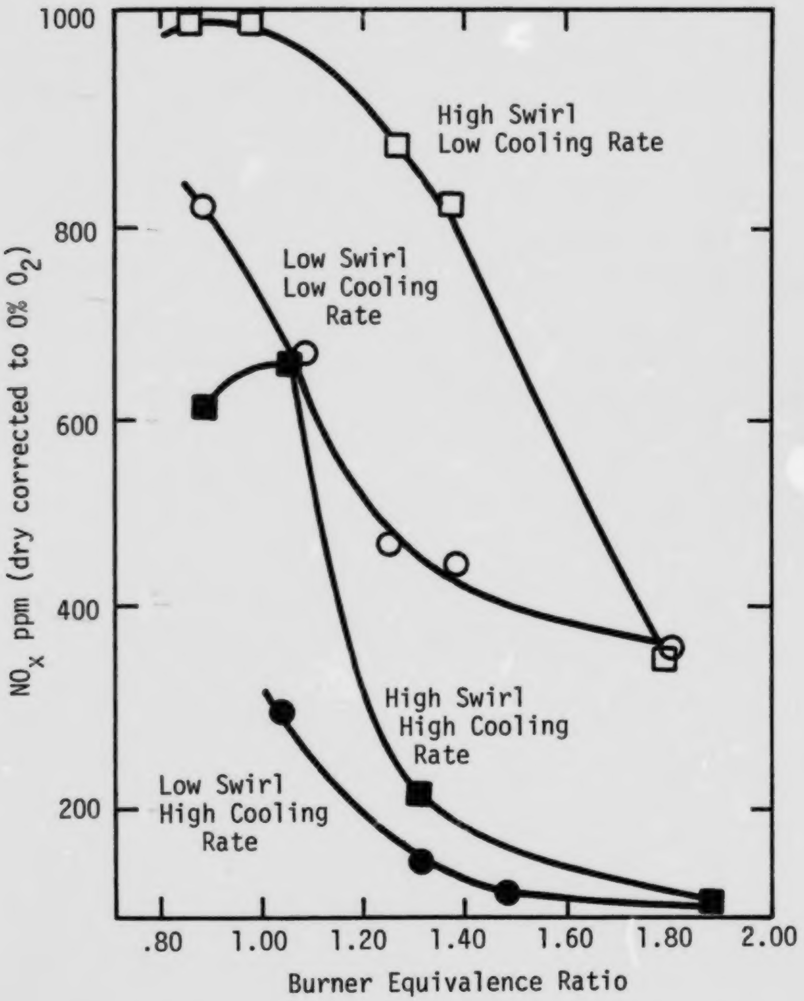

Figure 1-1. Effects of Swirl, Cooling Rate and Burner Equivalence Ratio on NO$_x$ Emissions for a Pilot Scale Distributed Mixing Burner.

pulverized coal were approximately twice those from pulverized petroleum coke. With axial fuel injection at particular swirl levels, emissions were similar for the two fuels. These data suggest that high NO_x emissions from high turbulent pulverized coal flames primarily result from the oxidation of volatile fuel nitrogen fractions. Delayed mixing produced either by the formation of a long thin flame (using axial fuel injection) or with the Distributed Mixing Burner (DMB) reduce emissions because they minimize fuel NO formation from the volatile fuel nitrogen fragment, but they have little impact on char nitrogen oxidation.

The Influence of Oil-Water Emulsions on Pollutant Formation

Attempts to reduce NO_x emissions from fuel oil fired combustors are quite often limited by an increase in particulate emissions because of the need to operate with fuel rich zones. A brief series of tests were conducted with the TOTAL® emulsifier to ascertain whether the use of oil-water emulsions could alleviate this problem. The results of these tests indicated that:

- the addition of water in the form of an emulsion decreased particulate emissions from heavy oil flames;
- when operating under low NO_x conditions the addition of water reduced particulate emissions by a factor of three and had only a minor impact (a slight increase) on NO_x emissions.

Pollutant Measurements in Multi-Burner Systems

All of the previous experimental studies carried out in this program involved single burners and yet it is possible that interactions between burners could influence pollutant formation in multi-burner arrays. Tests were carried out to compare the characteristics of a three burner system firing natural gas and fuel oil (total heat input of 2.0 MW) with a single burner of equivalent heat input. The burners were scaled geometrically and were operated similarly.

Two basic burner types were investigated, namely:

- Type A (high momentum) - the total combustion air was supplied through the throat with a relatively high primary velocity

($50\ \mathrm{msec}^{-1}$),

- Type B (low momentum) - the air flow through the throat was halved, and the remainder supplied via a secondary duct. A common duct was used for the multiple burners.

An axial fuel gun was used for all cases; natural gas was injected radially and a 90° steam atomized Y jet was used for fuel oil. A disc swirler was necessary to stabilize the fuel oil flames. The excess air levels for type A and B flames were 5 percent and 9 percent of the stoichiometric requirements, respectively.

For natural gas flames it was found that a decrease in burner momentum increased emissions (i.e., emissions from the single type A burner were less than those measured with the single type B burner). The data presented in Figure 1-2 indicates that burner spacing does not have a significant influence upon NO_x emissions until the burners are in close proximity. With the low momentum burners maximum emissions were observed at intermediate burner separations.

The influence of burner type and spacing on NO_x emissions from fuel oil is presented in Figure 1-3. In general emissions increase with reductions in burner spacing. With large single burners the emissions are reversed from those observed with natural gas. The higher emission from the high momentum burner could be attributed to increase fuel NO formation because of the more rapid fuel air mixing. Comparison between the small and large burners is difficult because of the problems assciated with scaling oil nozzles.

The Use of a Television Pyrometer to Control Low Emission Burners

Increased complexity and the need to operate low NO_x burners within close limits places stringent demands upon control systems. A test was carried out with a television pyrometer (TVP) developed by Hartel(1.3) at the University of Stuttgart to determine whether this system could be used as a sensor in a burner control system. A schematic illustration of the composite units of the TVP is given in Figure 1-4. The instrument setup

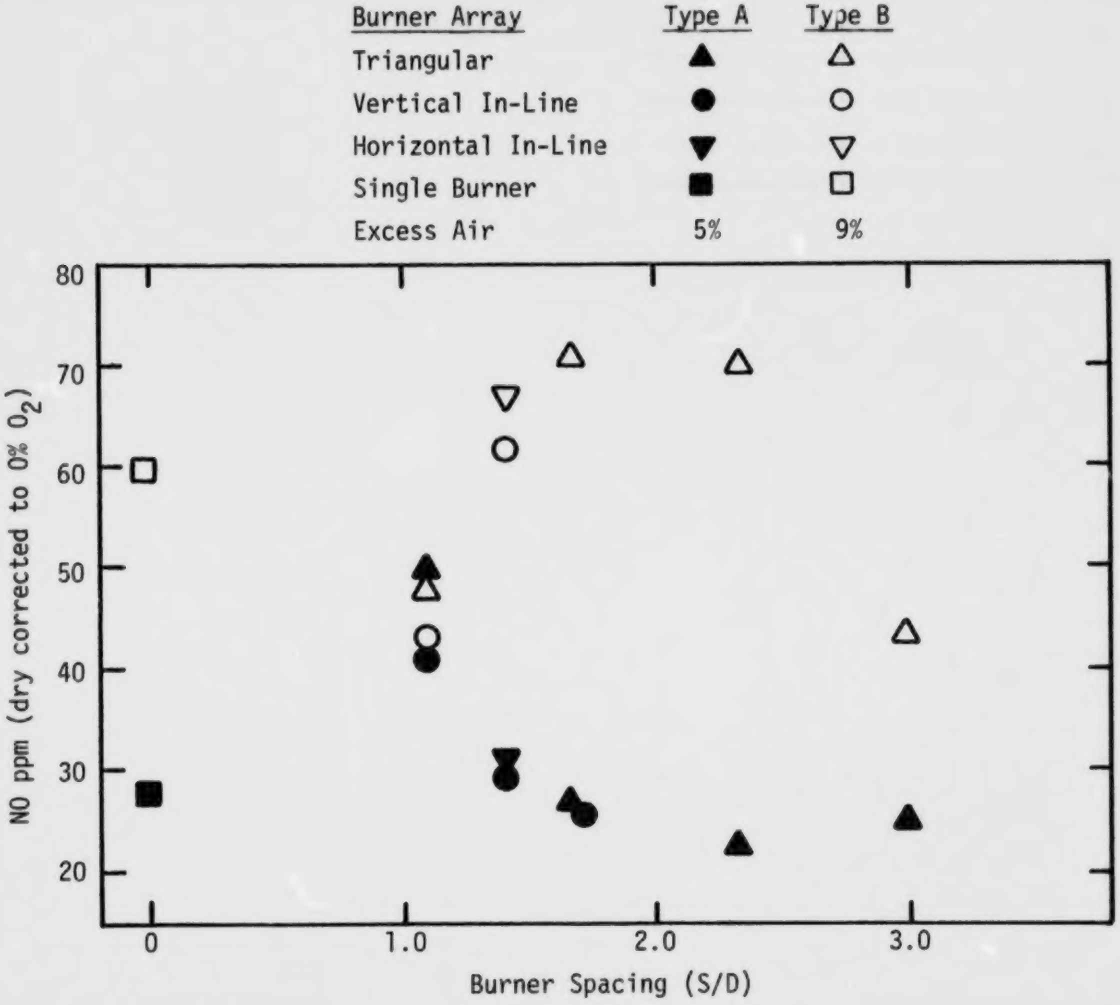

Figure 1-2. The Influence of Burner Spacing, Type and Configuration on NO Formation in Natural Gas Flames.

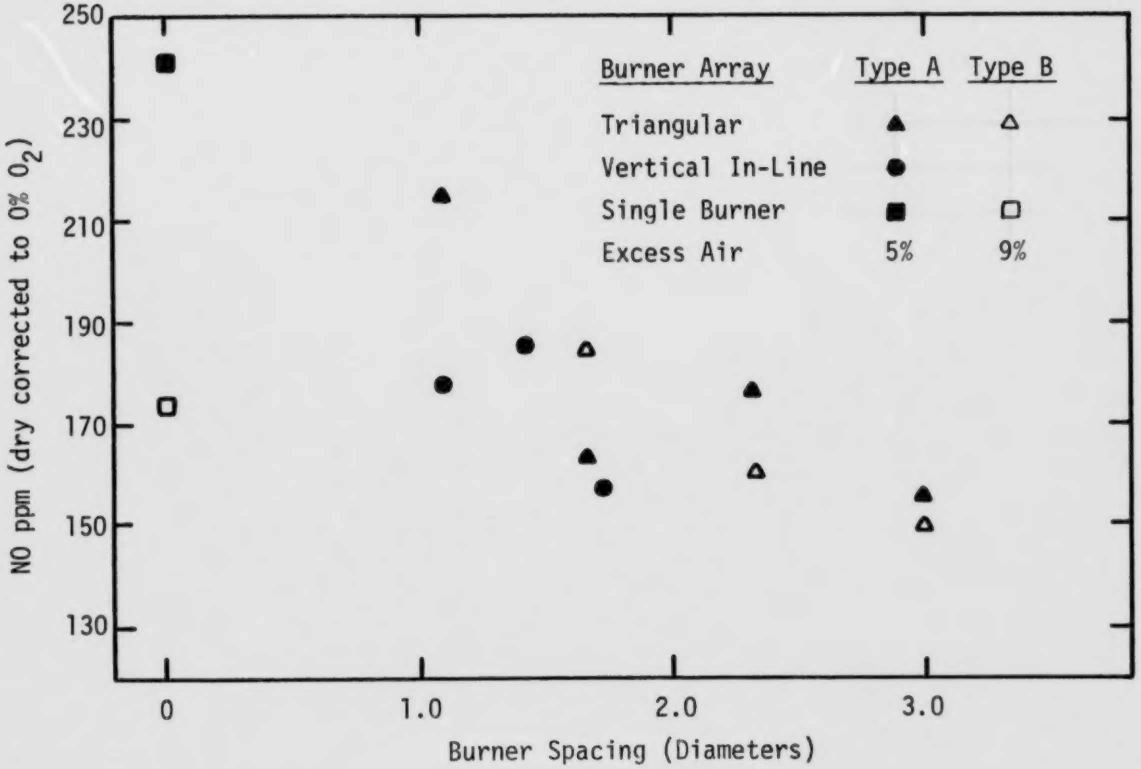

Figure 1-3. The Influence of Burner Spacing, Type and Configuration on NO Formation in Fuel Oil Flames.

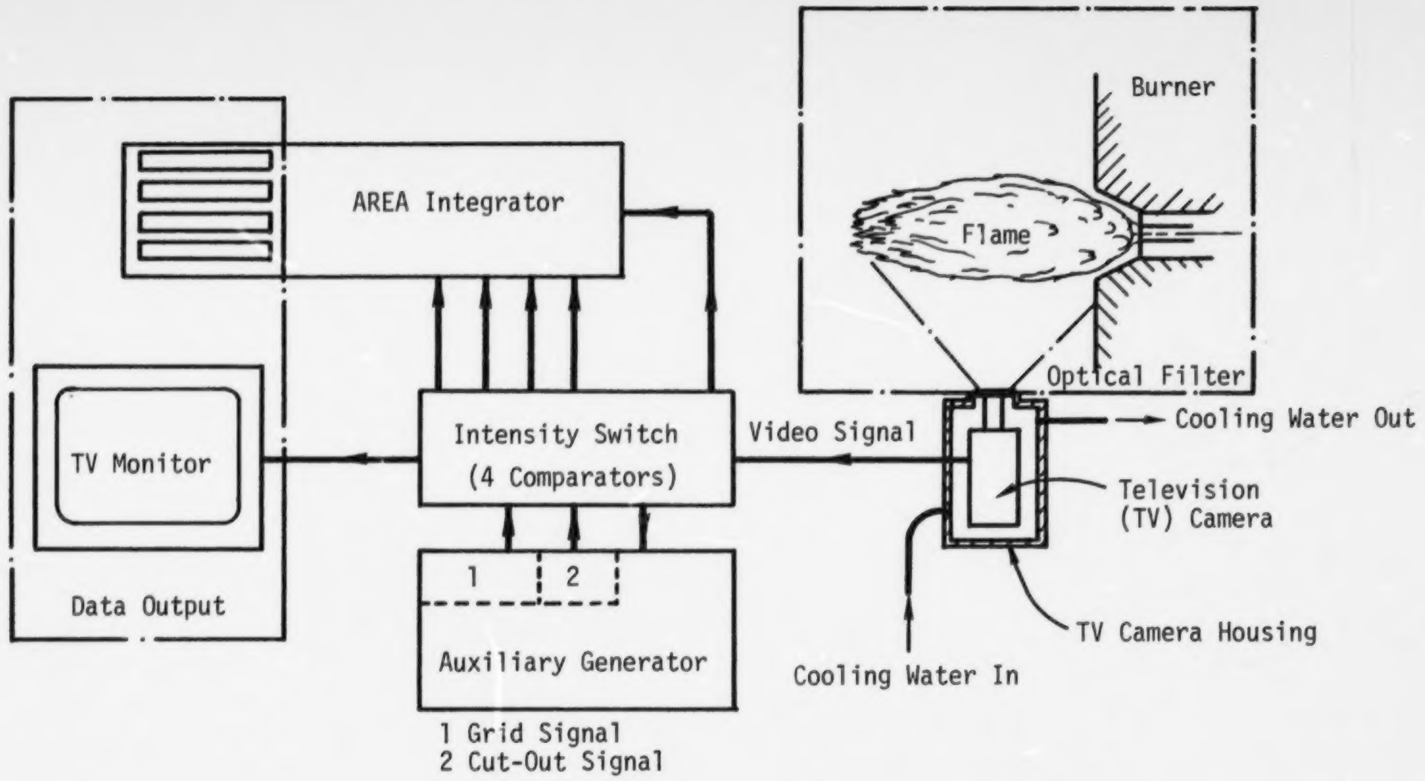
Burner
Flame
Optical Filter
Cooling Water Out
Television
(TV) Camera
TV Camera Housing
Cooling Water In
Video Signal
AREA Integrator
Intensity Switch
(4 Comparators)
TV Monitor
Data Output
1
2
Auxiliary Generator
1 Grid Signal
2 Cut-Out Signal

Figure 1-4. Schematic Setup of the Composite Units of the Television Pyrometer (TVP).

consists of five electronic units:

- a commercial TV camera;
- an intensity switch;
- an area integrator;
- an auxiliary generator;
- a commercial black and white or color TV monitor.

The TV camera views the flame through an optical filter and transforms the flame image into an electrical signal, the videosignal. This videosignal contains all the optical information from the object which penetrates the optical filter. Entering the intensity switch, the signal is modified by four comperators which subdivide the flame image into areas of four intensity ranges, each of which is displayed on the TV monitor in either four different gray shadings or, when a color TV monitor is used, in four different colors. The threshold value of each comperator can be varied continuously in the full range between 0 and 100 percent; however, during this test series, the intensity distribution was kept constant.

An integration of the number of screen points which lie within each range of equal intensity and the total number of points within the flame image on the screen can be carried out by the area integrator.

The auxiliary generator permits the display of an electronic grid on the TV monitor which gives the observer a visual scale for dimensions, thus avoiding possible parallactic aberrations. Furthermore, this generator can cut out by electronic means undesired parts of the monitor screen and thus allows an intensity analysis, for instance, to be confined to one flame only even when more than one flame lies within the angle of vision of the TV camera.

The main objective of testing the television pyrometer (TVP) was to investigate its potential application as an external burner control for industrial furnaces fired by multiple burner systems. First results of the test have indicated that nitric oxide flue gas concentrations emitted by natural gas flames can be correlated with the data of the intensity distribution obtained by the TVP. However, better controlled experiments are required to establish correlation data for a wider range of burner and/or flame types, respectively.

It has been suggested that under the conditions considered in this study (non-luminous natural gas flames), the TVP mainly detects the light emission from exited CH and C_2 radicals. It, therefore, offers itself also for the control of other input parameters which influence the radical concentration and temperature, as, for example, the excess air level.

REFERENCES

1.1 Heap, M. P., et al. The Development of Combustion Systems from Heavy Oil and Coal-Fired Furnaces. Volume I. Influence of Burner Variables on NO_x Formation in Pulverized Coal Flames. EPA 600/2-76-061a, March 1976.

1.2 Heap, M. P., et al. The Development of Combustion Systems from Heavy Oil and Coal-Fired Furnaces. Volume II. Further Furnace Investigations and the Evaluation of Radiative Heat Transfer Models. In publication, 1982.

1.3 Hartel, H. "Fue Answertung von Flammenbildern Technesche Flammen." University of Stuttgart Thesis, 1974.

2.0 POLLUTANT GENERATION AND CONTROL DURING PULVERIZED COAL COMBUSTION

2.1 The Problem

Increased coal utilization is undoubtedly the key to decreased reliance upon imported crude oil. However, there are several alternative methods available to convert coal into electrical energy. Economic and environmental considerations will be significant factors in the choice of energy conversion alternatives since there is a need to utilize coal in an efficient, but environmentally acceptable, manner. Coal contains constituents which have the potential to form pollutants which unless controlled will be emitted into the atmosphere during the energy conversion process. These constituents are:

- Sulfur which forms SO_2 and SO_3 under oxidizing conditions.
- Mineral matter which results from the biological, chemical and environmental conditions existing during the formation of coal is converted to ash or slag or is vaporized. Coal contains almost all the elements in the periodic table.
- Nitrogen which can also be oxidized to give nitric oxide which subsequently oxidizes to nitrogen dioxide, and the sum of these which can be referred to as NO_x.

The above compounds, together with the products of incomplete combustion (CO, hydrocarbons, carbonaceous particulate, and large molecular weight organic molecules), are potential pollutants resulting from coal utilization.

For SO_x, one of the major pollutants produced from coal, there are pollutant control options. The sulfur can be removed from the fuel or from the products of combustion. Removal from the fuel involves the production of a liquid or gaseous fuel or a clean, solid fuel. Coal gasification converts the majority of the sulfur to hydrogen sulfide which is then scrubbed from the fuel gas. Neglecting sorbent efficiency, the reduced gas volume ensures that the task of removing H_2S from the fuel gas is easier than the removal of SO_2 from the combustion products. Although coal gasification is not a new technology, its application to today's needs is far from straightforward. Fluidized bed combustion of coal offers the possibility to burn coal as mined and yet control sulfur emissions by in-bed absorption of SO_2. Flue gas scrubbers are current state-of-the-art for sulfur oxide control, but their size, complexity, and cost provide incentives to find alternative control options. Although nitrogen oxides can be removed from the combustion flue gas treatment is not the preferred control option. Coal gasification can be considered as removal of nitrogen from the fuel since the product gas can be nitrogen free. Liquification does not remove nitrogen. Extensive hydrotreatment is required to produce a low nitrogen liquid fuel from coal. Fortunately the formation of nitrogen oxides from fuel bound nitrogen can be controlled by modifying the combustion process.

This report describes an investigation which was primarily concerned with the control of one pollutant, NO_x, produced during the combustion of pulverized coal and heavy fuel oil. It has been estimated that the total production of NO_x by stationary combustion sources in 1972 was 11.665×10^6 tons, and that 32 percent of this can be attributed to coal-fired utility boilers.(2.1) Another 16 percent was attributed to gas and oil-fired utility boilers. Unless there is a breakthrough in advanced coal conversion technology, the only possibility for a near term increase in coal usage will come about by the application of existing technology--direct combustion. This might be accomplished by a combination of two possibilities:

- Reconversion of those boilers which were originally built for coal firing, but have been converted to oil or gas firing.
- Construction of new boilers either with SO_2 scrubbers or burning low sulfur fuel for pulverized coal or stoker firing.

However, as coal utilization is increased in this way, there is the potential that coal-fired utility boilers will account for an increased fraction of the total NO_x emissions necessitating the development of demonstrated low NO_x combustion technology.

NO_x emissions can be moderated by combustion modification (i.e., changing the processes by which fuel and oxidant are brought together, reaction takes place, and heat is released) or they can be removed from the flue gas. The application of simultaneous NO_x/SO_x scrubbing would be attractive;

however, the economic projections indicate that these processes may be expensive. Combustion modification for NO_x control has been successful and boilers are being operated within the New Source Performance Standards (NSPS). However, the level of NO_x control must be improved if the status quo is to be maintained as coal utilization increases. Table 2-1 lists the Combustion Research Branch Technical Goals for new systems.$^{(2.1)}$ In this section, present day control technology will be reviewed. It should be remembered that the technical goal for 1985 requires a coal-fired boiler to operate with NO_x emissions of less than 20 percent of the existing New Source Performance Standards.

Table 2-1. New System Goals--Average NO_x (ppm @ 3% O_2)$^{(2.1)}$

Utility Boiler Fuel	NSPS	1980 Goal	1985 Goal
Gas	150	100	50
Oil	225	150	90
Coal	550	200	100

2.2 The State-of-the-Art of NO_x Control

Boiler manufacturers, utilities, KVB, Inc., and the Exxon Research and Development Company have all carried out extensive testing with utility boilers firing pulverized coal to tune the boiler for low NO_x emissions. This section will briefly review the state-of-the-art as far as utility boiler operation and NO_x emissions are concerned before discussing some of the fundamental aspects of NO_x formation and their impact upon future control possibilities.

2.2.1 Overall Excess Air

Figure 2-1 taken from the work of Crawford et al$^{(2.2)}$ shows the effect of overall excess air on the emission of NO_x from several coal-fired boilers. Emissions decrease as excess air is reduced and tangential fired boilers have lower emissions than wall fired boilers. Figure 2-2 shows the increase in CO concentration that accompanies the decrease in NO concentration at low excess air firing.

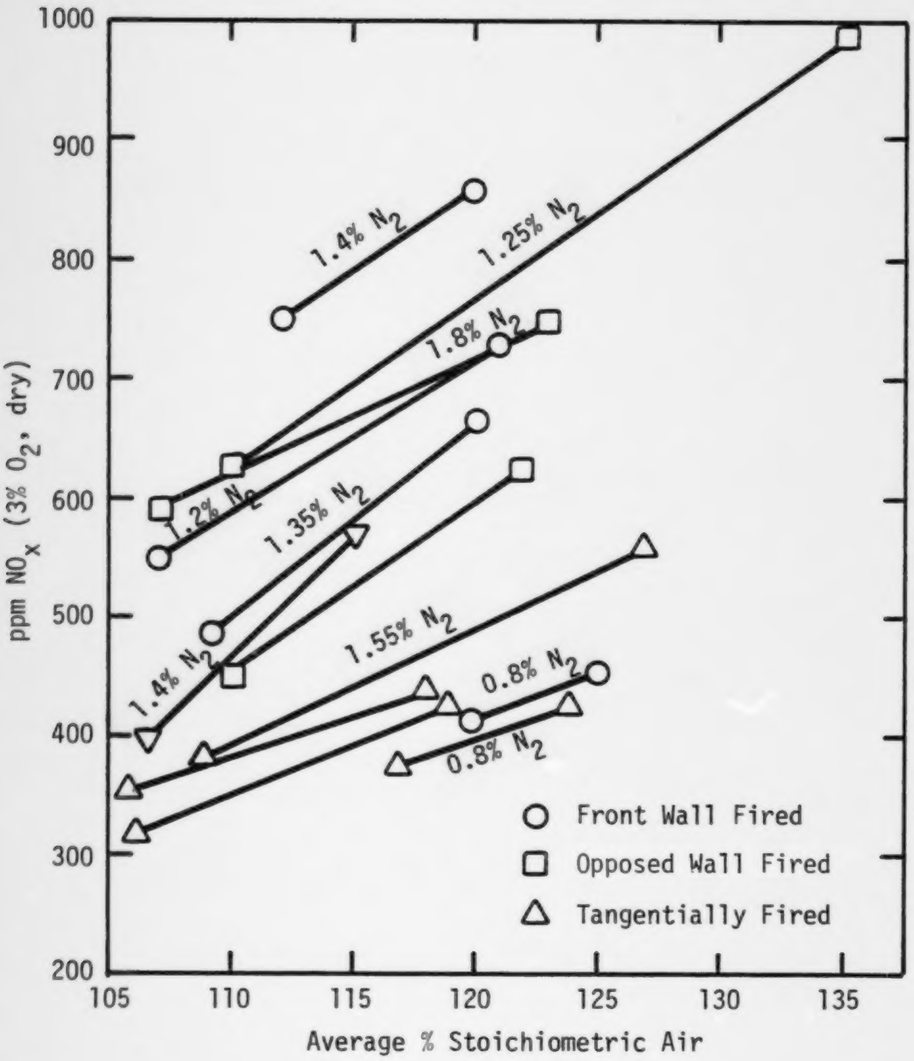

Figure 2-1. ppm NO_x vs % Stoichiometric Air for Coal Fired Boilers.

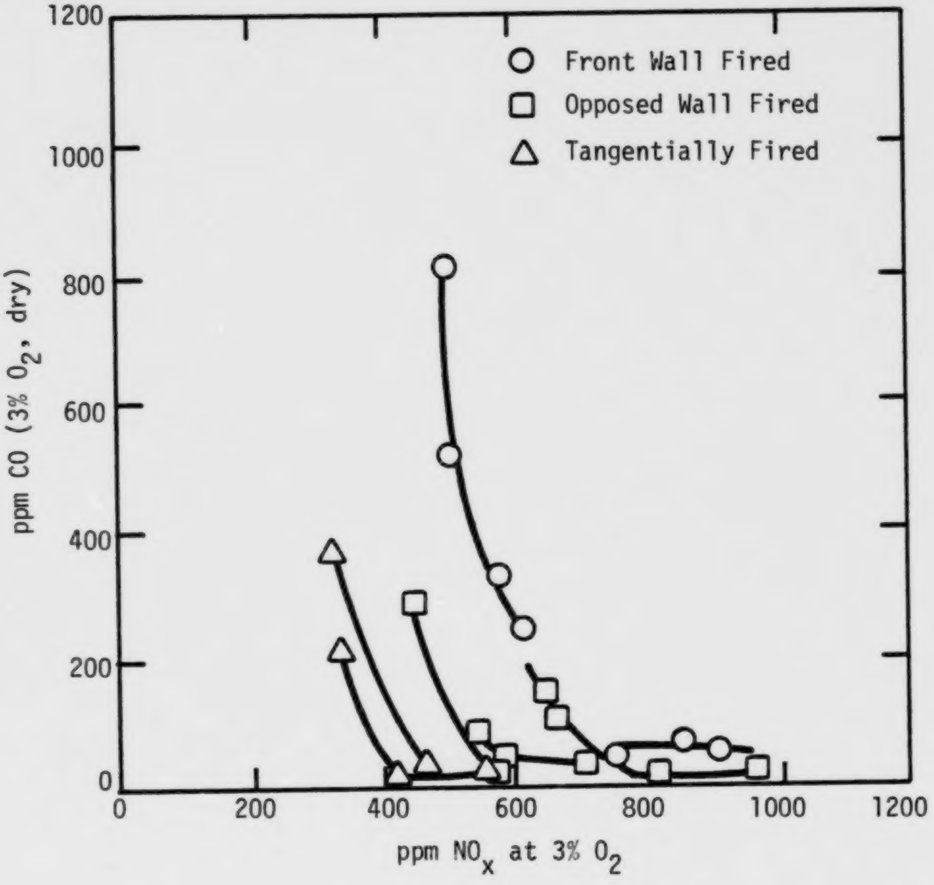

Figure 2-2. CO Emissions as a Function of NO_x Emissions for Coal-Fired Boilers as the Excess Air is Changed.

2.2.2 Flue Gas Recirculation

NO_x emissions from coal-fired boilers are primarily due to the oxidation of coal bound nitrogen producing fuel NO_x. Flue gas recirculation reduces flame temperatures, thereby reducing thermal NO production. It would be surprising if flue gas recirculation had a significant effect upon NO_x emissions from coal flames since fuel NO_x formation is not very temperature sensitive. This supposition has been confirmed by Thompson et al.(2.3) These investigators added flue gas to the combustion air supply of a 560 Mw horizontally opposed wall-fired boiler. Results are presented in Figure 2-3 which show the effect of percent flue gas recirculation on NO_x emissions during normal boiler operation. Emissions were reduced by about 20 percent for 20 percent recirculation which was the fraction of the total NO attributed to oxygen fixation by Pershing et al.(2.4)

2.2.3 Staged Heat Release

The "traditional" method of reducing NO_x emissions from boilers firing fuels which contain bound nitrogen is to stage the heat release process by removing some burners found in service. Air alone flows through these burners to make up for the air deficiency caused by reducing the air flow to the burners receiving fuel. This is an ad hoc process, and each boiler is tuned on an individual basis. Figure 2-4, taken from the work of Crawford et al,(2.2) shows the effect of this process on NO_x emissions which are plotted as a function of the fraction of stoichiometric air supplied to the active burners. In general, reductions of the order of 50 percent of the baseline emissions can be achieved. This type of reduction is normally accompanied by an increase in CO emissions.

2.2.4 Burner Modifications

Babcock and Wilcox(2.3) is the only boiler manufacturer to report NO_x emissions from a boiler which has been modified to accept a new design of low NO_x burner. The boiler was an opposed wall-fired boiler with division walls (see Figure 2-5) and originally utilized 18 36-inch circular burners. Six dual register low NO_x burners were installed in the front and rear sections of one zone. The remaining 12 burners were left as initially supplied. Figure 2-6 summarizes the baseline performance of the boiler.

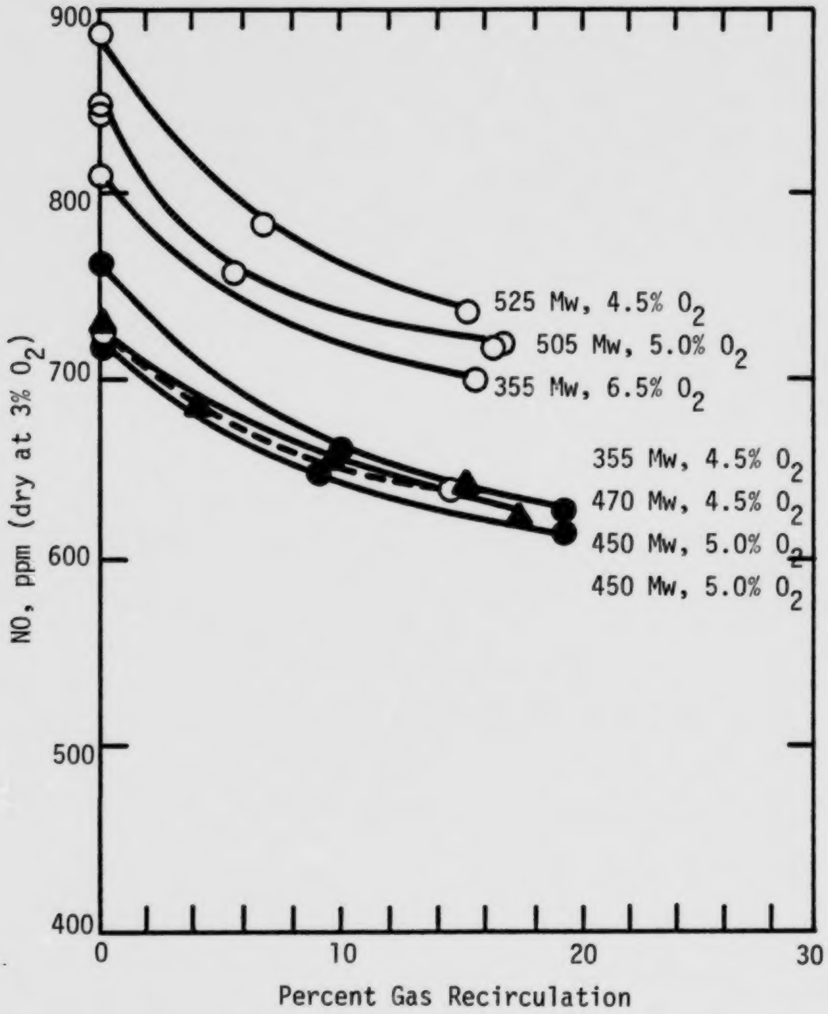

Figure 2-3. NO Dependence on Gas Recirculation During Normal (Air-Rich) Operation.

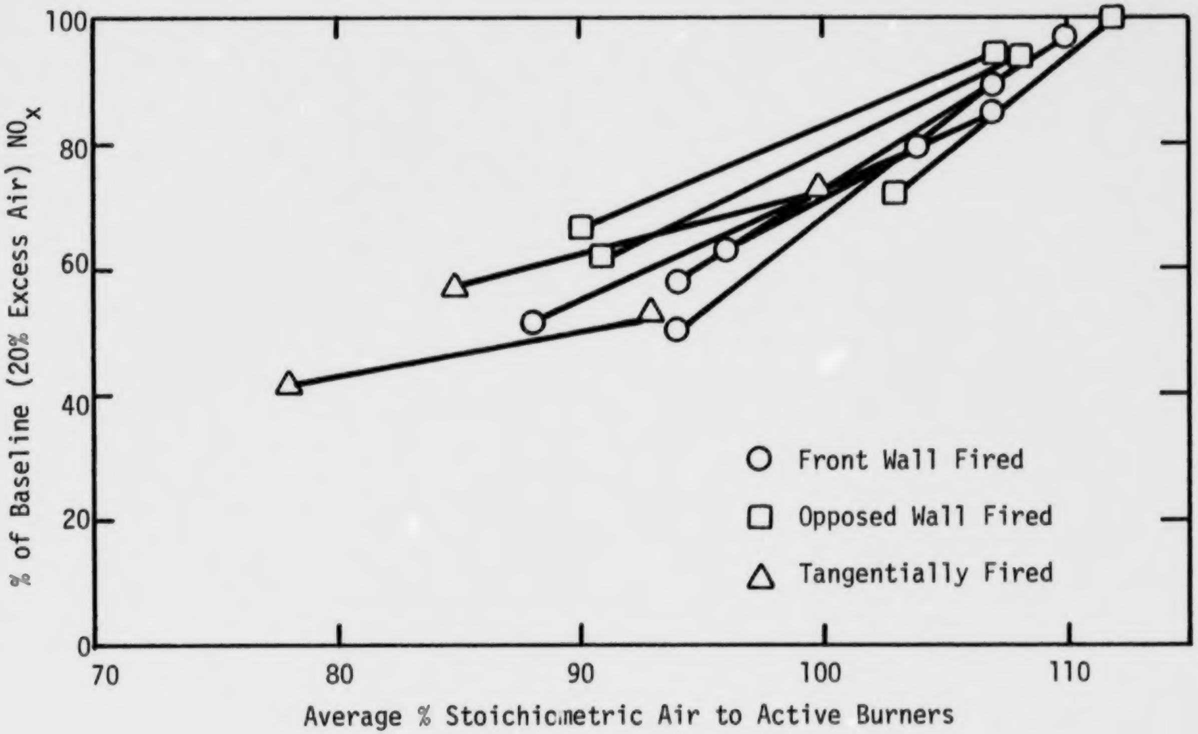

Figure 2-4. Effect of Excess Air on NO_x Emissions Under Modified Firing Conditions.

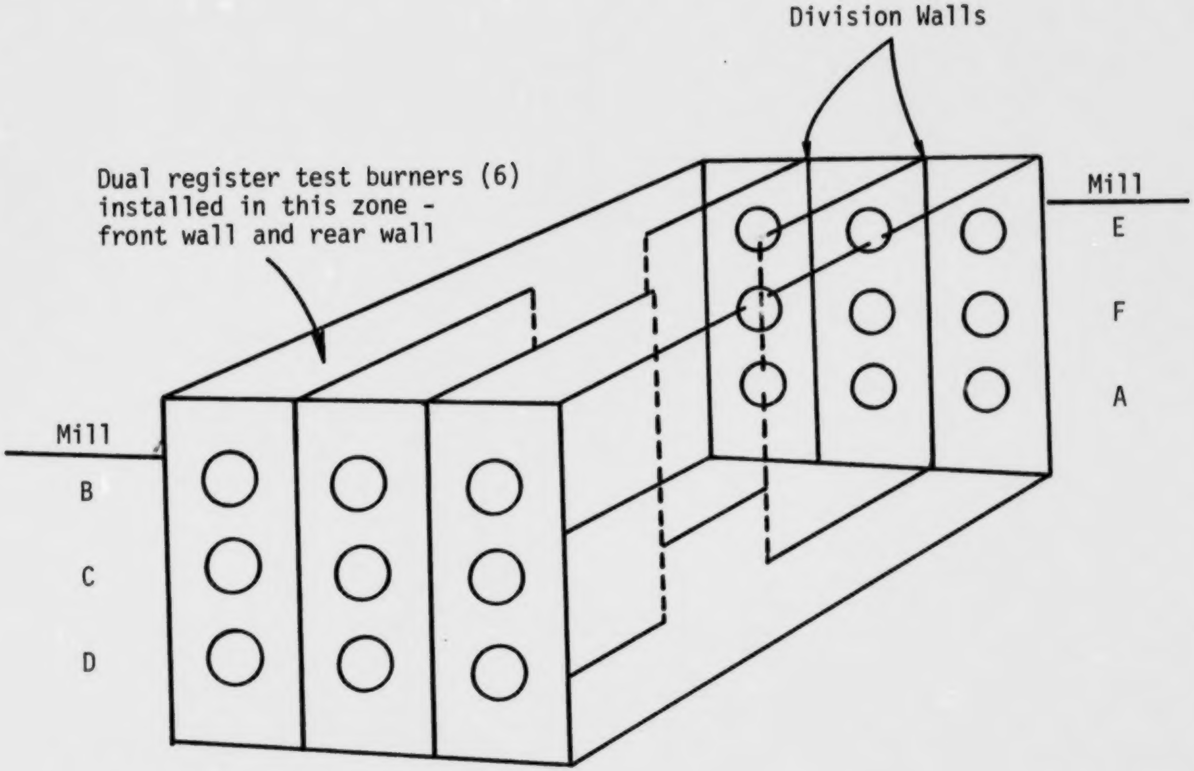
Division Walls
Dual register test burners (6) installed in this zone - front wall and rear wall
Mill
E
F
A
Mill
B
C
D

Figure 2-5. Burner Arrangement - Opposed Fired.

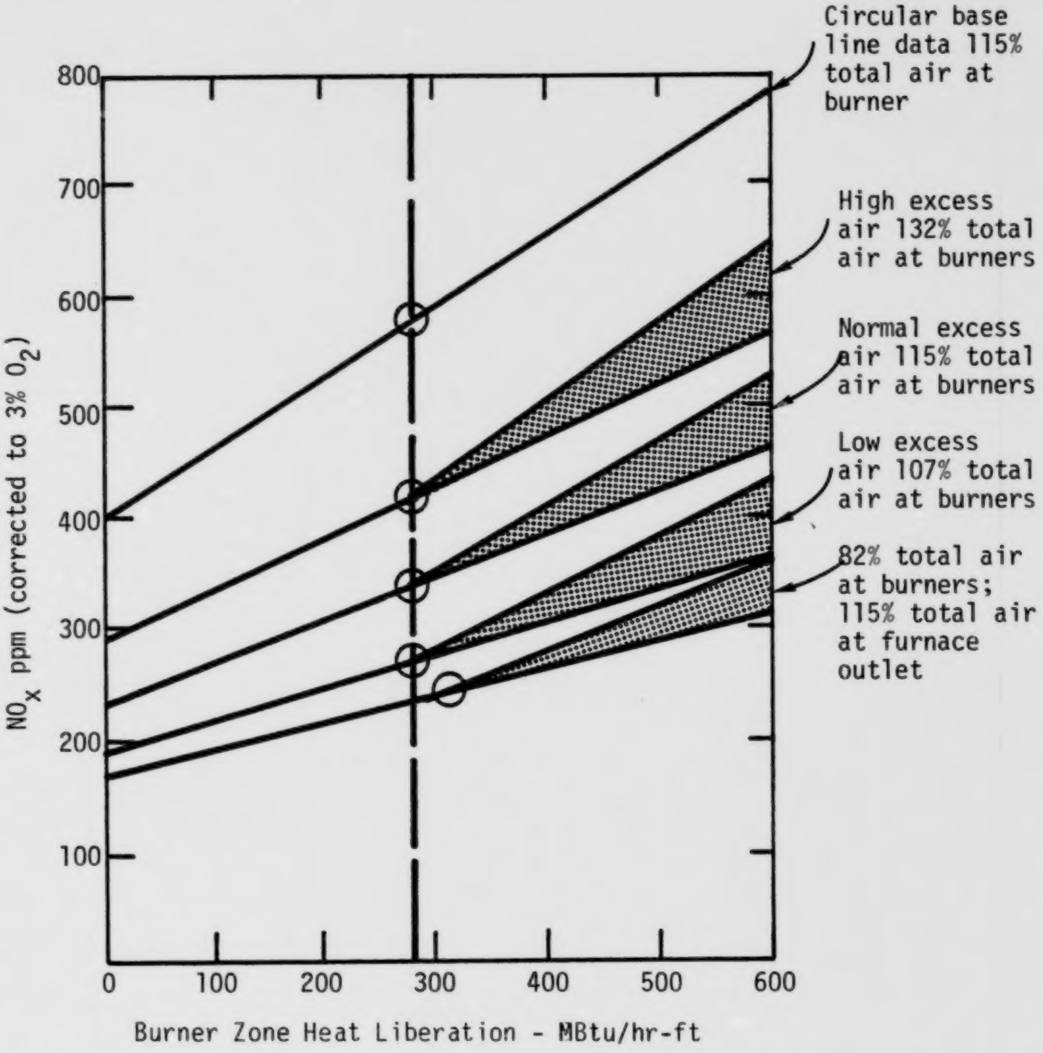

Figure 2-6. Boiler Baseline Performance with Unmodified Burners.

NO_x emissions are plotted as a function of the total heat available divided by the adjusted burner zone water-cooled surface. With the new burners, emissions were reduced by approximately 40 percent (435 ppm versus 725 ppm). Exxon tested the same boiler after all the burners had been changed and estimated a 35 percent reduction in emissions due to the burner change.(2.2) Emission levels as low as 182 ppm were measured by reducing the boiler load to 66 percent capacity, taking some burners out of service, and firing at low excess air.

2.3 Pollutant Formation in Pulverized Coal Flames

The previous section discussed the state-of-the-art of NO_x control for pulverized coal-fired boilers. In this instance, state-of-the-art can be considered as "boiler applied;" however, it does not represent our total knowledge concerning NO_x formation in pulverized coal flames. There is also a considerable body of data from small-scale burner studies and fundamental experiments which adds to our basic knowledge. The flow diagram presented in Figure 2-7 attempts to relate the various input parameters and the basic phenomena associated with NO production in pulverized coal flames. Input parameters control the coal particle environment throughout its lifetime via mass transport and heat exchange. Particle physics in combination with the particle environment dictate the particle heating rate, a factor which is of major importance with regard to coal chemistry. NO production in pulverized coal flames is most strongly linked to the fate of the nitrogen bound in the char. The split between volatile and char nitrogen and the rate of evolution of volatile nitrogen are all important for fuel NO production. The ultimate NO level is dependent upon the homogeneous and heterogeneous reactions involving various hydrocarbon species, nitrogen-containing radicals, sulfur radicals, char, and molecular nitrogen. Although fuel NO_x is a major contributor to the total uncontrolled NO_x emission, thermal NO production might well be important under controlled conditions.

Figure 2-8 attempts to explain the complex phenomena that occur during heat release and pollutant formation in a pulverized coal flame. It is believed that volatile fuel nitrogen fragments (XN) are mainly responsible for fuel NO production. There are homogeneous reactions allowing the production of either N_2 or NO from the volatile XN species. The availability

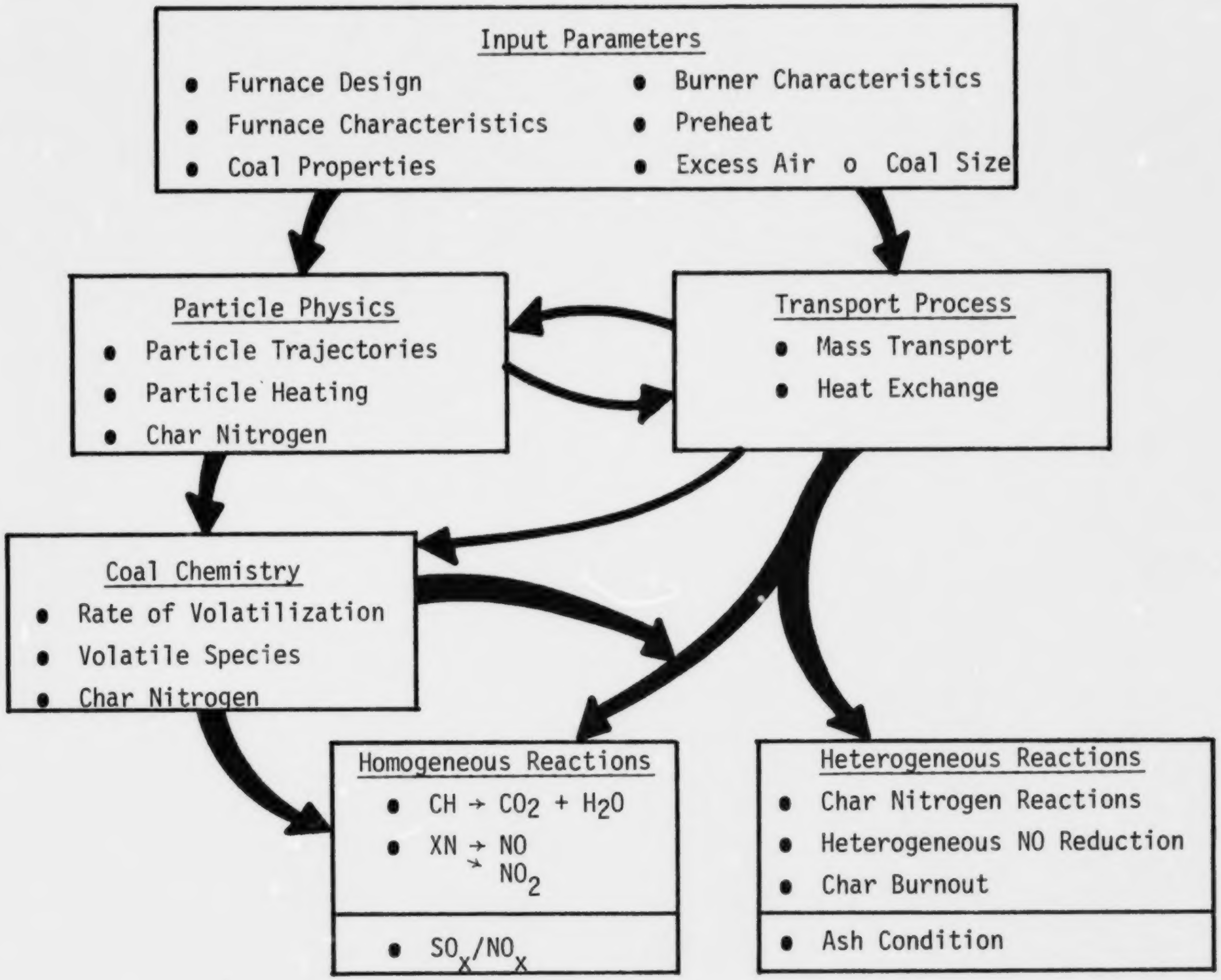
Input Parameters
Furnace Design
Furnace Characteristics
Coal Properties
Burner Characteristics
Preheat
Excess Air o Coal Size
Particle Physics
Particle Trajectories
Particle Heating
Char Nitrogen
Transport Process
Mass Transport
Heat Exchange
Coal Chemistry
Rate of Volatilization
Volatile Species
Char Nitrogen
Homogeneous Reactions
CH → CO2 + H2O
XN → NO
→ NO2
SOx/NOx
Heterogeneous Reactions
Char Nitrogen Reactions
Heterogeneous NO Reduction
Char Burnout
Ash Condition

Figure 2-7. NO Production in Pulverized Coal Flames.

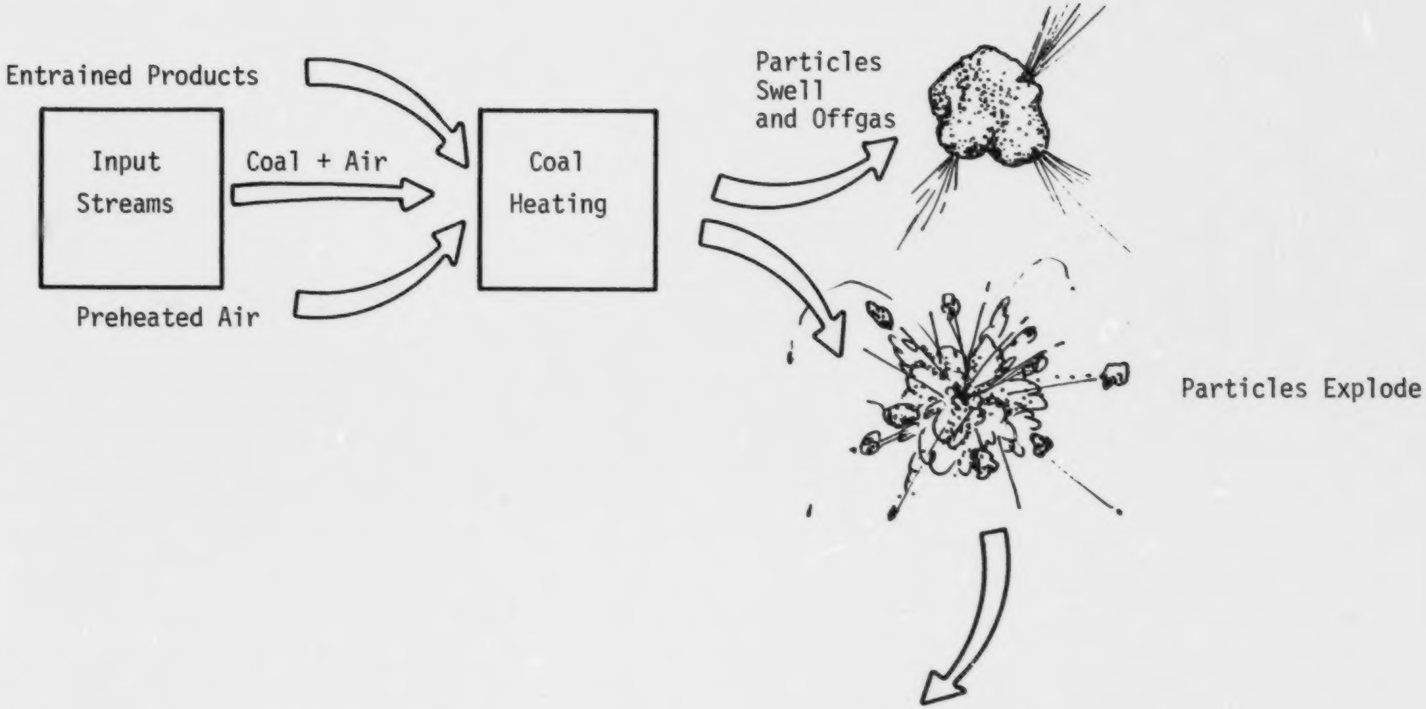
Entrained Products
Input Streams
Coal + Air
Preheated Air
Coal Heating
Particles Swell and Offgas
Particles Explode

Solid Reaction	Gas Phase Reaction
Char + OX → CO_2 + H_2O	CH + OX → CO_2 + H_2O
Char N → NO	XN + OX → NO + ...
Char + NO → N_2	XN + YN → N_2 + ...
Char + XN → Char XN (absorbed)	CH + NO → XN

Figure 2-8. Phenomenological Model of NO Production in Coal Flames.

of oxygen is probably the overwhelming factor in the production of NO which will be controlled by:

- Fuel/air mixing rates,
- Particle devolatilization rate and time of evolution of the nitrogen compounds, and
- Availability of CH fragments.

The fate of char nitrogen is pure speculation at present, and char might act to reduce nitric oxide. Thus, the key to NO production in coal flames is strongly associated with:

- Coal chemistry,
- Homogeneous reactions, and
- Heterogeneous reactions.

2.3.1 Coal Chemistry

Coal chemistry is rather a misnomer. In the restricted sense of this review, it refers to those reactions which take place during particle heating and dictate volatile evolution. Available information is restricted to cause and effect studies rather than details of the process. Particles in pulverized coal flames are subjected to heating rates between 10,000 K/sec and 100,000 K/sec causing a loss of volatiles from the coal. The particle might swell and offgas as a jet, it might explode, or the volatilization process might occur with little physical change in the particles. Blair et al(2.5) and Pohl and Sarofim(2.6) have shown that the total quantity of volatiles produced is a strong function of pyrolysis temperature. It has been postulated that the total volatile evolution can be split into two sections referred to as early and late volatiles.

Blair et al(2.5) carried out a series of controlled pyrolysis experiments with single particles and found that:

- Total nitrogen volatilized is a more sensitive function of pyrolysis temperature than is total mass pyrolyzed (see Figure 2-9).
- Twenty percent of the volatile fuel nitrogen appears to be released from the coal as light gases (HCN, NH_3).

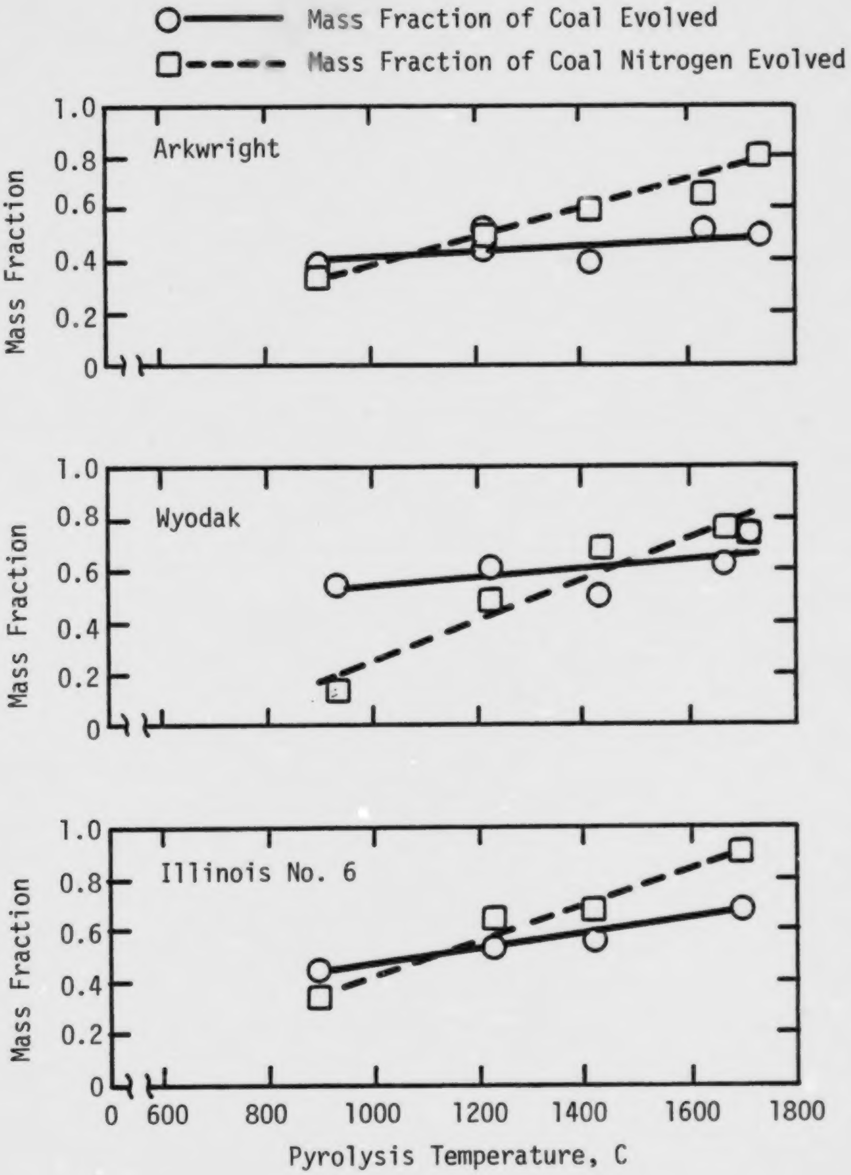

Figure 2-9. Fractional Coal Mass and Coal Nitrogen Loss as Functions of Pyrolysis Temperature.

This latter conclusion may have less significance because even though the initial nitrogen fragments may be heavy molecular weight compounds, it is probable that the nitrogen finally ends up as HCN.

Pohl and Sarofim(2.6) have carried out a series of studies in a laminar flow furnace. The nitrogen retention in the char under inert pyrolysis conditions is shown as a function of temperature and time in Figure 2-10. From these results, it can be seen that for a residence time of one second, which exceeds the usual residence time in flames, temperatures in excess of 1500 K are required to reduce the nitrogen content of the char to less than 40 percent of the value of the original coal.

Oxidation experiments have also been performed at M.I.T. on coals and on chars prepared from them. The conversion of coal and char nitrogen to nitric oxide are shown in Figures 2-11 and 2-12 as a function of fuel/air equivalence ratio for a furnace temperature of 1500 K. Conversion of char nitrogen to nitric oxide is seen to occur with lower efficiency tha that of coal nitrogen under comparable conditions of temperature and fuel/air equivalence ratio. The data on pyrolysis and on coal and char oxidation can be combined to infer the fraction of the total NO_x contributed by oxidation of volatiles and the percent conversion to NO_x of the volatiles as a function of fuel/air equivalence ratio.

The above studies provide some insight into the process that occurs during the staging of a coal combustor. In the first stage, part of the fuel nitrogen is devolatilized and is converted to NO_x in amounts that decrease with an increase in the local fuel/air ratio. Part of the nitrogen is retained by the coal char or coked residue and is converted to NO_x with a lower efficiency than the nitrogen in the volatiles. Some of the fuel nitrogen may persist into the second stage if the temperature and time in the first stage are not high enough, but any nitrogen carried into the second stage in the coal char will be converted to nitric oxide with an efficiency that depends on the local stoichiometry. The studies suggest that the amount of nitrogen carried over to the second stage can be decreased by increasing the first stage temperature. The effects of increasing the furnace temperature to 1750 K on the emissions of NO_x and nitrogen in the unburned char are shown in Figure 2-13. Comparison with the results

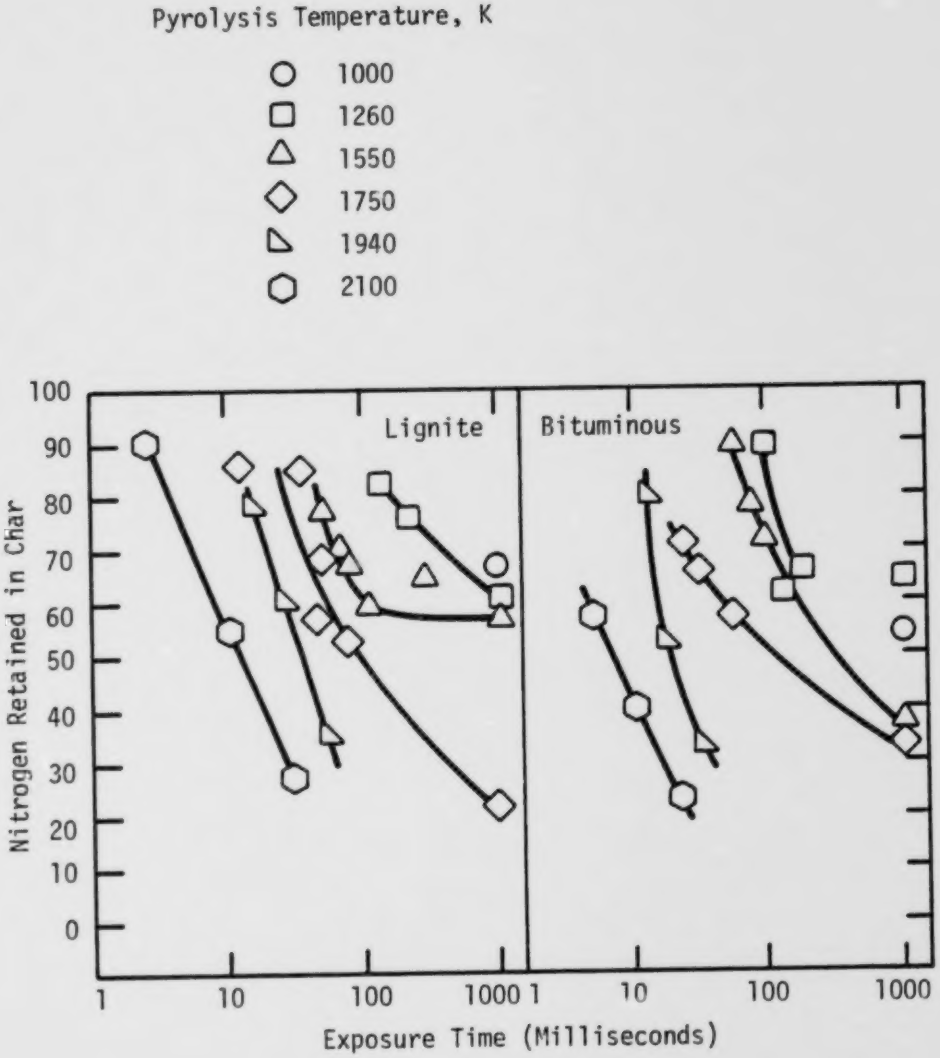

Figure 2-10. Retention of Nitrogen in Devolatilized Lignite and Bituminous Coal Chars.

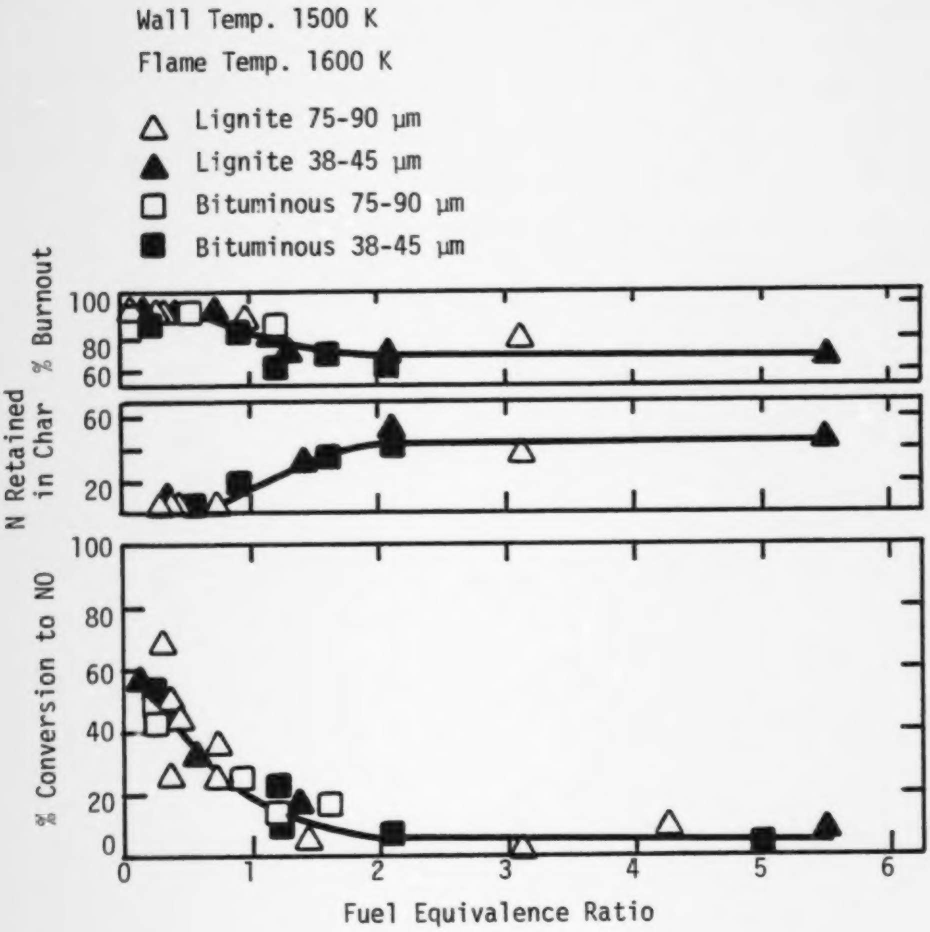

Figure 2-11. Conversion of Coal Nitrogen as a Function of Fuel Equivalence Ratio in a 1500 Furnace.

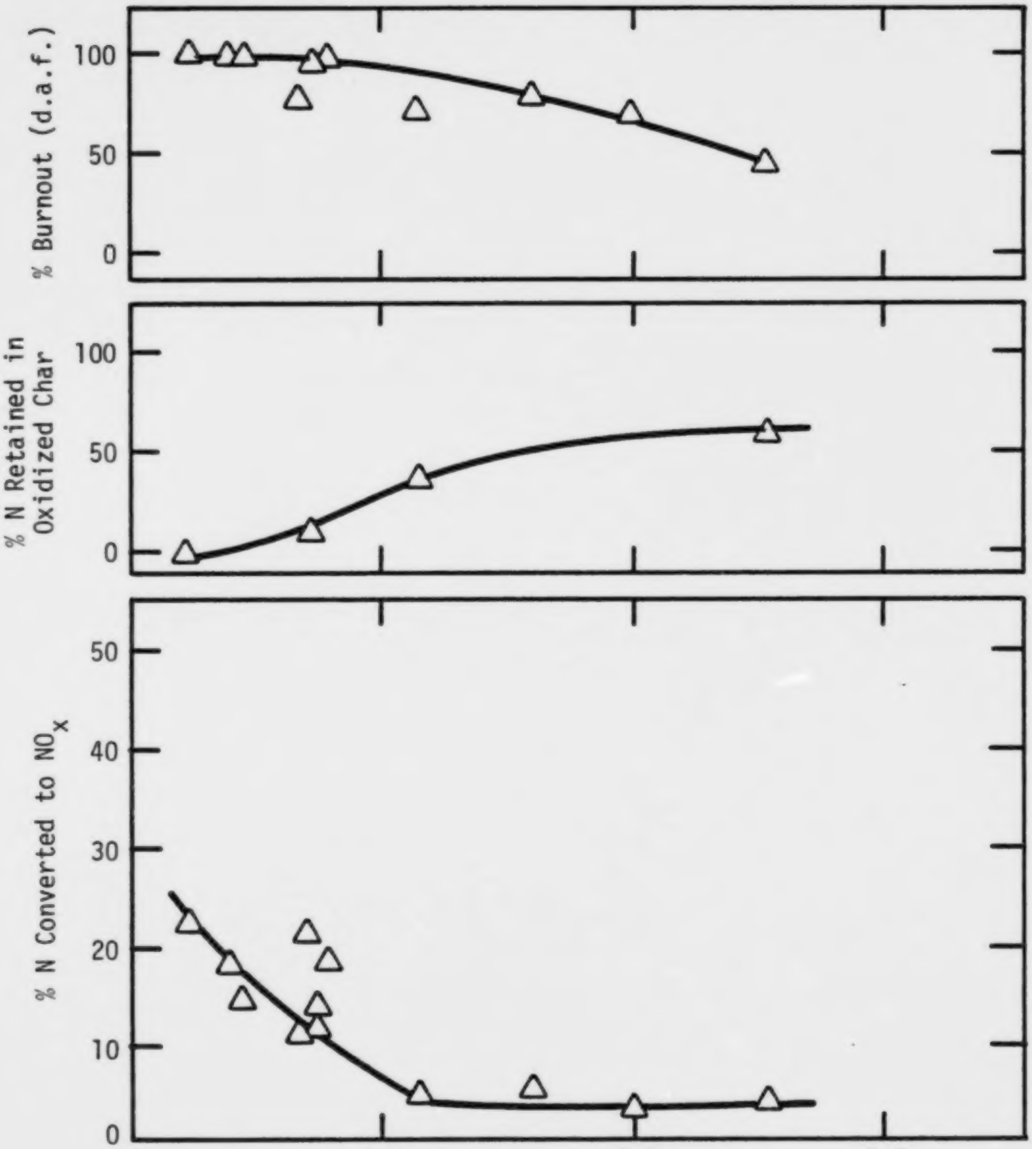

Figure 2-12. Conversion of Nitrogen vs Fuel Equivalence Ratio in a 1500 K Furnace for a Lignite Char Previously Devolatilized at 1500 K for One Second.

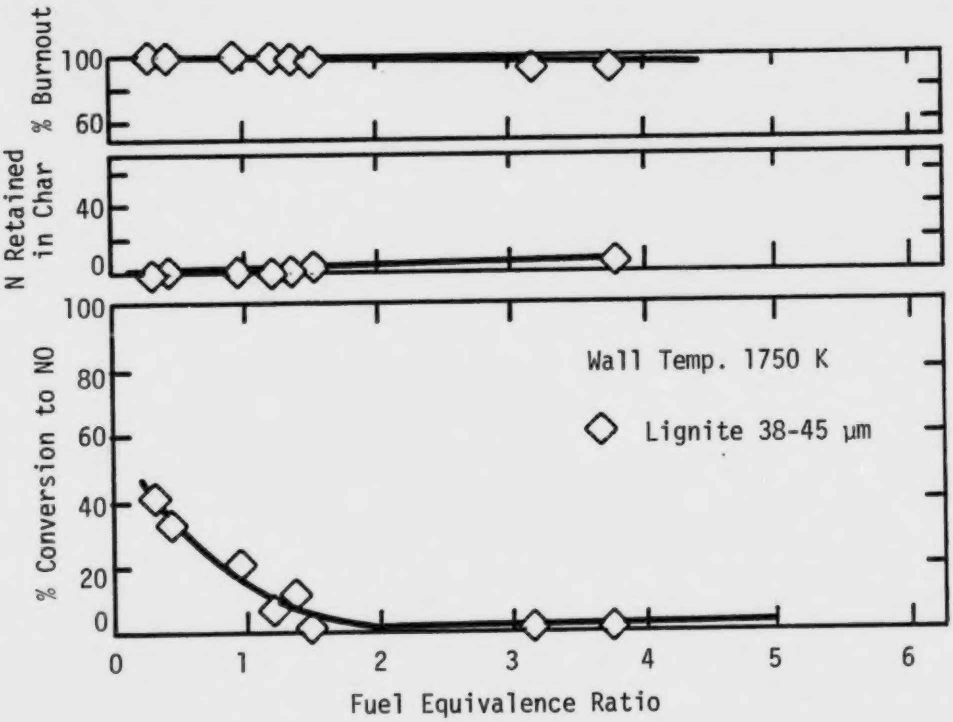

Figure 2-13. Conversion of Coal Nitrogen as a Function of Fuel Equivalence Ratio in a 1750 K Furnace.

at 1500 K in Figure 2-11 clearly shows the beneficial effect of increasing temperature under fuel-rich conditions (fuel equivalence ratio > 1).

2.3.2 Homogeneous Gas Phase Reactions

It appears reasonable to assume that all of the volatile fuel nitrogen fractions will be converted to HCN in the region around the coal particle. There have been many studies on gas phase fuel nitrogen reactions. A short review of the major findings of these studies is presented below. Qualitative conclusions indicate that:

- Fuel nitrogen conversion to NO is most sensitive to reaction zone stoichiometry and only slightly sensitive to reaction zone temperature.
- Fuel nitrogen conversion appears to be almost independent of the nitrogen bonding (i.e., NH or CN).
- For fuel-rich mixtures, conversion is higher with hydrogen than with hydrocarbon fuels.
- The presence of sulfur reduces fuel nitrogen conversion to NO for fuel-lean mixtures and increases it for fuel-rich mixtures.
- NO can be considered as a fuel nitrogen compound.
- HCN, NH_i, NO and N_2 have been found in products of combustion of fuel rich flames doped with NH_3, NO, and HCN.

The mechanism of fuel NO formation in overall NO formation in homogeneous systems is not completely understood, but a model which explains the observables involves HCN oxidation:

$$HCN + H \rightarrow CN + H_2 \qquad (1)$$

$$CN + OH \rightarrow NCO + H \qquad (2)$$

$$H + NCO \rightarrow NH + CO \qquad (3)$$

and hydrogen abstraction:

$$NH + H \rightarrow N + H_2 \qquad (4)$$

The ultimate NO level is then dictated by two competitive reaction paths:

$$N + O_2 \rightarrow NO + O \qquad (5)$$

$$N + OH \rightarrow NO + H \qquad (6)$$

$$N + NO \rightarrow N_2 + O \qquad (7)$$

Under Fuel-Lean conditions, Reaction (5) is most likely to occur. In fuel-rich conditions, Reactions (6) and (7) are more likely. NO itself will produce CN radicals by:

$$NO + CH \rightarrow CN + OH \qquad (8)$$

Thus NO formed in an early part of the flame could be reduced by hydrocarbon radicals.

The presence of sulfur might interfere with these reactions either directly via:

$$NH + S \rightarrow HS + N \qquad (9)$$

$$N + SO \rightarrow NO + S \qquad (10)$$

or indirectly via such reactions as:

$$CH + S \rightarrow CS + H \qquad (11)$$

or

$$CH_2 + S \rightarrow CH + HS \qquad (12)$$

In a staged combustion system, the major impact of homogeneous kinetics is associated with the time required in the rich primary zone to minimize the sum of the XN (NO_x and reduced nitrogen compounds) species before secondary air is added and the mixture becomes overall oxidizing.

2.3.3 Heterogeneous Reactions

Compared to the wealth of data on gas phase nitrogen reactions, very little is known concerning char nitrogen reactions. Char nitrogen conversion to NO appears to be low, but considering system requirements, there is very little that can be done from a combustion viewpoint to modify conditions in the char burnout region.

There is evidence that at lower temperatures, carbon in the form of soot or coal will reduce NO. More information of a fundamental nature is needed in this area to provide input for low NO_x burner development.

REFERENCES

2.1 Martin, G. B., and Bowen, J. S. "Development of Combustion Modification Technology for Stationary Source NO_x Control: Health, Environmental Effects, and Control Technology of Energy Use." EPA Report 600/7-76-002.

2.2 Crawford, A. R., et al. "Field Testing: Application of Combustion Modifications to Control NO_x Emissions from Utility Boilers." EPA 650/2-74-066, June 1974.

2.3 "The Proceedings of the NO_x Control Technology Seminar." EPRI Special Report, February 1976.

2.4 Pershing, D. W. Ph.D. Dissertation, Department of Chemical Engineering, University of Arizona, Tucson, 1976.

2.5 Blair, D. W., Wendt, J. O. L., and Bartok, W. "Evolution of Nitrogen and Other Species During Controlled Pyrolysis of Coal." Presented at the Sixteenth Symposium (International) on Combustion, Cambridge, Mass., August 1976.

2.6 Pohl, J. H., and Sarofim, A. F. "Devolatilization and Oxidation of Coal Nitrogen." Presented at the Sixteenth Symposium (International) on Combustion, Cambridge, Mass., August 1976.

3.0 BURNER DESIGN TO CONTROL NO_x FORMATION IN TURBULENT DIFFUSION FLAMES

The basic mechanisms of nitric oxide formation during the combustion of pulverized coal and heavy oil were described in the previous section. The total emission of NO was divided into two groups based upon the source of the nitrogen:

- thermal NO is formed by the fixation of molecular nitrogen by a process which is extremely sensitive to temperature;
- fuel NO is formed from fuel bound nitrogen by a process which is relatively insensitive to temperature but very dependent upon oxygen availability.

Fuel NO forms the most significant fraction of the total NO produced by the combustion of both pulverized coal and heavy oil. Consequently pollutant control strategies for these fuels should be primarily based upon minimizing the formation of fuel NO. This section will discuss the objectives of the overall program on the development of burner design evidence for NO_x control and discuss the results of the earlier phases. Since all of the experimental investigations involve swirling turbulent diffusion flames, a discussion of the characteristics of these flames will be presented.

3.1 The Characteristics of Swirling Flames

Burner designs which introduce a rotational flow component to the combustion air (referred to as swirl) are commonly used to improve flame stability and to increase the combustion intensity of turbulent diffusion flames. The increase in ignition stability is due to the formation recirculation vortex near the burner axis which causes burning gases to reverse direction and travel back towards the burner where they provide a continuous ignition source. The application of swirl tends to give a shorter and wider flame. A complete characterization of a swirling jet requires a knowledge of the initial distribution of both the tangential and axial velocities across the burner throat. This is because the tendency to spread more rapidly for a free jet is only present in forced vorticies (i.e., those in which the tangential velocity is constant or increases with radius). In a free vortex, where the tangential velocity varies inversely as the radius, the pressure field balances the centrifugal force, and the jet does not show the characteristic tendency to spread more rapidly than the non-swirling jet. In addition, an inner recirculation zone does not develop with a free vortex and most practical swirl burners give rise to forced vorticies.

Swirl number(s) is a dimensionless number which is used to characterize swirling flows and it is defined as:(3.1)

$$S = \frac{\text{Axial Flux of Angular Momentum}}{\text{Axial Flux of Linear Momentum x Radius of the Burner Throat}}$$

Although this parameter is referred to frequently it has one major deficiency, it does not take account of angular momentum as a function of burner throat radius and this is known to affect the characteristics of swirling flows. Consequently, swirl number is most useful to compare swirl levels produced by burners of similar design.

A convenient way to describe the characteristics of swirling flames is to consider the changes that occur as swirl is applied to the combustion air flow of a simple double concentric burner with an axial fuel jet. Without swirl the flame is ignited several burner diameters downstream of the fuel injector. This will be termed a lifted jet flame. Ignition occurs because the combustion air and the fuel jet mix and entrain high temperature gases from the furnace, "external" recirculation. Consequently, the ignition distance is very sensitive to the furnace temperature and, therefore, heat extraction.

When swirl is applied to the annular combustion air flow the jet expands faster, the rate of entrainment of external recirculation increases and eventually the flame is stabilized at the burner. Three types of burner stabilized flame can be distinguished, namely:

- Annular recirculation zone stabilized (Type I) - the fuel jet completely penetrates the swirl induced internal recirculation zone. The resulting flame is divided into two sections: a short bulbous zone close to the burner and a longer tail section. These two sections are connected by a short neck and under certain circumstances the connection may consist of only a few filaments of flame which may be severed leaving only the bulbous front section. Alternatively the two sections may merge and become almost indistinguishable.

- Axial recirculation zone stabilized (Type II) - the swirl induced internal recirculation zone divides the fuel jet as it leaves the injector. The rapid mixing in the near burner region produces a short high intensity flame. This flame type is produced most readily when: (1) low fuel velocities; (2) annular, radial or divergent fuel injectors, or (3) high swirl levels are used. At zero swirl this flame type can be produced by bluff body recirculation.
- Burner jet flames (Type III) - although the flame is stable on the fuel injector, no internal recirculation zone has been established. It is not necessary to use swirl to achieve this type of flame. Ignition close to or at the fuel injector can be achieved with axial flows if they have the appropriate momentum ratio.

Type I flames are rarely used in industrial applications. Type II are very common in practical situations. The flames used in wall fired boilers would be classified as type II flames. Jet flames are encountered in cement kilns and glass tanks. In addition, a tangential firing system for boilers can be considered as four impinging lifted non-swirling jet flames. Figure 3-1 shows sketches of these various flame types.

The four flame types described above can be produced with gaseous, liquid or solid fuels. Figure 3-2 illustrates the different characteristics of these flame types with natural gas as the fuel by comparing the axial temperature distribution and flame length indicating:

- that the application of low level of swirl to a jet flame ($S < 0.5$) increases the rate of temperature increase on the axis and decreases the flame length;
- that axial recirculation zone stabilized flames (Type II) are high intensity flames with high initial axial temperatures which correspond to the location of the axial recirculation zone.
- that type II flames are shorter than type I flames.

The application of swirl to pulverized coal flames intensifies mixing and improves ignition stability. Since the rate of decay of axial velocity

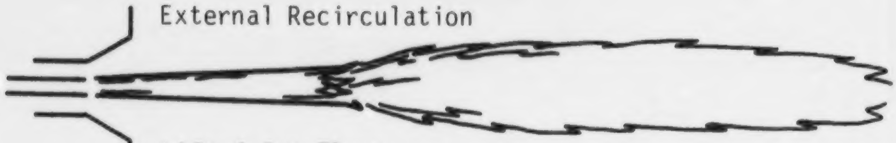
External Recirculation

Lifted Jet Flame

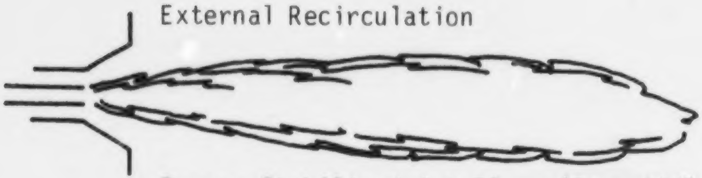
External Recirculation

Burner Stabilized Jet Flame (Type III)

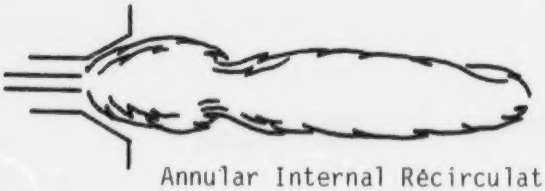

Annular Internal Recirculation Zone Stabilized (Type I)

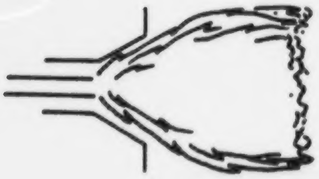

Axial Internal Recirculation Zone Stabilized (Type II)

Figure 3-1. Sketches of Four Typical Flame Types.

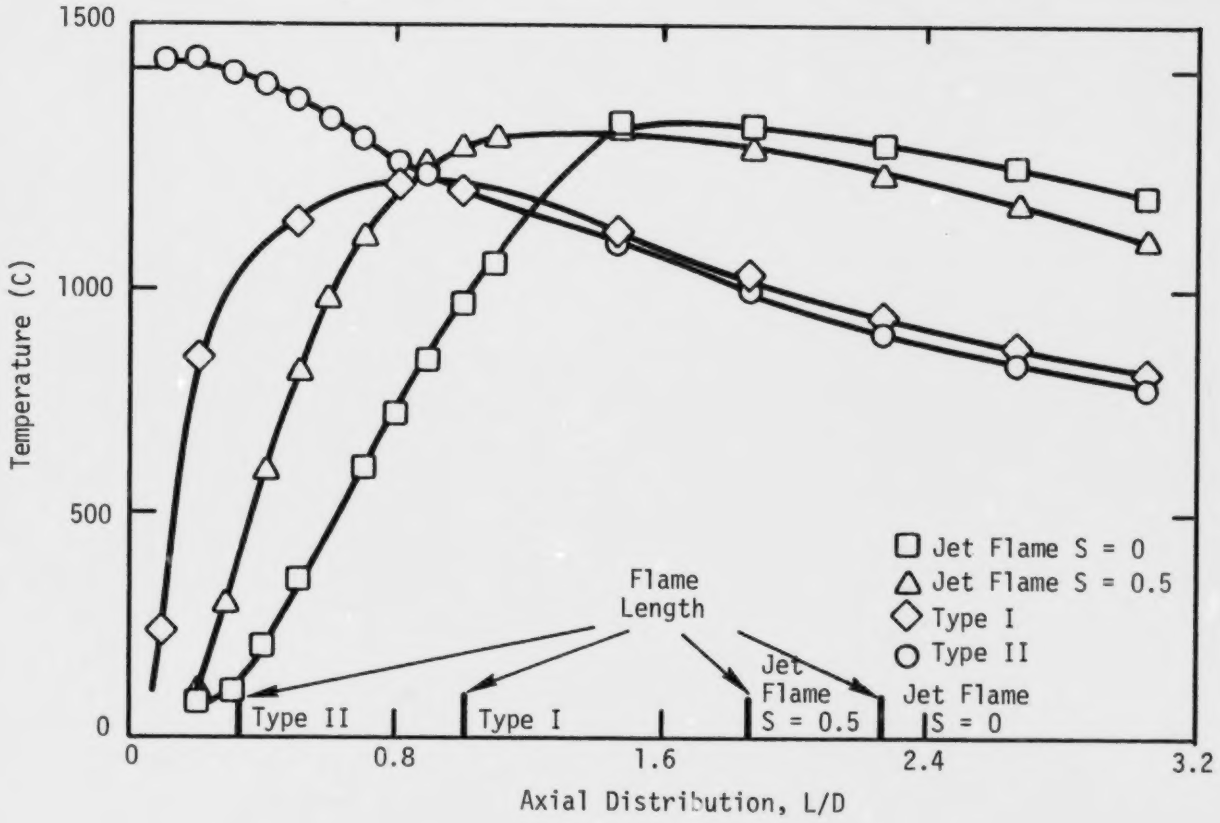

Figure 3-2. Axial Temperature Distribution Showing the Characteristics of Different Flame Types.(3.2)

is increased by the application of swirl and coal burnout is time dependent, burnout distances are reduced by the addition of swirl. The visible appearance of the flame is dependent upon the coal volatile content but it is possible to produce all the flame types shown in Figure 3-1 with pulverized coal. If low volatile coals are used, then the axial temperature distribution provides a measure of ignition stability since a visible ignition front may not be present. The optimum condition for ignition is considered to be a steep axial temperature gradient. Figure 3-3 indicates the influence of swirl on the axial and radial temperature distribution of anthracite flames as a function of swirl level. Ignition stability is favored by steep axial temperature gradients, and it can be seen that an optimum swirl exists for ignition stability and that this does not produce a type II flame (see Figure 3-3b) because the temperature is not a maximum on the axis. The optimum condition is close to the transition from type I to type II. However, the coal jet is not divided by the axial recirculation zone but just penetrates and then stagnates. After the critical conditions have been attained any further increase in swirl causes a deterioration in the combustion characteristics. Hein(3.4) has shown that the optimum swirl level for early stable ignition of anthracite flames increases with increases in primary jet momentum and secondary air velocity. The optimum swirl level is reduced if primary swirl is used, the burner exit is divergent rather than parallel, and the length of the divergent is increased.

Increasing the volatile content of the coal means that the ignition front will be visible and ignition stability can be judged by the location of the visible ignition front. The visible ignition front is caused by the combustion of the volatile coal fractions which are released from the coal particles when they are heated. Thus, the conditions for ignition are:

- rapid heating of the coal particles to ensure an adequate supply of combustible gas;
- mixing with the required amount of air to provide a flammable mixture;
- the presence of an ignition source.

To satisfy these conditions the coal particles must be mixed rapidly with high temperature recirculating products (i.e., internal recirculation).

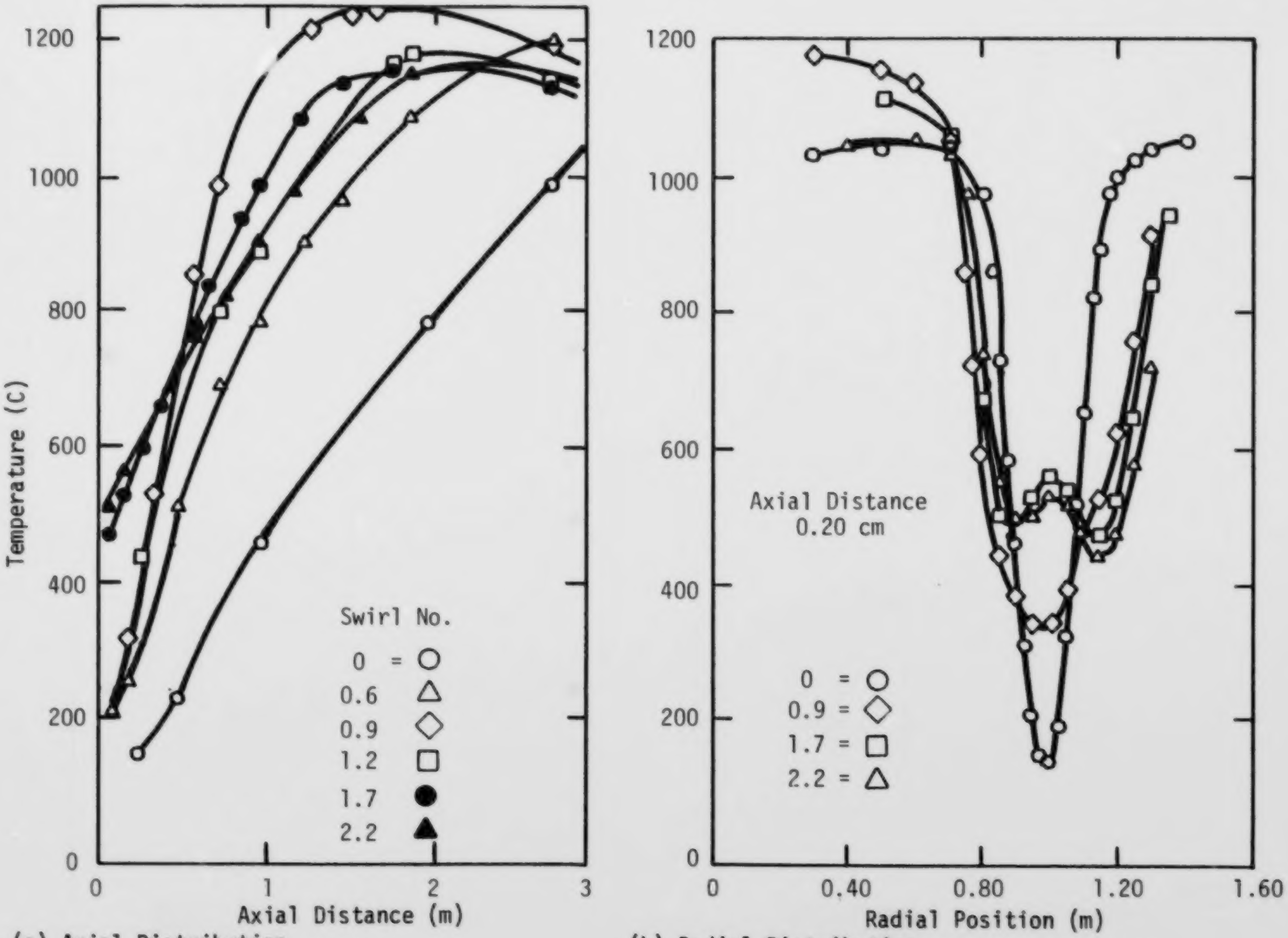

(a) Axial Distribution (b) Radial Distribution

Figure 3-3. The Influence of Swirl on the Characteristics of Anthracite Flames.(3.3)

Consequently the burner parameters which control the size and strength of the recirculation zone will influence ignition stability.

The characteristics of swirling flames are not dependent solely upon the level of swirl. Other burner parameters influence the level of swirl which is necessary to create a particular flame type. These burner parameters include:

- Fuel injector design. For pulverized coal three injector types are used most commonly: (1) axial single hole, (2) axial annular, and (3) some device to spread the coal (a deflector or radial injection system). The first type is used in corner fired boilers whereas the other options are used in circular burner designs.
- Burner geometry. The shape and size of the divergent exit influence flame characteristics.
- Register or swirl device design. Earlier in this section it was stated that total angular momentum does not define the characteristics of swirling jets; the distribution of angular momentum must be taken into account. The features of the mechanical system included in the burner design to provide rotation can influence the distribution of angular momentum.
- Air and fuel velocities. High air velocities are discouraged because of the cost penalties associated with high windbox pressures.

Based upon the discussions in the previous section it could be expected that those burner parameters which provided rapid fuel air mixing would promote nitric oxide formation from fuels containing bound nitrogen. However, since burner parameters control fuel air mixing it is possible that nitric oxide formation can be controlled by the optimization of burner parameters.

3.2 Phase I and Phase II Efforts

The overall program objective is the specification of burner design criteria for the minimization of pollutant formation in both pulverized coal and residual fuel oil fired combustors. In Phase I influence of several burner design parameters on the emission of nitrogen oxides from natural gas and pulverized coal flames was defined. The burner parameters investigated include:

- the method of fuel injection;
- the position of the fuel injector relative to the burner exit;
- the geometry of the burner exit;
- the burner throat cross-sectional area;
- the degree of swirl applied to the secondary air; and
- the fraction of the total air supplied with the coal at fixed excess air levels.

Three parameters were found to influence NO_x formation significantly: (1) the method of fuel injection, (2) the degree of swirl, and (3) the amount of primary air supplied with the coal.

The emission characteristics of two high volatile coals were investigated and it was found that NO_x levels varied by over 400 percent for fixed preheat and excess air levels. With the higher nitrogen coal, maximum emissions were found to be higher than those measured with the lower nitrogen coal, although the increase was not directly proportional to the increased nitrogen content. However, minimum emissions from both coals were similar. It was readily apparent from these studies that burner conditions giving rise to rapid coal/air mixing also produced high NO_x emissions. Conversely, those burner conditions which delayed coal/air mixing tended to give the lowest emissions. Unfortunately, the delayed mixing also produced long flames which could not be considered suitable for utility boiler applications since flame impingement upon the opposing wall would probably occur.

In order to explain the observations, two basic assumptions were postulated:

- Fuel NO accounted for the major portion of the total emission.
- Volatile fuel nitrogen fractions were mainly responsible for fuel NO formation.

Support for the former assumption was later provided by Pershing et al(3.5) who burned pulverized coal with both air and argon/oxygen mixtures.

Pershing reports that for a single coal flame 80 percent of the total NO_x emission can be attributed to fuel nitrogen oxidation. The latter assumption was based on the fact that significant quantities of nitric oxide were produced very early in the combustion process, and the conditions under which a large proportion of the char burns out are mainly dependent upon input conditions and not upon burner variables. Consequently, it appears that the design of low NO_x emitting combustion systems for pulverized coal and heavy fuel oil must delay the mixing of all the combustion air with the fuel for as long as possible consistent with the attainment of complete combustion.

These general conclusions drawn from the Phase I efforts are illustrated by the results presented in Figures 3-4 and 3-5. Figure 3-4 shows the emission characteristics of pulverized coal flames produced with a radial fuel injector. The coal and primary air are injected at right angles to the secondary air stream from the burner throat, thus providing rapid coal/air mixing. The emission characteristics for two fuels of different nitrogen contents are almost insensitive to the amount of primary air, and the level of secondary air swirl. These are the burner conditions which give short, stable, intense flames, unfortunately, they also correspond to the conditions which maximize NO production. Alternatively, the results presented in Figure 3-5 illustrate those burner conditions which restrict NO formation. The coal is maintained as a coherent jet on the flame axis and is injected with the minimum primary air and at the maximum velocity. The ignition front which surrounds the coal jet provides the "diffusion flame" type environment for reaction of the fuel nitrogen intermediates.

The major accomplishment of this first series of furnace investigations was the demonstration that under subscale conditions NO_x emissions from pulverized coal flames could be varied by a factor of four. This variation was achieved mainly by the selection of three burner design parameters:

- The method of fuel injection. Any tendency to rapidly mix the coal with all the combustion air resulted in higher emissions. The lowest emissions were achieved with a high velocity axial fuel injector which maintained a coherent fuel jet of high coal density.
- Optimum level of swirl to provide a stable ignition source at the

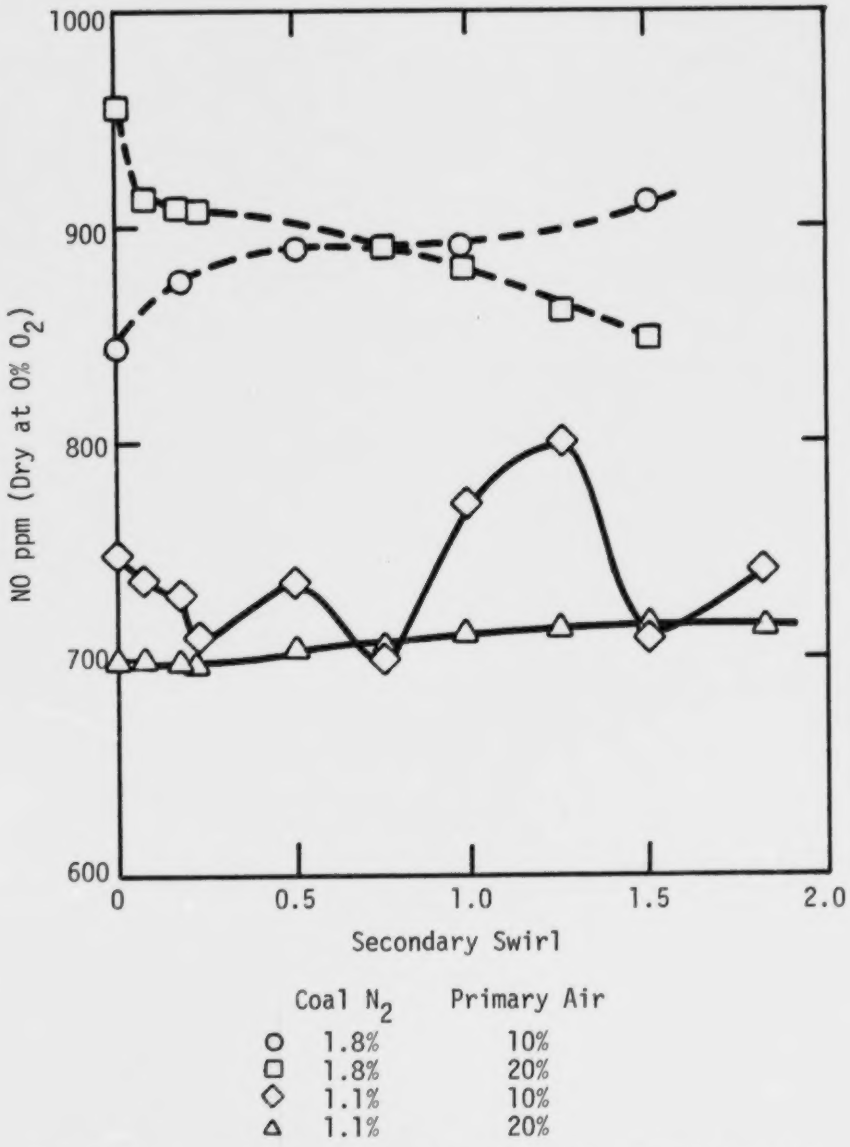

Figure 3-4. Emission Characteristics of Pulverized Coal Flames Produced with Radial Fuel Injection (5% Excess Air, 300 C Preheat).

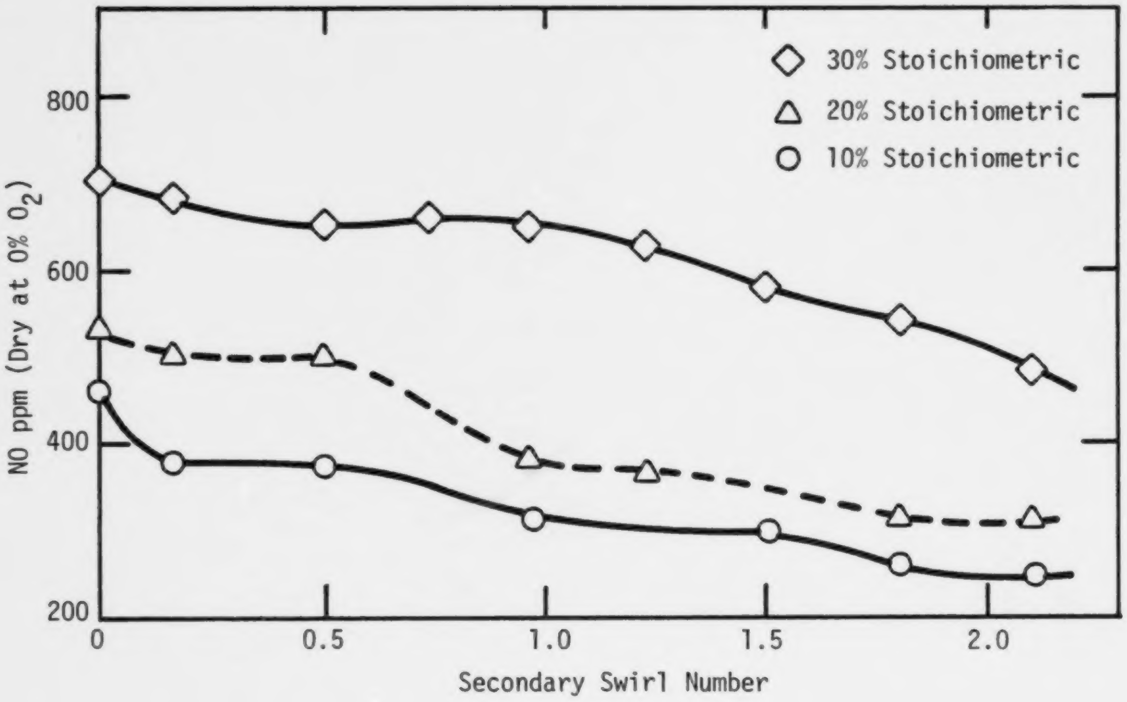

Figure 3-5. Emission Characteristics of Pulverized Coal Flames Produced with Axial Fuel Injection (300 C Preheat, 5 Percent Excess Air, and 1.1 Percent Nitrogen Coal).

fuel injector without mixing the fuel too rapidly with the secondary air.

- The degree of primary air. Primary air refers to that air which is mixed with the pulverized coal prior to delivery into the furnace. NO_x emissions were lowest when the minimum amount of primary air was used consistent with maintaining slow mixing of the fuel jet with the secondary air.

Although burner conditions had been identified which gave low NO_x emissions, it was readily recognized that such a burner design would be unsuitable for use in existing wall-fired utility boilers.

The second series of furnace trials were planned to achieve three major goals:

- to provide further information on the formation of NO_x in pulverized coal flames to aid in interpretation of the results;
- to extend the investigation to include residual fuel oil firing in order to define those parameters which give minimum emissions; and
- to investigate methods of satisfying process requirements and produce minimum emissions. This involves the definition of the combustion requirements of practical systems as well as an attempt to reduce emissions via burner design.

During the furnace trials emphasis was placed upon four separate areas:

- Emission Characteristics of a Subscale Practical Burner

Results were obtained in this study which were similar to those reported by Armento et al.(3.6) NO_x emissions increased with increasing excess air although the precise influence of preheat, excess air and firing rate were not duplicated. Very high NO levels (in excess of 1700 ppm) were recorded at high firing rates and 450 C preheat with an almost uncooled furnace. These high emissions are probably due to an increasing contribution of thermal NO and to more complete loss of nitrogen from the coal char because of the higher temperatures. The emissions from the subscale burner could be modified by changing the method of fuel injection and the amount of air supplied with the coal in the primary stream. Reducing the tendency of the coal jet to spread and mix rapidly with the combustion air reduces emissions by more than 28 percent for a given set of input conditions.

- Tertiary Air Injection to Reduce NO_x Formation

The total combustion air supply to be burned was divided into three streams to delay the mixing of the fuel with all the air by injecting one of these streams (tertiary air) from the periphery of the burner. In the most successful application of the technique, 40 percent reductions in emissions from the subscale practical burner were achieved with 20 percent of the stoichiometric air requirement supplied in the tertiary stream. Incorrect designs caused 300 percent increases in emission from natural gas-fired tertiary air systems.

- Emission Characteristics of Dual Fuel Systems

NO_x emissions resulting from the simultaneous firing of gaseous and solid fuels are not additive. The emission characteristics of dual fuel firing are dependent upon burner parameters such as fuel injector type and whether the gas is injected separately or mixed with the coal.

- Emission Characteristics of Fuel Oil Flames

The emission characteristics of fuel oil containing significant quantities of bound nitrogen appear to follow similar trends to those observed with coal. Lower NO emissions were generally obtained if the fuel spray was narrow. The lowest emissions of approximately 100 ppm were obtained with axial fuel oil injection produced with an air blast atomizer. Further work is required under cold wall conditions to ensure that low NO conditions do not produce excessive amounts of particulate matter. The influence of thermal effects (air preheat and furnace heat extraction rate) should be investigated more fully. Preliminary data was obtained indicating that the influence of air preheat was dependent upon fuel atomizer design.

3.3 Purpose of the Phase III Investigations

The third series of furnace investigations was planned to provide further insight into the formation of nitric oxide in turbulent diffusion flames. In addition further information was required to establish the design parameters for low NO_x burners. The experimental investigations can be grouped into three, namely:

- Further investigations with the distributed mixing involving pulverized coal, petroleum coke and oil water emulsions.
- Pollutant formation in multiple burner arrays.
- Flame detectors for low NO_x burners.

REFERENCES

3.1 Beer, J. M., and Chegier, N. A. Combustion Aerodynamics. Applied Science Publishers, Ltd., 1972.

3.2 Michelfelder, S., and Lowes, T. M. International Flame Research Foundation Report F36/a/4, 1974.

3.3 van Heyden, L., Heap, M. P., and Frieker, N. Daistillung Eeneger Ergebnisse von Kohlenstaub - Drallflammen im Hinblick auf Fregen der Modellerung Gas Worme Inlonaharal, p. 445, 12, December 1971.

3.4 Hein, K. Papers presented at the International Flame Research Foundation First Mentuo Conference, May 1969.

3.5 Pershing, D. W., Martin, G. B., and Berkau, E. E. "Influence of Design Variables on the Production of Thermal and Fuel NO From Residual Oil and Coal Combustion." AICHe Symposium Series, No. 148, 71, 1975.

3.6 Armento, W. J., et al. "Effects of Design and Operating Variables on NO_x from Coal-Fired Furnaces - Phase I." EPA-650/2-74-002a.

4.0 EXPERIMENTAL RESULTS

4.1 Evaluation of the Distributed Mixing Burner Concept

Earlier furnace investigations(4.1, 4.2) had demonstrated that the formation of NO_x in pulverized coal flames was strongly dependent upon those burner parameters which dictated the rate of fuel air mixing. It was argued that volatile nitrogen compounds accounted for the major portion of the NO_x formed in pulverized coal flames. Consequently, the design philosophy was directed towards ensuring that the volatile compounds were driven rapidly from the parent coal and reacted under oxygen deficient conditions. One method of satisfying these conditions had been identified in the first series of furnace tests.(4.1) Maintaining the fuel as a coherent jet, limiting the amount of primary air injected with the coal, and restricting the rate of secondary air penetration of the fuel jet by providing a stable ignition zone around the jet gave complete combustion of the fuel with minimum NO_x levels. NO levels approaching 200 ppm[*] were obtained even though "normal" emission levels were greater than 600 ppm for equivalent furnace input considerations. Unfortunately, the flame configuration which produced this minimum emission was unsuitable for the existing design of wall fired utility boilers. It is believed that the conditions which exist in this long low-NO flame are closely associated with conditions existing in a corner fired utility boiler, and it is reasonable to consider that the long axial flame described in an earlier report is in fact representative of one corner of a tangential unit.

Having identified those parameters which controlled NO formation, the major thrust of the work was directed towards satisfying those conditions while providing combustion conditions suitable for wall fired boilers. Initial attempts to produce such a combustion system met with mixed success.(4.2) The design objectives were:

1. To provide a well mixed rich primary zone with a sufficient residence time to minimize the quantity of XN compounds (NO, HCN or NH_i).
2. To supply air for burnout at the optimum time to maximize burnout and minimize pollutant formation.

---

[*] Unless stated otherwise, all NO concentrations are corrected to 0% oxygen.

The total combustion air supply was divided into three streams in an attempt to satisfy these design objectives. The rich primary zone was supplied with secondary air which could be swirled and the primary air injected with the pulverized coal. The third air stream was injected from the periphery of the burner exit on the firing wall to mix with the products of the primary zone some distance downstream. Optimization of the velocity of the third air stream was necessary to meet the design objectives. With low injection velocities for the tertiary air flow, NO emissions actually increased for coal, residual oil, and natural gas firing.

The following section describes a series of investigations carried out in the third series of furnace trials to further optimize a burner design to control NO formation in pulverized coal flames by controlling the fuel air mixing process. The parameters to be investigated included:

- air injector design;
- fuel injector design;
- air preheat; and
- furnace temperature

in an attempt not only to define design conditions, but also to establish the degree of NO_x control to be expected from this type of technique.

4.1.1 Delayed Mixing Burner Design

The investigations were carried out in a horizontal refractory tunnel furnace at the International Flame Research Foundation, IJmuiden, Holland. The sketch presented in Figure 4-1 shows a section through the almost 2m x 2m square furnace which is 6.25m long with probing access along one wall. Removable cooling tubes allowed the furnace cooling load to be varied. The versatile test burner shown in Figure 4-2 fired horizontally along the length of the furnace. The burner utilized the moving block swirl generator designed by Leuckel(4.3) and readily allowed the influence of several parameters on NO_x formation to be established. The burner parameters investigated included:

- the method of fuel injection;

Note: All Dimensions are in Millemeters (mm)

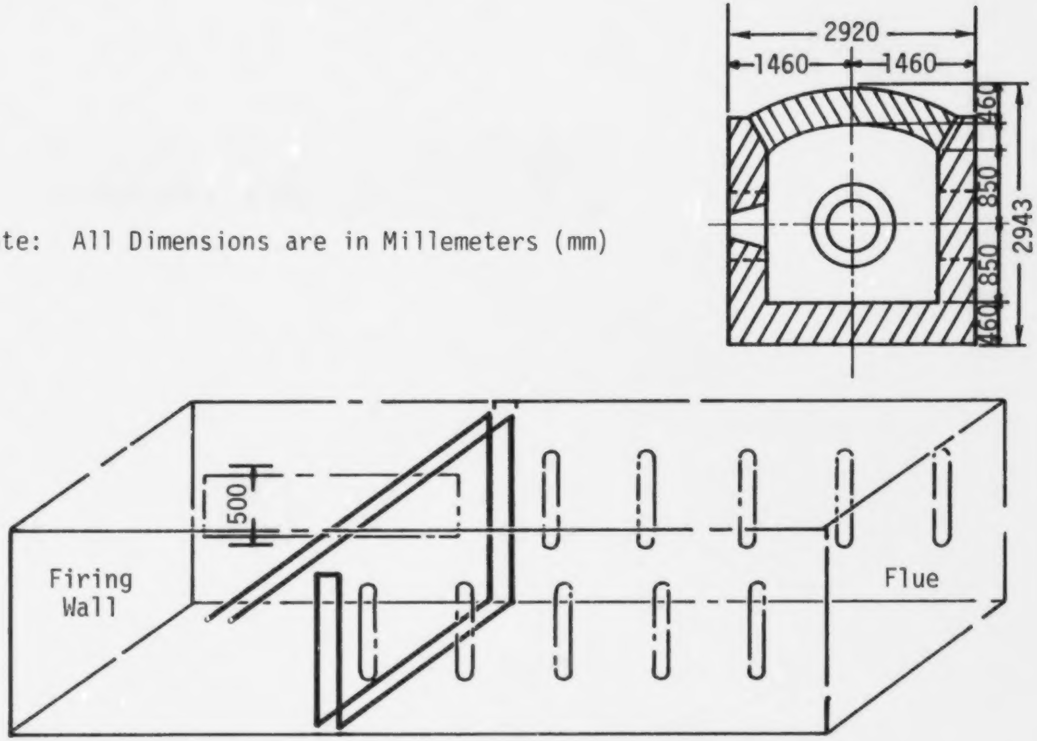
2920
1460
1460
460
850
850
460
2943
500
Firing Wall
Flue

Figure 4-1. Sketch Showing the Refractory Tunnel Furnace and the Cooling Loop Arrangements.

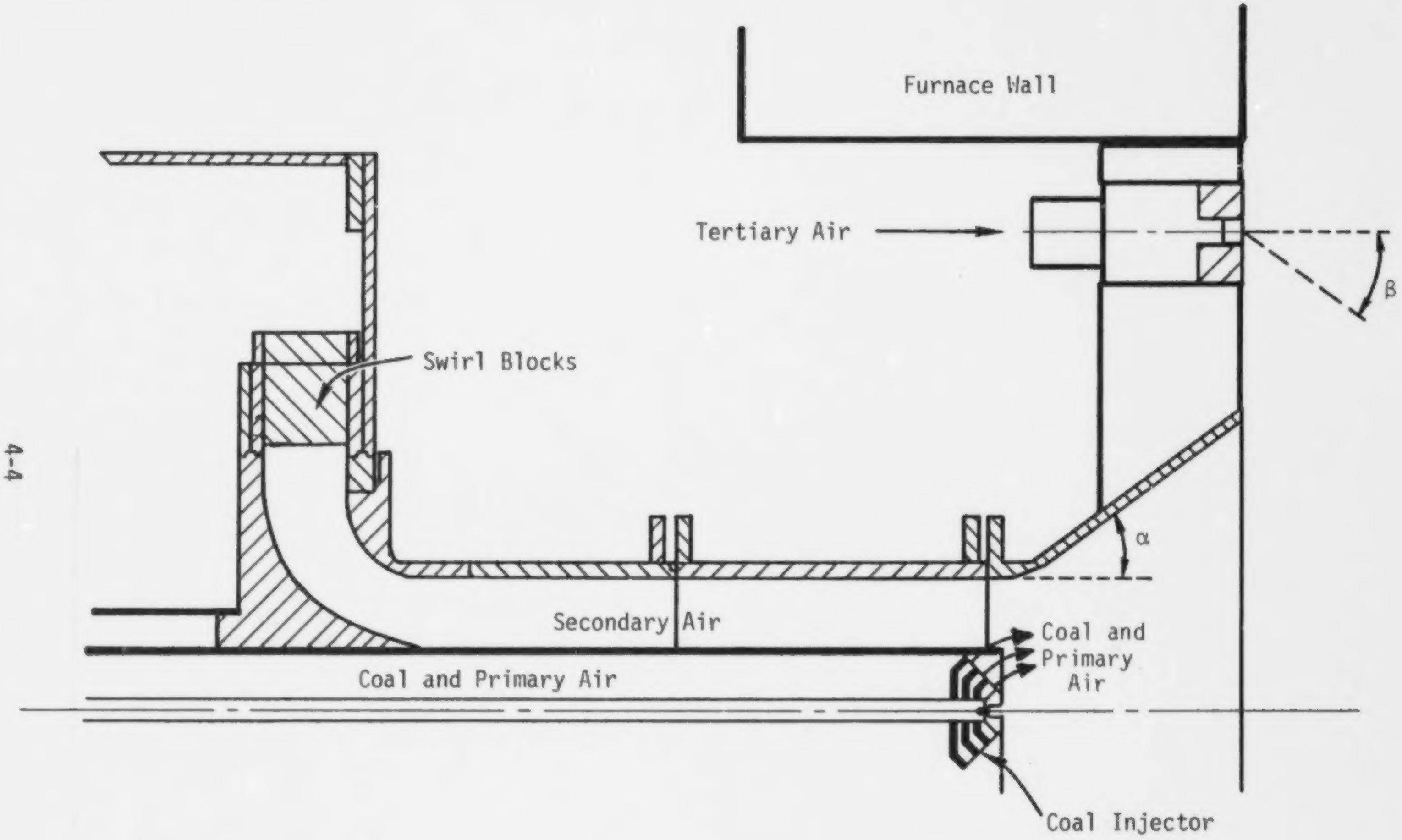
Furnace Wall
Tertiary Air
β
Swirl Blocks
α
Secondary Air
Coal and Primary Air
Coal and Primary Air
Coal Injector

Figure 4-2. Versatile Test Burner Showing the Position of Tertiary Air Injection and a Scaled Down Version of a Practical Type Coal Injector.

- the division of the total air supply between primary, secondary, and tertiary air streams;
- the tangential momentum imparted to the secondary air;
- the angle of the burner divergent;
- the number of injection points for the tertiary air;
- the position of the fuel injector relative to the burner exit.

Figure 4-3a presents details of the construction of the moving block swirl generator. The swirl register consists of two annular plates and two series of interlocking wedge shaped blocks each attached to one of the plates. Interlocked, the blocks form alternating radial and tangential air flow channels, such that the air flow splits into an equal number of radial and tangential streams which combine downstream from the actual swirl generator into one swirling flow. Rotating the back plate progressively closes the radial channels and opens the tangential ones (or vice versa). Thus the resulting flux of angular momentum increases (or decreases) continuously between zero and a maximum value dependent upon the dimensions of the system. Figure 4-3b shows the relationship between the relative position of the blocks, R_s, and the swirl number, S. It should be noted that swirl number is only a useful parameter when it refers to swirl devices of similar design.

4.1.2 Investigations Involving Pulverized Coal

Table 4-1 lists the flame conditions investigated in this series of tests. The overall excess oxygen level was maintained constant at 3 percent and the fuel[*] input at 184 kg/hr. The burner parameters which were varied were:

- Secondary air flow.
- α, the angle of the burner divergent.
- β, the angle of inclination of the tertiary (0 equals parallel to the fuel injector).
- The method of fuel injection. Three different fuel injectors were used: the coal spreader (CS), the radial fuel injector,

---

[*] The fuel composition is discussed in Section 4.1.3.

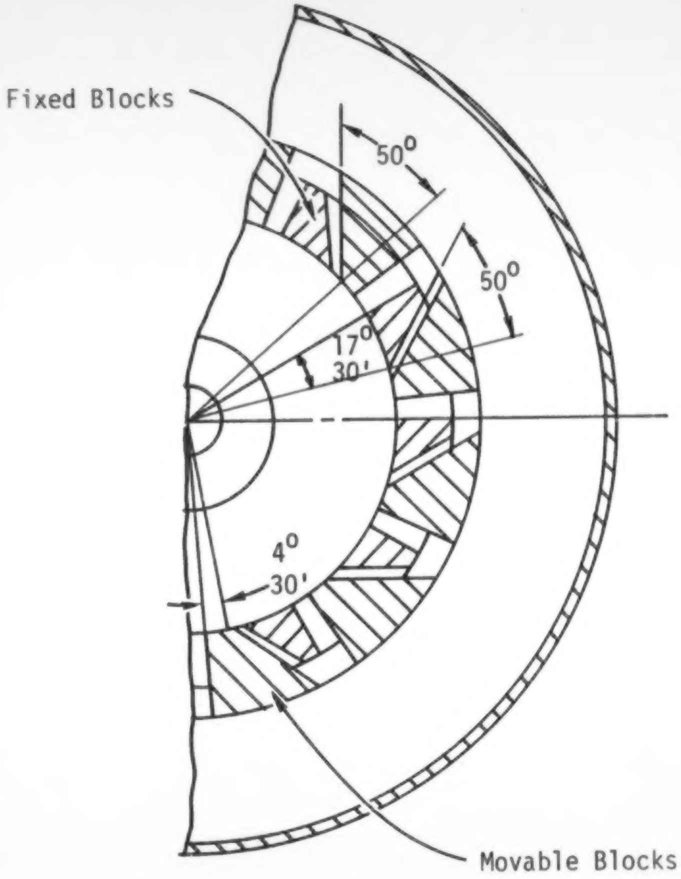
Fixed Blocks
50°
50°
17°
30'
4°
30'
Movable Blocks

Figure 4-3a. Double Concentric Burner System.

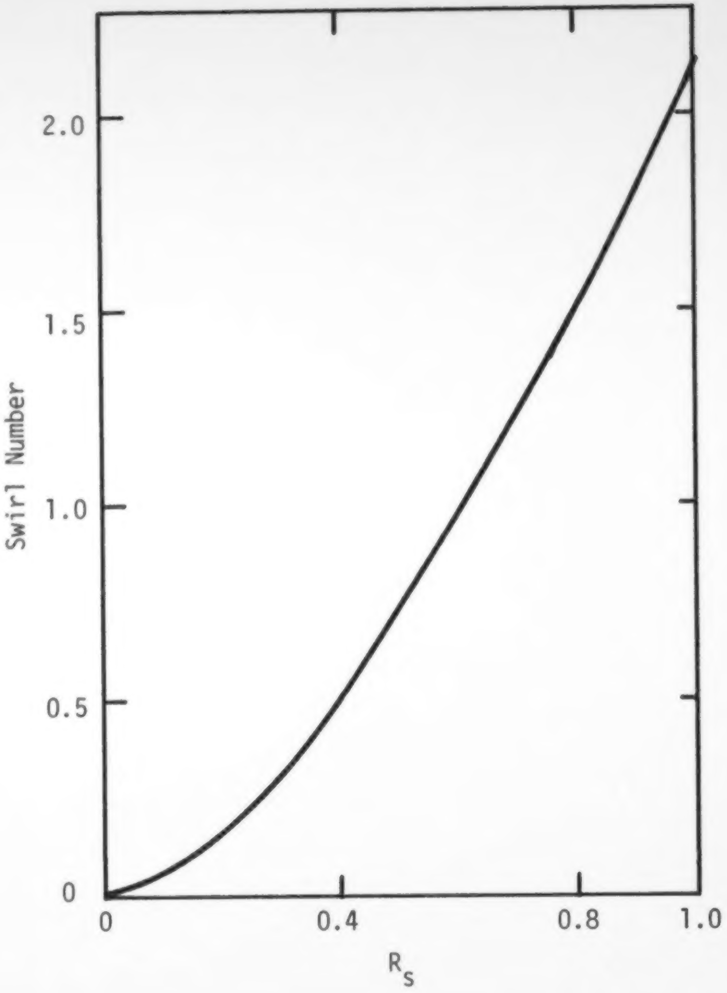

Figure 4-3b. The Relationship Between Relative Swirl Index, R_S, and Swirl Number, S.

Table 4-1. Flame Conditions

Run No.	α	β	Fuel Injector	Preheat	Tw	A_T	P_A%
84	25	0	CS	300 C	C	4	9
86	25	0	CS	300 C	C	4	28
87	25	0	CS	300 C	C	4	18
88	25	0	CS	300 C	C	4	18
89	25	0	CS	300 C	C	4	9
92	25	0	Radial	300 C	C	4	9
97	25	45	Radial	300 C	C	4	18
103	35	0	CS	450 C	C	4	9
104	35	0	CS	450 C	C	4	18
106	35	0	Axial	450 C	C	8	9
107	35	0	CS	300 C	C	8	9
108	35	0	CS	300 C	C	8	9
119	35	0	Axial	300 C	C	8	9
124	35	0	CS	300 C	h	8	18
125	35	0	CS	300 C	h	8	9
127	35	0	Radial	300 C	h	8	9
128	35	45	CS	300 C	h	8	9

c - high heat extraction

h - low heat extraction

and an axial injector.

- Air preheat. Two levels of preheat were investigated: 300 and 450 C.
- Heat extraction. Two levels of heat extraction were investigated by removing cooling tubes.
- The number of tertiary ports, A_T. Increasing the number decreases the velocity.
- The amount of air supplied with the coal expressed as a percentage of the stoichiometric air requirement (P_A).

Figures 4-4 and 4-5 show the impact of operating the burner throat fuel rich. The open symbols represent conditions without tertiary air injection and the closed symbols indicate that the maximum air flow possible was being supplied through the tertiary air injections which corresponds to a burner stoichiometry of approximately 55 percent of the theoretical air. It can be seen that there is a dramatic reduction in NO when the tertiary ports are opened. Under staged conditions, swirl level has a relatively minor impact on emissions compared to other factors, which is also shown by the data in Figures 4-6 through 4-8.

The burner parameters which influence emissions under staged conditions are:

- Burner exit. The lowest emissions were observed with a 35^o exit divergent.
- The influence of amount of air supplied with the burner appears to be dependent upon other parameters.

Experiments were carried out at a reduced cooling rate to investigate the effect of furnace temperature on NO emissions under staged conditions. These data are compared in Figure 4-9 for the coal spreader at high and low swirl levels. Unstaged and staged emissions increase. The high cooling rate represents a mean wall temperature of 950 C and with the lower cooling rate the temperature increases to 1250 C.

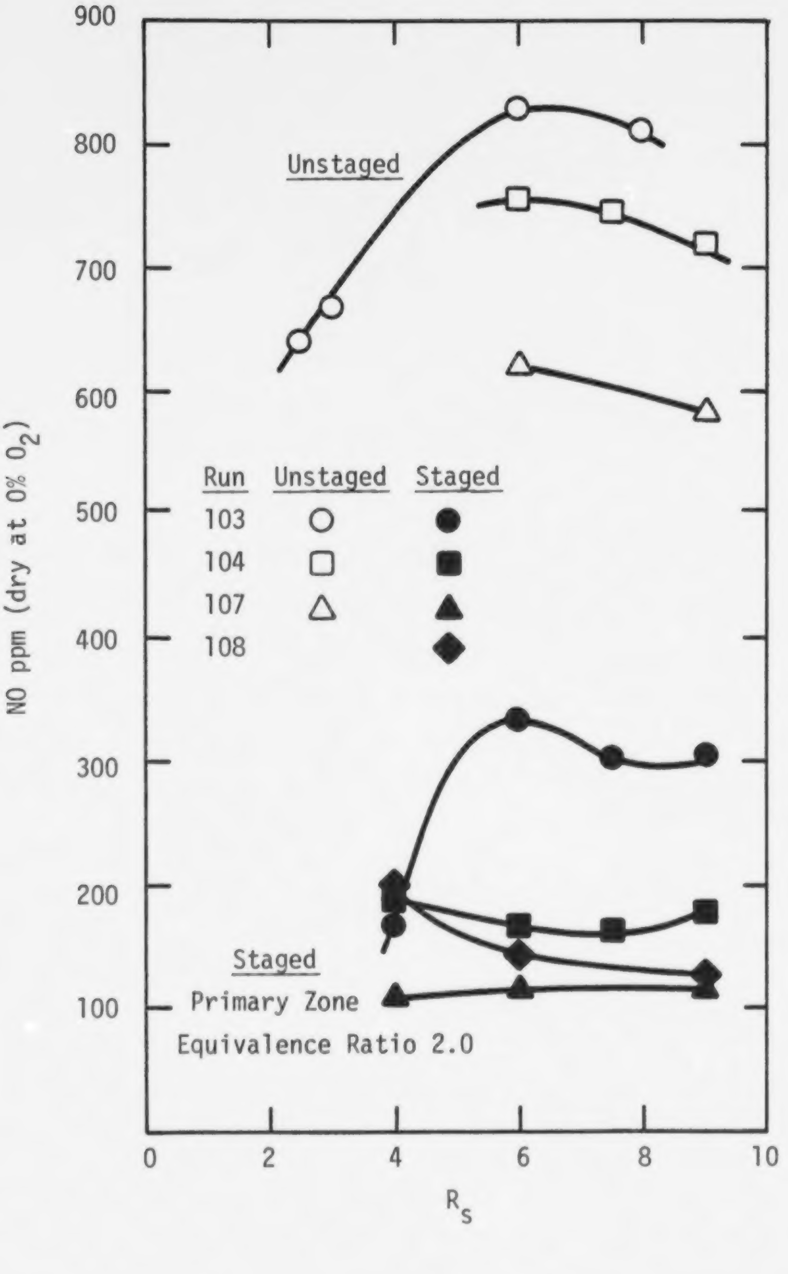

Figure 4-4. The Effect of Tertiary Air Injection on NO_x Emissions.

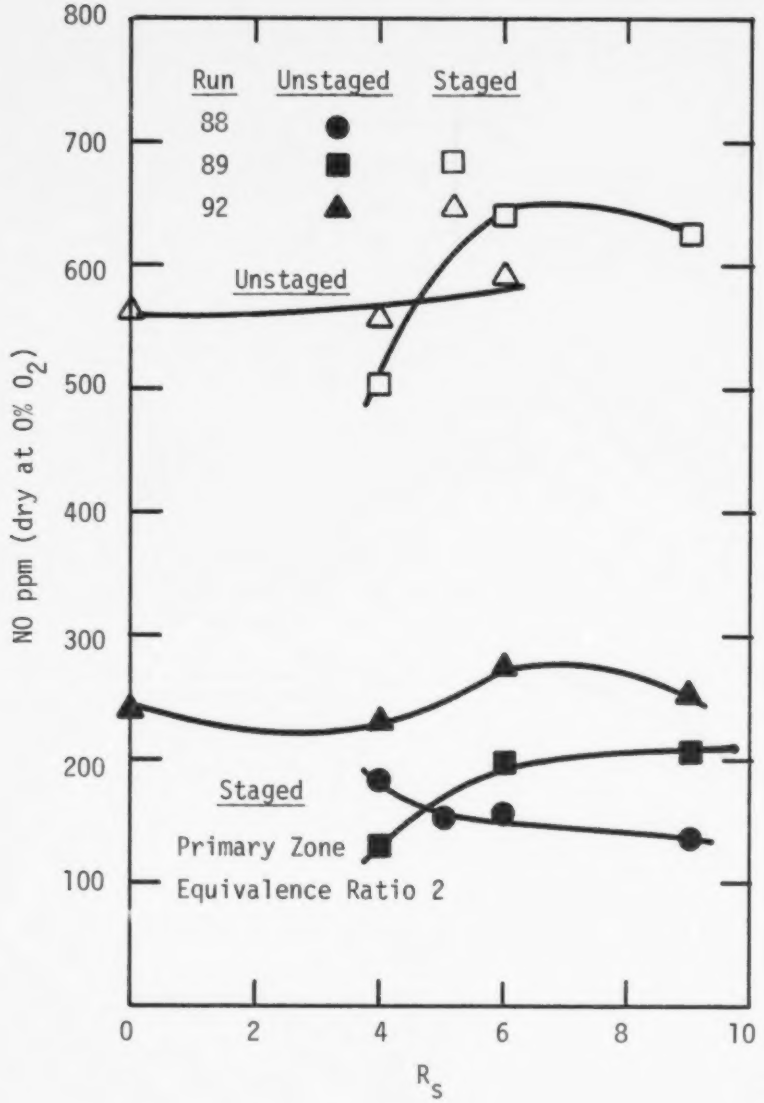

Figure 4-5. The Effect of Tertiary Air Injection on NO_x Emissions.

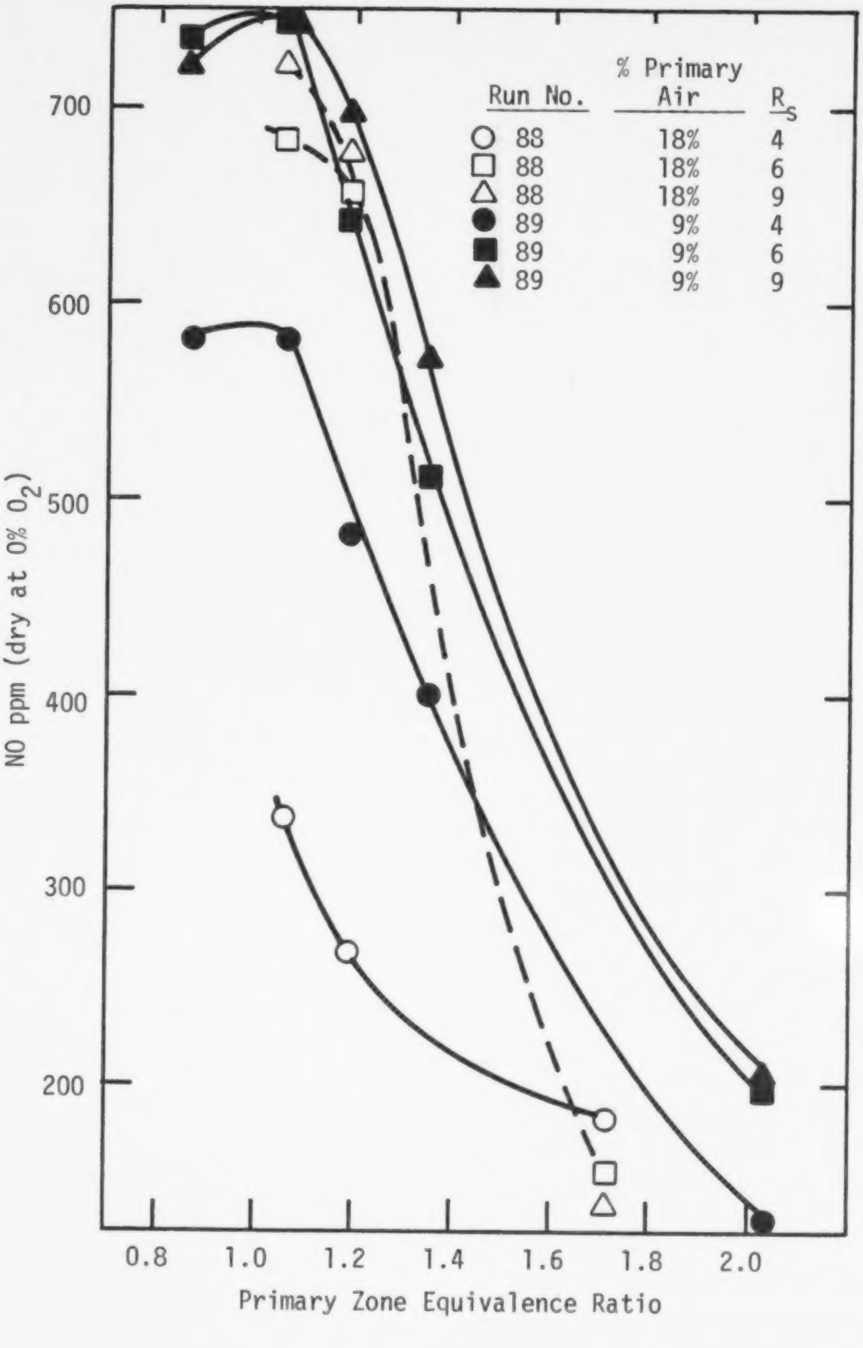

Figure 4-6. The Influence of Primary Air Percentage on NO Emissions.

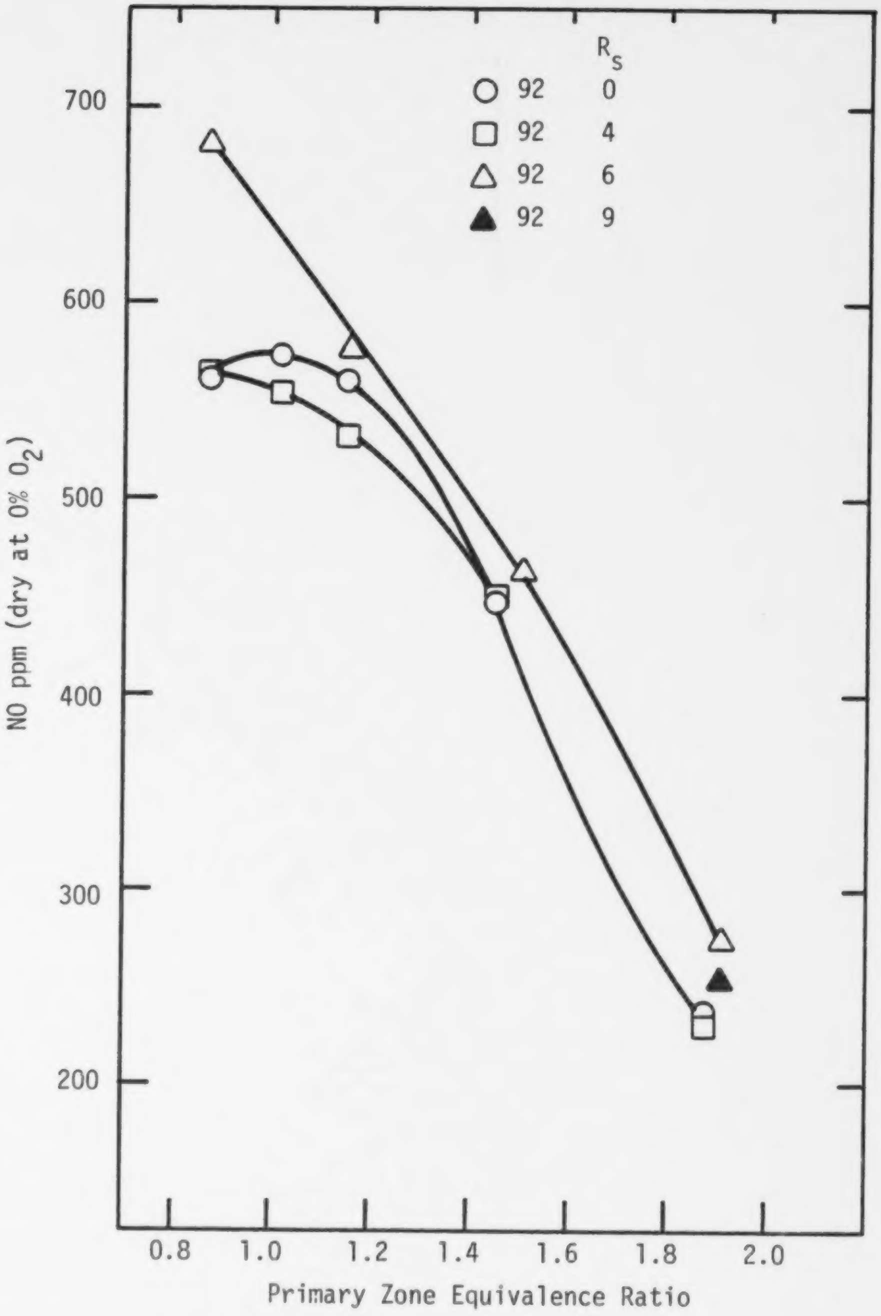

Figure 4-7. The Influence of Secondary Swirl Level.

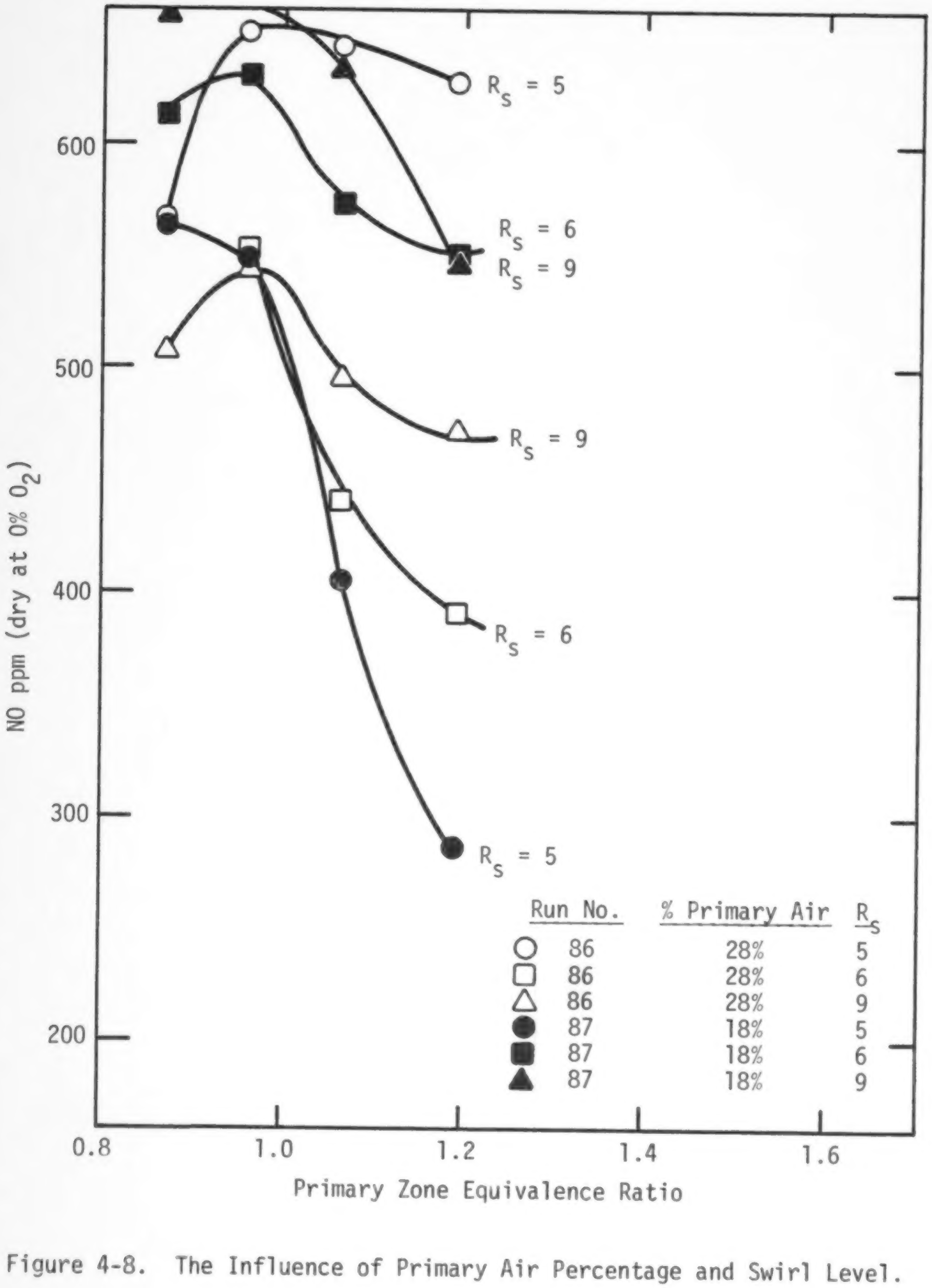

Figure 4-8. The Influence of Primary Air Percentage and Swirl Level.

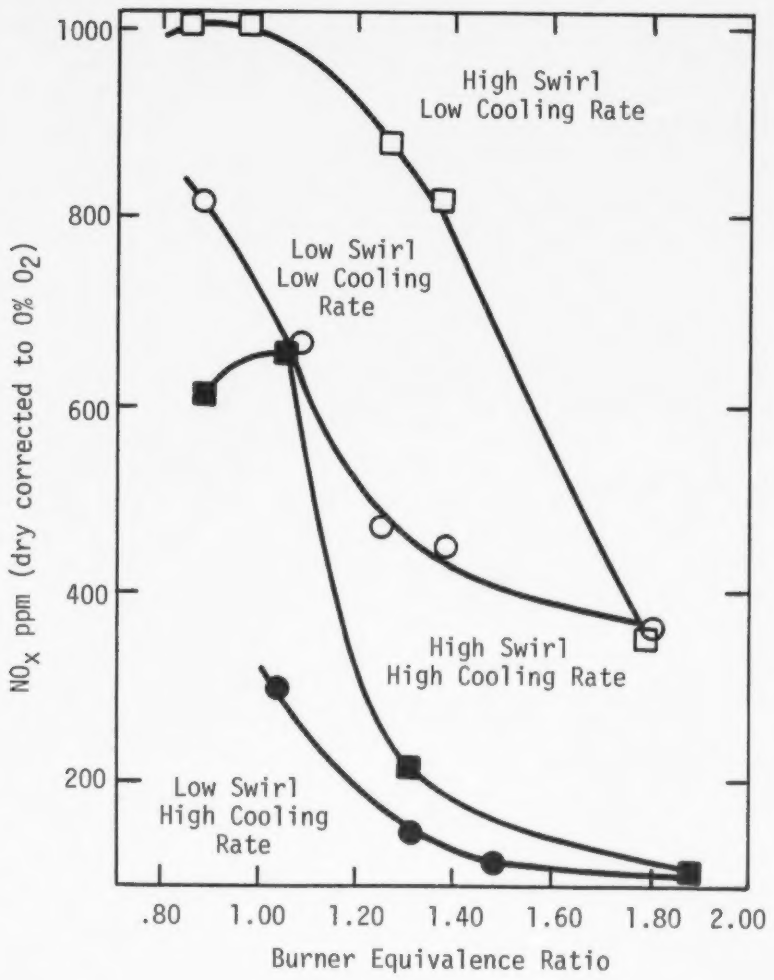

Figure 4-9. Effects of Swirl, Cooling Rate and Burner Zone Stoichiometry on NO$_x$ Emissions.

4.1.3 Investigations Involving Pulverized Coke

The discussions in Section 2 referred to the split of coal nitrogen between the volatile and char fractions. Under uncontrolled conditions with high turbulent burners, it is most probable that NO_x emissions are mainly the result of volatile coal nitrogen oxidation. This hypothesis is based upon observations of the impact of burner parameters on NO formation. NO formation is extremely sensitive to fuel air mixing conditions in the early stages of the flame. Experiments were carried out in the third series of trials conducted for the EPA at the IFRF with petroleum coke to provide greater understanding of the influence of volatile and char nitrogen. Petroleum coke is a high nitrogen low volatile solid produced by thermally cracking residual petroleum fractions. Therefore, it can be assumed that very little of the nitrogen will be volatile.

These investigations were carried out using the burner system described in the previous section. Three fuel injectors were used, namely:

- A single hole axial injector.
- A multi-hole radial injector.
- A coal spreader of commercial design.

The furnace was operated with the minimum cooling load and fired at approximately 1.76 MW.

Table 4-2 compares the properties of the coal and the petroleum coke which had volatile contents of 35 and 12 percent, respectively. It can be seen that the nitrogen content of the coal is somewhat higher than that of the coke but that the sulfur content of the coke is very much higher than that of the coal.

NO Formation from Pulverized Petroleum Coke

No practical problems were experienced burning the pulverized petroleum coke. Ignition occurred readily and a stable flame could be maintained without problem. Burnout was essentially 100 percent under all conditions. It can be seen from the data presented in Figure 4-10 that NO emissions from petroleum coke were relatively insensitive to the method of fuel injection but generally increased with increasing swirl level. Figure 4-11 shows the

Table 4-2. Ultimate Analysis (Dry)

	Coal	Petroleum Coke
Ash	6.35	0.63
Carbon	80.50	91.84
Hydrogen	4.68	3.36
Nitrogen	1.66	1.13
Sulfur	0.86	3.04
Oxygen (by diff)	6.05	-
Heating Value kcal/kgm	7,800	8,600

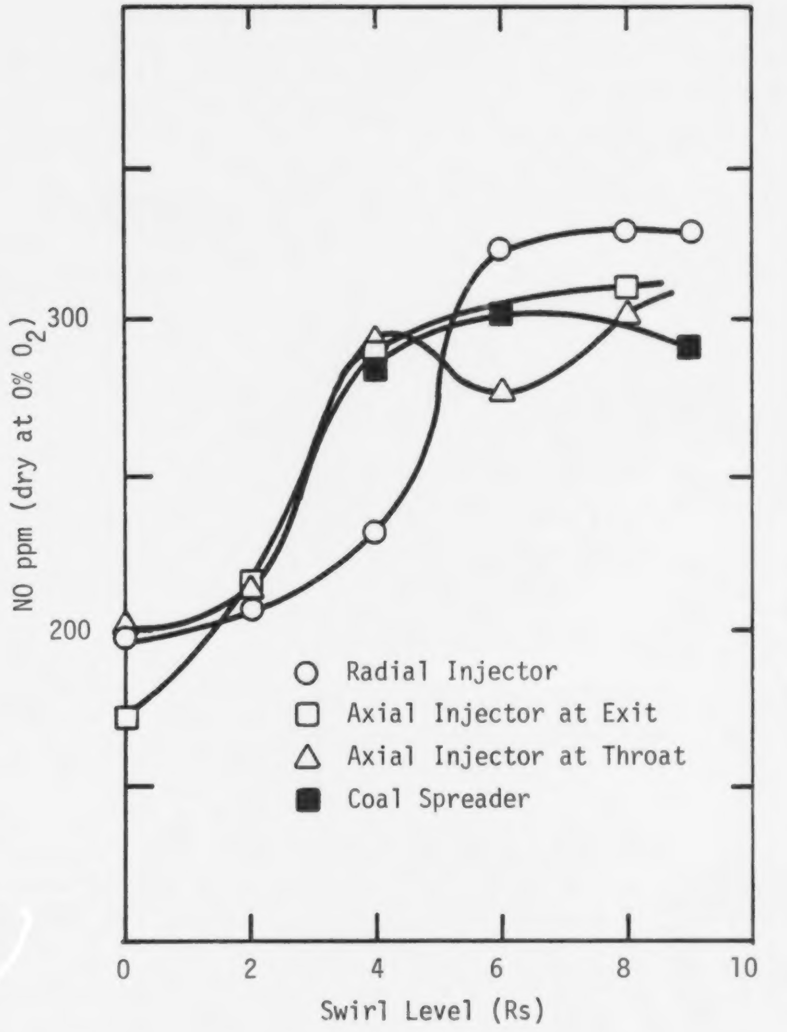

Figure 4-10. The Influence of Fuel Injector Type on NO Formation from Petroleum Coke (2.5% Excess Oxygen, 340 C Preheat).

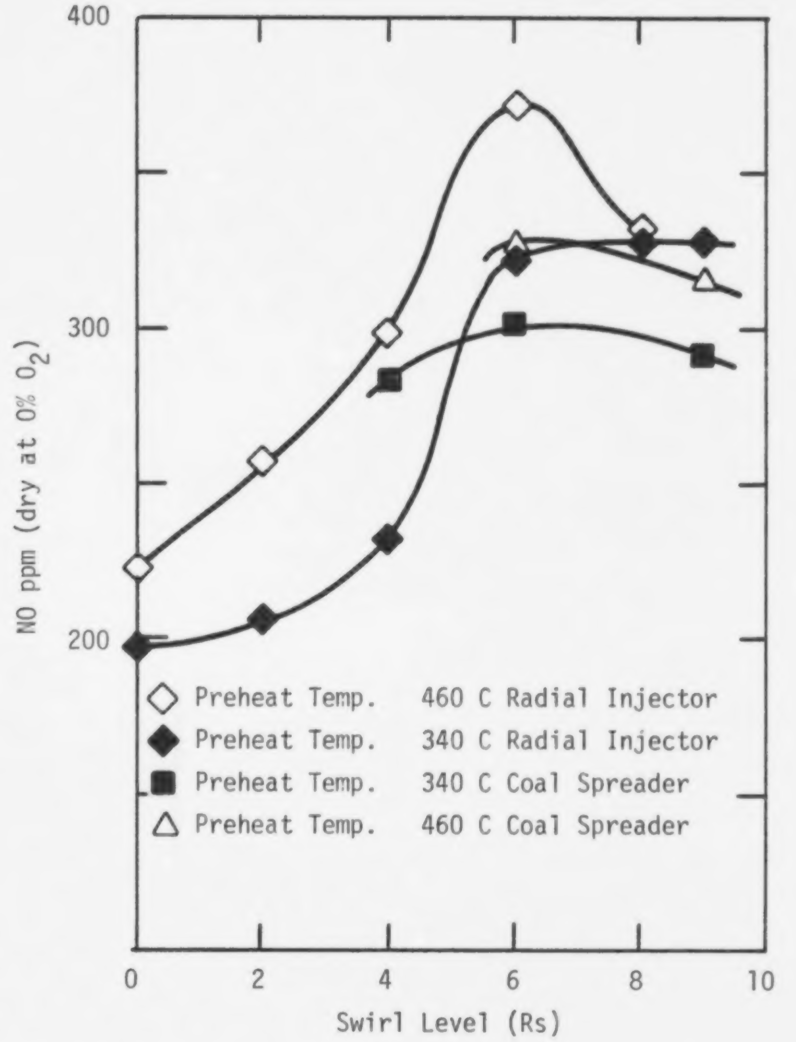

Figure 4-11. The Influence of Preheat on NO Emission from Petroleum Coke Flames.

influence of air preheat on NO_x emissions.

It has already been noted that petroleum coke emissions are less sensitive to burner parameters than those from coal flames. Figures 4-12 and 4-13 compare directly emissions from the two fuels with the coal spreader and the axial fuel injector. With the coal spreader, emissions from coal were approximately twice those produced with petroleum coke. At one swirl level, axial fuel injector emissions were lower with coal than with petroleum coke.

Figure 4-14 shows the relative increase of NO as a function of fuel flowrate for the two fuels. Emissions increase almost linearly with increasing firing rate for coke, but there is some evidence that emissions from coal increase steeply at high firing rates. This is consistent with the high emissions measured in the previous trial with an uncooled furnace and high firing rate.

Figure 4-15 compares the influence of tertiary air injection on NO emissions for the two fuels. Emissions from petroleum coke were not reduced by the same fraction as those from coal by the use of tertiary air injection. A 30 percent reduction was observed with coke compared to a 65 percent reduction with coal. This reduction may be due to one or a combination of the following:

- Burner staging through the use of tertiary air injection reduces peak temperatures, thereby reducing NO formation.
- Petroleum coke contains some volatile nitrogen and its conversion to NO is being reduced by staging.
- The coke produces NO initially because, even though the throat is fuel rich overall, the gas phase will burn fuel lean for a short time. This NO which is formed at short times is then reduced in the fuel rich burner zone.

4.1.4 The Influence of Fuel Oil-Water Emulsions on Nitrogen Oxide and Particulate Formation

A fuel oil emulsifier developed by TOTAL® was used in this investigation to determine the effect of emulsions on NO and particulate emissions. The emulsifier was provided on the condition that no details were presented con-

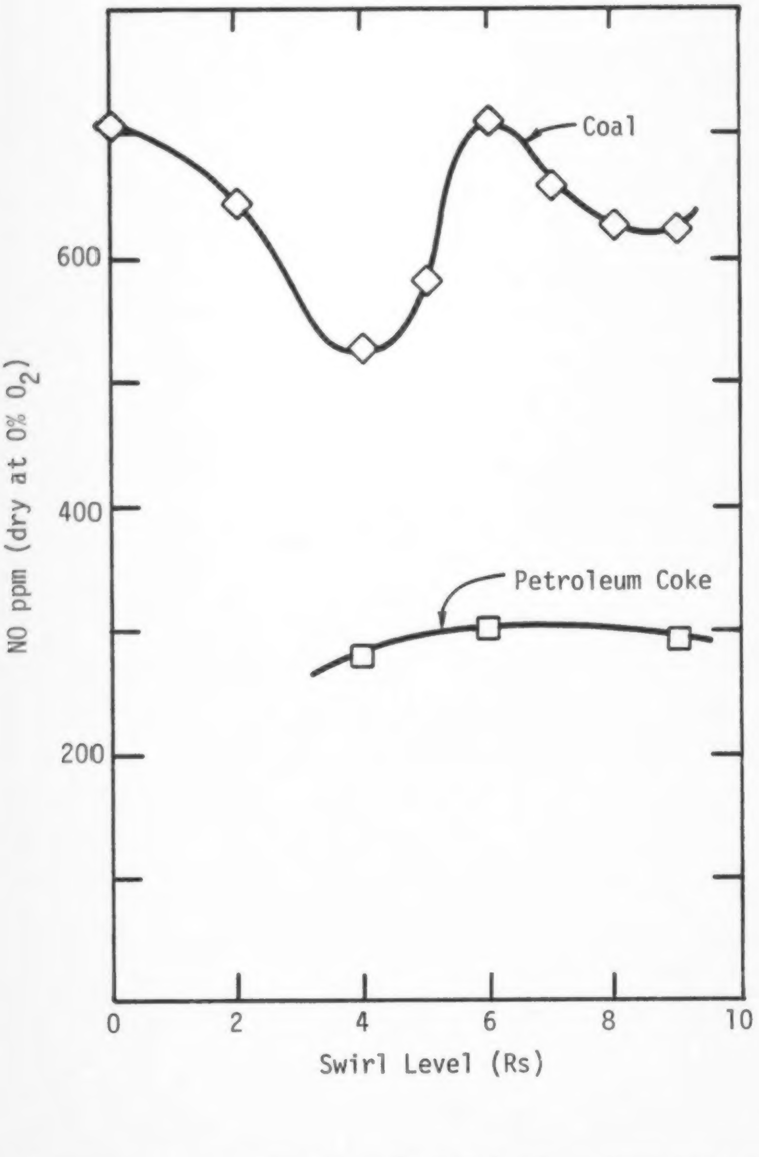

Figure 4-12. Comparison of NO Emissions from Coal and Petroleum Coke Using a Coal Spreader.

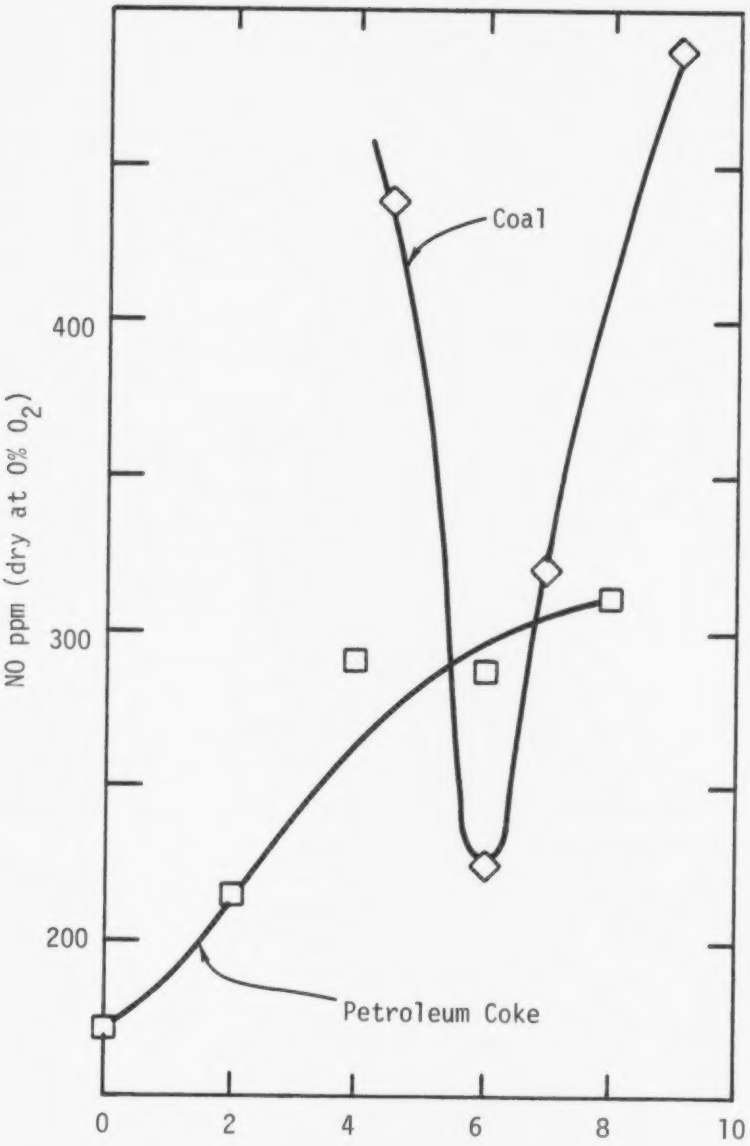

Figure 4-13. Comparison of NO Emission from Coal and Petroleum Coke with Axial Fuel Injection.

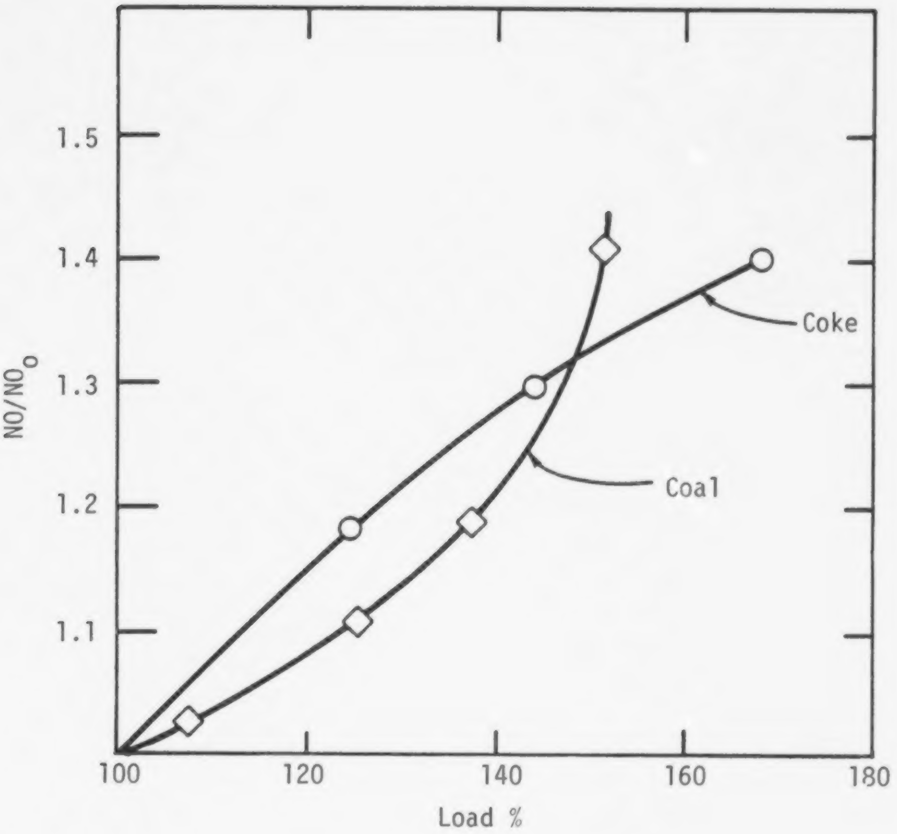

Figure 4-14. Relative Increase in NO Emissions with Increased Fuel Flow.

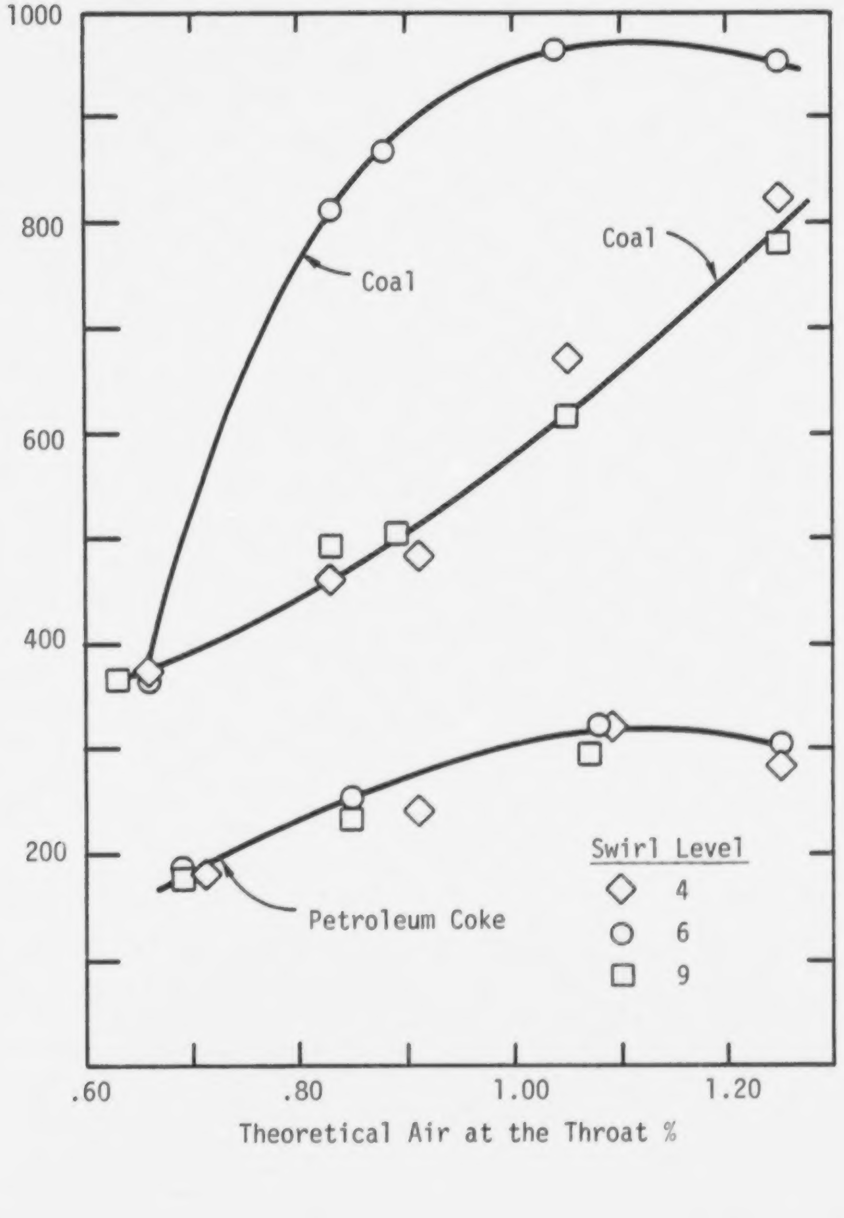

Figure 4-15. The Influence of Burner Stoichiometry on Emissions from Pulverized Coal and Petroleum Coke.

cerning its design and construction.

Experimental Systems

Figure 4-16 shows the installation of the TOTAL emulsifier in the oil supply system. The fuel oil preheated to 45 C is stored in a holding tank fitted with a steam heat exchanger. The water flow was metered by a rotameter and mixed with the oil in a premixer prior to a constant volume pump (40 bars, 40 kg/hr). The total flow was forced through the emulsifier and the fraction of the flow which did not pass to the burner was recycled via the recycle loop and heated to 80 C. The flow to the burner was heated to 120 C and delivered to the nozzle at 10 bars for the twin fluid atomizers and 25 bars for the mechanical atomizers.

The burner used in these studies was the same as that described in Section 3 except that the coal injector was replaced by a fuel oil nozzle. Three different fuel nozzles were used in the investigation:

- Axial air blast atomizer which produced an axial high velocity fuel spray.
- Pressure jet atomizer with a spray angle of 70^o.
- A steam atomized Y jet with a distributor cap (see Section 7).

The following parameters were maintained constant during the tests:

- heat input 136 kg/hr of oil corresponding to 1.3 MW_{Th};
- overall excess air 5%;
- air preheat temperature 300 C;
- burner exit divergent 25^o;
- parallel tertiary air injection.

The fuel oil had a viscosity of 800 reduced secs at 50 C and sulfur and nitrogen contents of 1 and 0.3 percent, respectively.

The Influence of Emulsion Water Content on NO_x and Particulate Emissions

The reduction of particulate mass with increasing emulsion water content can be seen in the results presented in Figure 4-17. Water contents greater than 10 percent were necessary to maximize the reductions in

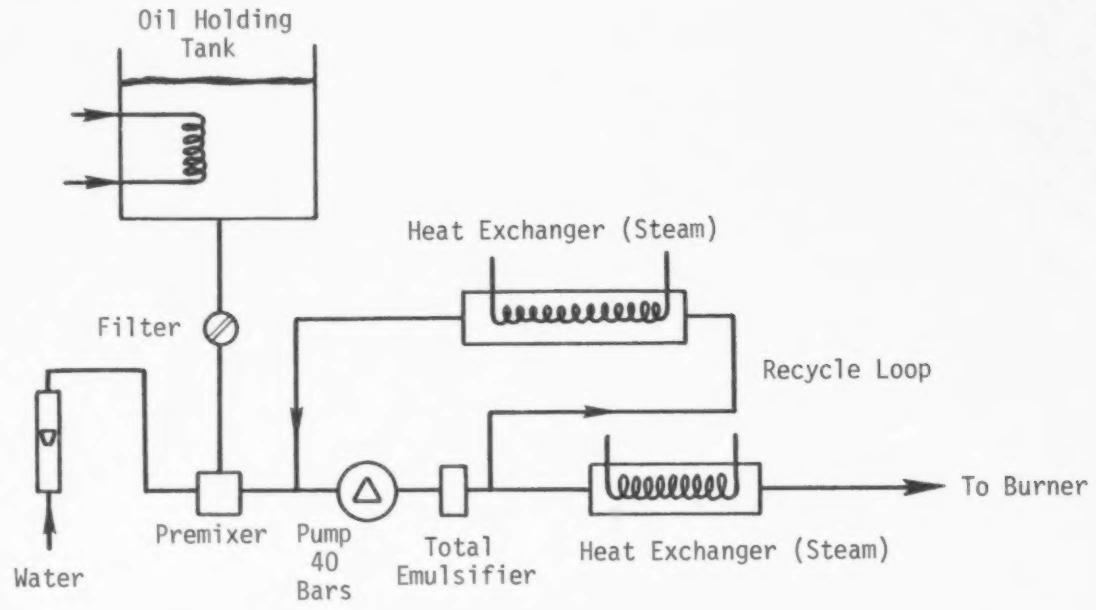
Oil Holding
Tank
Heat Exchanger (Steam)
Filter
Recycle Loop
To Burner
Water
Premixer
Pump
40
Bars
Total
Emulsifier
Heat Exchanger (Steam)

Figure 4-16. Installation of TOTAL Emulsifier in the IFRF Oil Delivery System.

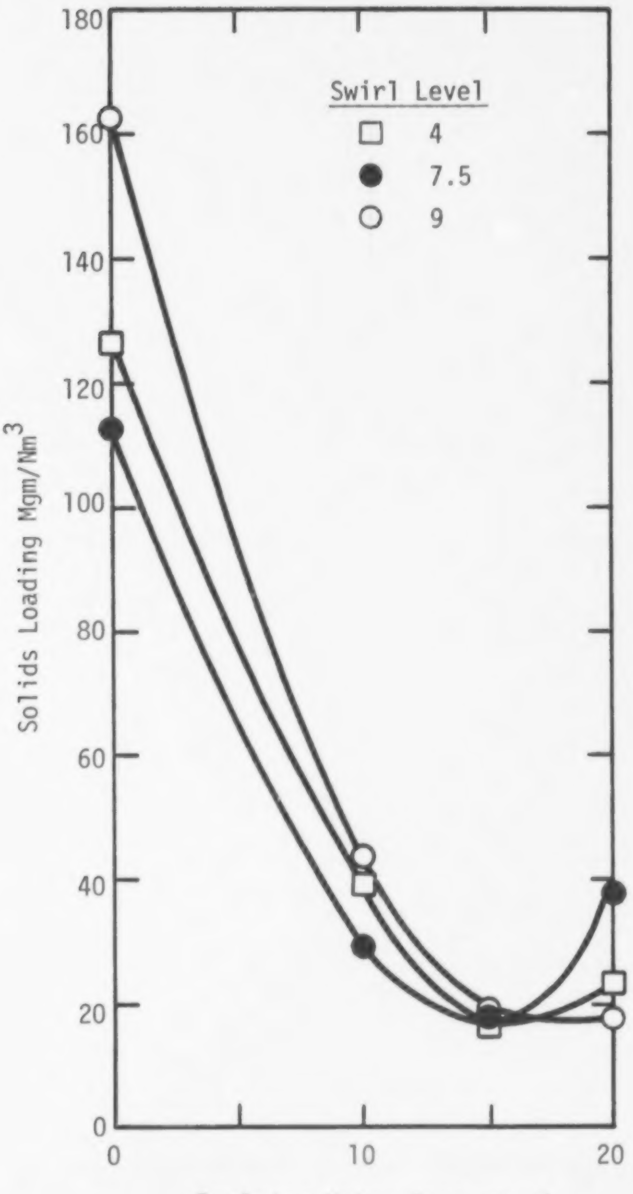

Figure 4-17. The Influence of Emulsion Water Content on Particulate Mass Emissions (Steam Atomization, 5% Excess Air, 300 C Preheat).

particulate emissions. There is also some evidence for an increase in particulate emissions as the water content increases beyond 15 percent. For the particular burner conditions investigated, the influence of emulsion water content on particulate mass is almost independent of secondary air swirl. This does not apply to the influence of emulsion water content on NO emissions. As can be seen in Figure 4-18, NO emissions tend to increase with increasing water content but the percentage increase is dependent upon burner swirl level. At low swirl levels, emissions from the pure oil and 10 percent water oil emulsions are similar. At all swirl levels, emissions are increased by adding 15 or 20 percent water to the oil. With regard to NO formation, the influence of water addition could be considered to have two conflicting effects:

- reduction of temperature reducing thermal NO formation; and
- secondary atomization could improve fuel/air mixing, thus causing an increase in the formation of fuel NO.

The Influence of Atomizing Air Flow

The results presented in Figure 4-19 and 4-20 illustrate the influence of atomizing air flow rate on NO and particulate emissions. These results were obtained with the axial twin fluid atomizer with and without staged air flow. Unstaged pure oil, both NO and particulate emissions are high but both decrease as the atomizing air flow increases. When an emulsion containing 11 percent water was burned, both NO and particulate emissions were reduced. (Particulate emissions were reduced by a factor of three, presumably because secondary atomization occurs.) However, it is surprising that NO emissions were also reduced by the addition of water. NO emissions were drastically reduced when the staged air injectors were used, but there was a considerable increase in particulate emissions unless an emulsion was burned. It is worthy of note that with this atomizer an NO emission level of 80 ppm was achieved with particulate loadings of less than 50 mg/Nm^3.

The Influence of Emulsions Under Staged Conditions

One of the problems associated with staged combustion and heavy fuel oil is the increase in particulate emissions as the burner zone becomes more fuel rich. The data presented in Figures 4-21 and 4-22 dramatically demon-

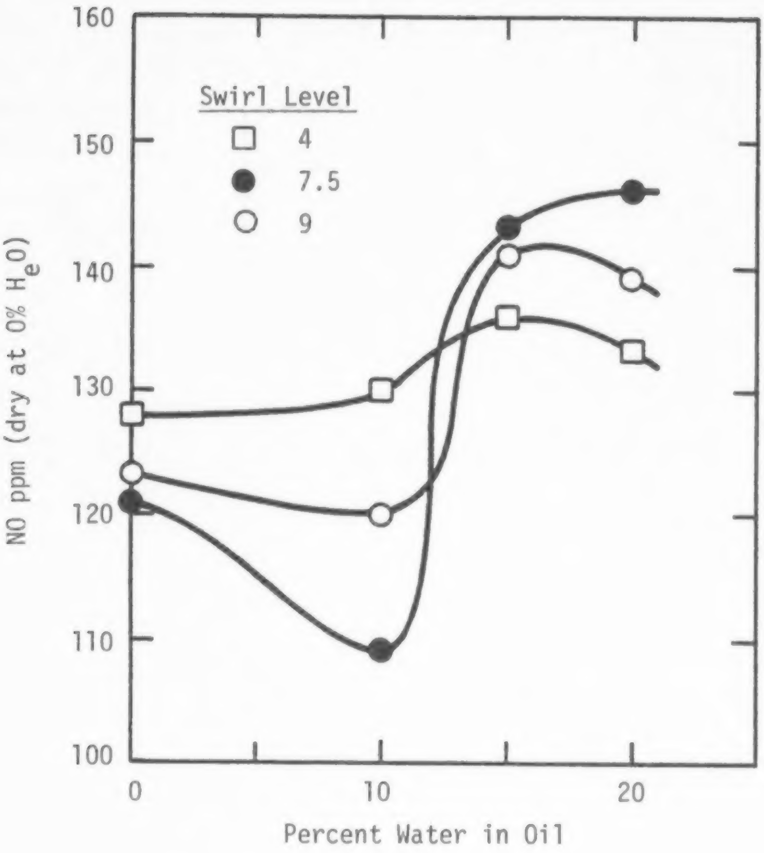

Figure 4-18. The Influence of Emulsion Water Content on NO Emissions.

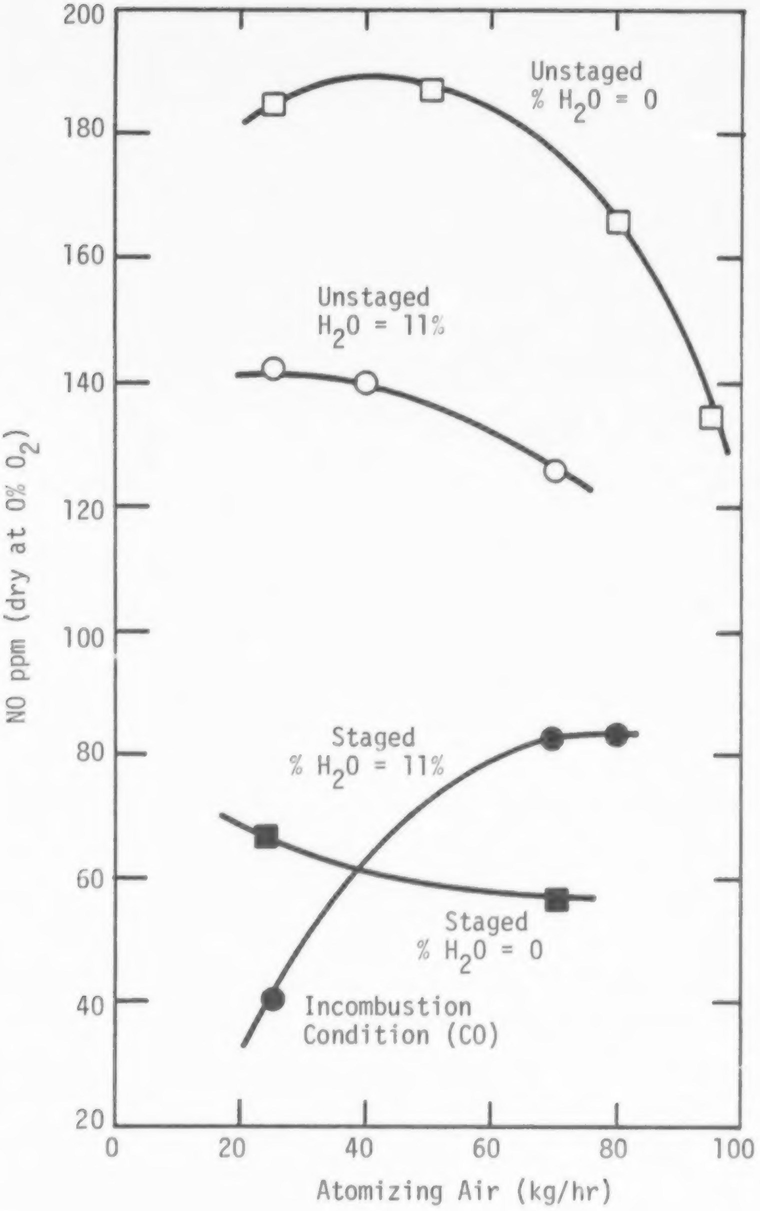

Figure 4-19. The Influence of Atomizing Air Flow Rate on NO Emissions (5% Excess Air, 300 C Preheat, S_I = 9).

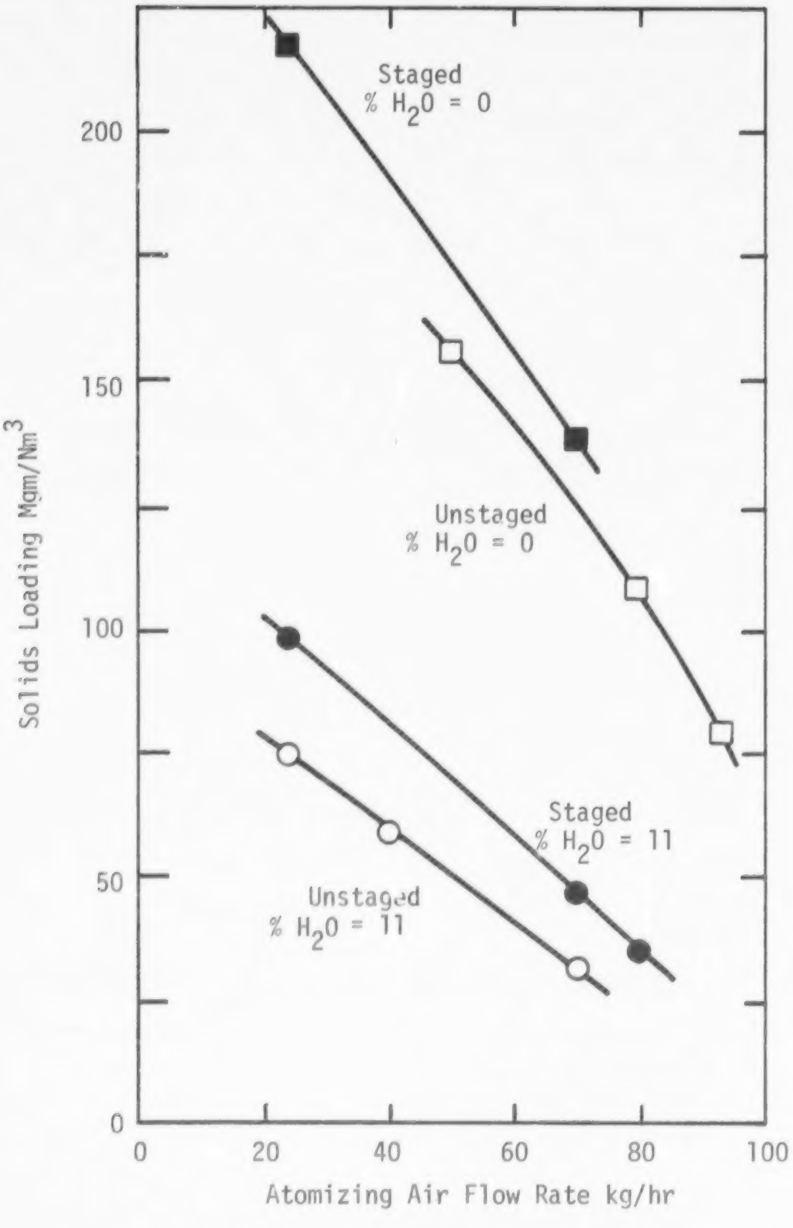

Figure 4-20. The Influence of Atomizing Air Flow Rate on Particulate Emissions (5% Excess Air, 300 C Preheat, S_I = 9).

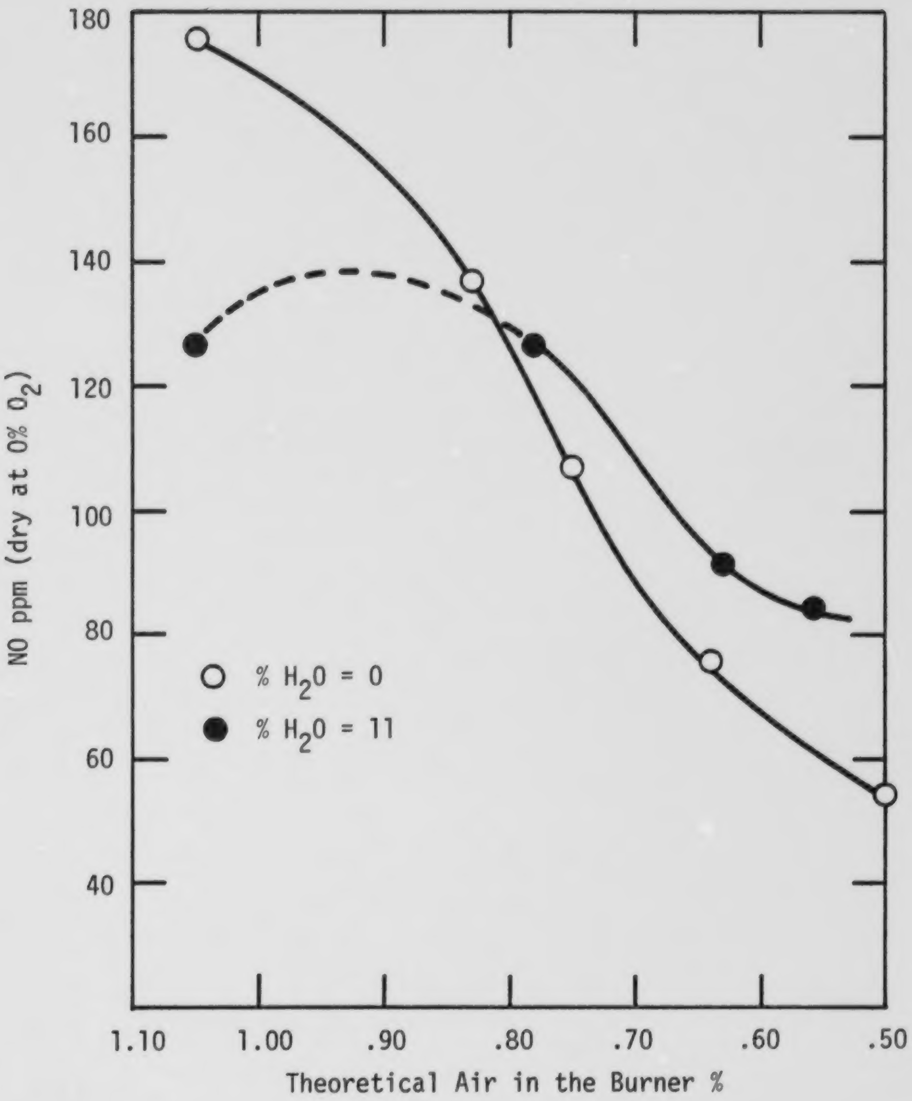

Figure 4-21. The Influence of Tertiary Air Flow on NO Emissions (Air Atomized, 5% Excess S_I = 9, Preheat 300 C).

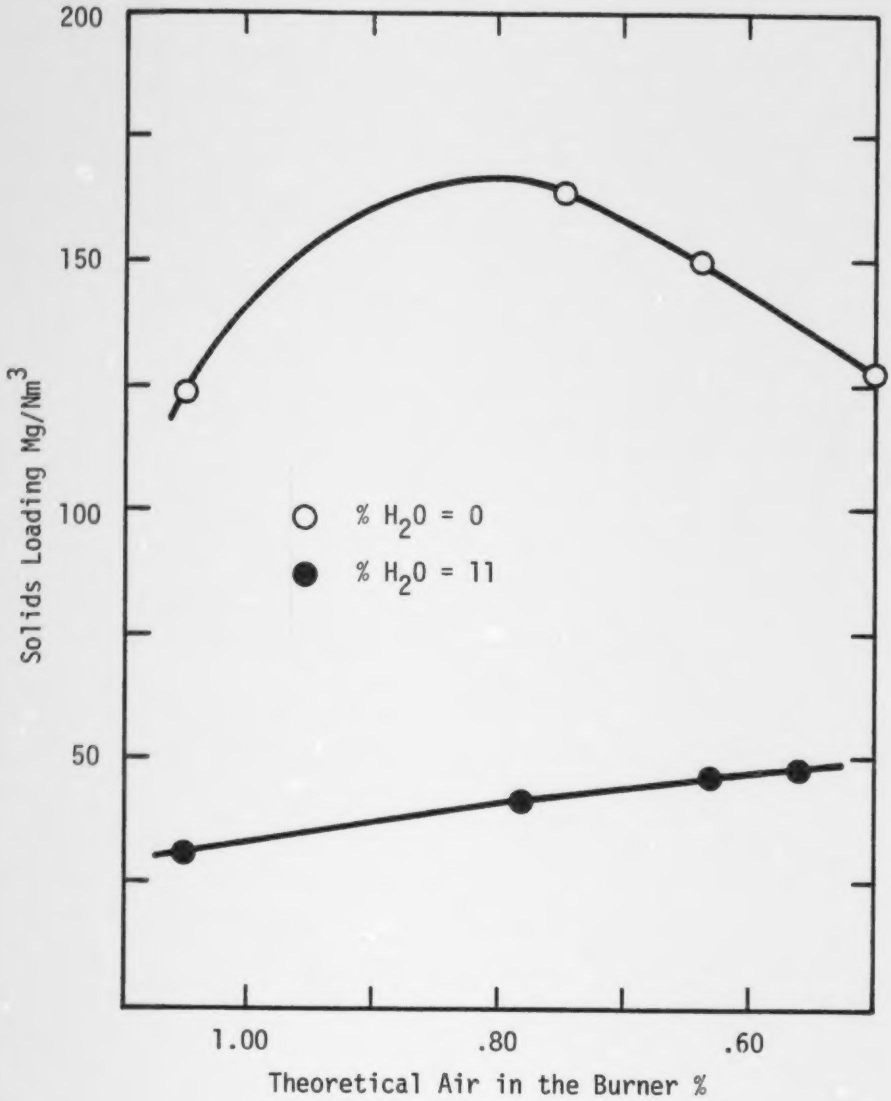

Figure 4-22. The Influence of Tertiary Air Flow on Particulate Emissions (Air Atomized, 5% Excess S_I = 9, Preheat 300 C).

strate that emulsions can alleviate this problem. These data were obtained at low atomization flow rates and the axial air atomized nozzle. Under these conditions, NO emissions are low but are reduced even further by the injection of tertiary air. However, particulate emissions are high. Addition of 11 percent water as an emulsion reduces the particulate emissions by a factor of three, but has only a minor effect on NO levels.

Summary

This brief series of tests with the TOTAL emulsifier indicated that:

- The addition of water in the form of an emulsion decreased particulate emissions from heavy oil flames.
- Under low NO_x conditions, the addition of water reduced particulate emissions by a factor of three but caused only a minor increase in NO_x levels.

The addition of water represents a significant loss of efficiency. Consequently, the use of emulsions is not optimum unless very low NO_x and particulate emissions are required and no satisfactory alternative can be found.

4.1.5 NO Formation and Fuel Oil Injector Design

In the previous series of furnace trials it was found that NO_x emissions from heavy fuel oil were affected by the design of the fuel injector. Minimum emissions were obtained with a single hole axial air blast-injector which produced a flame which was analogous to the long coal flame. The excessive flame length produced with this type of injector makes it unsuitable for many practical applications. The distributed mixing burner was modified to investigate the effect of producing a flame from several discrete jets.

A primary swirl zone was added (30^{o}) and a distributor tip over a standard Y-jet (see Figure 4-23). Figure 4-24 shows NO emission characteristics, plotted as a function of secondary swirl intensity. It can be seen that at low secondary swirl levels emissions from standard Y-jets are considerably higher than those obtained with distributor tips. However, as the swirl level is increased, the emissions from flames produced with distributor tips increase and for tip 3 approach those obtained with standard Y jets.

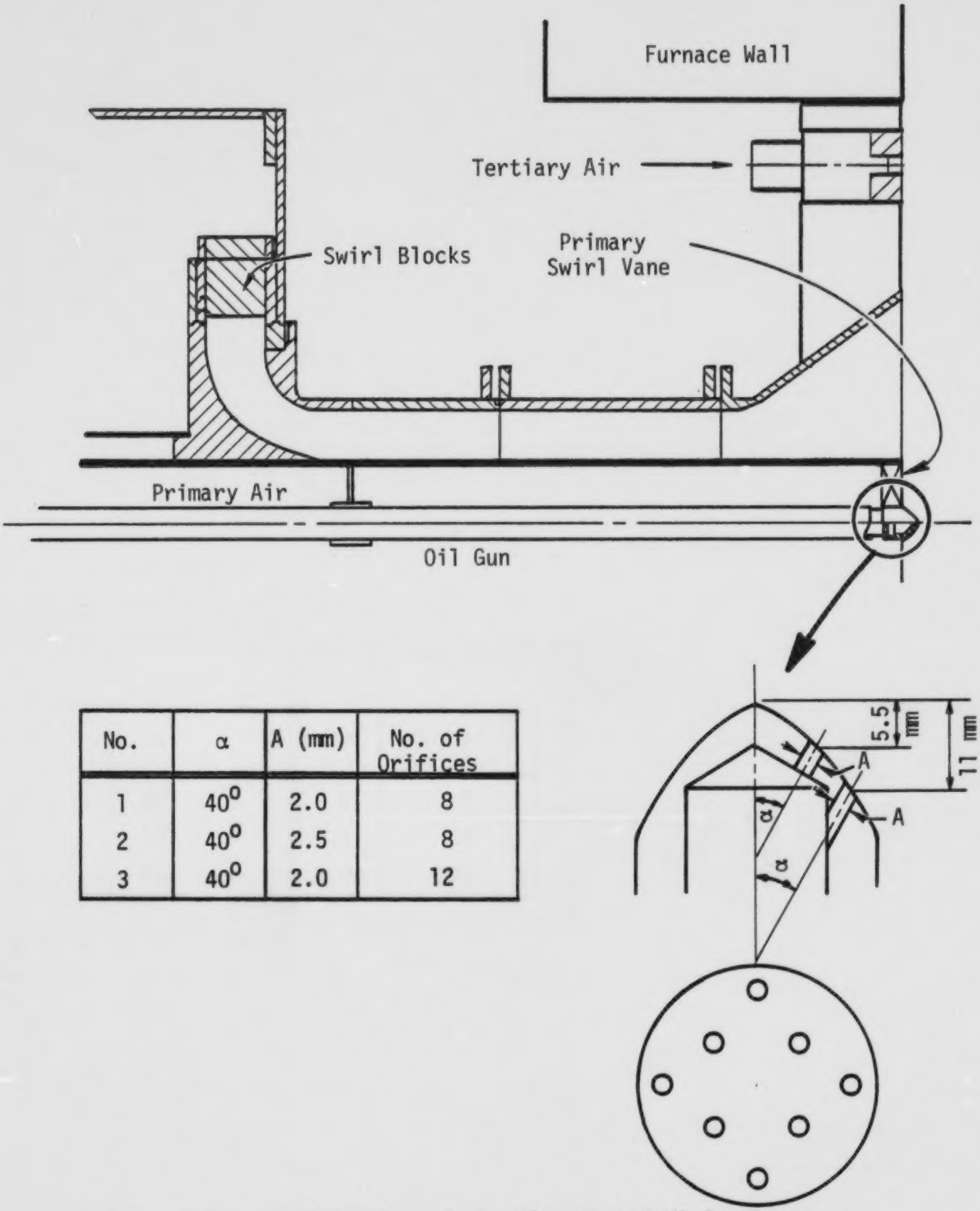
Furnace Wall
Tertiary Air
Swirl Blocks
Primary
Swirl Vane
Primary Air
Oil Gun
5.5 mm
11 mm
A
A
α
α

No.	α	A (mm)	No. of Orifices
1	40°	2.0	8
2	40°	2.5	8
3	40°	2.0	12

Figure 4-23. Modification of the Distributed Mixing Burner Showing Primary Swirl Vanes and Oil Injector Cup.

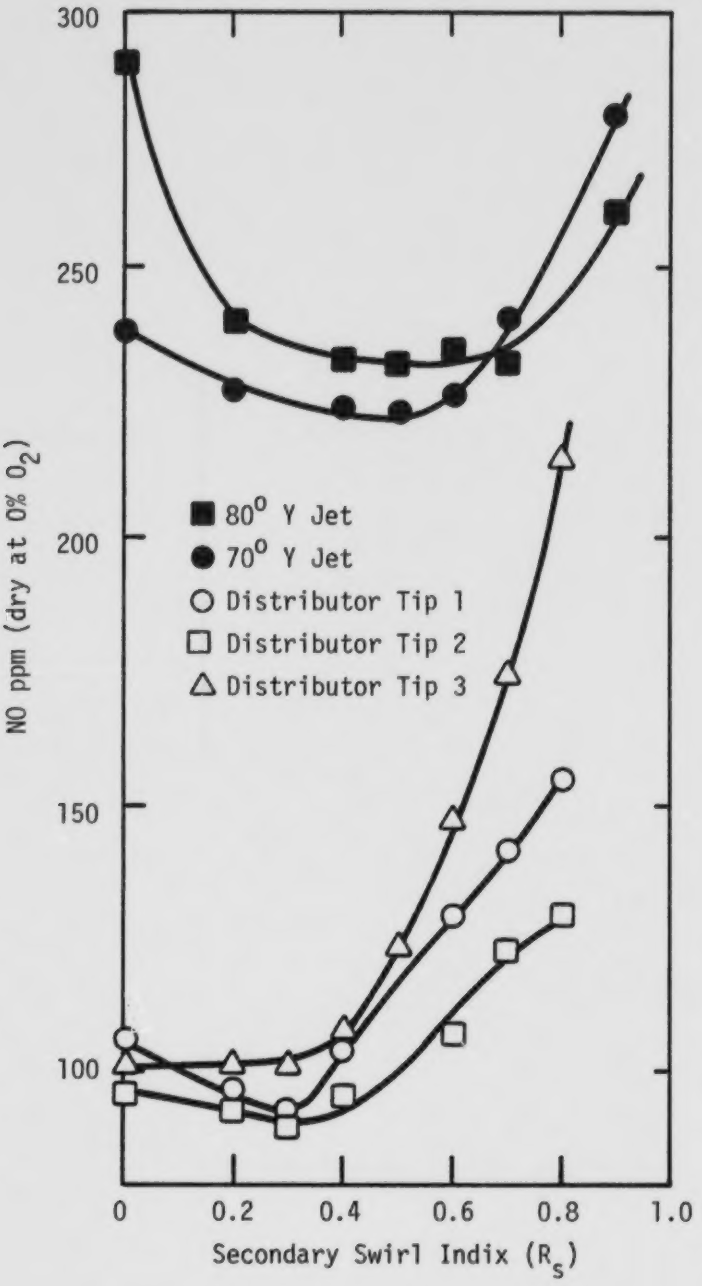

Figure 4-24. Comparison of NO Emissions from Standard Y Jets and Y Jets Fitted with Distributor Caps.

4.2 Pollutant Measurements in Multi-Burner Systems

A series of trials were planned by the members of the International Flame Research Foundation to assess the impact of multi-burner arrays on flame characteristics and heat transfer. This series of experiments provided the opportunity to evaluate the impact of multiple burner systems on pollutant formation and this section presents the results of these findings.

4.2.1 Experimental Systems

The investigations were carried out in the IJmuiden No. 1 furnace which was described in Section 4.1. In these studies the furnace was cooled by a series of pipe loops positioned along its length. The characteristics of a three burner system firing natural gas and fuel oil with a total heat input of 3.0 MW were compared with a single burner of equivalent heat input. The burners were scaled geometrically (i.e., $R = r\sqrt{3}$) and were operated in a like manner.

Two basic burner types were investigated during the trials:

(1) Type A (high momentum) - the total combustion air was supplied through the throat with a relatively high primary velocity (50 m/sec).

(2) Type B (low momentum) - the air flow through the throat was halved, and the remainder supplied via a secondary duct. A common duct was used for the multiple burners.

An axial fuel gun was used for all cases, natural gas was injected radially and 90° steam atomized Y jet was used for fuel oil. A disc swirler was necessary to stabilize the fuel oil flames. The excess air levels for Type A and B flames were 5 percent and 9 percent of the stoichiometric requirements, respectively.

Figure 4-25 presents a sketch showing the arrangement of the small burners in the common duct. For the high momentum burner all the air was supplied to the burner throat, however, as shown in Figure 4-25 for the low momentum burner, part of the air was supplied to common windbox. The high momentum burners had a short (L/D = 0.45) burner exit with a 25° divergent. Two configurations were investigated: three burners in line

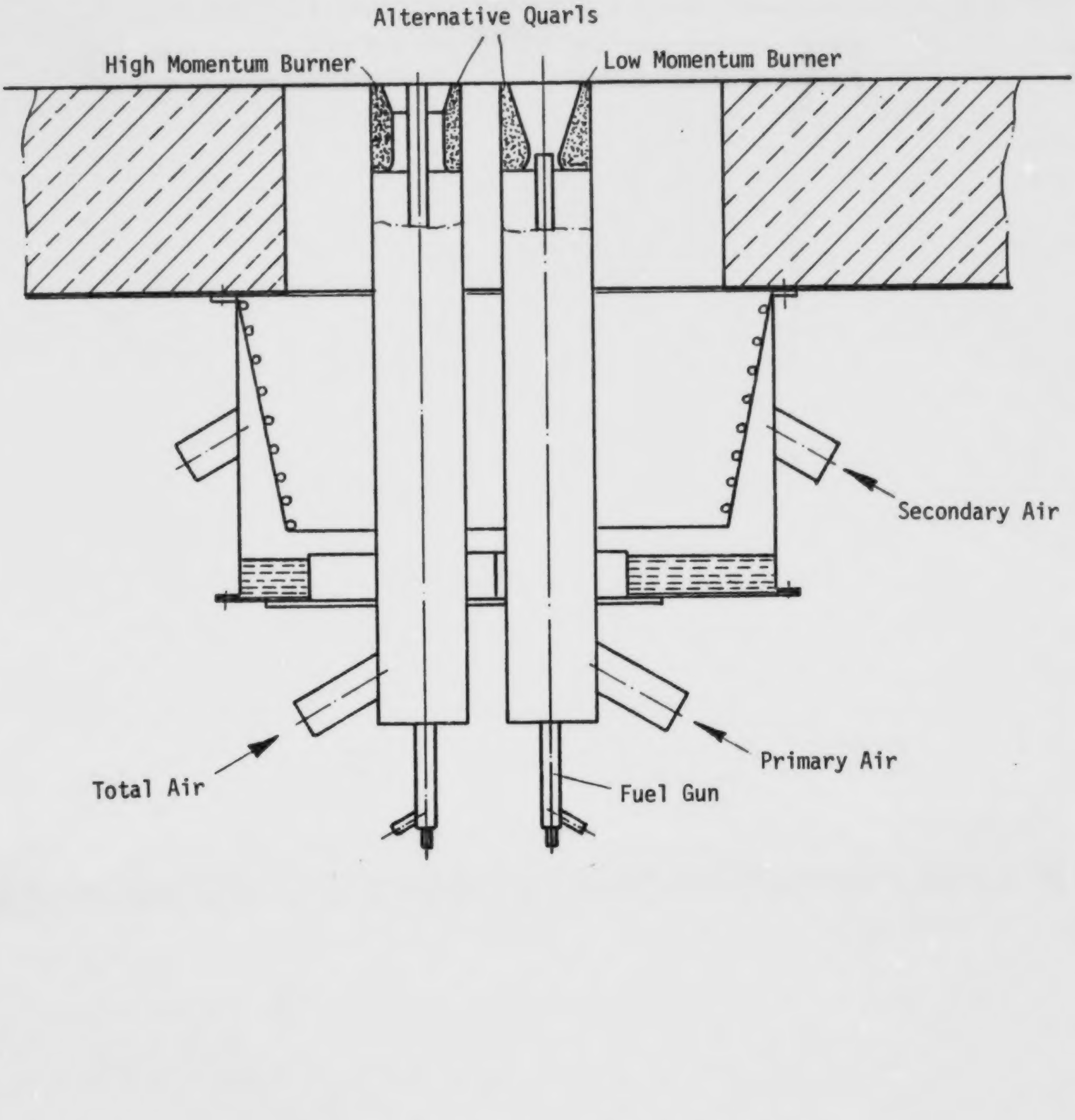
Alternative Quarls
High Momentum Burner
Low Momentum Burner
Secondary Air
Primary Air
Total Air
Fuel Gun

Figure 4-25. Multiple Burner System.

vertically and the triangular arrangement shown in Figure 4-26. The burner center to center distance could be varied in discrete intervals. Burner spacing is denoted by S/D where S is the centerline distance and D is the burner exit diameter.

4.2.2 Results

The organization of the trials enabled the influence of burner type, number, orientation and spacing on the following characteristics to be investigated:

- heat transfer to the cooling load;
- ignition stability and burnout;
- pollutant formation;
- noise generation.

Gross measurements were backed up by partial flame mapping to allow an explanation of the observed phenomena.

The Influence of Multiple Burner Systems on Ignition Stability and Burnout

One of the findings of the first multiple burner trials carried out at IJmuiden was that burner spacing had no significant influence upon the stability or turndown limits of natural gas flames. This result was confirmed during the MJ-2 Trials. Also, the turndown limit for both the small and large gas burners, at constant air rate, was approximately the same.

For oil flames, the stability characteristics of the large burner were a significant improvement of those obtained with the small burner. The large burner could be turned down from 2.9 to 0.7 MW whereas the three small burners could not, in general, stabilize a flame below 2.6 MW. Also, the large burner produced a satisfactory flame with a pressure jet atomizer. This was not the case for the smaller burners.

Gas flames showed a tendency to increase in length as the burner spacing was reduced. Axial carbon monoxide concentrations are presented in Figure 4-27 for the middle burner of the three inline vertical high momentum gas flames for three burner spacings. Flame lengthening is indicated by the increased CO burnout distance.

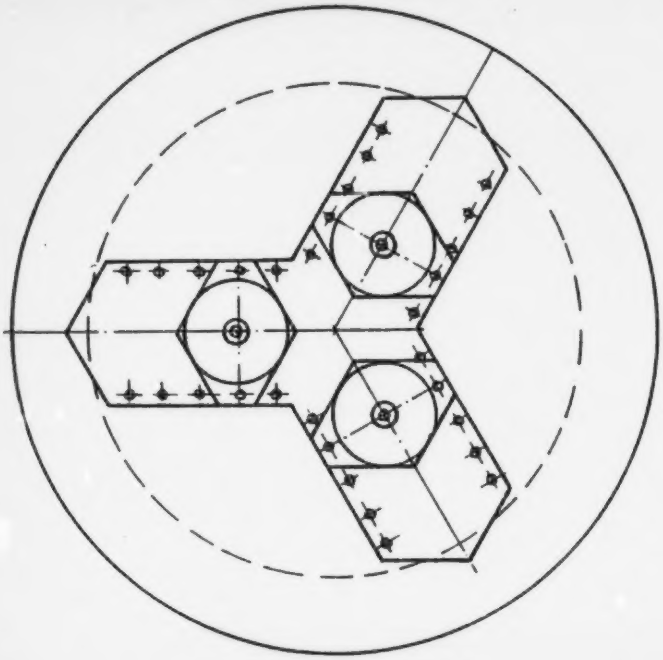

Figure 4-26. Triangular Multiple Burner Array.

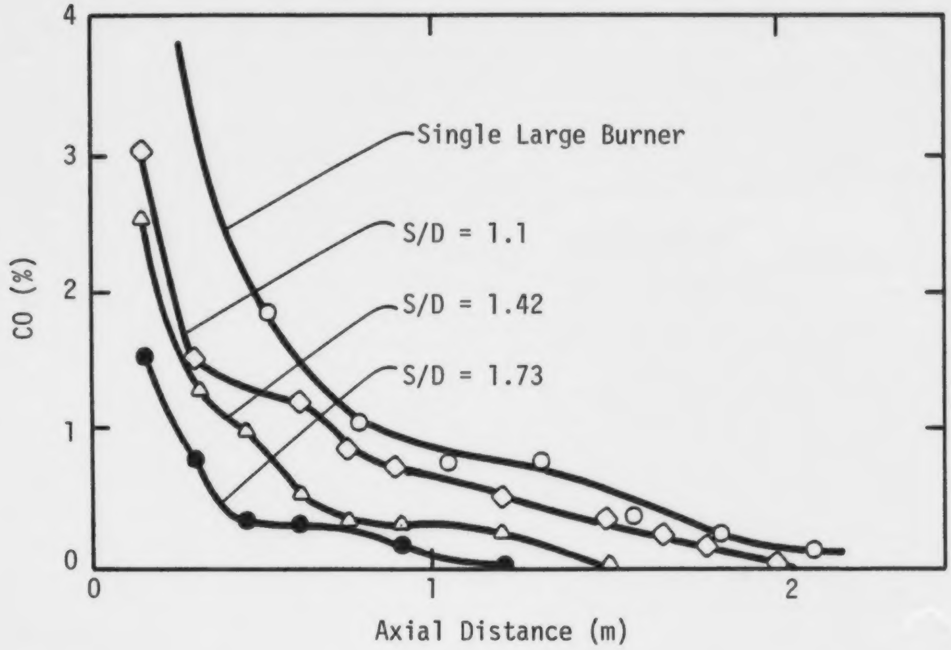

Figure 4-27. CO Concentration on Axis of the Central Burner of Three-In-Line, Configuration (Type A), and Larger Burner.

Photographic records of an oil flame tended to indicate that the flame length was reduced slightly as the burner spacing was reduced. This suggests that droplet burning rather than mixing is the factor controlling the visible length of oil flames. As the burner spacing is reduced, peak temperatures are increased which will tend to accelerate droplet combustion.

The Influence of Multiple Burner Systems on Heat Transfer to the Cooling Load

It was found that the heat transferred to the cooling load increased with increased burner separation. The proportion of heat transferred to the cooling loops is presented in Figure 4-28 and 4-29 for the type A gas and oil flames. The values for the single scaled up burners are shown in comparison. The increased heat transfer may be the result of the reduced distance of the load to flame. The axial distribution of heat flux (Figure 4-30) shows an increase in the heat transferred in the first half of the furnace as the separation between burners is increased.

The Influence of Multiple Burner Systems on Noise Generation

Noise measurements were made with a sound level meter, the microphone of which had a flat frequency response in the range of 20-8000 Hz. Measurements were made 2m behind the burner to give an indication of the noise levels [db(A)] likely to be encountered during industrial operation. Sound level measurements were also made with the measuring slot full open and the meter positioned in the center of the slot 2m from the furnace. With these measurements, both weighting networks (A) and (C) were used. These weighting factors were developed to account for the dependence of perceived loudness upon frequency. The A scale is the one used most frequently to assess environmental noise. Preliminary measurements indicated that the region in front of the slot was essentially reverberatory. Therefore, a single measurement could be used to characterize flame noise.

Frequency analysis through 1/10 octave band filters indicated that the spectrum was broad band with a broad peak around 500 Hz except for a resonance at 58 Hz which was present in all cases. The resonant frequency corresponded to the first longitudinal harmonic of the furnace, calculated with a gas temperature of 1100 C. When the fuel flow was turned off and measurements were made with the correct input frequency, analysis indicated that

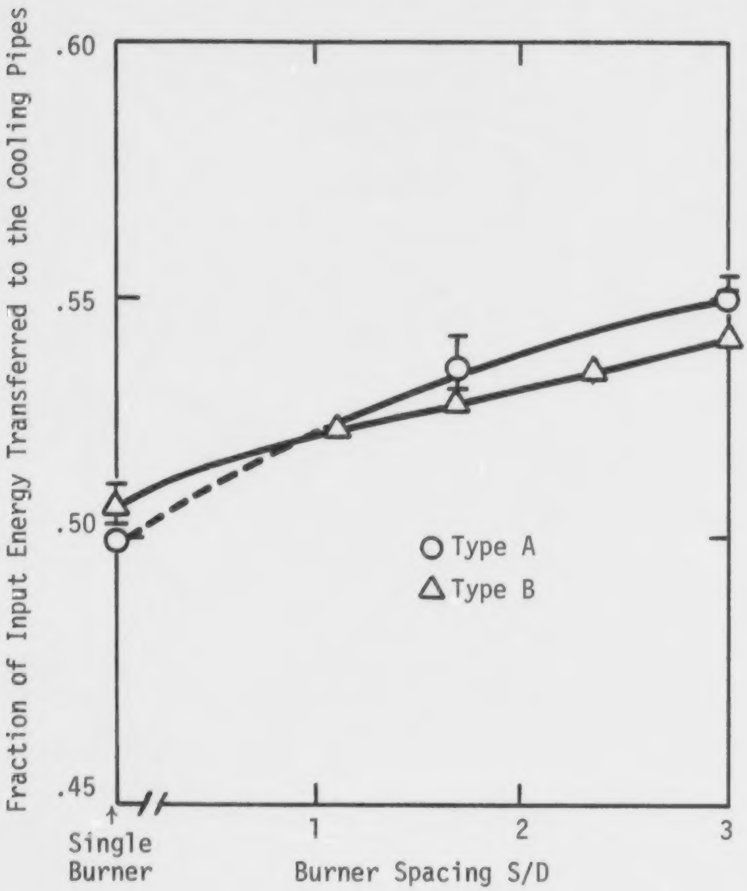

Figure 4-28. Heat Transferred to Cooling Pipes. Natural Gas Flames in a Triangular Array.

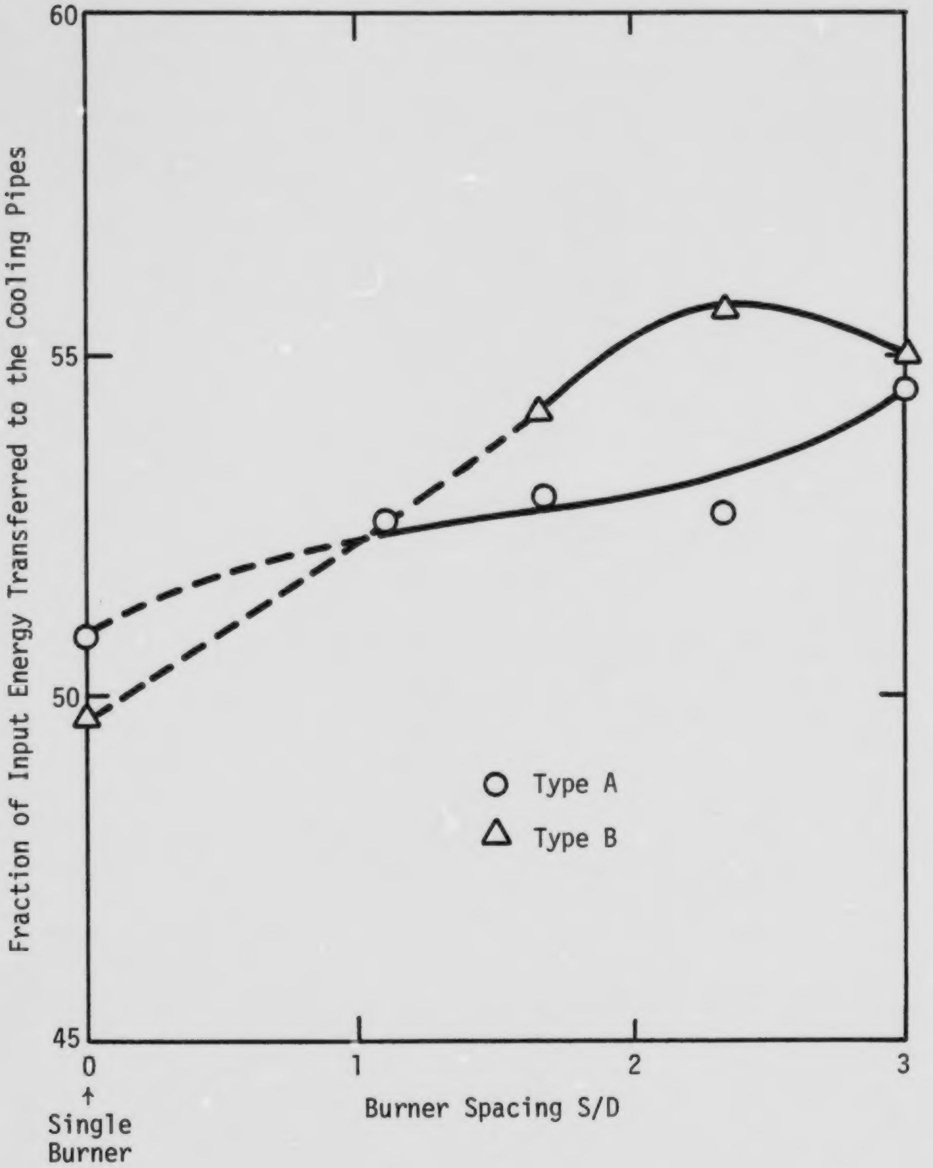

Figure 4-29. Heat Transferred to the Cooling Pipes. Oil Flames in a Triangular Array.

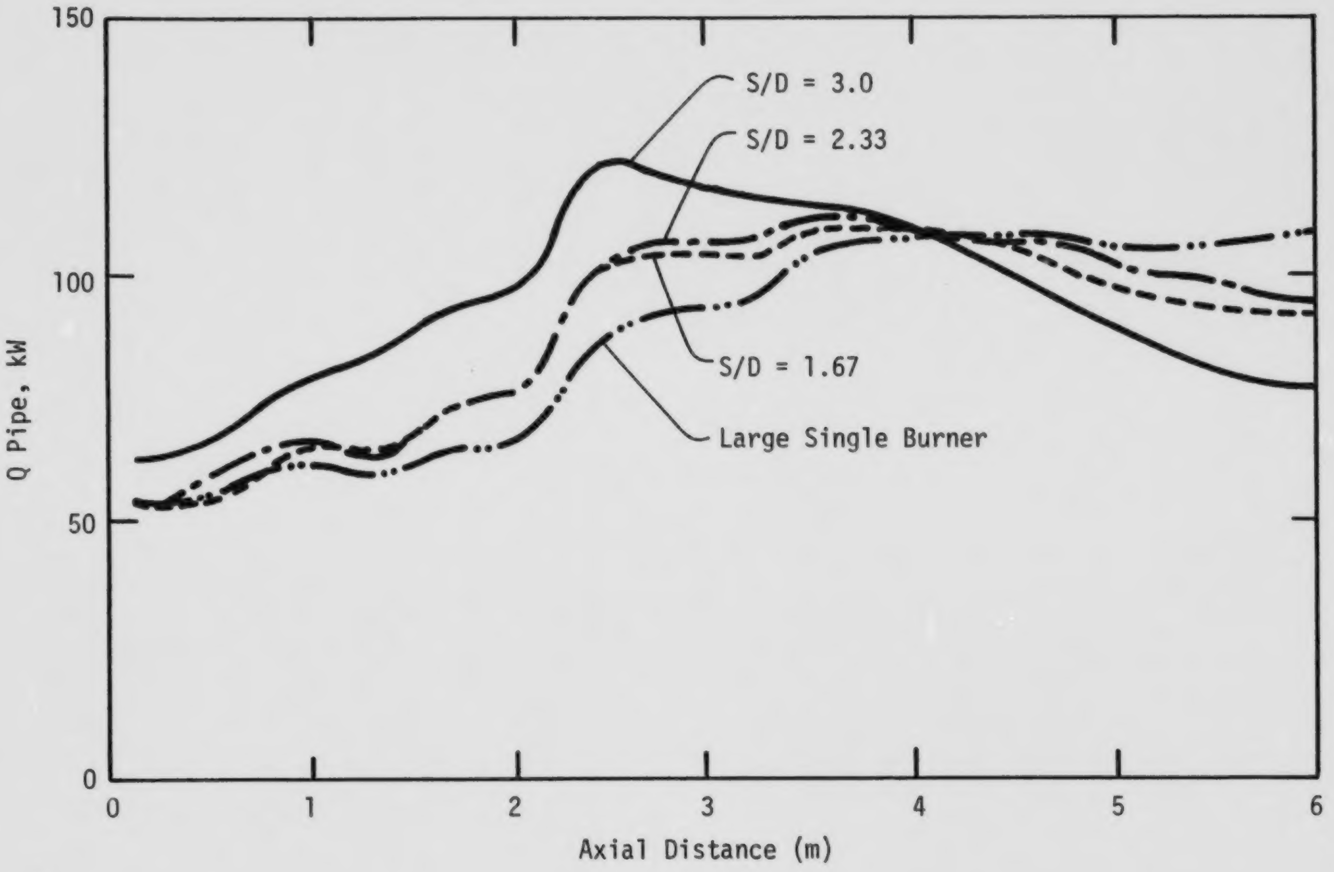

Figure 4-30. Axial Distribution of Heat Flux to the Cooling Pipes. Type A Oil Flames in a Triangular Array.

the combustion noise was restricted to frequencies below 1500 Hz - 2000 Hz.

Figure 4-31 and 4-32 present the sound pressure levels measured opposite the measuring slot for gas and oil firing, respectively. Weighting network A attenuates strongly at frequencies below 1000 Hz, whereas network C has a flat response. The results exhibit the following characteristics.

(1) There is a small influence of burner spacing on noise generation, particularly at small burner separations.

(2) With weighting network C, there appears to be little effect of flame type or array configuration on noise generation in gas flames. With network A low momentum gas flames (Type B) generated more noise.

(3) For oil flames, the higher momentum oil flames produced more noise (both A and C scales).

(4) For multiple systems, noise generation is greater with gas flames. The difference between the two fuels is most marked on the A scale, this indicates that a greater proportion of noise is generated at lower frequencies in oil flames than in gas flames.

(5) The large single burner was noisier than the corresponding three burner system. In gas flames, this increase was due to low frequency generation since measurements with the C scale showed a greater effect than with the A scale. The opposite trend was observed with oil flames.

(6) The Type B flame produced slightly more noise than the Type A single gas flame. The reverse effect was observed with oil flames.

The noise levels measured behind the burner were all below 90 dB(A), the generally accepted 8 hour per day exposure limit for accupational noise. These results showed an effect of burner spacing and configuration. However, the level of these results are peculiar to the experimental system. A different arrangement of valves, etc., would undoubtedly alter the sound level.

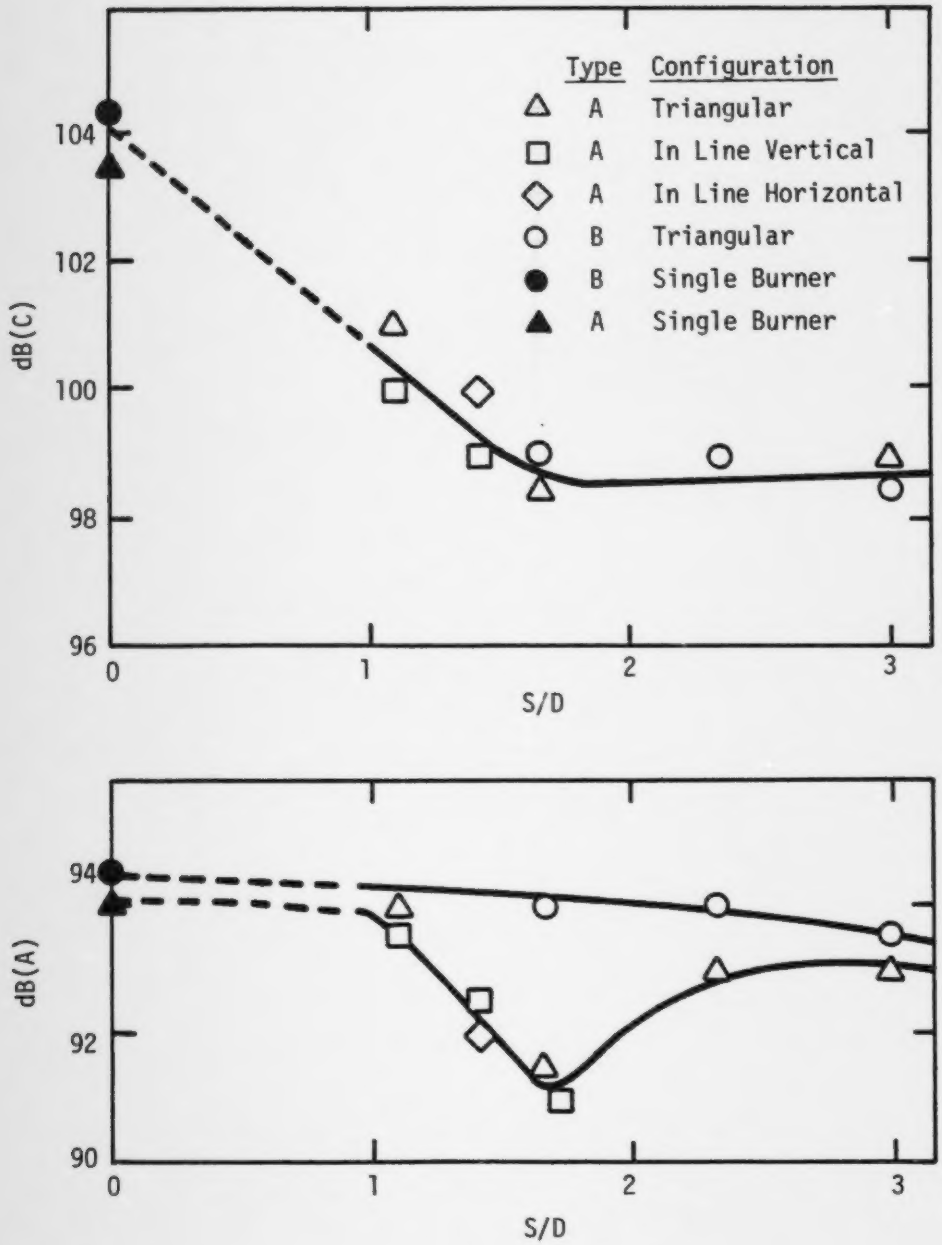

Figure 4-31. The Influence of Burner Spacing, Type, and Orientation on Noise Generation in Natural Gas Flames.

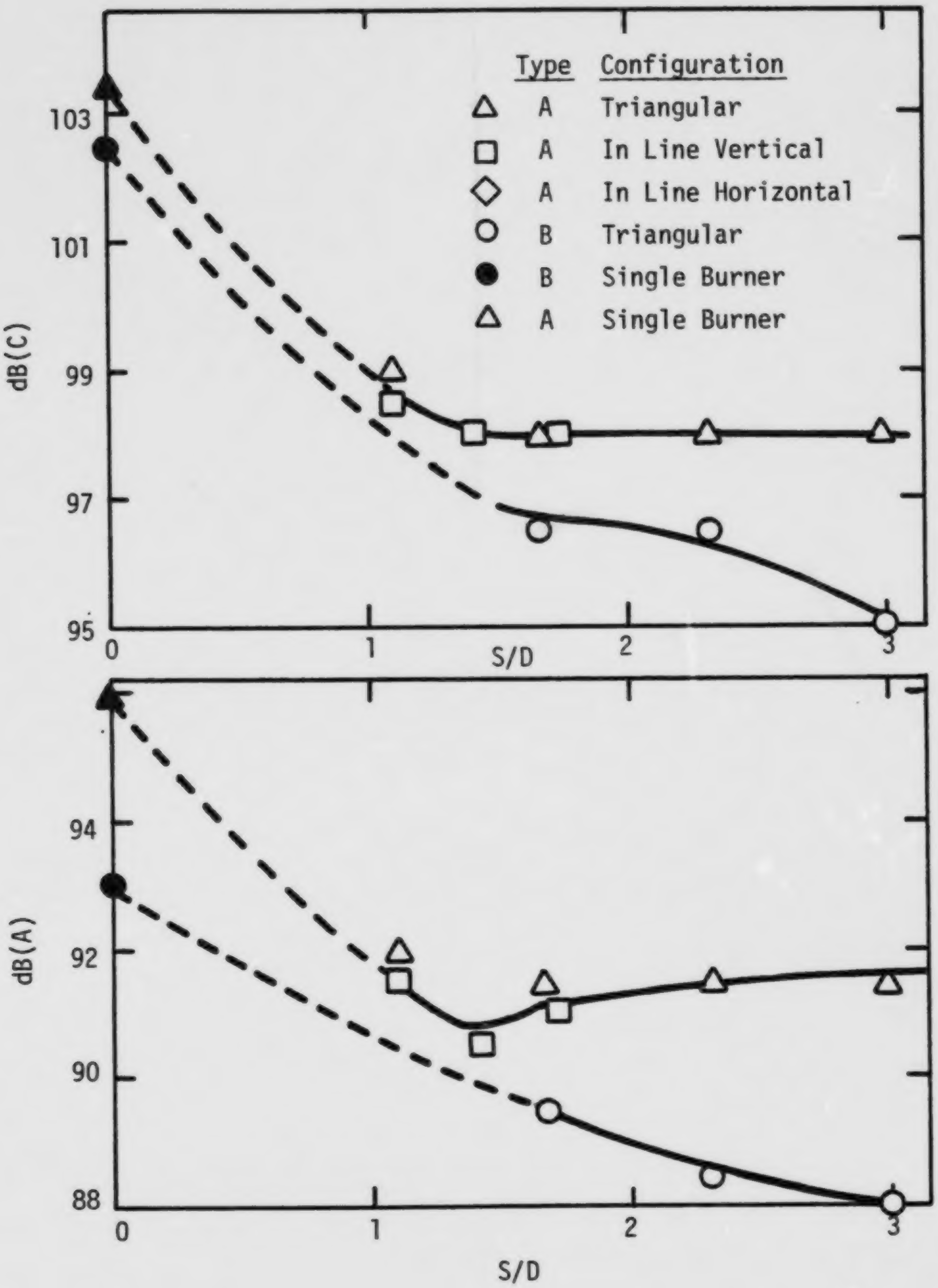

Figure 4-32. The Influence of Burner Type, Spacing, and Orientation on Noise Generation in Oil Flames.

The Influence of Multiple Burner Systems on Nitric Oxide Formation in Natural Gas Flames

Flue gas nitric oxide concentrations are presented in Figure 4-33 for Type A and B flames. In agreement with previous EPA trials results(4.1) reduced burner momentum causes an increase in NO emission because of a reduction in the mass of relatively cool external recirculation entrained by the flame jet. Burner spacing does not appear to have a significant influence upon emission from Type A until the burners are close together (S/D = 1.1). With the Type B flames reduced, emissions were observed at both large and small burner separations. Emissions from single burners are not higher than those from the three burner systems (cf. noise generation), but are similar to emissions measured at intermediate burner spacings.

The increase of NO emission with increase in burner momentum is further illustrated in Figure 4-34 which shows emissions as a function of the ratio of air supplied through the throat (primary) to the total air. Comparisons are possible for the large single burner and three burners at one pitch, either in-line horizontal or in-line vertical. It can be seen that the configuration has an increased influence as the mass of primary air is reduced. Excess air levels were reduced to accentuate carbon monoxide emissions. It can be seen that as the burner momentum is reduced, CO emissions increase and there is an effect of configuration. Carbon monoxide emissions were lower with the three in-line horizontal array.

Emission from natural gas-air flames in the lowly loaded highly cooled furnace are low. Oxygen was added to the air supply to exaggerate any effects of spacing and configuration to enable a better understanding of the influence of burner interactions on NO_x formation to be obtained. Figure 4-35 presents the results of this experiment showing both the influence of burner spacing and configuration. It can be seen that:

- Emissions from horizontal arrays are higher than vertical arrays.
- The effect of burner separation increases as emissions increase.
- At moderate levels of oxygen enrichment there is a strong decrease in NO formation as the burner spacing is increased.

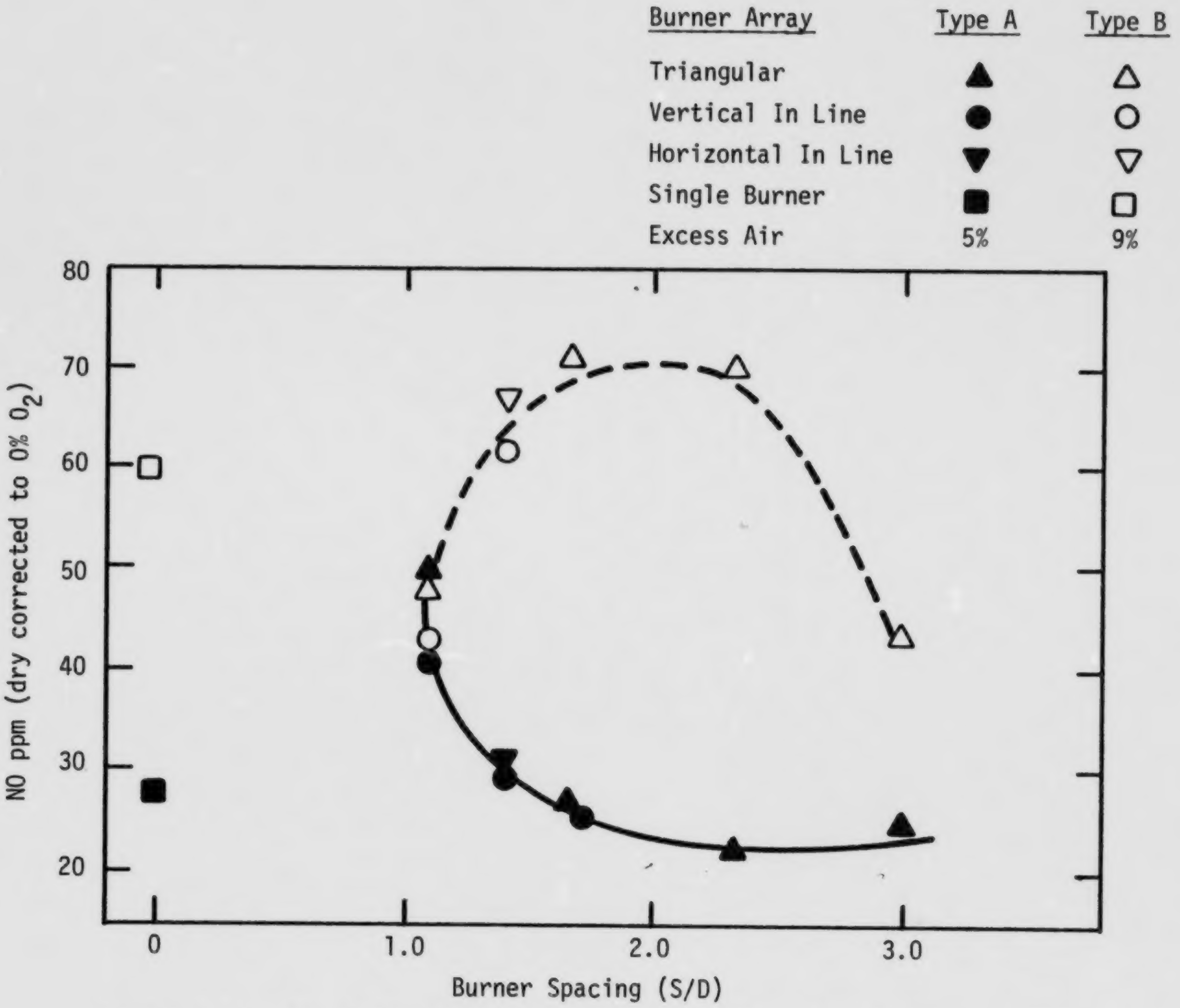

Figure 4-33. The Influence of Burner Spacing, Type, and Configuration on NO Formation in Natural Gas Flames.

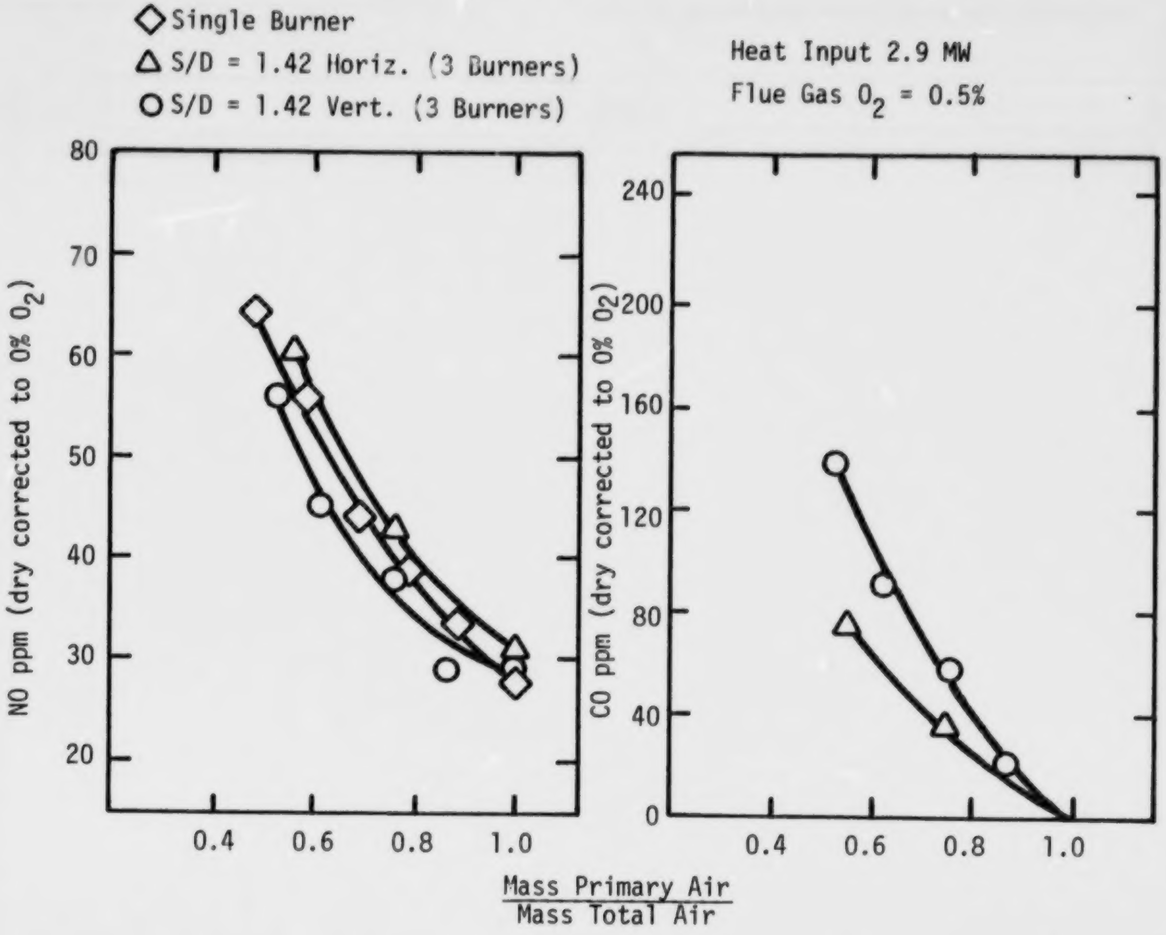

Figure 4-34. The Effect of the Primary Secondary Mass Ratio on NO and CO Formation.

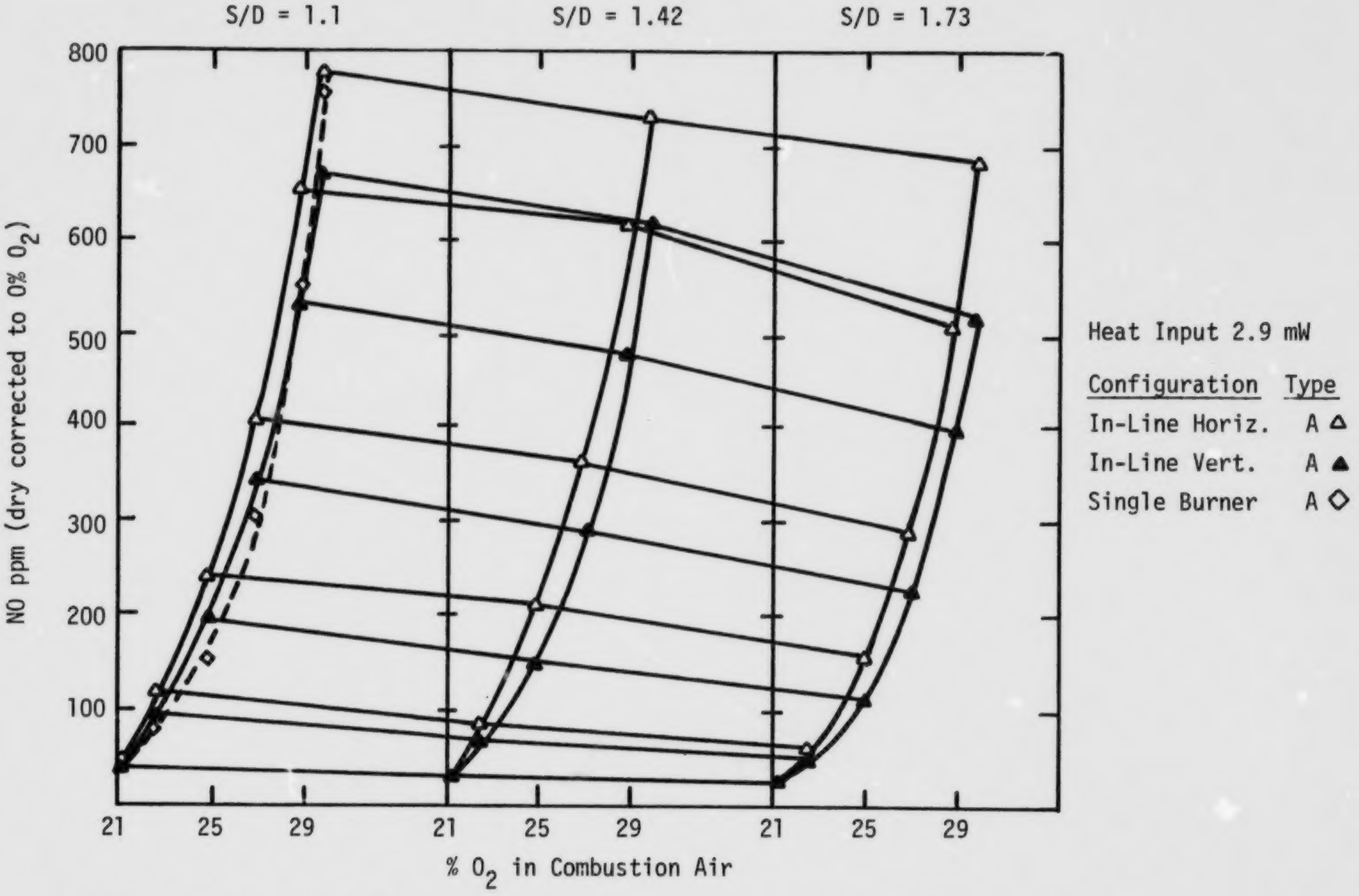

Figure 4-35. The Influence of Burner Spacing, Type, and Configuration on NO Formation in Natural Gas Flames Supported by Oxygen Enriched Air.

- Emissions from the single large burner are lower than those from the three burner systems at low levels of oxygen addition. At high levels of oxygen addition, emissions from the single burner are only lower than the 3 burners in-line horizontal at small burner separations.

The results presented in Figure 4-35 were obtained with a constant burner momentum thus the excess air increases with increasing oxygen enrichment. When the oxygen was added and the air flow reduced in order to reduce the excess air to give 0.5% O_2 in the flue, the burner momentum was naturally reduced, the vertical array gave a higher emission than the horizontal array. Table 4-3 gives the NO emissions for this system when the air distribution to each burner was varied to allow burners to be fired rich and lean with constant overall excess air. Carbon monoxide levels were zero for these conditions. The curves presented in Figure 4-36 were obtained by reducing the oxygen flow rate. This was done to give an indication of which configuration would be most likely to produce carbon monoxide.

An important feature in practical combustors is turndown. Figure 4-37 compares the effect of reducing heat input by turning down or turning off burners. Emissions were found to increase as the firing rate was reduced by turning down burners, whereas emissions were reduced when one burner was turned off.

The Influence of Multiple Burner Systems on NO Fomation in Fuel Oil Flames

It was originally intended that the investigations involving fuel oil would be more extensive. However, the use of oil was limited due to the Arab oil boycott. The influence of burner spacing and configuration on NO formation in oil flames can be seen in Figure 4-38. The results are not consistent. In general, emissions increase with reducing burner distance, but there is some scatter within the individual results. With the large single burner Type A flames give a higher emission than Type B flames (cf. natural gas results where the opposite effect was observed). With the three burner systems, the only comparison possible shows that for two out of three cases Type A flames produced less NO than Type B flames.

Table 4-3. The Influence of Non-Uniform Air Distribution on NO Formation in Type A Natural Gas-Oxygen-Air Flames (Flue Gas O_2 Concentration 0.5%) for Three In-Line Configuration

Burner Stoichiometry	NO ppm	
	Horizontal In-Line	Vertical In-Line
All Lean	275	300
Outside burners lean $\phi \simeq 1.2$ Middle burner rich $\phi \simeq 1.6$	210	220
Outside burners rich $\phi \simeq 0.9$ Middle burner lean $\phi \simeq 1.2$	240	220

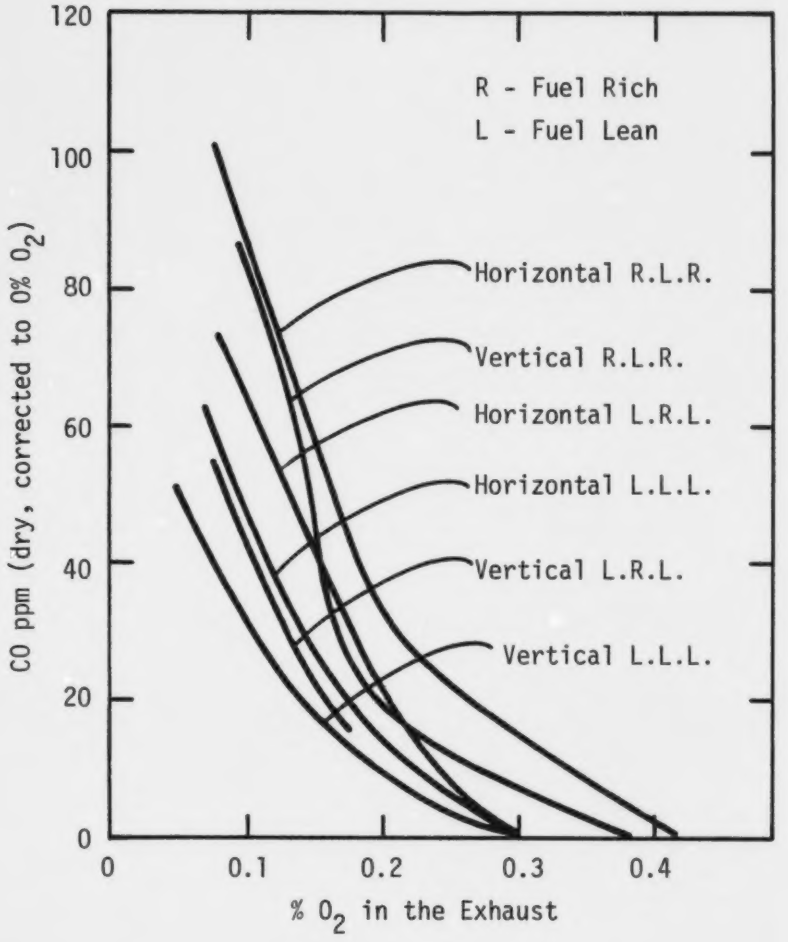

Figure 4-36. Carbon Monoxide Formation as a Function of Burner Configuration and Excess Air with Non-Uniform Air Distribution.

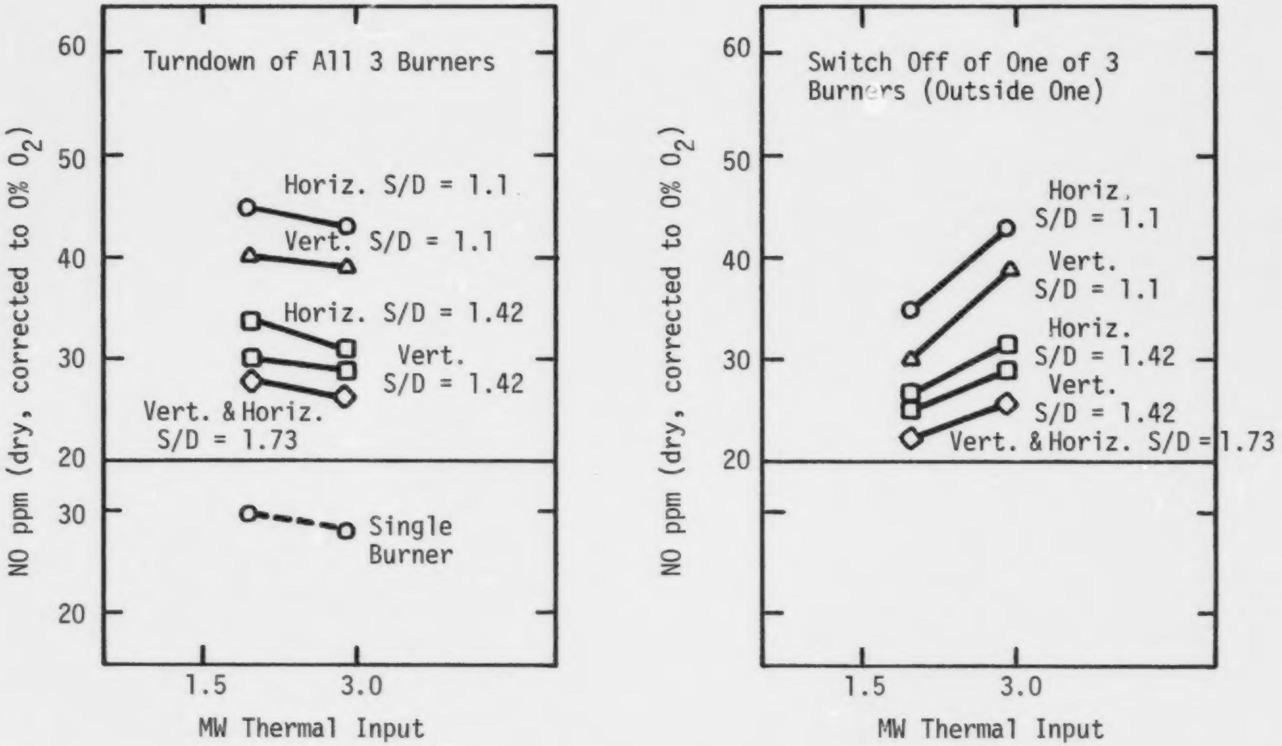

Figure 4-37. Effect of Load on NO Emissions from Type A Gas Flames Produced with a Single Burner and a 3 Burner In Line System.

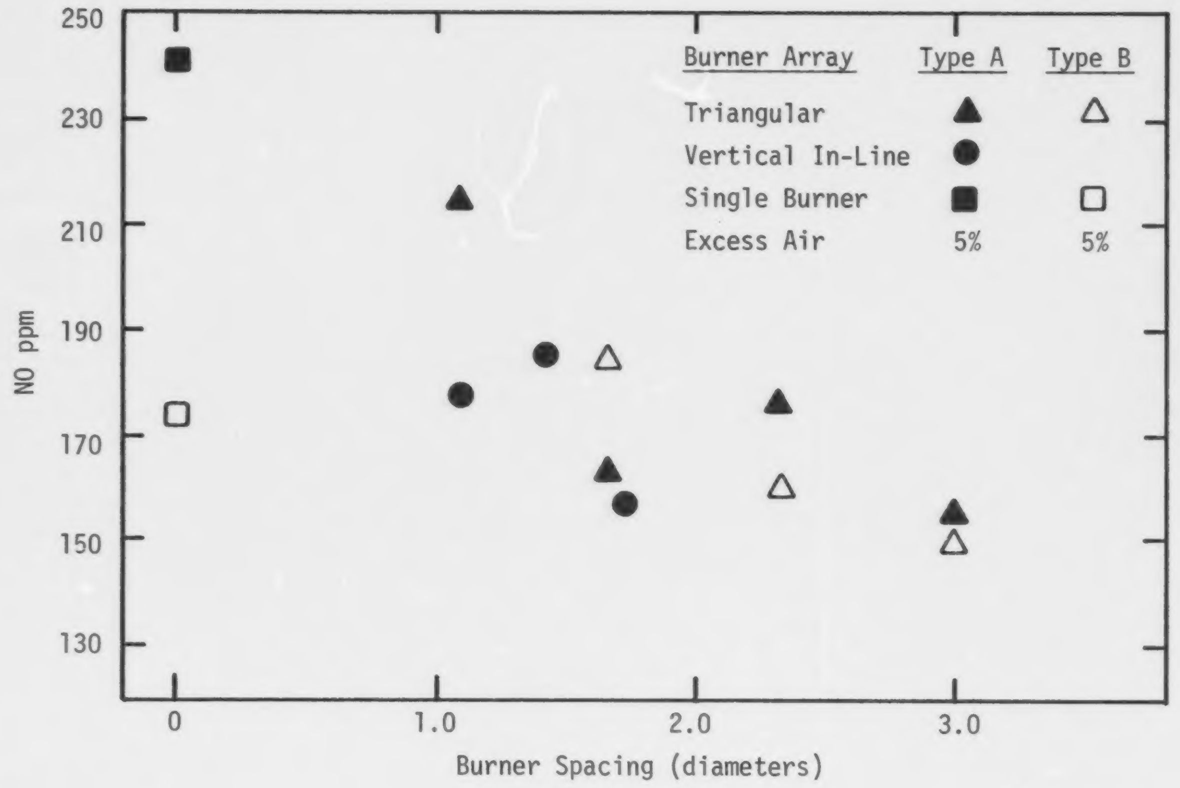

Figure 4-38. The Influence of Burner Spacing, Type, and Configuration on NO Formation in Fuel Oil Flames.

Figure 4-39 shows the reduction of NO when the fraction of total air added through the primary duct was reduced for the large single burner. The excess air was held constant to give a flue gas O_2 concentration of 0.5 percent. It can be seen that a reduction in NO formation is accompanied by a sharp increase in CO production.

4.2.3 Discussion

A considerable body of data exists concerning the influence of burner parameters on nitric oxide formation. There are almost no data available on the influence of burner arrays on pollutant formation other than those obtained in real systems (e.g., utility boilers). A qualitative model was used to explain the effect of burner parameters on NO formation in turbulent natural gas diffusion flames measured in earlier experiments.(4.1) The same approach will be used to help explain the phenomena observed in the multi-burner tests. It is believed that the formation of NO in oil flames is less well understood and the results will be used merely to illuminate the problem areas.

NO Formation in Multiple Natural Gas Flames

Nitric oxide formation in natural gas flames is dependent upon the rate of fuel air mixing, the entrainment of external recirculation both before and after reaction, and the enthalpy of the entrained matter. The three small burners were identical and for Type A flames it can be assumed that the fuel air mixing patterns would also be similar. This assumption is reasonable because the burner input conditions, and not the burner spacing, should be the dominating influence upon the fuel air mixing rate. The rate of entrainment of recirculation is dependent upon the burner momentum and the density of the recirculating matter. The density will be neglected because, over the temperature range encountered, its influence will be secondary.

Earlier investigations involving multiple burner systems found that axial temperatures in a multi-burner system were higher than those encountered in an equivalent single burner. As burners are moved closer together, the cooler recirculating gases cannot penetrate to the center of the multiple system. Consequently, each flame entrains hot products from its neighbor and NO formation will be promoted because the entrained gases have

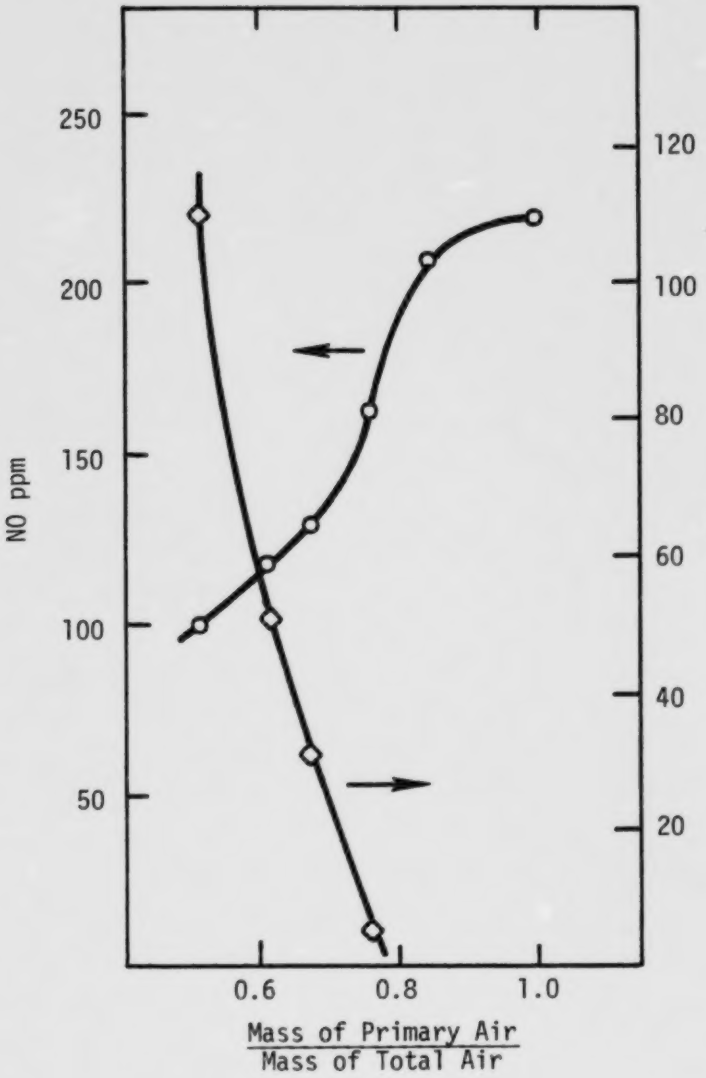

Figure 4-39. The Influence of Primary Air Rate on NO and CO Emissions from the Large Single Type Oil Burner (Oxygen Flue Gas Cone 0.5%).

a higher enthalpy. Therefore, flame temperatures will be higher and the rate of temperature decrease of flame gases will be less than would be obtained if cooler recirculating gases were to be entrained. The temperature traverses presented in Figure 4-40 were measured along the axis of the center flame for the in-line configuration and along the axis of one flame for the triangular configuration. The temperatures were measured by a suction pyrometer and show that the highest temperatures were attained at the smallest burner distances for the two configurations. It is not suggested that these temperatures characterize the conditions under which NO is formed. However, it is reasonable to assume that the burner spacing which gives the highest bulk gas temperature will also produce the highest flame temperature and the lowest rate of flame product quench

The emission levels presented in Figure 4-33 show that for the Type A flame, more NO is produced with the triangular array than with the vertical in-line array at S/D = 1.1. The temperature profiles presented in Figure 4-40 follow the same trend; higher temperatures were attained with the triangular array. This is not surprising since, with the in-line array, more of the "flame surface" is exposed to cool recirculation and can "see" the furnace walls than with the triangular array.

When the total air supply is split between the burner throat and the common secondary duct for the low momentum Type B flames the assumption that the fuel air mixing pattern is independent of the burner spacing may be no longer valid. This is because the flow through the secondary duct will be influenced by the relative position of the burners. Consequently, the decreased emission at small burner spacings with Type B flames is probably associated with non-uniform air distribution around the burners.

4.3 An Investigation to Assess the Use of a Television Pyrometer to Control Low Emission Burners

This section presents the results of a 3 day test conducted to determine whether a Television Pyrometer system could be used as part of a control sequence for a low NO_x burner system. This system was developed by Hartel(4.4) at the University of Stuttgart.

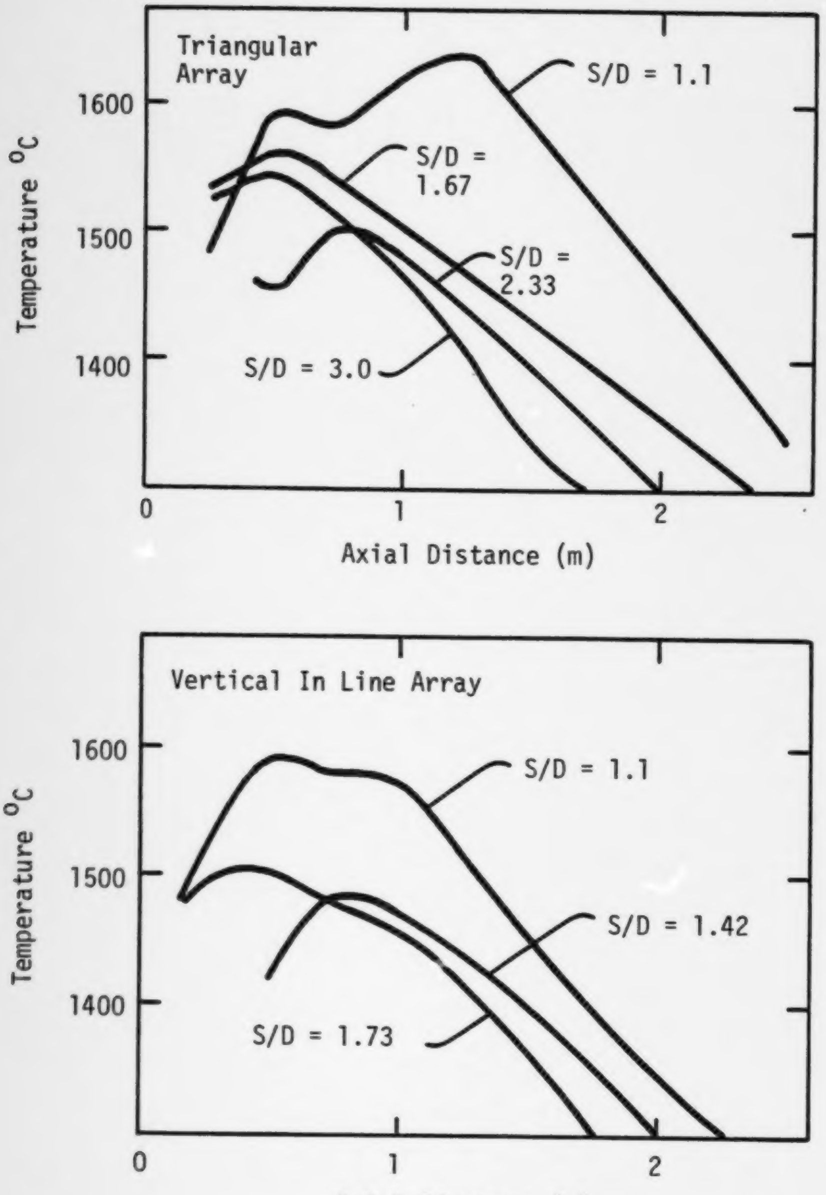

Figure 4-40. The Influence of Burner Spacing on Temperature Profiles Measured Along a Flame Axis (Type A Burner)

4.3.1 Description of the Television Pyrometer (TVP)

A schematic illustration of the composite units of the TVP is given on Figure 4-41. The instrument setup consits of five electronic units:

- A commercial TV camera
- An intensity switch
- An area integrator
- An auxiliary generator
- A commercial black and white or color TV monitor.

The TV camera views the flame through an optical filter and transforms the flame image into an electrical signal, the videosignal. This videosignal contains all the optical information from the object which penetrates the optical filter. Entering the intensity switch, the signal is modified by four comparators which subdivide the flame image into areas of four intensity ranges, each of which is displayed on the TV monitor in either four different gray shadings or, when a color TV monitor is used, in four different colors. The threshold value of each comparator can be varied continuously in the full range between 0 and 100 percent; however, during this test series, the intensity distribution was kept constant as indicated in Table 4-4.

Table 4-4. Selected Ranges of Intensity Distributions

Comparator No.	Intensity Range	Colored Display	Black & White Display
1	0 - 25%	blue	dark grey
2	25 - 50%	red	medium grey
3	50 - 75%	yellow	light grey
4	75 - 100%	white	white

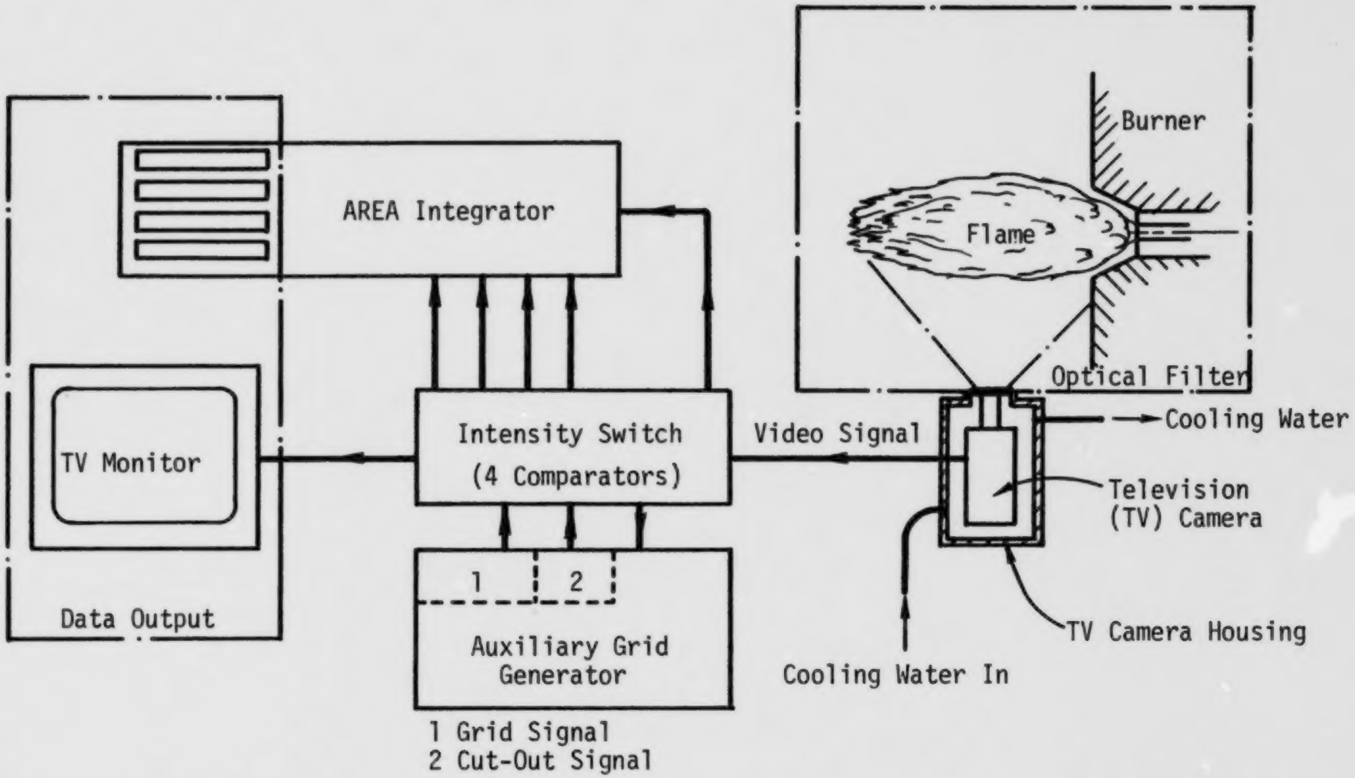
Burner
Flame
Optical Filter
Cooling Water
Television
(TV) Camera
TV Camera Housing
Cooling Water In
Video Signal
AREA Integrator
Intensity Switch
(4 Comparators)
1
2
Auxiliary Grid
Generator
1 Grid Signal
2 Cut-Out Signal
TV Monitor
Data Output

Figure 4-41. Schematic Setup of the Composite Units of the Television Pyrometer (TVP)

An integration of the number of screen points which lie within each range of equal intensity and the total number of points within the flame image on the screen can be carried out by the area integrator.

The auxiliary generator permits the display of an electronic grid on the TV monitor which gives the observer a visual dimensional scale. Furthermore, it allows undesired parts of the monitor screen to be electronically cut out. This allows an intensity analysis to be confined to one flame even when more than one flame lies within the angle of the viewer of the TV camera.

A detailed description of the TVP including the electronic circuits is given by Hartel.(4.4)

4.3.2 Connection Between the Videosignal and the Intensity Distributions and Flame Properties

Before trying to correlate the videosignal or the intensity distributions with NO-flue gas concentration measurements, it is important to assess the nature of the videosignal and its connection to the properties of the flame. Ordinary TV cameras operate in the visible part of the spectrum, similarly to the human eye, which lies in between the 0.4 and 0.8 um wavelength range which falls within the wavelength range encompassed by "thermal radiation" which is approximately 0.4 to 5 μm. Thermal radiation is defined as radiant energy emitted by a medium that is due solely to the temperature of the medium. It can therefore be expected that the videosignal is a function of the temperature of the object seen by the TV camera.

For an object which has the radiation properties of a black body ($\varepsilon = 1$) the emitted radiation intensity can be calculated from the temperature by Planck's law:

$$I\lambda = a \frac{\lambda^{-5}}{e^{\frac{b}{\lambda T}} - 1} \qquad (1)$$

where

I is intensity

λ is wavelength

T is the temperature, and
a and b are constants

By approximating the transmittance curve of the optical filter and the TV camera with a hat function between the wavelengths in consideration (λ_1, λ_2) (see Figure 4-42), one can write for the videosignal (Voltage U):

$$U = A \int_{\lambda_2}^{\lambda_1} I_\lambda \, d_\lambda \qquad (2)$$

where

U is the voltage, and
A is the amplitude of transmittance

When Planck's law is replaced by Wien's law - the 1 in the denominator of equation 1 disappears ($e^{b/\lambda t} >> 1$) - then the integration of equation 2 yields:

$$U = A \cdot \frac{aT}{b^{\lambda 3}} \; e^{\frac{-b}{\lambda t}} \left[1 + 3 \frac{T\lambda}{b} + 6 \left(\frac{T\lambda}{b}\right)^2 + 6 \left(\frac{T\lambda}{b}\right)^3\right] \Bigg/_{\lambda_1}^{\lambda_2} \qquad (3)$$

Equation 3 describes the relation between the videosignal and the temperature for a black body emitter under the above mentioned assumptions. For the spectral region between $\lambda_1 = 0.58\ \mu$ and $\lambda_2 = 0.78\ \mu$ a comparison of the actual videosignal with the signal calculated by Equation 3 is shown in Figure 4-43. The agreement between prediction and measurement is very good and indicates that the TVP can be used for the detection of surface temperatures of black emitters. It can also be applied to measure the temperature of gray emitters when their emissivity (ε) is known.

Non-luminous gas flames, however, have neither black nor gray radiation properties. The spectral nature of radiation from gases is very different from solid body emission as they emit only at certain frequency ranges of the spectrum. Furthermore, gas flames are not surface but volume emitters. Unfortunately, those different radiation characteristics of gases make it virtually impossible to relate the radiation intensity arriving at the TVP from a gas flame (and such as the videosignal) to a local temperature in

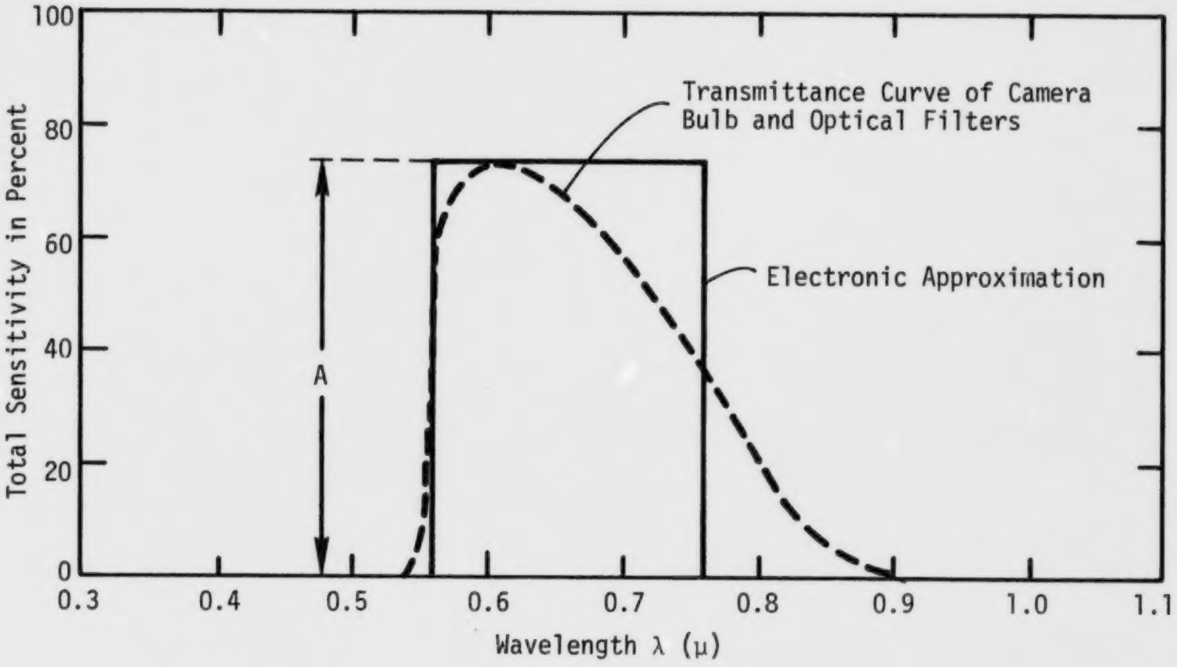

Figure 4-42. Approximation of the Transmittance of the Optical Filter ($\lambda = 0.58 - 0.78\ \mu$) and the TV Camera by a Hat Function.

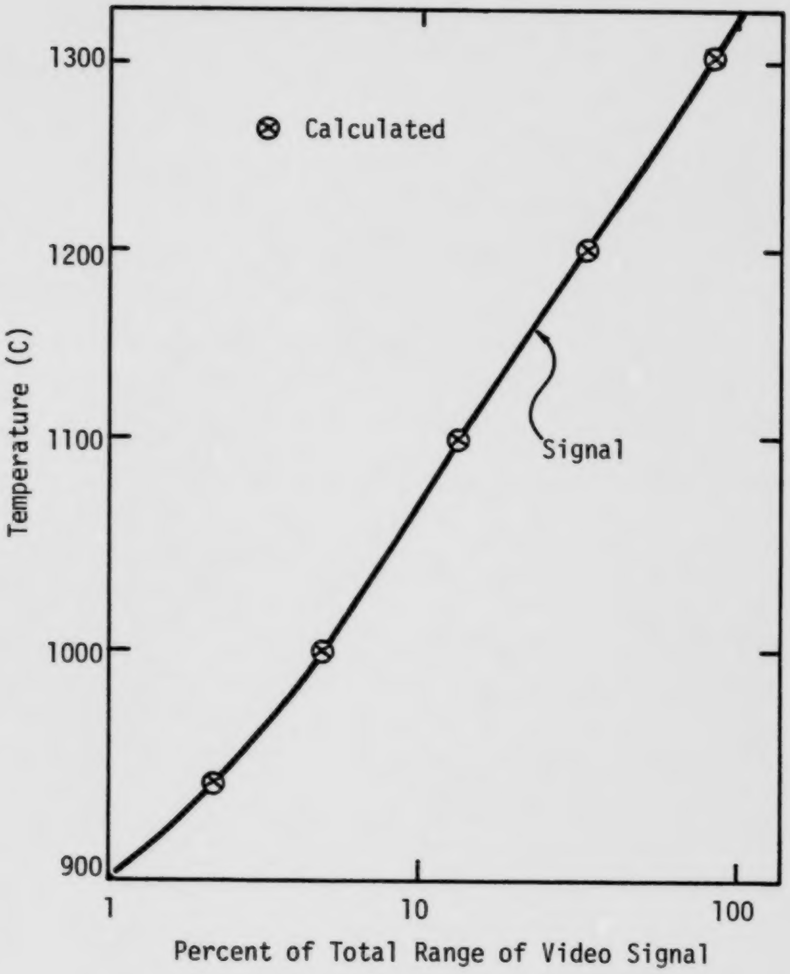

Figure 4-43. Comparison Between Calculated (Eqn. 3) and Measured Video Signal.

the flame.

The most important contributions to the thermal emission from gas flames in furnaces come from the band radiation of water vapor (H_2O), carbon dioxide (CO_2) and to a smaller amount from carbon monoxide (CO). Apart from a weak emission in the visible frequency range (blue) which is characteristic for the combustion of CO, these gases emit solely in the infra-red region of the spectrum. The lowest frequency bands center around 1.1 μm for H_2O and 1.4 μm for CO_2. Also, at relatively low temperatures (600 - 800°C) black or gray surface emitters have a very small radiation intensity in the visible range of the frequency spectrum. At these temperatures, the intensity maximum lies in the infra-red and their appearance in an enclosure is dark red. Refractory materials, although their radiation properties can be approximated by a gray body assumption for engineering calculations of radiation heat transfer, are not "gray" in reality. Their monochromatic emissivity at short wavelengths (λ) is usually much lower than their average emissivity, in some cases as low as 0.1 to 0.2 in the region of $\lambda \approx 0.5$ μ.

The above considerations indicate that all the visible light emitted by non-luminous gas flames has to be attributed to other sources than H_2O, CO_2, and CO band radiation. Furthermore, the influence of furnace wall radiation on the videosignal at relatively low temperatures (600 - 800°C) can practically be excluded because it contributes less than 1 percent of the video signal. The light emission detected by the TVP also includes emission from intermediate radicals produced during the combustion process (i.e., CH^* around 0.43 μm and C_2^* around 0.52 μm). Consequently, the TVP signal is dependent both upon temperature and the concentration of certain radical species. That applies even more for the videosignal when an optical filter is used in front of the TV camera (Figure 4-41) which absorbs all but the light frequency range between 0.38 μ and 0.58 μ (Figure 4-44).

The formation of NO in natural gas (NG) flames in furnaces with a bulk gas temperature below 1300°C occurs primarily in the flame zone by two mechanisms:

- The reactions commonly referred to as the extended Zeldovich mechanism

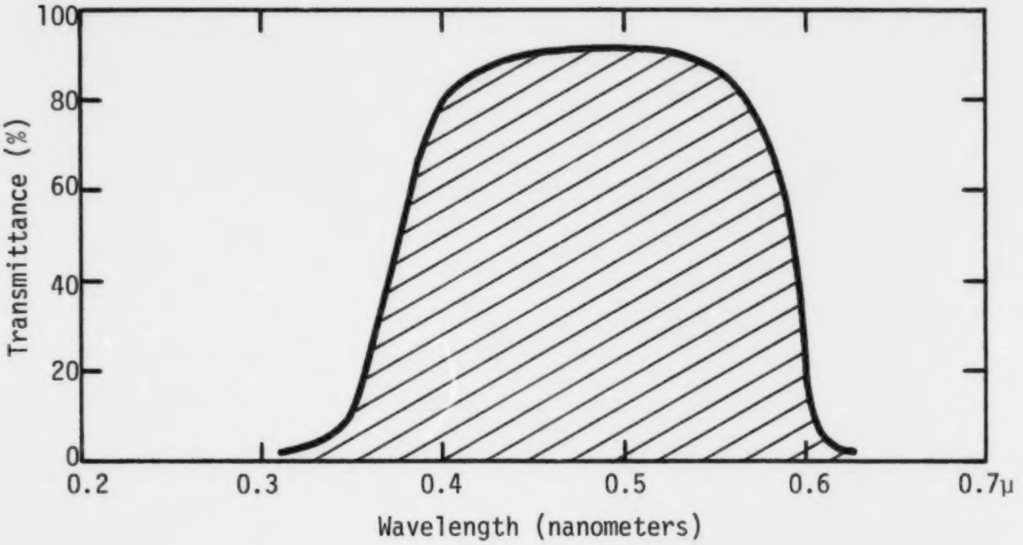

Figure 4-44. Transmittance Characteristic of the Optical Blue Filter Used in Front of the TV Camera.

$$O + N_2 \rightleftarrows NO + N$$

$$N + O_2 \rightleftarrows NO + N$$

$$N + OH \rightleftarrows NO + H$$

- Breaking of the N $\equiv$-N bond by hydrocarbon fragments

$$CH + N_2 \rightarrow HCN + N$$

In summary, it can be stated:

- The videosignal obtained from the TVP observing non-luminous natural gas flames in enclosures with a moderate wall temperature of 600 - 800 C through an optical filter restricting the light transmission to $\lambda = 0.38\ \mu - 0.58\ \mu$ can mainly be attributed to the light emission from exited CH and C_2 radicals. The intensity distribution displayed on the TV monitor (four different ranges) and evaluated by the area integrator (Figure 4-41) is a function of the local gas temperature and the concentration of CH and C_2 radicals. In the flame front, these radicals are usually present in high super equilibrium concentrations.
- The NO-formation in non-luminous NG flames is a flame phenomenon and is strongly temperature dependent. Also as flame radicals such as C_2 and CH influence NO formation, it can be expected that there is a substantial interrelation between the videosignal or intensity distribution respectively and the nitric oxide emission from such flames.

4.3.3 Experimental Arrangements and Flames Investigated

General Setup

The tests were performed in the horizontal No. 1 furnace at IJmuiden, with the burners firing along the furnace axis. This furnace is a refractory box of approximately 2 x 2 m cross-section and 2.26 m length. To ensure moderate refractory temperatures, a series of water-cooled double loop pipe systems were fitted along the furnace side walls to act as a heat sink. The TV camera of the TVP was placed in a water-cooled metal housing in front of the horizontal slots at the furnace side wall and directed towards the burner wall. As indicated before, an optical filter, the characteristics of which are given on Figure 4-44 was mounted in front of the camera lens. The camera aperture was kept at 3.5 throughout these test cases.

Burner Design

The burner described in Section 3 was used in this study and the natural gas was supplied through a central fuel lance. The fuel injectors are shown in Figure 4-45.

Flame Type

The influence of burner parameters on the NO emission from large turbulent NG-flames was extensively investigated during the earlier EPA studies.(4.1) During these investigations, it was found that the mixing between fuel, oxidant, and recirculating combustion products can substantially influence the NO emission. The burner permits significant changes in the mising process by varying the swirl intensity, fuel injection method, and injection position; the conditions were chosen based upon previous experience with three geometrically different burner configurations:

- RUN 7, radial injector positioned at the burner exit (see Figure 4-45);
- RUN 8, radial injector positioned in the burner throat;
- RUN 9, divergent injector positioned in the burner throat.

The mass input into the furnace was kept constant for all nine flames. 200 Nm^3/h NG corresponding to 1.76 MW thermal input were fired at an excess air level of 5 percent. A listing of the input conditions and the NO flue-gas concentrations as measured with a chemiluminescent analyzer for the 9 flames is presented in Table 4-5.

4.3.4 Experimental Results

Two minutes of the videosignal of each flame were recorded on a video recorder to allow the evaluation of the measurements to be carried out after the test period. For the analysis of the signal the following procedure was adopted:

- From each two minutes record a random distribution of fifty frames

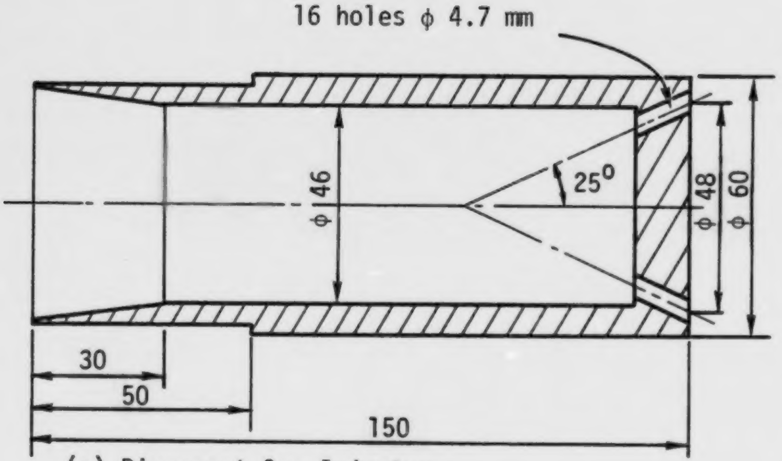
16 holes φ 4.7 mm
φ46
25°
φ48
φ60
30
50
150

(a) Divergent Gas Injector

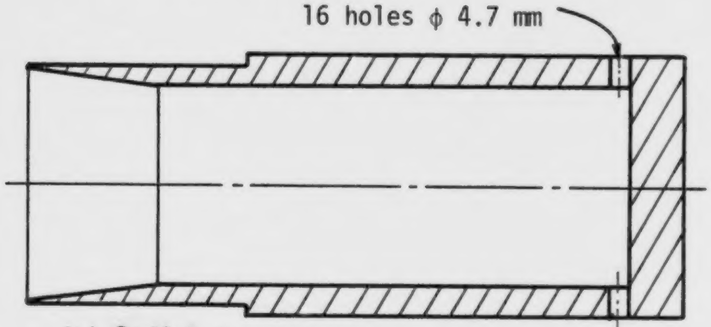
16 holes φ 4.7 mm

(b) Radial Gas Injector

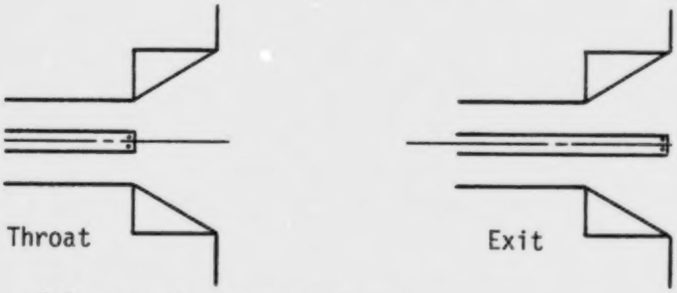
Throat
Exit

(c) Position of Injector

Figure 4-45. Construction and Positioning of the Natural Gas Injectors as Used for the TVP-Test.

Table 4-5. Input Conditions in the Flames Investigated and Nitric Oxide Concentrations Measured in the Fluegas

Condition / Run	Swirl No. S	Injector Type	Injection Position	Massflow in kg/h		Fluegas NO concentration in ppm as Measured
				NG	Air	
7.5	0.2	radial	burner exit	159	2160	56
7.2	0.73	radial	burner exit	159	2160	75
7.3	1.49	radial	burner exit	159	2160	38
8.1	0.3	radial	burner throat	159	2160	55
8.2	0.73	radial	burner throat	159	2160	46
8.3	1.49	radial	burner throat	159	2160	48
9.1	0.17	divergent	burner throat	159	2160	78
9.2	0.73	divergent	burner throat	159	2160	44
9.3	1.49	divergent	burner throat	159	2160	35

which were analyzed for the area weighted intensity distribution. The results referred to in this report represent the arithmetic mean values obtained from fifty single frames.

The number of picture points was chosen as the dimension for the total area and the area distribution within the four intensity ranges. During the evaluation of the results, the threshold values of the four comparators which determine the intensity distribution were changed to compensate for the loss in the total videosignal to produce approximately the same size of areas of equal intensity as the original setting with the real time signal.

The TVP measurements have been analyzed for all nine flames listed in Table 4-6. The results are presented in Figures 4-46a, 4-47a, and 4-48a where the integrated areas are plotted against the intensity distribution on a semilogarithmic scale against the swirl intensity for identical geometrical burner configurations.

In Figures 4-46b, 4-47b, and 4-48b the corresponding nitric oxide flue gas concentrations are given as a function of the swirl intensity. As one would expect from the considerations outlined earlier, comparison of the TVP intensity distribution with the corresponding NO measurements indicates little interrelation between the signals in the low intensity ranges (i.e., 0 - 40 percent). For two flame series (RUN 7 and 9) the highest intensity range analyzed (60 - 100 percent) is, however, similar to the NO concentrations strongly influenced by the swirl intensity.

The correlation between the integrated areas of TVP intensities in the ranges 40 - 100 percent and 60 - 100 percent of the total signal with the flue gas NO concentrations is illustrated in Figure 4-49. Only the 60 - 100 percent intensity range has a sufficiently strong correlation with the nitric oxide concentration to be useful for practical purposes. Unfortunately, promising results were achieved for two burner configurations only, namely RUN 7 and RUN 9 whereas RUN 8 deviates from the expected tendency--larger high intensity areas independent of swirl number.

Although RUN 7 and RUN 9 follow the expected tendency, the NO-TVP intensity values do not fall on one line. For premixed flat flames one could assume that a direct relationship would exist between NO emission

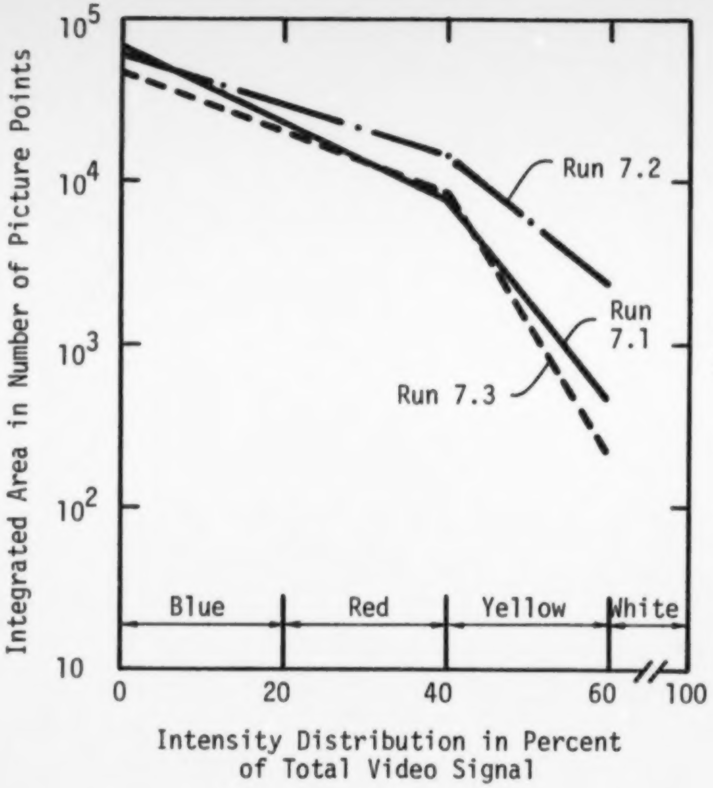

Figure 4-46a. Intensity Distribution Within the Range of the Total Video Signal from the TVP for Run 7.1, 7.2, and 7.3.

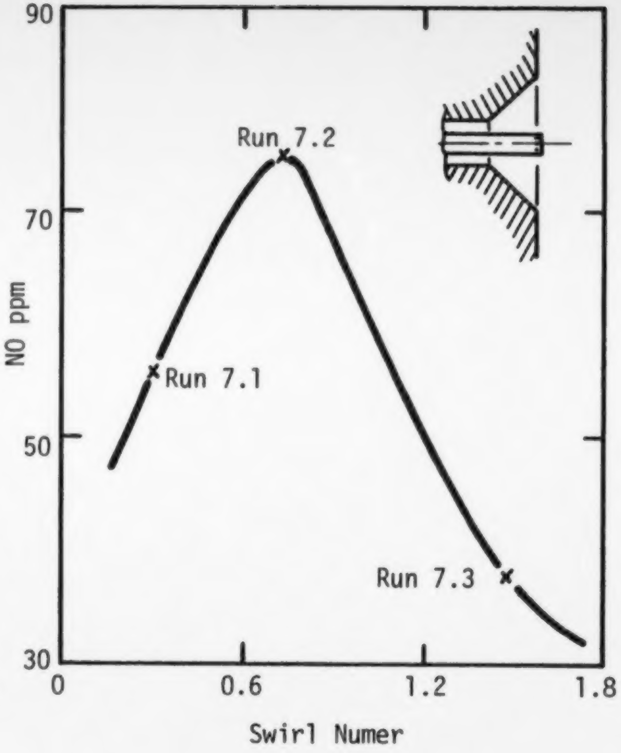

Figure 4-46b. NO Flue Gas Concentrations as Measured For Run 7.1, 7.2, and 7.3.

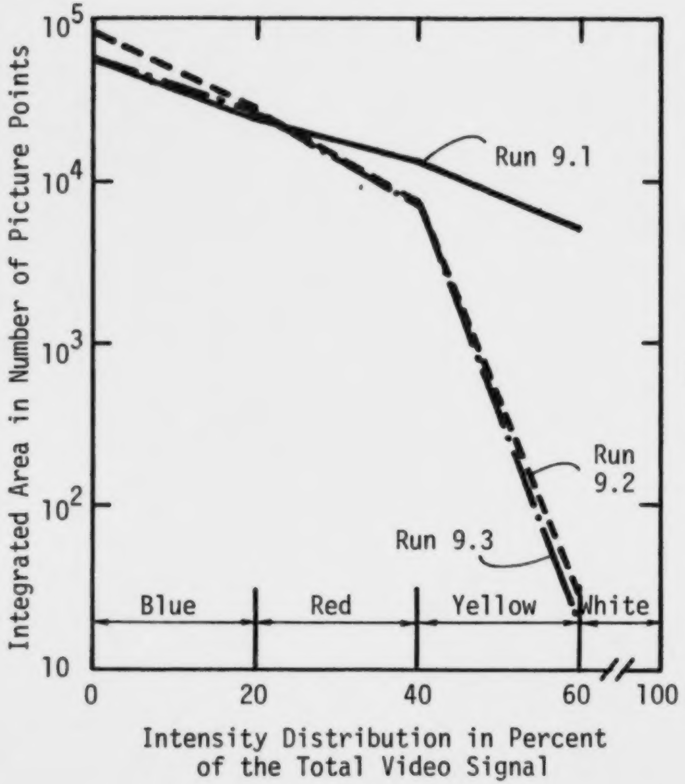

Figure 4-47a. Intensity Distribution with the Range of the Total Video Signal from the TVP for Run 9.1, 9.2, and 9.3.

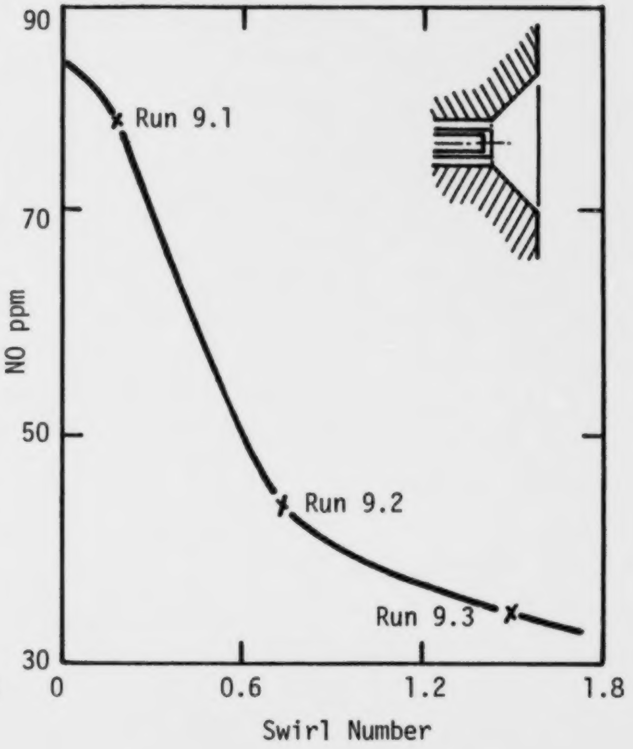

Figure 4-47b. NO Flue Gas Concentrations as Measured for Run 9.1, 9.2, and 9.3.

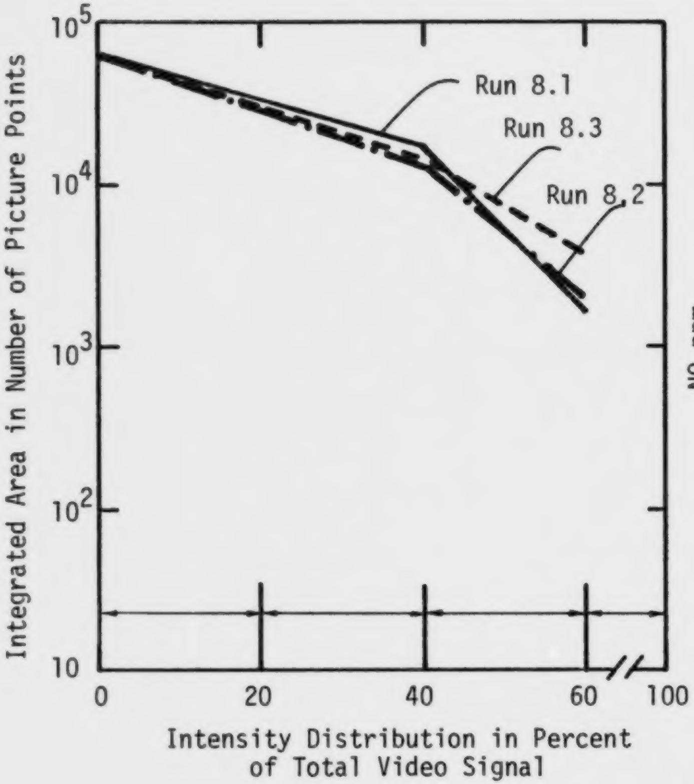

Figure 4-48a. Intensity Distribution Within the Range of Total Video Signal from the TVP for Run 8.1, 8.2, and 8.3.

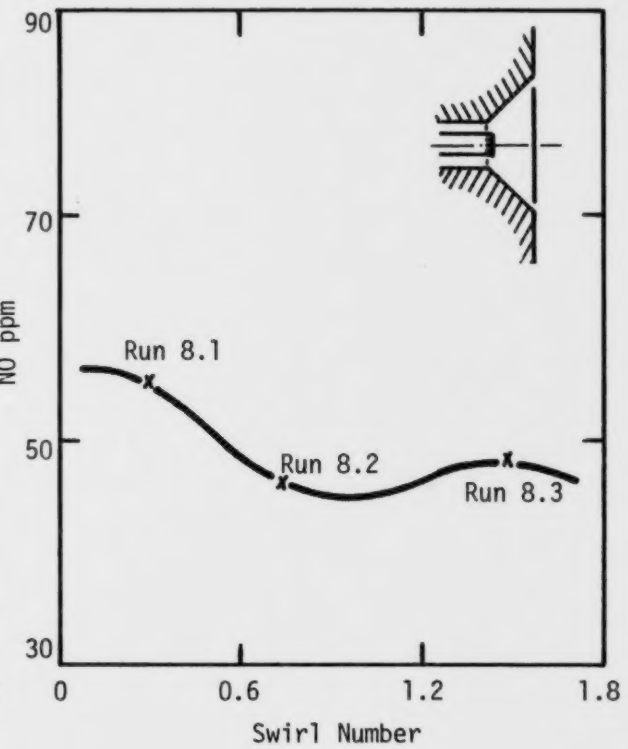

Figure 4-48b. NO Flue Gas Concentrations as Measured for Run 8.1, 8.2, and 8.3.

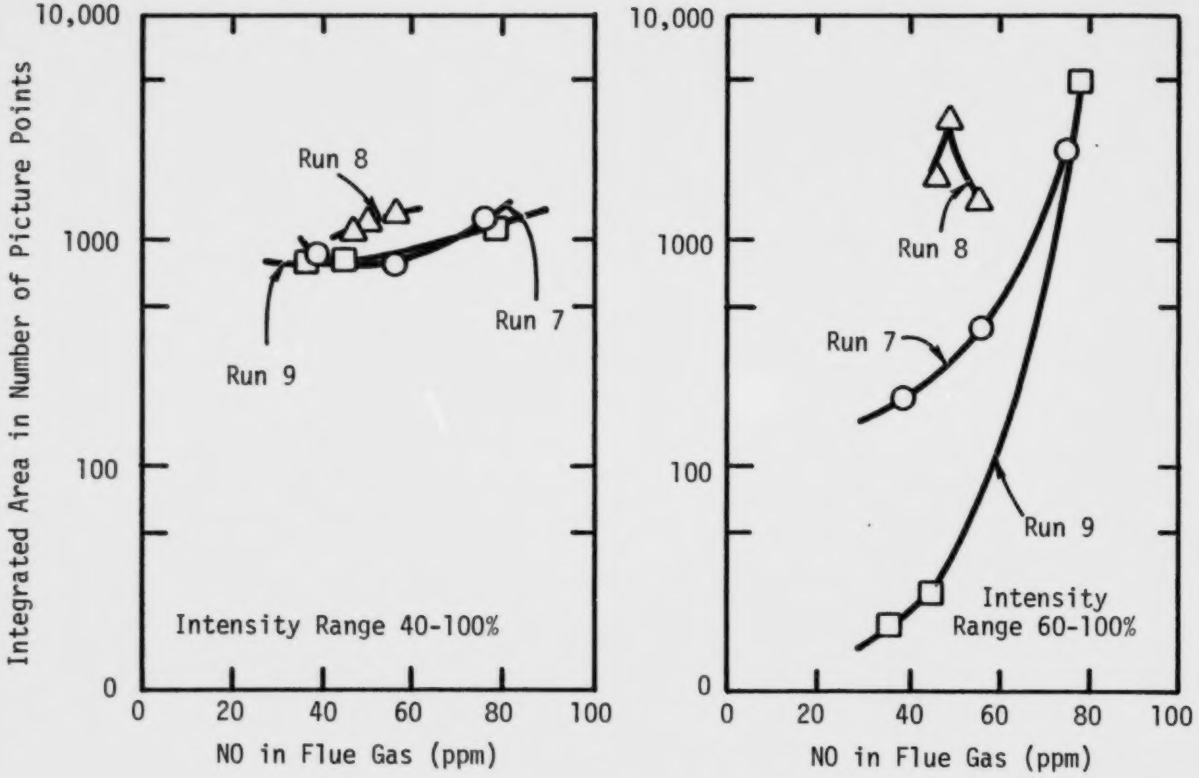

Figure 4-49. Correlation of TVP Intensity Data with Flue Gas Nitric Oxide (NO) Concentrations for Two Intensity Ranges; 40-100% and 60-100% of Total Video Signal.

and TVP intensity. The flames investigated here were, however, turbulent diffusion flames produced with various burner configurations and with different geometries and flow patterns. As the radiant characteristics of non-luminous NG flames are strongly influenced by the flame volume (pathlength of radiating gases), which does not apply to the same extent for the NO formation, one cannot expect a direct relation between both. Nevertheless, the correlation found for RUN 7 and RUN 9 is of great practical importance as it indicates the potential application of the TVP technique in external burner control for flames of similar shape produced with the same burner. The latter limitation does not impede the industrial use of the TVP since in most practical multiple burner systems, identical burners with similar thermal heat inputs are employed.

Due to the radial fuel injection which enhances early mixing between fuel and oxidant, the flames of RUN 8 were all stabilized inside the burner quarl, only a part of which was in the direct view of the TV camera (Figure 4-50). Thus, a substantial part of the flame root, where a significant amount of NO can be formed, was out of sight of the TV camera and, therefore, could not contribute to the videosignal.

Particularly for the flame of RUN 8.1, it can be expected that near stoichiometric combustion accompanied by high NO formation rate and light emission occurs within the invisible part of the quarl. As a result of the very low swirl intensity, the internal recirculation zone is weak which, together with the good mixing between fuel and air due to the radial fuel injection, leads to near stoichiometric combustion and high flame root temperatures. By increasing the swirl intensity (RUN 8.2 and 8.3), the mass of the internally recirculating combustion products increases, resulting in a dilution of the combustible mixtures and lower flame root temperatures. Therefore, the shadow effect of the burner quarl has less influence on the correlation of the NO/TVP intensity at higher swirl levels. In addition, swirl level will have a reduced effect upon NO when the radial fuel injector is placed in the throat, because fuel air mixing is rapid and controlled by the fuel injector.

This hypothesis is confirmed by the isotherms plotted in Figure 4-51 (RUN 7), Figure 4-52 (RUN 8) and Figure 4-53 (RUN 9):

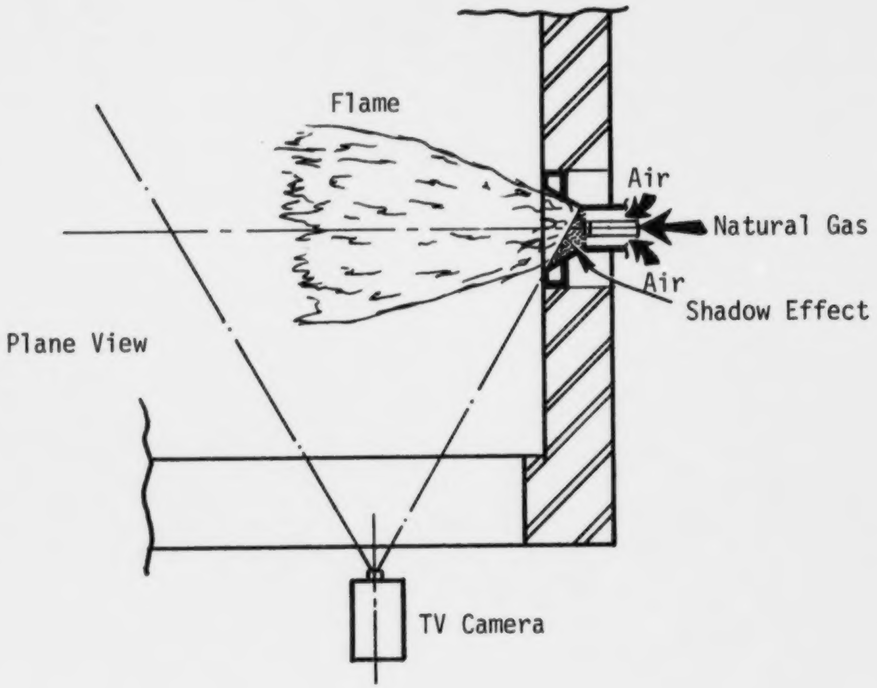
Flame
Air
Natural Gas
Air
Shadow Effect
Plane View
TV Camera

Figure 4-50. The Burner Quarl as Viewed by the TV Camera (Shadow Effect).

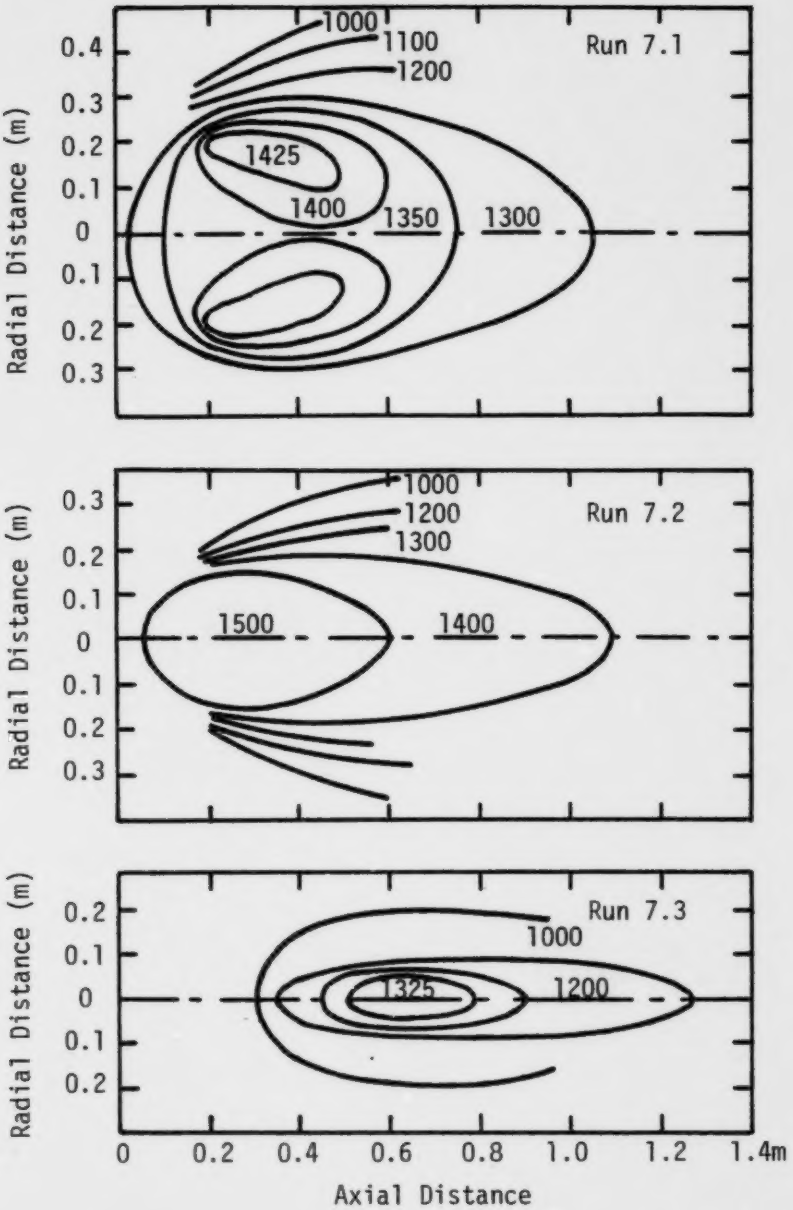

Figure 4-51. Isotherms (C) in the Flames of Run 7 as Measured by a Suction Pyrometer.

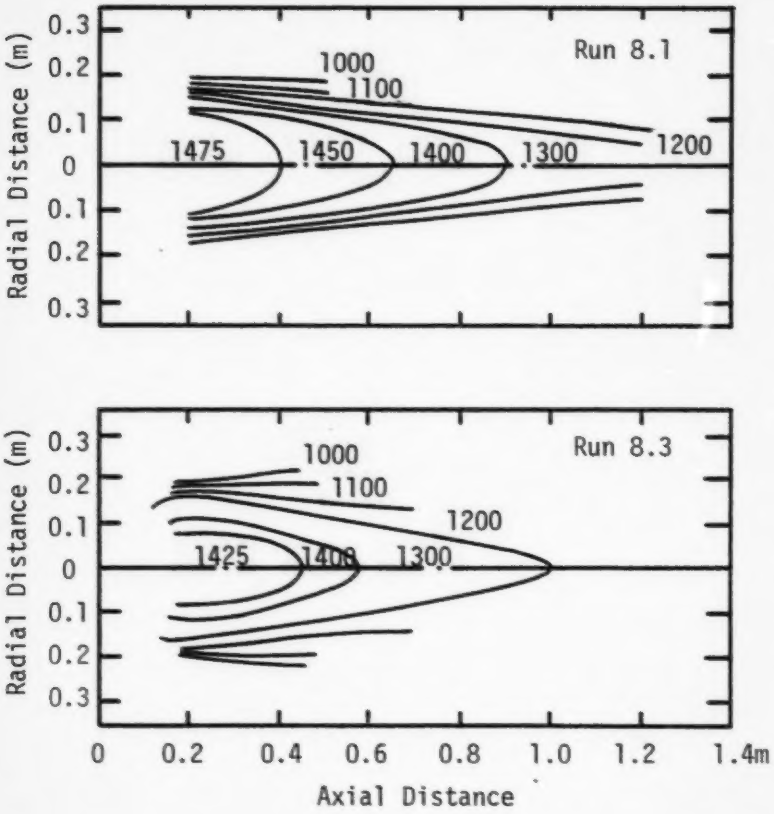

Figure 4-52. Isotherms (C) in the Flames of Run 8 as Measured by a Suction Pyrometer.

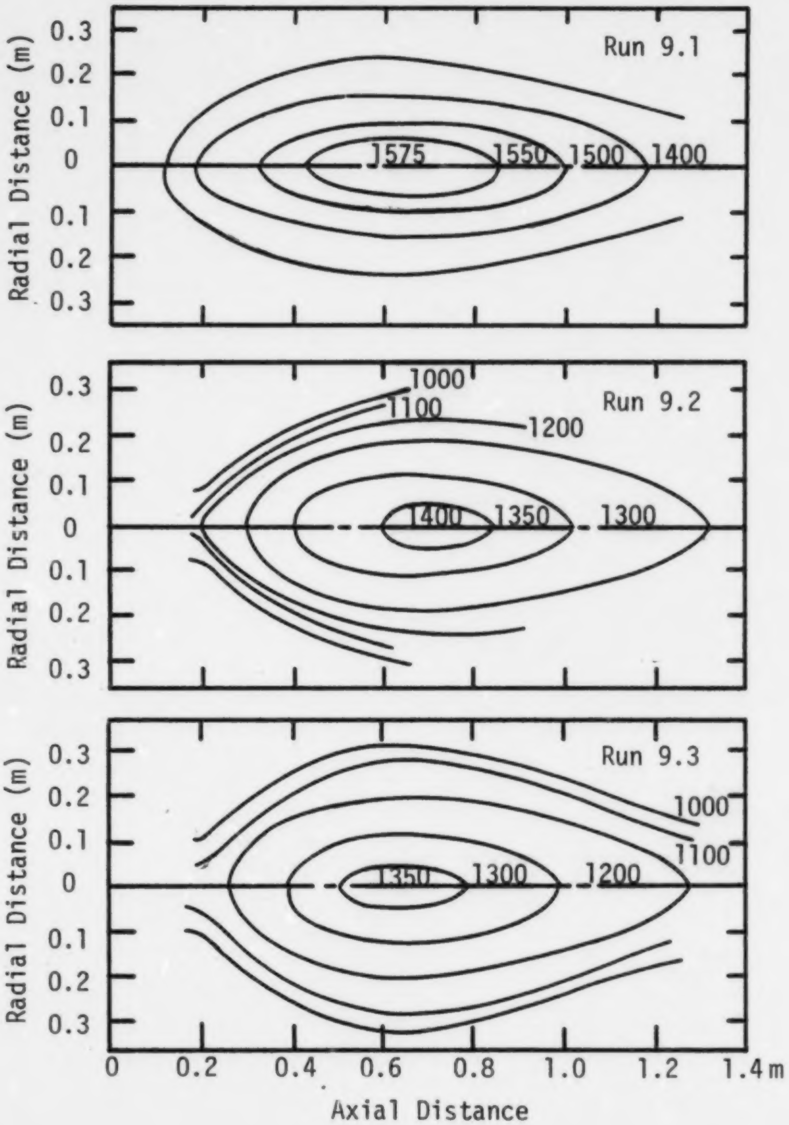

Figure 4-53. Isotherms (C) in the Flames of Run 9 as Measured by a Suction Pyrometer.

- A comparison of the isotherms between the flames of RUN 8.1 and 8.3 indicates that the maximum temperature for both flames lies within the quarl.
- The flames of RUN 9 were also stabilized within the quarl and yet the correlation followed the expected trends. The reason lies in the divergent fuel injection which does not provide rapid mixing in the burner throat so most of the combustion occurs downstream of the burner quarl. That is shown by the isotherms (Figure 4-52) which clearly indicate a temperature maximum 0.4 to 0.9 m downstream of the burner.

4.3.5 Conclusions

The main objective of testing the television pyrometer (TVP) was to investigate its potential application as an external burner control for industrial furnaces fired by multiple burner systems. First results of the test have indicated that nitric oxide flue gas concentrations emitted by natural gas flames can be correlated with the data of the intensity distribution obtained by the TVP. However, better controlled experiments are required to establish correlation data for a wider range of burner and/or flame types, respectively.

It has been suggested that under the conditions considered in this study (non-luminous natural gas flames), the TVP mainly detects the light emission from exited CH and C_2 radicals. It, therefore, offers itself also for the control of other input parameters which influence the radical concentration and temperature, as for example the excess air level.

As the instrument does not come in contact with the flame, its application is not limited to gas flames. One can think of its application as a detector for thermal emission and also for the control of various input parameters in oil flames when the appropriate wavebands are selected by optical filters.

4.4 Detailed Measurements in Natural Gas and Coal Flames

During an earlier trial series detailed measurements were made in two natural gas and four pulverized coal flames to provide information of NO formation in turbulent diffusion flames. This section summarizes the results of these measurements and discusses the significance of the obervations. A complete listing of the data is presented in Appendix A.

4.4.1 Flame Conditions and Measurement Systems

The measurements were made in the IJmuiden furnace, with almost no cooling, and the burner was a moving block swirl burner which was described earlier. Table 4-6 lists the input conditions for the six flames. The radial hole injection system produces a flame on axial recirculation zone. The axial fuel injection produced flames which were stabilized by an annular recirculation zone. Thus, by selecting these conditions it was possible to determine the characteristics of both flame types for two fuels. Since the parametric studies had indicated the importance of primary air percentage with pulverized coal, two flames were measured (123 and 124) with different primary air flows.

Measurements were made of:

- Temperature. Suction pyrometers were used to measure temperature since these give an accurate direct reading of temperature. The temperature is measured by a thermocouple positioned on the axis of a system of shields and the gas whose temperature is to be measured is passed through the annular channels formed by the shields (see Figure 4-54). The shields serve a dual purpose:
    - they isolate the thermocouple from the surrounding radiation;
    - they protect the thermocouple from contamination by the furnace matter.
- Velocity. Measurements of magnitude and direction of the velocity were made with a hemi-spherical five hole pitot probe. These properties are determined from the measured pressure distribution around the head of the probe when it is placed in the flowing stream.

Table 4-6. Conditions for Detailed Flame Measurements

Flame No.	Fuel	Fuel Injection Type	Fuel Stream Velocity	Fuel Injector Location	Swirl Number	Primary % of Stoichiometric	Excess Air
119	Natural Gas	Radial Holes	200 m/sec	Throat	0.8	-	5
120	Natural Gas	Single Hole	380 m/sec	Throat	2.0	-	5
121	Coal	Radial Holes	54 m/sec	Throat	2.0	20	25
122	Coal	Single Hole*	38 m/sec	Throat	2.0	20	25
123	Coal	Single Hole	38 m/sec	Exit	2.0	30	10
124	Coal	Single Hole	38 m/sec	Exit	2.0	20	10

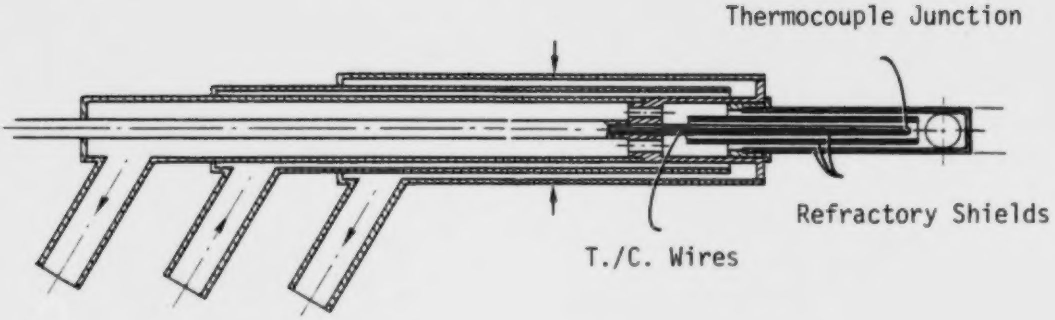
Thermocouple Junction
Refractory Shields
T./C. Wires

Figure 4-54. Suction Pyrometer with Replaceable Refractory Shields.

- Gas Concentration. A gas chromatograph was used to analyze for O_2, CO_2, CO, H_2, CH_4, C_2H_6, C_3H_8, and C_2H_4. NO and NO_x were measured by a chemiluminescent analyzer and special care was taken when extracting the gas samples from the furnace. Figure 4-55 shows the construction of the NO sample probe which was used for the gas flames. The water quench probe which is shown in Figure 4-56 was used to extract gaseous samples from coal flames for NO analysis.
- Solid Concentration. Two probe designs were used to determine solid concentrations and extract solid samples for analysis. In the regions of high solids loadings (i.e., in the initial stages of the flame) the probe shown in Figure 4-57 was used. A probe with a smalller volume filter was used for regions of low solids loadings (see Figure 4-58).

4.4.2 Results

Section 3 discussed the general characteristics of swirling turbulent flames. The data presented in Figures 4-59 through 4-63 illustrate these characteristics for natural gas and pulverized coal flames. Figure 4-59 compares the radial distribution (HP - horizontal position in m from the side wall; 1.00 indicates the burner and furnace axis) at 0.10 m from the firing wall (AD = .10). Flame 119 has an axial recirculation zone which corresponds to the high temperature region on the axis. Whereas flame 120 has a minimum temperature on the axis and the maximum temperatures are found in the annular recirculation zones. The different characteristics of the two flame types is also shown in the isotherms presented in Figure 4-60. Figures 4-61 and 4-62 present a similar comparison for flames 121 and 122 indicating that general flame characteristics are independent of fuel type.

Figure 4-63 compares radial profiles for flames 123 and 124 both of which are stabilized by annular recirculation zones. The difference in the two flames is that flame 123 has a greater percentage of primary air. It can be seen that this is reflected by the increased availability of oxygen on the flame axis. The exhaust NO levels measured for flames 123 and 124 were 625 ppm and 284 ppm, respectively. This reduction in emissions of greater than fifty percent was achieved by a small change in burner param-

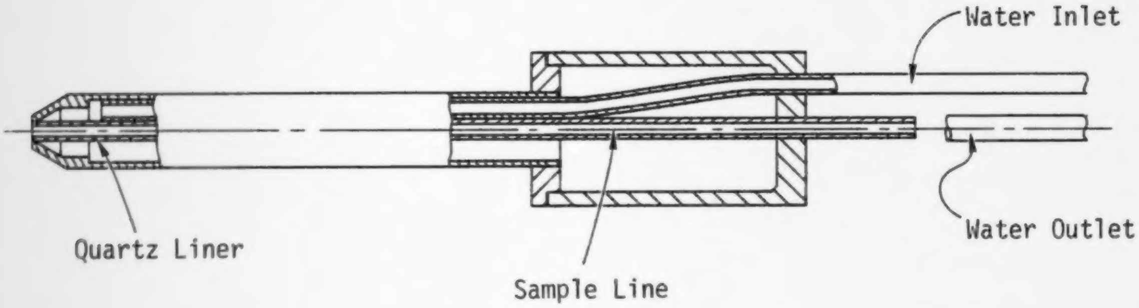
Water Inlet
Water Outlet
Quartz Liner
Sample Line

Figure 4-55. Water Cooled Quartz Lines Probe for Sampling from Gas Flames.

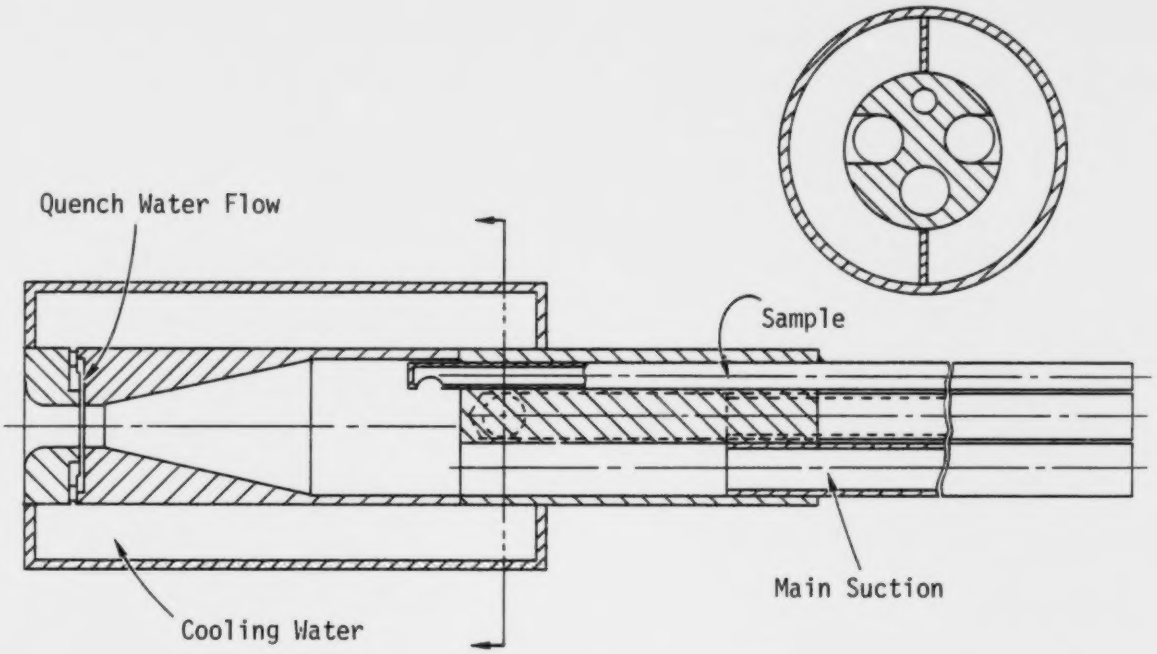
Quench Water Flow
Sample
Main Suction
Cooling Water

Figure 4-56. Water Quench Probe for NO Measurement.

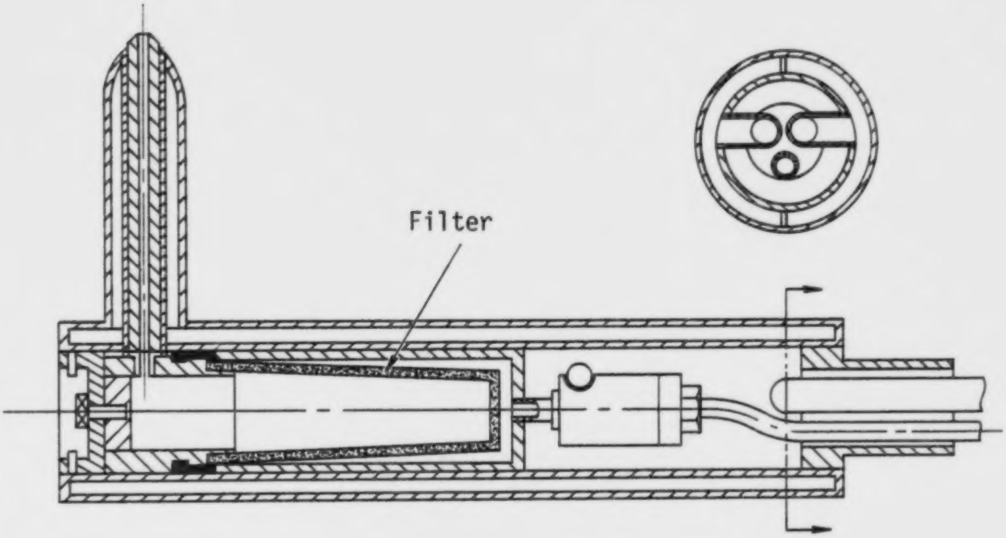

Figure 4-57. Solid Sampling Probe (High Loadings)

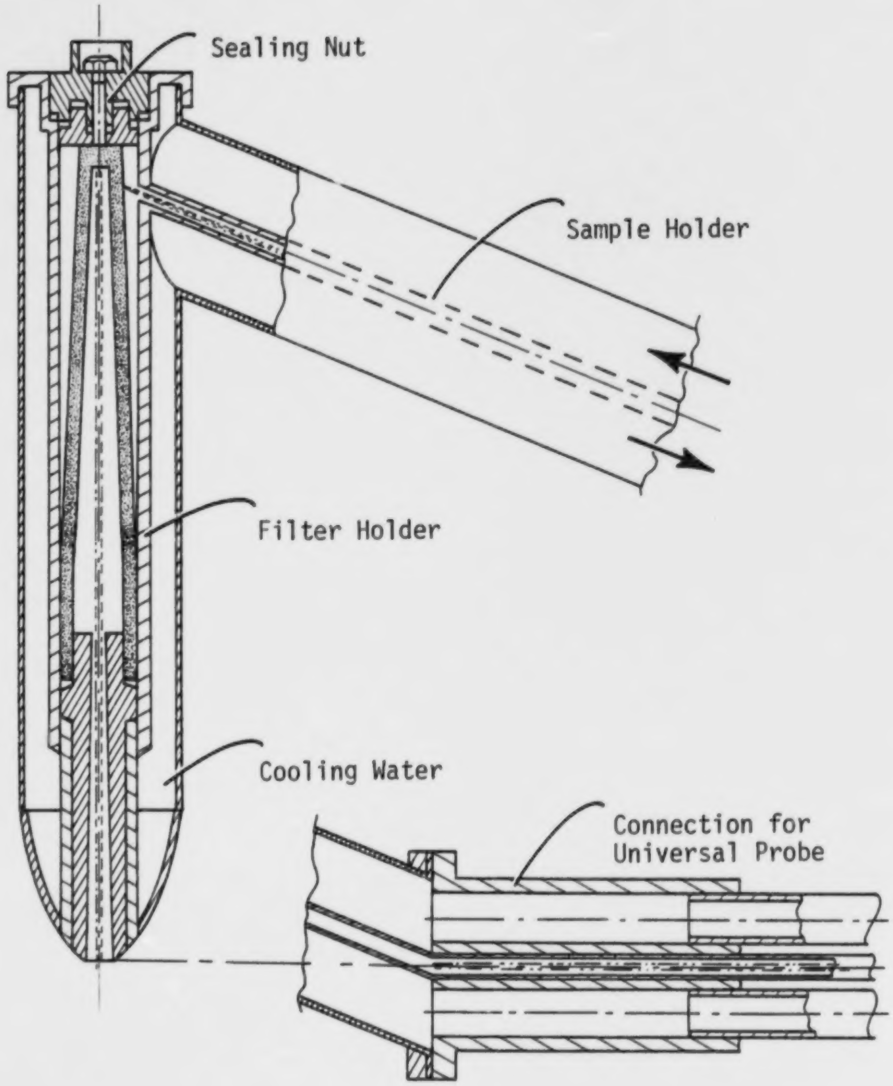
Sealing Nut
Sample Holder
Filter Holder
Cooling Water
Connection for
Universal Probe

Figure 4-58. Solid Concentration Sampling Probe (Low Loadings).

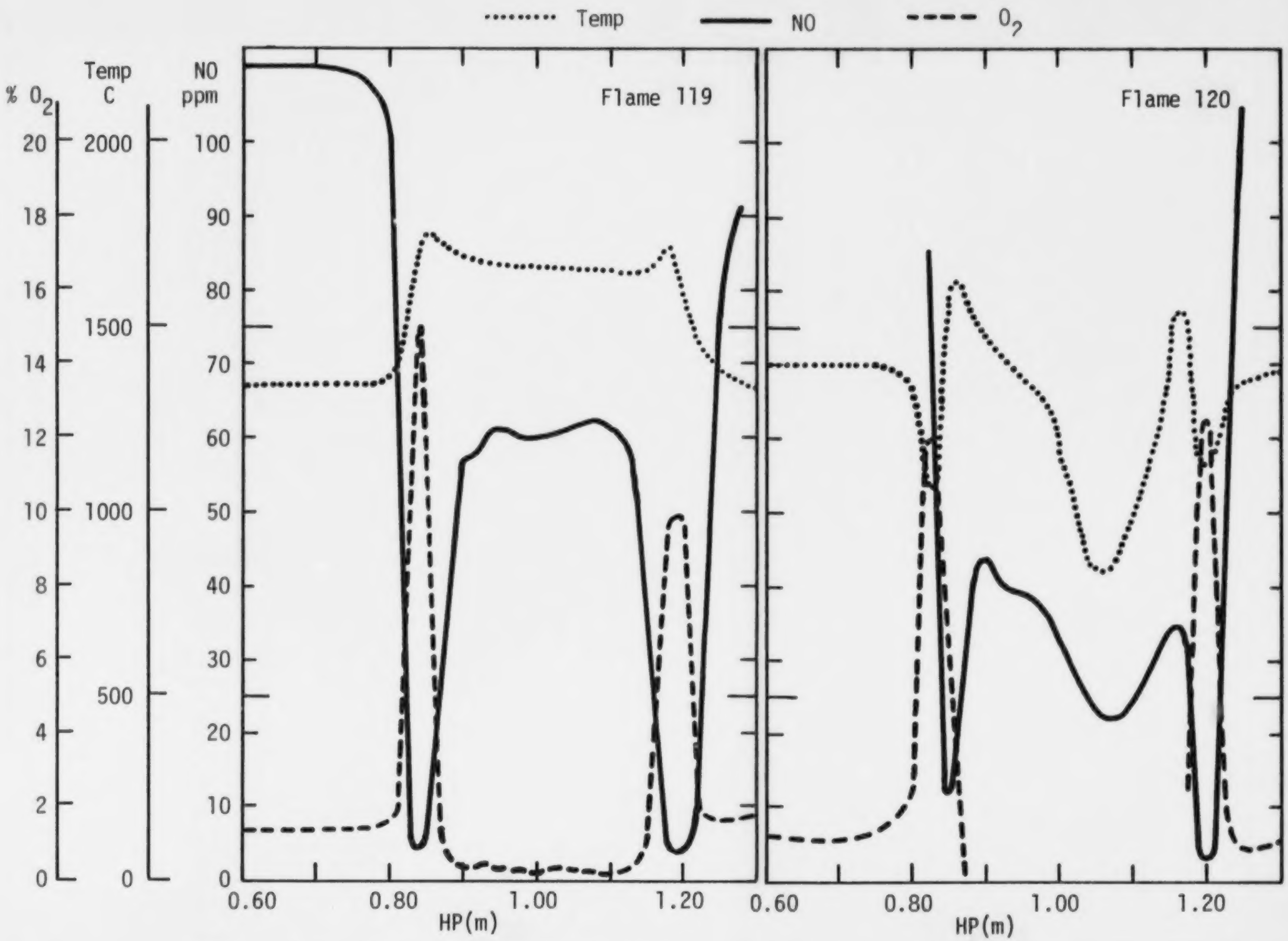

Figure 4-59. Radial NO, O_2 and Temperature Distribution in Natural Gas Flame.

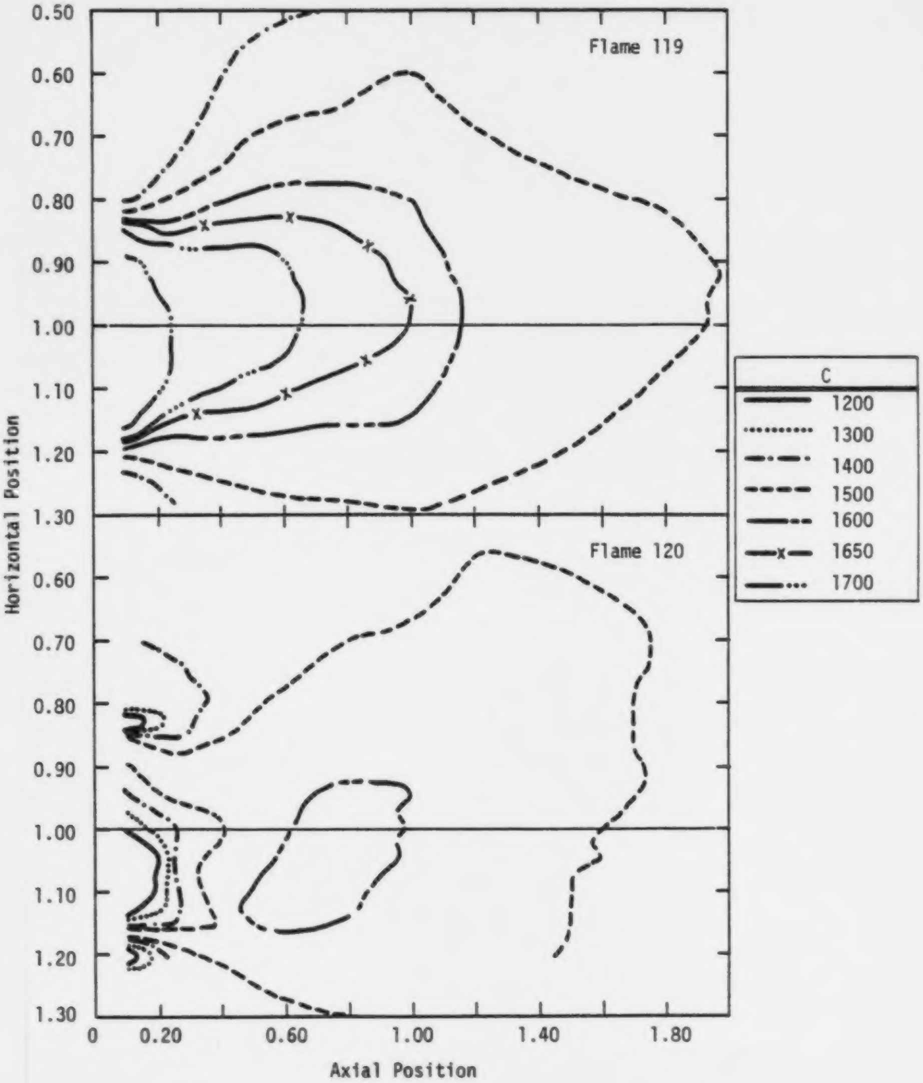

Figure 4-60. Isotherms Measured in Natural Gas Flames.

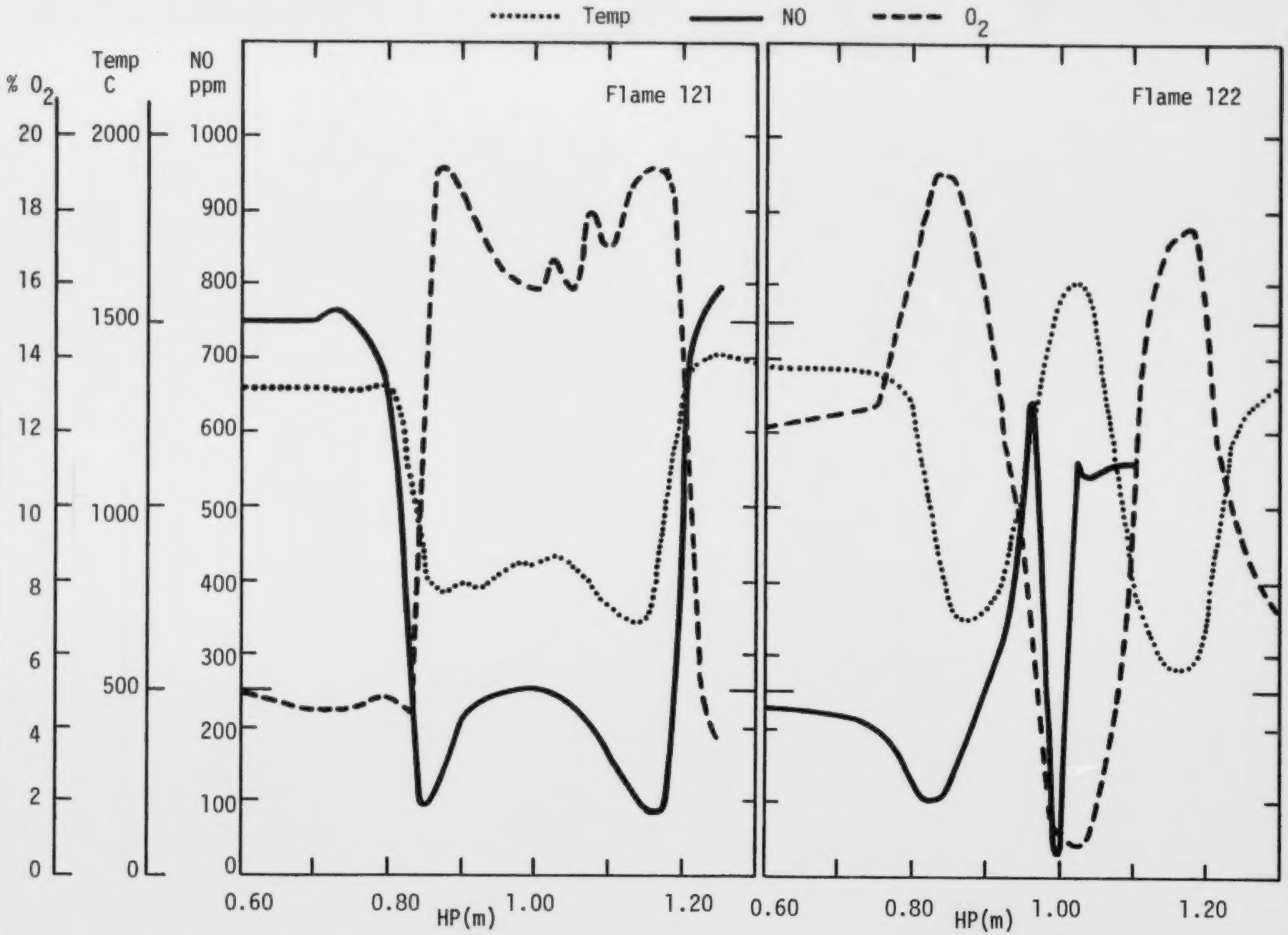

Figure 4-61. Radial Distributions of NO, O_2 and Temperature.

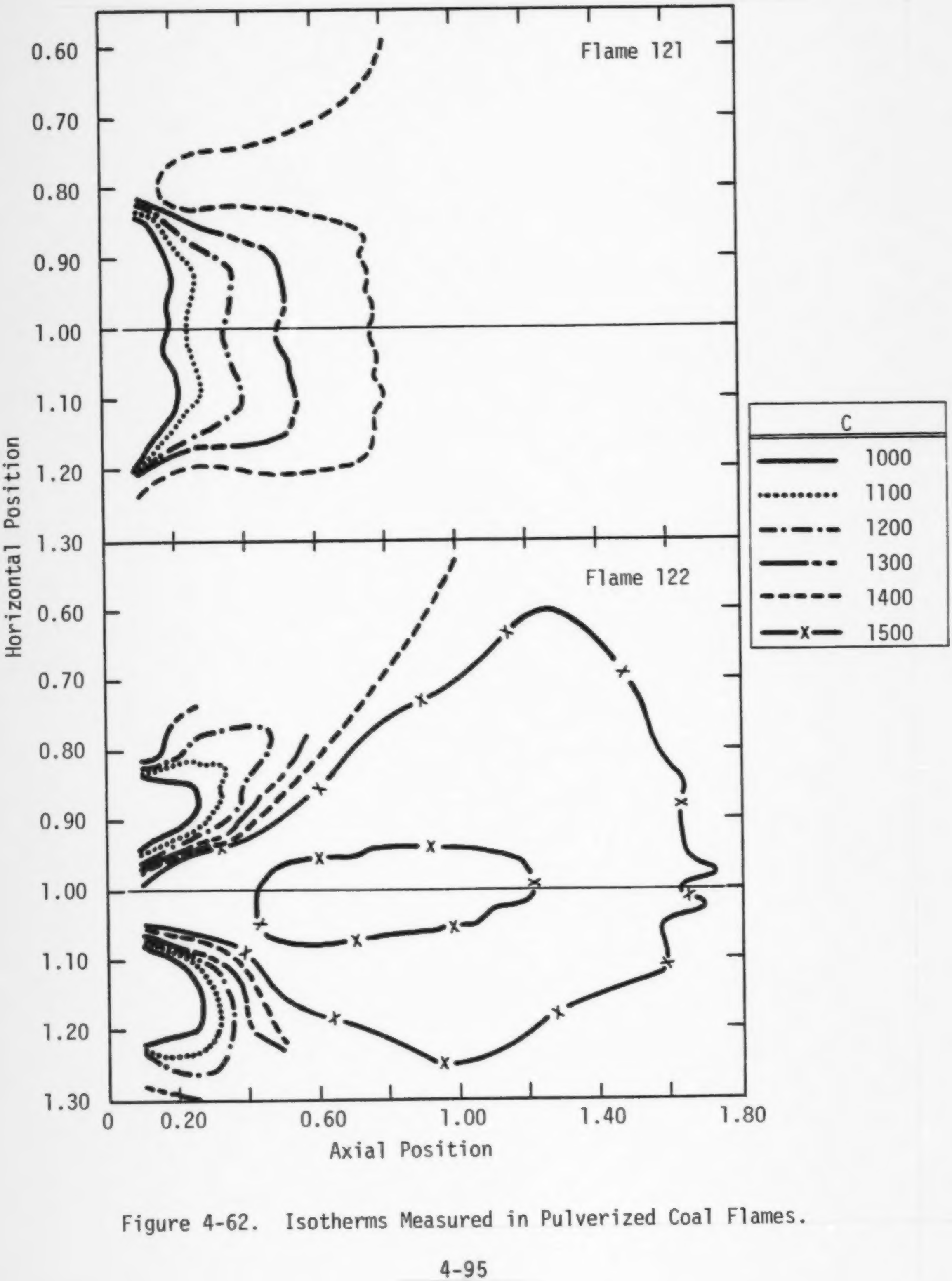

Figure 4-62. Isotherms Measured in Pulverized Coal Flames.

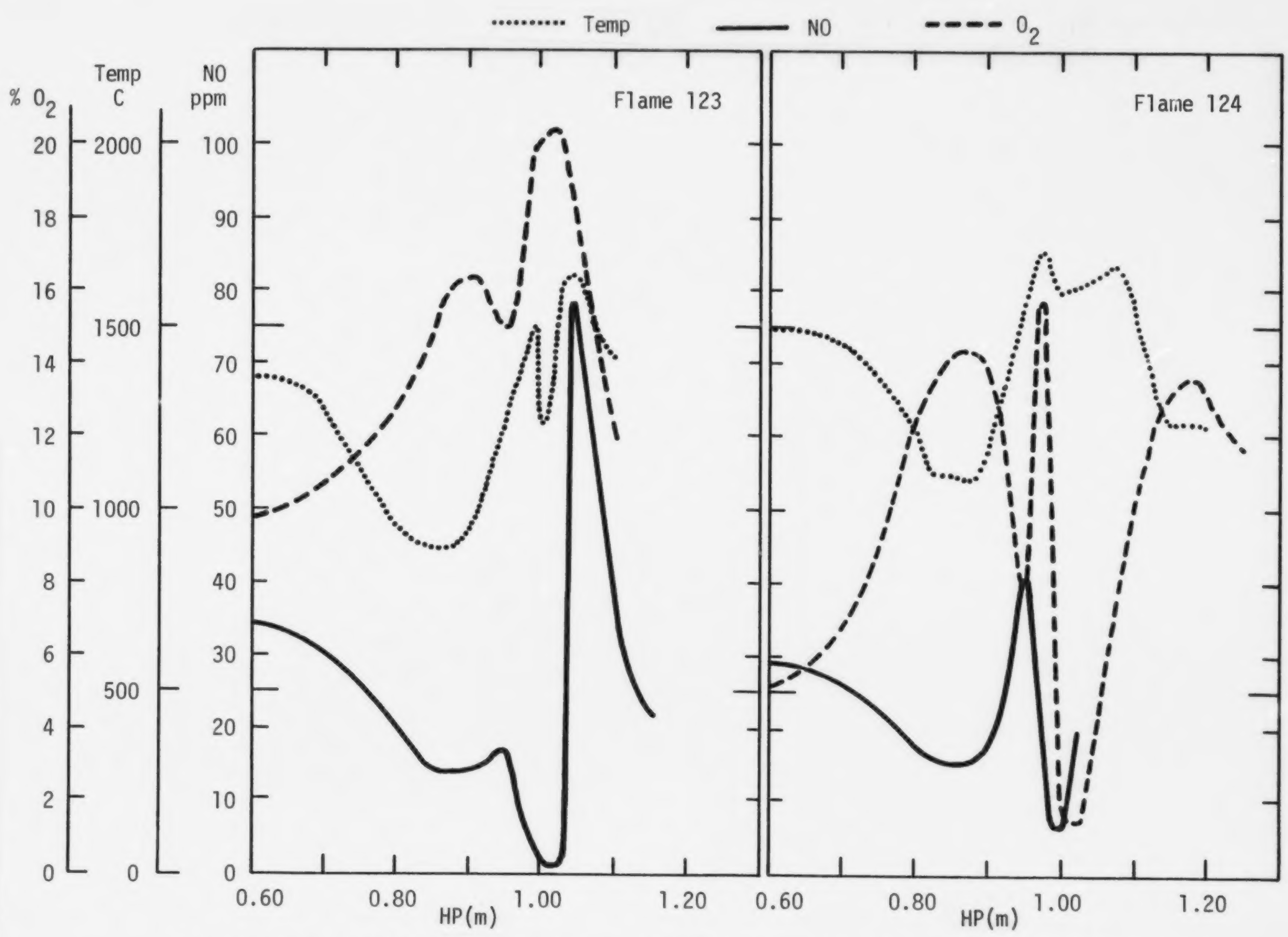

Figure 4-63. Radial NO, O_2 and Temperature Distribution in Pulverized Coal Flames.

eters - a modification in the amount of primary air. The axial profiles shown in Figure 4-64 indicate that the reduced oxygen availability results in an increase in carbon monoxide concentration and the presence of methane. The lower exhaust level attained with flame 124 can be attributed to a combination of:

a. reduced conversion of fuel nitrogen species to NO because of the fuel rich conditions;

b. reduction of NO by hydrocarbon radicals as the coal volatiles burn.

These studies indicate that burner parameters effect the fuel air contacting conditions which either promote or prevent NO formation.

REFERENCES

4.1 Heap, M. P., et al. The Development of Combustion Systems from Heavy Oil and Coal-Fired Furnaces. Volume I. Influence of Burner Variables on NO_x Formation in Pulverized Coal Flames. EPA 600/2-76-061a, March 1976.

4.2 Heap, M. P., et al. The development of Combustion Systems from Heavy Oil and Coal-Fired Furnaces. Volume II. Further Furnace Investigations and the Evaluation of Radiative Heat Transfer Models. In publication, 1982.

4.3 Leuckel, W. IFRF Document No. F, 72/a/12.

4.4 Hartel, H. "Fue Answertung von Flammenbildern Technesche Flammen." University of Stuttgart Thesis, 1974.

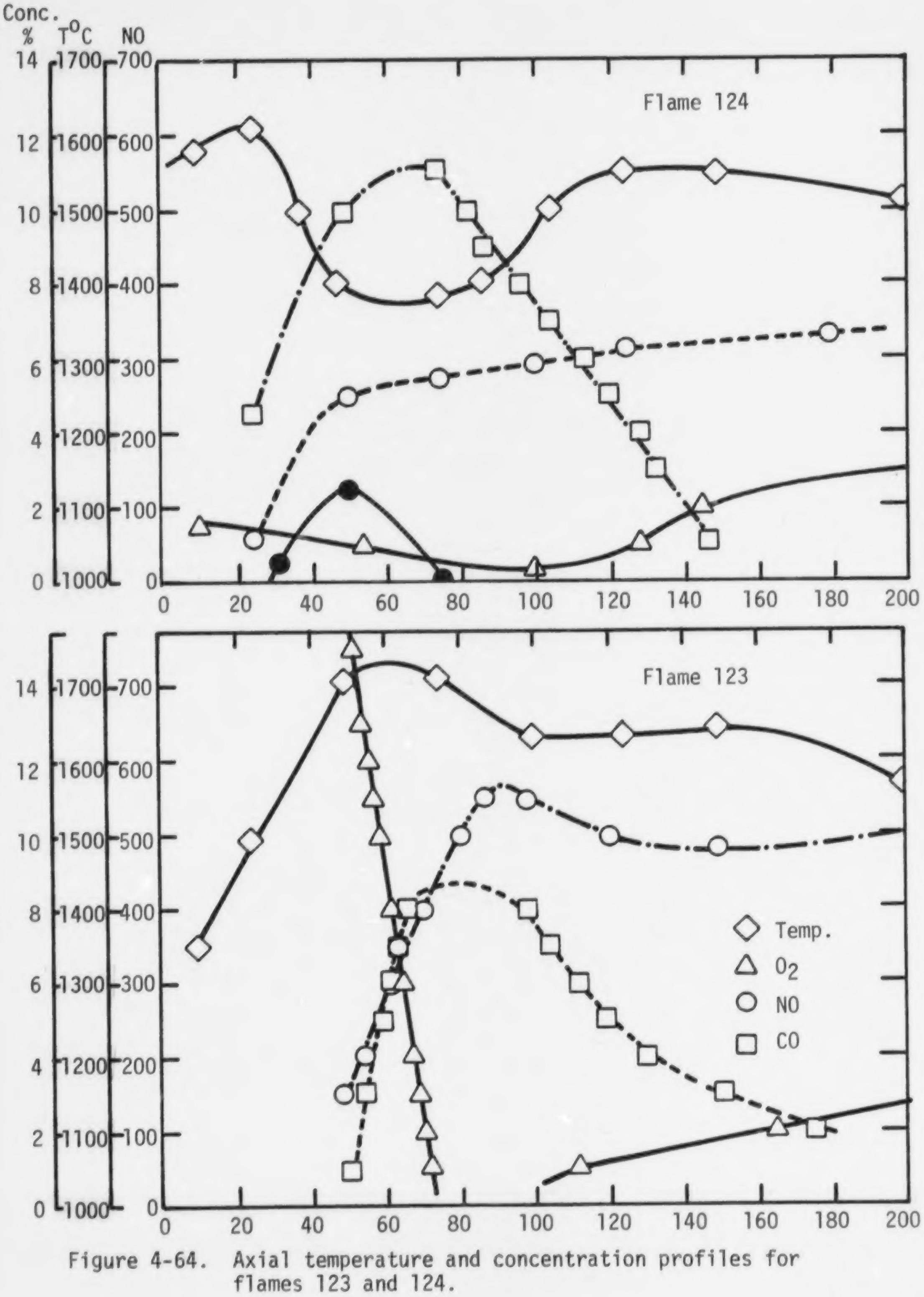

Figure 4-64. Axial temperature and concentration profiles for flames 123 and 124.

5.0 DISCUSSION AND CONCLUSION

This investigation on the influence of burner criteria on NO_x formation involved gaseous, solid, and liquid fuels. Therefore the results apply to fuels which when burned produce considerable quantities of fuel NO and also to those fuels which produce only thermal NO. Burners used in boilers have several design parameters which can be varied and which impact flame characteristics. These include:

- swirl level and swirl distribution;
- fuel injector design;
- burner geometry;
- air velocity.

It has been shown that all of these parameters influence NO formation because they impact fuel air mixing and the entrainment of cooler bulk gases. Thus they control local oxygen availability and flame temperatures, the factors which dictate fuel and thermal NO formation.

5.1 Natural Gas Flames

Peak time averaged flame temperatures measured in these studies were of the order of 1550 C and the bulk gas temperatures were 1200 C and below. Thus, for the flames under discussion in this report, nitric oxide formation can be considered solely as a flame phenomenon since insignificant amounts of nitric oxide will be formed in the bulk gases. The nitric oxide measurement cannot be accounted for on the basis of the flame temperatures presented in Section 4. However, these temperatures are time mean values for the suction pyrometer and neither the response time nor the spatial resolution are sufficient to measure the peak temperatures which are believed to be of importance for NO formation in turbulent diffusion flames.

The temperature reaction zone will depend on the composition and enthalpy of the mixture prior to reaction. It is important to note that this is not dependent on the local fuel air ratio alone, but also on the degree of dilution of the reactants and the temperature of any combustion products. Maximum temperatures will occur when the fuel and air are undiluted with combustion products and react in proportions close to stoichiometric. The rate at which the temperature of the freshly formed products of combustion will be reduced depends upon:

- the bulk gas temperature;
- the rate of mixing with the bulk gases;
- the amount of radiative heat loss which will be dependent on the volume and emissivity of the combustion products and the temperature of the furnace enclosure and the bulk gases.

Burner variables influence the amount of nitric oxide produced in natural gas flames because they control the mixing history of the four components of interest:

- the fuel;
- the air;
- internally recirculating combustion products;
- externally recirculating combustion products.

The mixing history of these components will dictate the degree of dilution and the reaction zone equivalence ratio and therefore the temperature reaction zone temperature. Also the rate of mixing will influence the rate of temperature decrease of the combustion products.

The influence of burner variables on the mixing history of the four separate components can be summarized by:

- the type of fuel injector and its position will affect both the fuel air mixing pattern and the mass exchange between the fuel and internally recirculation vortex;
- the degree of swirl will control the rate of entrainment of external recirculation and the size, intensity and position of the internal recirculation vortex;
- the throat velocity will influence the fuel air mixing pattern and the rate of entrainment of external recirculation;
- the geometry of the burner exit will influence the size and

intensity of the recirculating gases.

These same parameters affect the type of flame that is produced. Figure 5-1 illustrates the emission characteristics of general flame types.

5.2 Pulverized Coal Flames

For the most part, pulverized coal flames can be divided into the two general classes of flames shown in Figure 5-2. In the burner stabilized flame, the coal/air and high temperature recirculation products are mixed rapidly and form a conical flame around the axial recirculation zone. These characteristics are more readily discerned by the temperature concentration and NO data presented in Figure 5-3. The measurements were taken very close to the burner exit and clearly show that the coal is concentrated in a region away from the axis. In the high-fineness ratio diffusion flame (shown in Figure 5-2), the coal is maintained in a coherent stream for a substantial distance within the furnace. Measurements made in this flame are shown in Figure 5-4. The solids are concentrated in a region near the axis and NO concentration peak outside the fuel jet. Oxygen concentration peak in the annular combustion airstream and are a minimum on the flame axis. The measured peak flame temperatures are similar for both flame types.

These results suggest that the difference in NO_x emission characteristics is primarily due to the availability of oxygen during the lifetime of the coal volatile fractions. In the burner-stabilized flame, which gives high NO levels, the fuel and air mix rapidly, and the gas phase is always overall oxidizing. As a result, any NO that is formed in the early regions of the flame has little opportunity to be reduced. This can be contrasted with the long diffusion flame where the flame formed from the volatile fuel fractions separates the combustion air and the pulverized coal jet. After the oxygen supplied to the primary air has been depleted, the gas phase is reducing within the fuel jet. Thus, there is ample opportunity to form N_2 from the various XN species. To minimize the oxygen available on the coal jet axis, it is necessary that a flame front be established at the fuel injector. If the flame is lifted, then mixing can take place between the coal and the air even though the primary air level is low, thus increasing the oxygen availability during devolatilization.

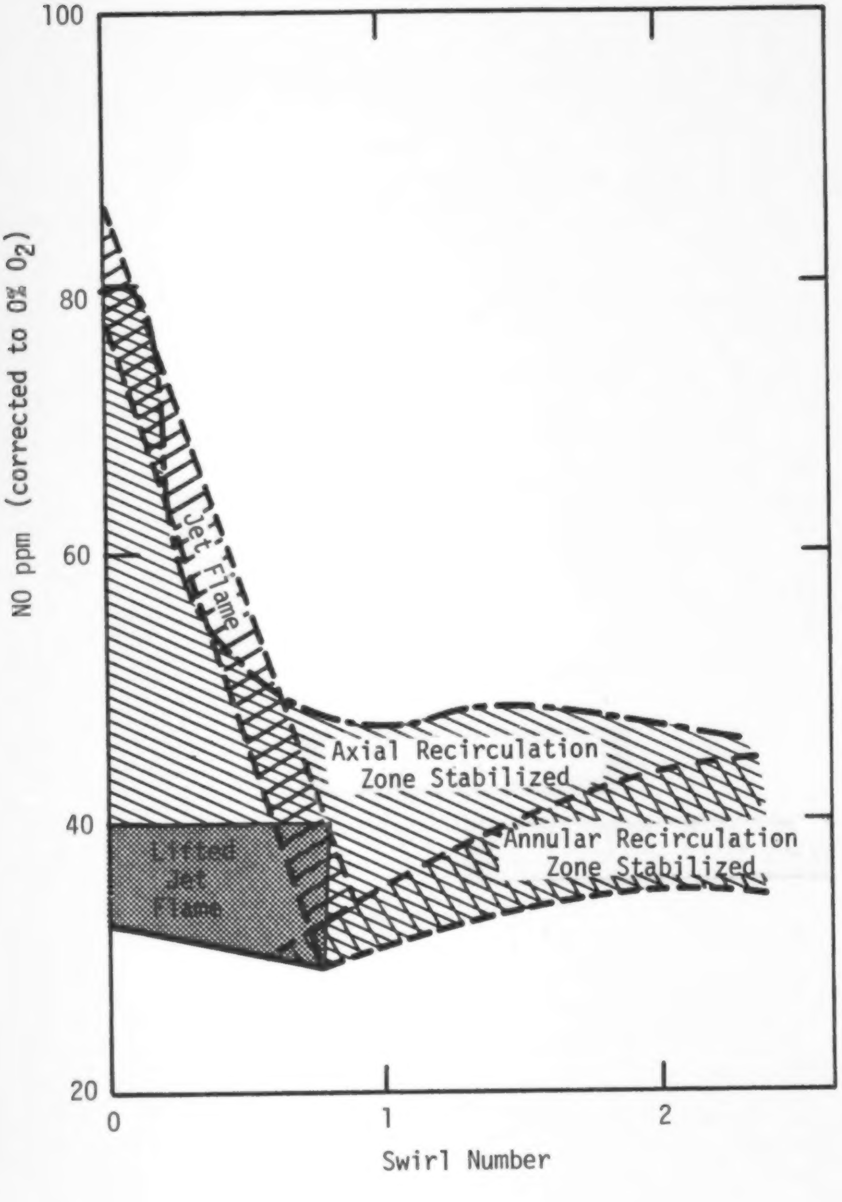

Figure 5-1. NO Emission Characteristics of the Various Natural Gas Flame Types.

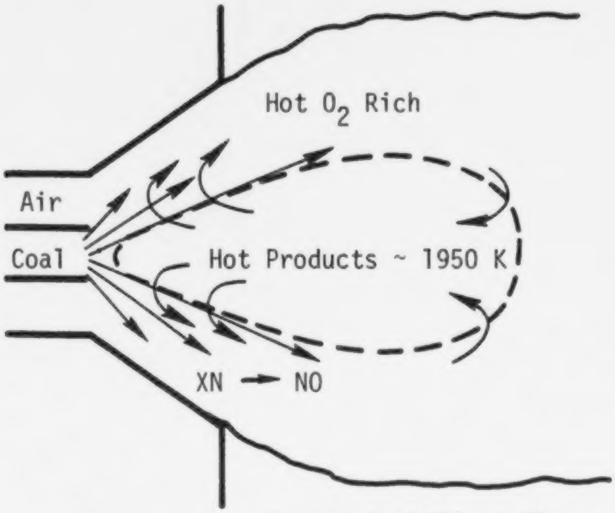
Hot O_2 Rich
Air
Coal
Hot Products ~ 1950 K
XN → NO

Burner Stabilized Flame

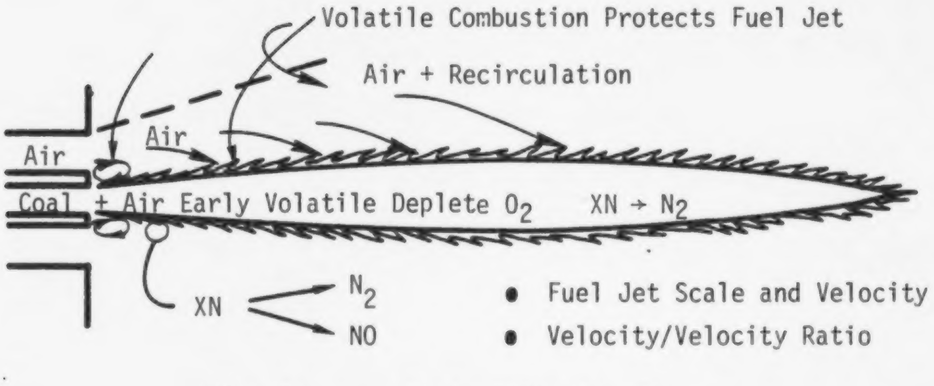
Volatile Combustion Protects Fuel Jet
Air + Recirculation
Air
Air
Coal + Air Early Volatile Deplete O_2
XN → N_2
XN
N_2
NO
● Fuel Jet Scale and Velocity
● Velocity/Velocity Ratio

High Fineness Ratio Diffusion Flame

Figure 5-2. Flame Characteristics.

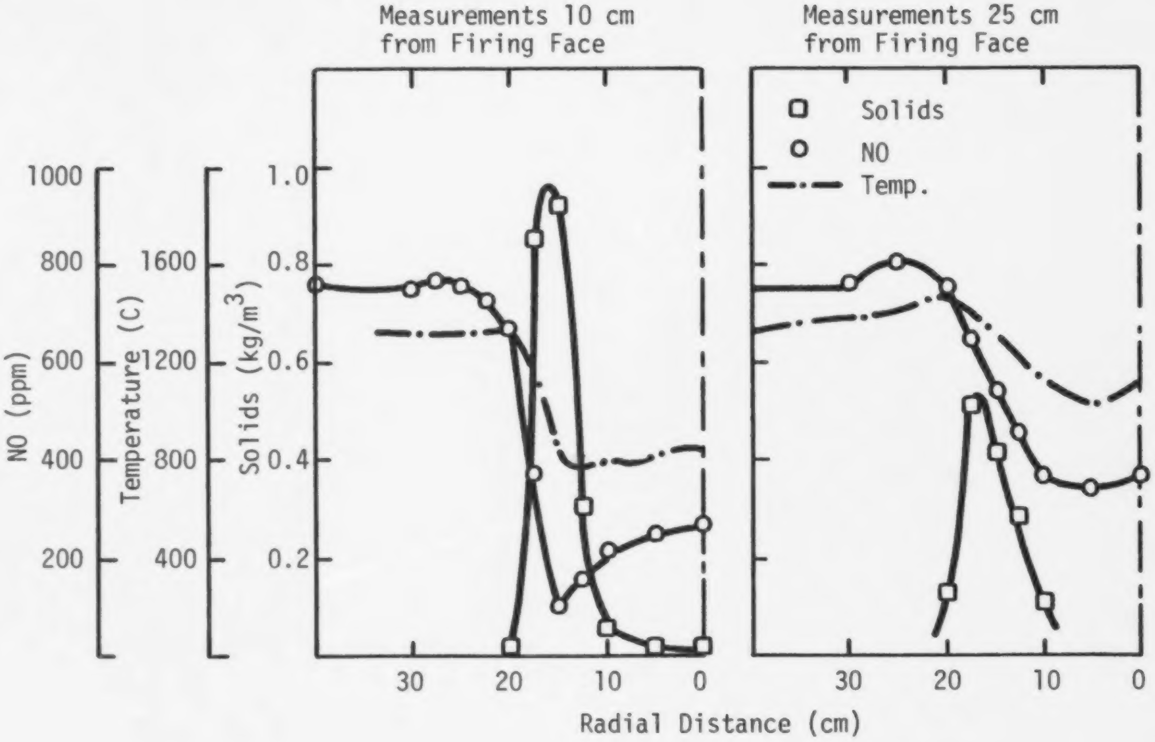

Figure 5-3. Measurements Within a Burner Stabilized Flame.

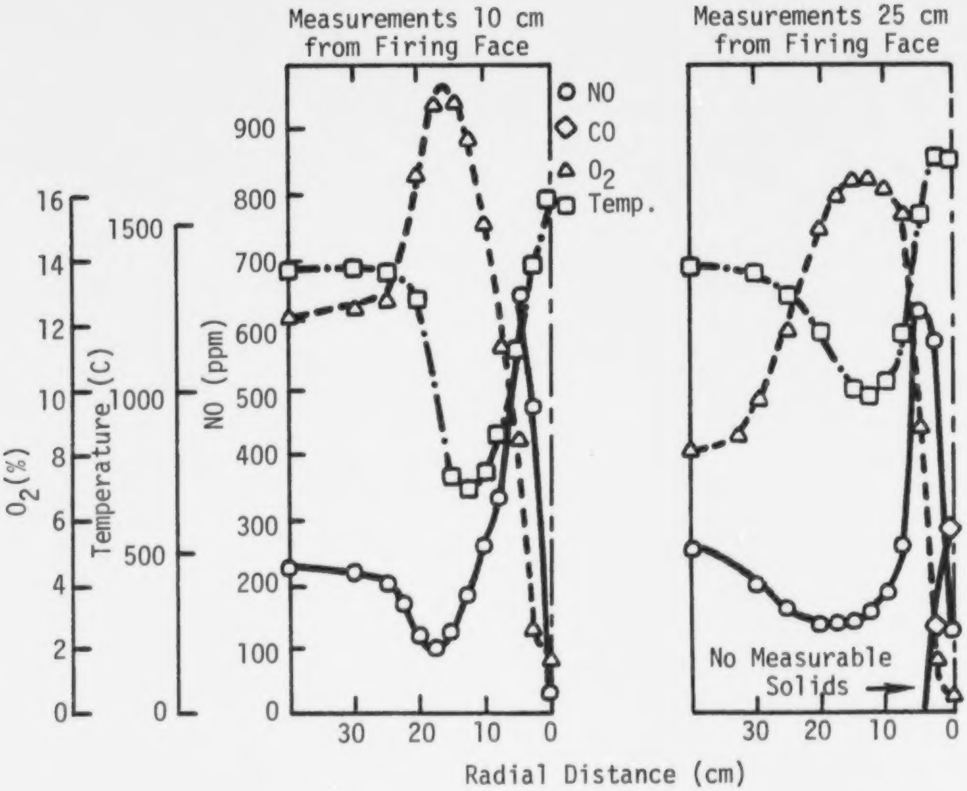

Figure 5-4. Measurements Within a High Fineness Ratio Diffusion Flame.

The effects of primary air on the gas composition within a swirl-stabilized flame are shown in Figure 5-5. The measurements were taken in two flames differing only in the amount of primary air. With high primary stoichiometry, Figure 5-5a, the oxygen concentration remains high for some distance down the flame and NO is rapidly formed. NO is only reduced slightly after the oxygen is reduced to zero. With the low level of primary air, the oxygen levels are very rapidly reduced to low concentrations on the flame axis. Measured flame temperatures are very simlar for both conditions; however, the exhaust emissions are a factor of two less for the low level of primary air.

5.3 Heavy Oil Flames

Heavy oil also contains fuel nitrogen and primary source of NO is fuel NO. Liquid fuel flames can have similar characteristics to natural gas and pulverized coal flames, although because of the conical nature of the fuel spray, for the most part they are stabilized by an axial recirculation zone. In liquid fuel flames the fuel injector serves two functions, namely:

- it produces a spray of droplets;
- it injects the droplets into the combustion air stream.

Both of these functions can influence NO formation. These studies have indicated that all things being equal the angle of fuel spray has a strong impact on NO formation.

The conditions which exist at the base of a residual fuel oil flame are shown conceptually in Figure 5-6 for two limiting conditions. These conditions are dependent upon the residence time of the liquid spray in an internal recirculation zone. This recirculation zone could be produced because of the divergence of flow caused by a swirling combustion air flow, or because of the use of a bluff body flame stabilizer. In one case (Figure 5-6a), the spray is assumed to have a relatively narrow angle and its trajectory provides a relatively long residence time within the internal recirculation zone. This recirculation zone will consist of hot combustion products deficient in oxygen. The liquid fuel will vaporize, mix with the inert products, and burn along the boundary of the recirculation zone when they contact air. In contrast to this condition, if the spray angle were

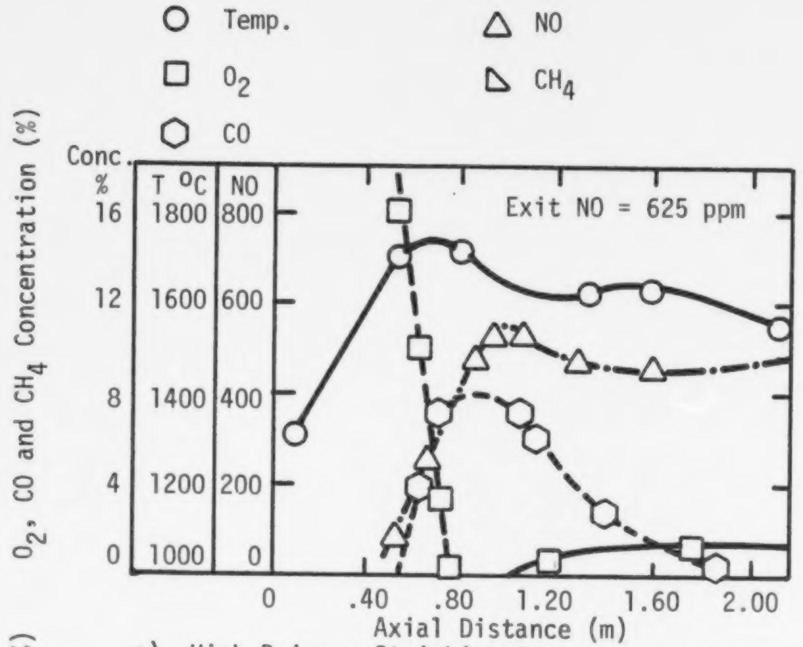

a) High Primary Stoichiometry

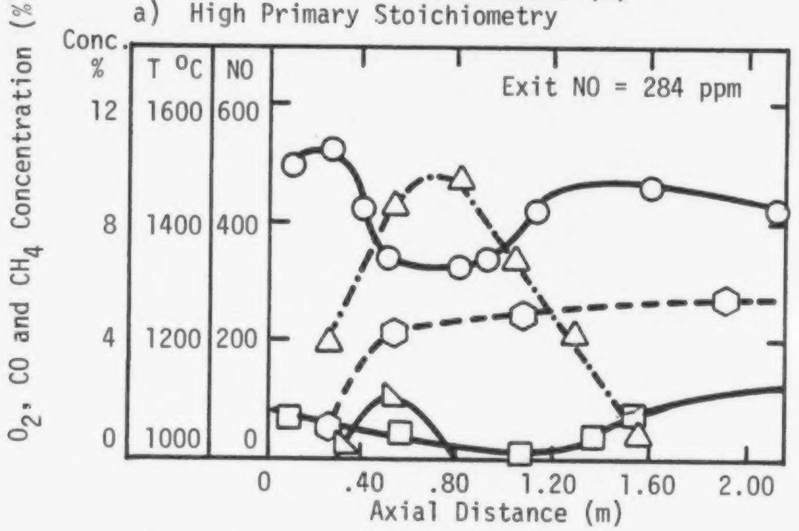

b) Low Primary Stoichiometry

Figure 5-5. Effects of Primary Stoichiometry on Gases Within a Swirl Stabilized Flame.

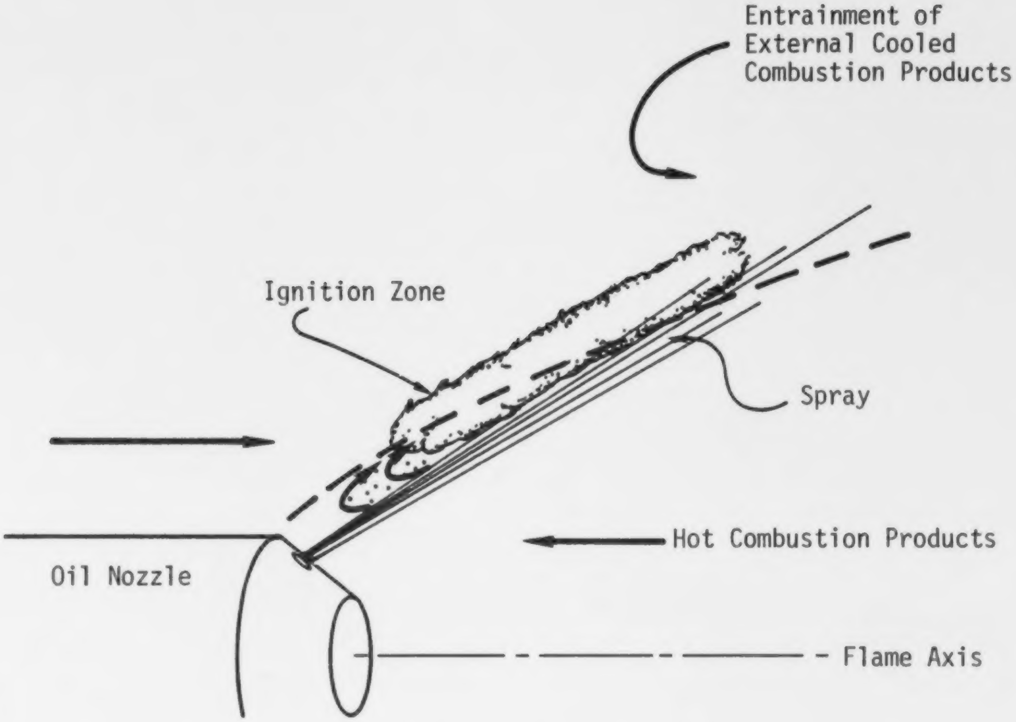
Entrainment of
External Cooled
Combustion Products
Ignition Zone
Spray
Hot Combustion Products
Oil Nozzle
Flame Axis

Figure 5-6a. Spray Trajectory Passes Through the Internal Recirculation Zone.

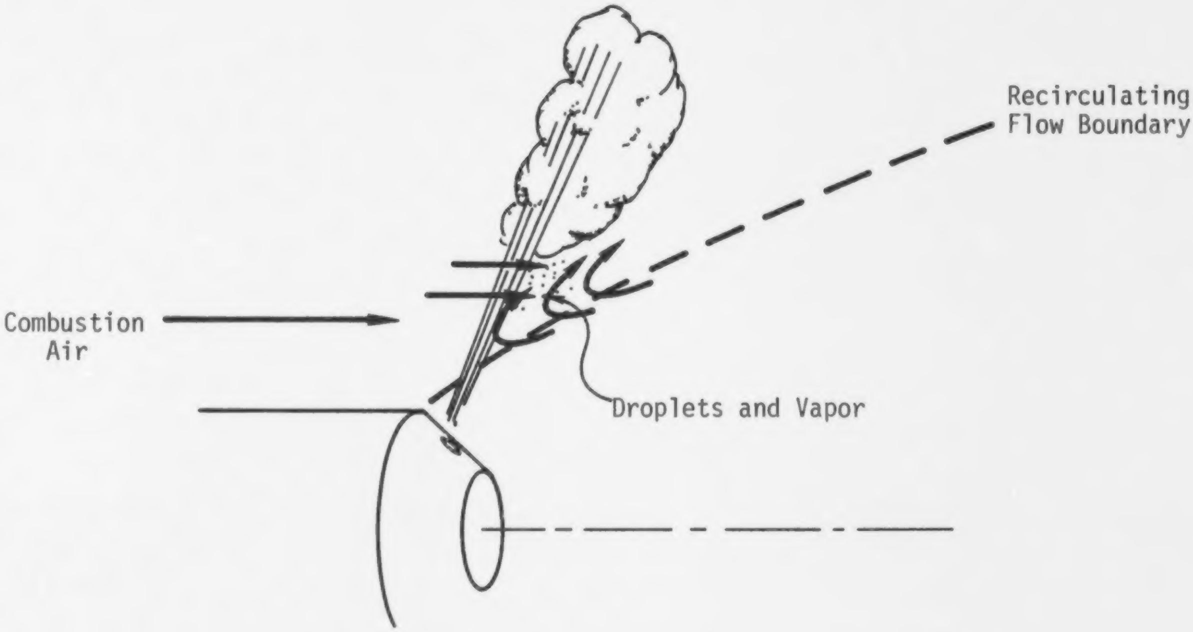
Recirculating
Flow Boundary
Combustion
Air
Droplets and Vapor

Figure 5-6b. Concept of Fuel Air Contacting at the Base of a Residual Oil Flame.

wide (Figure 5-6b) the spray has a very short residence time within the recirculation zone. Small drops and vapor are entrained with the combustion air prior to entraining high temperature products which will provide an ignition source. The major difference between the two limiting cases is that in (a) the fuel vaporizes in the absence of oxygen, in (b) the spray is first mixed with air before high temperature combustion products are entrained, and the droplets vaporize. If the angle in (b) is too wide, then the flame may not be stable. However, if a stable flame is achieved these are normally the conditions which will maximize NO production since oxygen is available when the fuel nitrogen compounds are released from the liquid droplets. Alternatively, condition (a) is one which will tend to minimize fuel nitrogen production since the droplets vaporize in the absence of oxygen and heat release takes place in a diffusion flame region, thus providing optimum conditions for the conversion of XN to N_2.

5.4 The Importance of Volatile and Char Nitrogen

Fuel nitrogen is the major source of NO which is produced by the combustion of pulverized coal. The nitrogen is bound in the organic matrix and can be considered in two fractions:

- one fraction is evolved with the coal volatiles (volatile nitrogen) and is probably rapidly converted to HCN before reacting to produce NO;
- the char nitrogen is that fraction which will remain with the solid after devolatilization and be converted to NO or N_2 during the char burnout phase.

The division of the total nitrogen between these two fractions could be dependent upon the type of coal and will certainly be dependent upon final particle temperature.

The experiments with petroleum coke indicate that the conversion of char nitrogen to NO is less than the conversion of volatile nitrogen to NO. It appears that the primary impact of burner parameters on NO formation is to reduce the conversion of volatile fuel nitrogen. This is reasonable since for the most part char burnout occurs remote from the burner and burner parameters will have less opportunity to influence the overall process other than to ensure that mixing is complete before the temperatures are too low to ensure the burnout of the char.

5.5 Burner Parameters and NO_x Control

Information generated in these studies culminated in the identification of three major design variables which influence NO formation. These are:

- The fuel injector which can either maintain the pulverized coal in a coherent jet along the flame axis, or divert the coal into the combustion airstream, thus producing rapid fuel/air mixing.
- The swirl level of the combustion air defined as the ratio of the flux of angular momentum to the flux of axial momentum multiplied by a characteristic burner dimension (such as throat diameter). The introduction of swirl to the combustion airflow increases entrainment rates and promotes the formation of internal recirculation zones. It should be noted, however, that the distribution of angular momentum is just as important or more important than the total angular momentum flux.
- The primary airflow which is mixed with the pulverized coal. In practical systems the amount of transport air is dictated, to some extent, by the coal pulverizer requirements. However, the amount of primary air influences the level of oxygen available during coal devolatilization.

Figure 5-7 shows the impact of two of the variables discussed above on NO formation. It can be seen that both swirl level and method of fuel injection have a significant impact upon NO formation. With radial injection, emissions are almost independent of the swirl level. This is because the fuel/air mixing is dictated by the method of fuel injection. With the medium velocity axial injector, an axial recirculation zone is formed at some critical swirl level splitting the fuel jet and causing it to mix more rapidly with the combustion air. This increases NO_x emissions. The lowest emissions are obtained with a high velocity axial fuel injector. Once sufficient swirl is provided to give a stable ignition zone at the fuel injector, NO_x emissions are almost independent of swirl level. The NO_x emission data in Figure 5-7 can be grouped into high and low levels. The

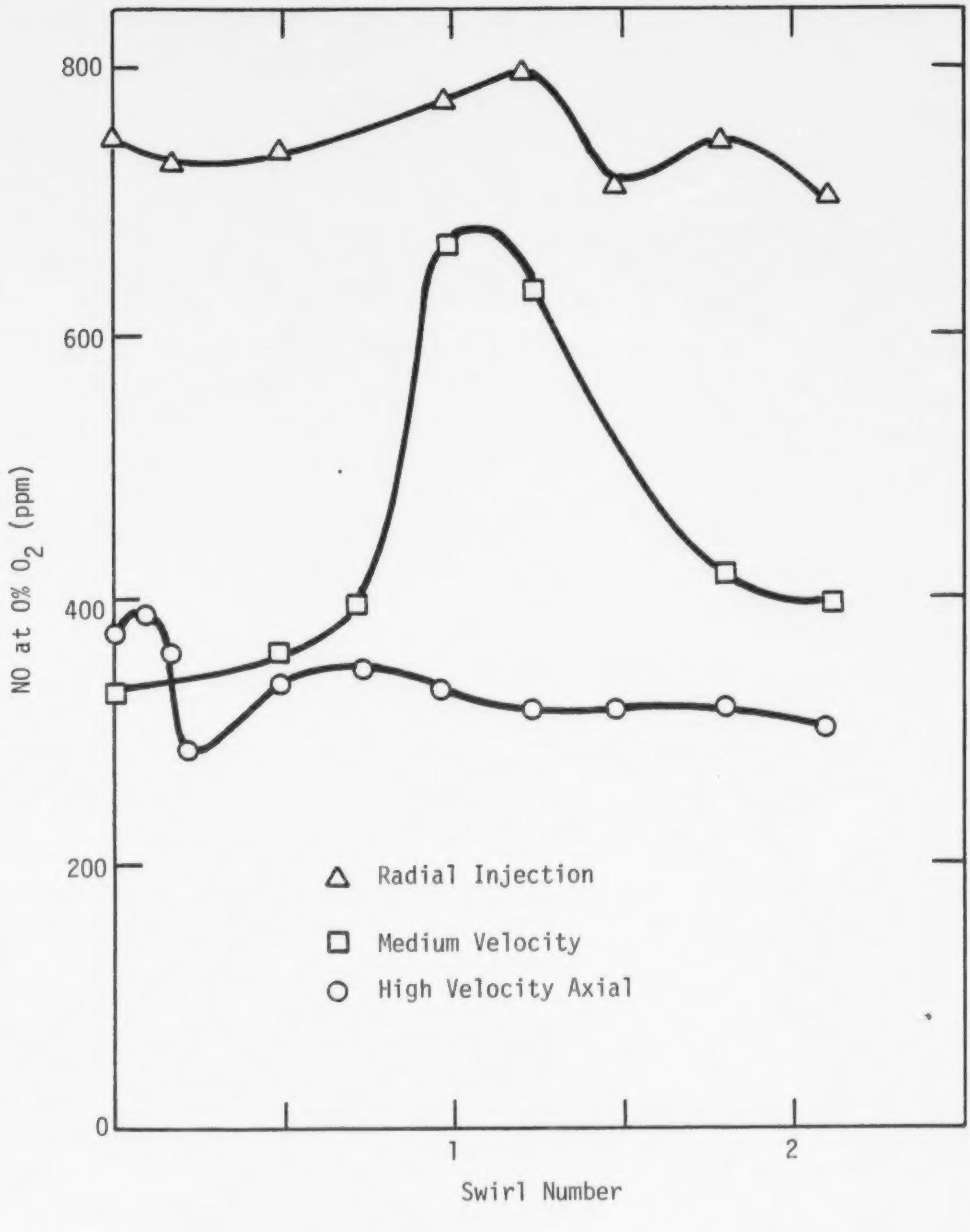

Figure 5-7. Effects of Air Swirl and Coal Injection on NO Emissions from Versatile Pilotscale Burner.

high levels are characteristic of burner-stabilized flames with axial recirculation zones, and the lower levels are characteristic of long flames in which the coal jet remains on the flame axis.

Figure 5-8 shows further evidence of the importance of early oxygen availability on NO formation in pulverized coal flames. The data shown in Figure 5-8a were obtained by varying the axial fuel injector diameter to maintain the axial velocity as the primary air was varied from 10 to 30 percent of the stoichiometric requirement. Under these high velocity conditions, a long flame was produced. As the oxygen level was progressively reduced, the NO emissions were also reduced. A subscale high-turbulence circular burner was used to generate the data shown in Figure 5-8b. The emissions with the normal coal impeller are very similar to those obtained in field-operating boilers.

Although long diffusion flames give inherently low NO emissions and can be stabilized at the fuel injector by the utilization of swirl, they are not easily accommodated in wall-fired boilers because of the firing depth required to prevent flame impingement. Thus, to satisfy both low NO emission requirements and the need for a minimum firing depth, it is necessary to produce a rapidly mixed fuel-rich zone with sufficient delay before air is added to complete combustion. This can be accomplished by physically separating the secondary combustion air into two streams. One stream is injected through the burner throat in the usual manner, while the other "tertiary air" is injected outboard of the throat. The fuel and air passing through the burner throat form a fuel-rich combustion zone. The tertiary air combines with the fuel-rich combustion products on the periphery of the burner zone to burn out the combustibles to overall fuel-lean conditions. With this "physical staging," the fuel-rich combustion characteristics of the long-diffusion flame can be produced in a short burner stabilized flame.

Figure 5-9 shows the results of this staging with tertiary air using a subscale high turbulence burner. It can be seen that when 20 percent of the overall air supply is injected from the tertiary air ports, emission levels are reduced by approximately 50 percent. The data presented in Figure 5-9 were obtained without any optimization of either the secondary swirl level

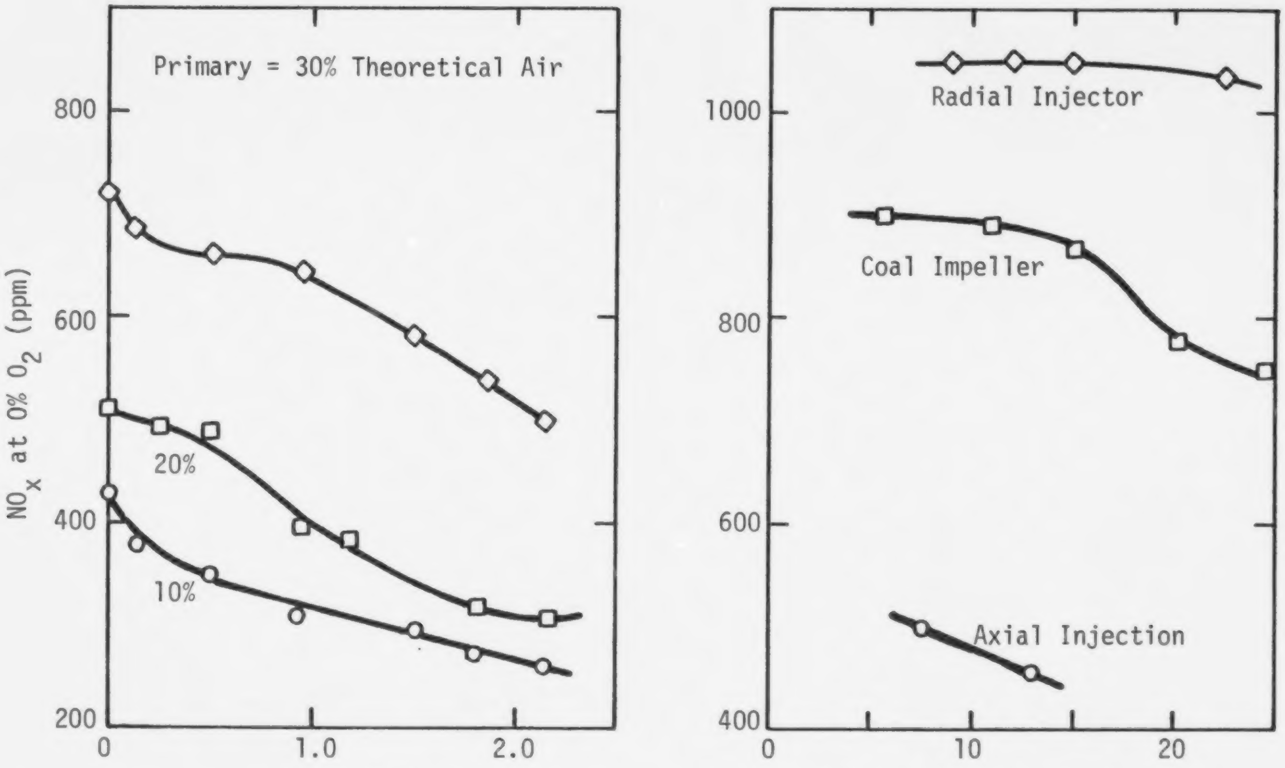

A) Versatile Burner with Axial Fuel Injection

B) Subscale High Turbulence Circular Burner

Figure 5-8. Effects of Primary Stoichiometry, Air Swirl, and Coal Injection on NO_x Emissions.

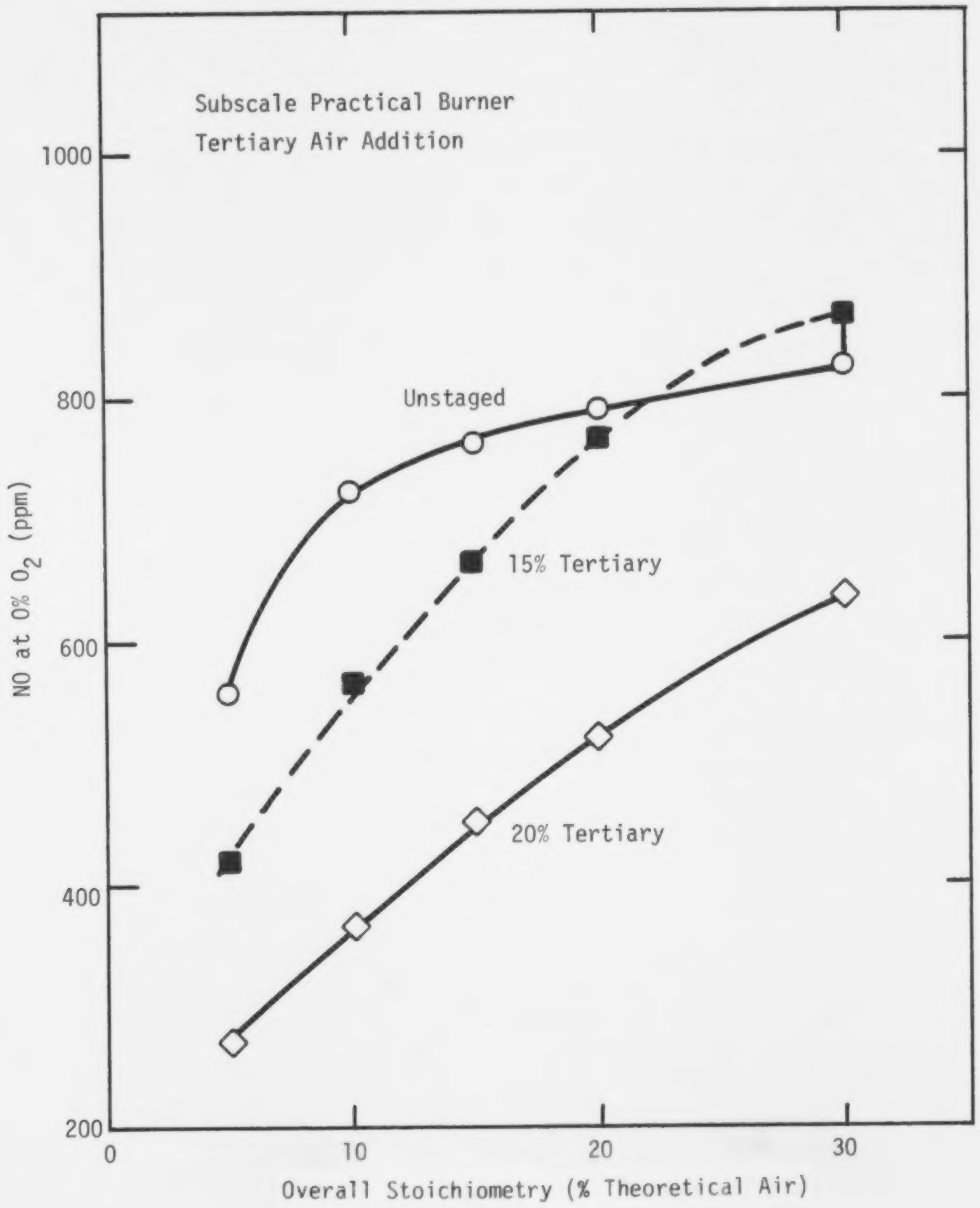

Figure 5-9. NO Emissions from IFRF Burner Operating with Tertiary Air.

or the fuel injection system. The data shown in Figure 5-10 were obtained with the versatile burner shown in Figure 5-10. It can be seen that the use of an optimum swirl level can have a significant impact on NO emissions at all burner zone stoichiometrics (the stoichiometry of the reactants supplied through the burner throat). In addition, it can be seen that the heat extraction from the flame has an impact upon the emission levels of NO without tertiary air.

This approach appears to offer promise of reducing NO_x emissions and producing a flame with characteristics which are suitable for application to wall fired boilers. Further work is necessary to:

1. Optimize the design criteria.
2. Establish scale effects.
3. Investigate multi-burner effects.

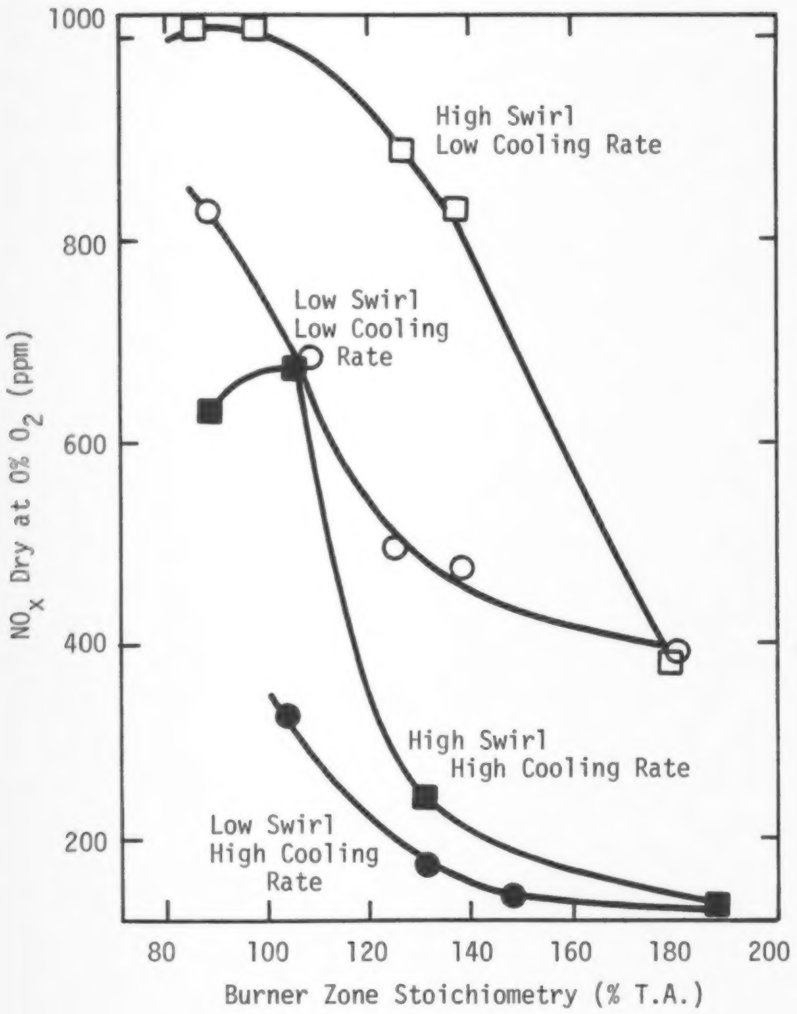

Figure 5-10. Effects of Swirl, Cooling Rate, and Burner Zone Stoichiometry on NO_x Emissions.

APPENDIX A

DETAILED FLAME MEASUREMENTS

AD - Axial Distance, m

HP - Horizontal Position, m

CO_2 - Concentration Dry, Nm^3/Nm^3

C_2H_4 - "

O_2 - "

CO - "

H_2 - "

CH_4 - "

N_2 - "

C_2H_6 - "

NO - Concentration Dry, ppm

NO_x - "

S - Solid Concentration, kg/Nm^3 dry gas

C - Fixed Carbon Content of Solid, kg/kg dry solid

A - Ash Content of Solid, kg/kg dry solid

T - Temperature, °C

V_x - Axial Velocity Component, $msec^{-1}$

V_y - Radial Velocity Component, $msec^{-1}$

V_z - Tangential Velocity Component, $msec^{-1}$

FLAME: 119

A.D.	H.P.	CO_2	C_2H_4	O_2	CO	H_2	CH_4	N_2	C_2H_6	NO	NO_x	S	T	V_x	V_y	V_z
m.	m.	Nm^3/Nm^3 dry gas								ppm		solids	°C	m/s		
.100	.200	.116	0	.016	0	0	0	.901	0	109	126	0	1340	0	0	0
.100	.400	.116	0	.016	0	0	0	.596	0	110	125	0	1340	0	0	0
.100	.600	.117	0	.014	0	0	0	.967	0	110	124	0	1340	0	7.1	-4.6
.100	.700	.119	0	.014	0	0	0	.907	0	110	124	0	1340	0	7.7	-6.3
.100	.750	.117	0	.016	0	0	0	.907	0	110	124	0	1345	1.8	6.8	-4.6
.100	.800	.116	0	.017	0	0	0	.907	0	97	113	0	1355	4.6	6.3	-6.6
.100	.815	.104	0	.036	0	0	0	.890	0	44	75	0	1450	70.0	6.2	-7.4
.100	.825	.091	0	.055	0	0	0	.885	0	18	49	0	1510	83.5	6.1	-8.8
.100	.840	.031	0	.149	0	.004	0	.800	0	4	25	0	1620	83.0	6.1	-8.4
.100	.850	.053	0	.098	.011	.009	0	.830	0	6	31	0	1720	62.3	6.1	-8.5
.100	.875	.074	0	.009	.028	.046	0	.830	0	35	37	0	1710	16.3	6.8	-7.8
.100	.900	.077	0	.003	.031	.049	0	.830	0	59	57	0	1685	-11.0	10.6	-5.2
.100	.925	.079	0	.004	.029	.044	0	.820	0	58	48	0	1675	-16.0	12.0	-2.7
.100	.950	.080	0	.003	.027	.043	0	.841	0	61	46	0	1665	-20.8	12.4	-8.1
.100	.975	.082	0	.003	.027	.040	0	.841	0	60	46	0	1660	-15.5	12.1	2.4
.100	1.000	.084	0	.002	.027	.039	0	.841	0	60	46	0	1660	-13.3	11.3	4.7
.100	1.025	.084	0	.003	.026	.039	0	.841	0	60	47	0	1660	-18.0	11.3	9.0
.100	1.058	.084	0	.003	.025	.038	0	.859	0	61	48	0	1650	-16.5	11.3	11.0
.100	1.075	.084	0	.002	.025	.039	0	.852	0	62	49	0	1650	-16.7	8.5	10.7
.100	1.100	.084	0	.002	.026	.040	0	.869	0	61	48	0	1650	-12.0	4.6	8.9
.100	1.125	.084	0	.003	.030	.045	0	.841	0	58	56	0	1640	8.3	3.0	7.3
.100	1.158	.070	0	.010	.033	.055	0	.820	0	40	35	0	1640	37.0	1.4	6.2
.100	1.175	.039	0	.087	.021	.030	0	.775	0	6	10	0	1700	92.5	.4	5.8
.100	1.180	.051	0	.092	.018	.017	0	.808	0	4	9	0	1700	91.5	.3	5.7
.100	1.200	.054	0	.098	.005	.003	0	.841	0	4	23	0	1560	23.0	-0.3	5.2
.100	1.225	.116	0	.018	0	0	0	.907	0	17	54	0	1425	9.0	-1.2	4.4
.100	1.250	.118	0	.016	0	0	0	.907	0	76	92	0	1380	1.0	-1.4	3.5
.100	1.275	.117	0	.017	0	0	0	.907	0	90	104	0	1340	0	-1.4	3.0
.100	1.300	.116	0	.018	0	0	0	.907	0	92	104	0	1330	0	-0.8	2.3
.250	.200	.111	0	.019	0	0	0	.885	0	117	136	0	1330	0	0	0
.250	.400	.111	0	.019	0	0	0	.885	0	121	139	0	1345	0	0	0
.250	.600	.112	0	.018	0	0	0	.885	0	121	138	0	1355	0	0	0
.250	.700	.111	0	.019	0	0	0	.891	0	118	134	0	1365	6.2	-2.0	-0.5
.250	.750	.106	0	.024	0	0	0	.885	0	97	114	0	1410	12.7	-2.0	-10.5

FLAME: 119

A.D.	H.P.	CO_2	C_2H_4	O_2	CO	H_2	CH_4	N_2	C_2H_6	NO	NO_x	S	T	V_x	V_y	V_z
m.	m.	Nm^3/Nm^3 dry gas								ppm		solids	^oC	m/s		
.250	.775	.103	0	.034	0	0	0	.885	0	50	94	0	1450	39.0	-2.7	-12.5
.250	.800	.096	0	.041	0	.002	0	.869	0	62	79	0	1515	45.5	-3.3	-15.0
.250	.825	.099	0	.037	0	.003	0	.875	0	50	74	0	1580	60.8	5.5	-17.2
.250	.840	.098	0	.027	0	.007	0	.870	0	47	73	0	1640	67.7	10.5	-18.5
.250	.850	.097	0	.016	.011	.012	0	.865	0	49	75	0	1645	67.7	16.0	-19.0
.250	.875	.092	0	.008	.017	.025	0	.852	0	55	79	0	1690	22.3	35.3	-20.5
.250	.900	.088	0	.003	.024	.034	0	.841	0	63	63	0	1725	14.7	20.3	-21.8
.250	.925	.083	0	.002	.023	.037	0	.830	0	70	65	0	1710	-5.7	13.0	-21.0
.250	.950	.085	0	.002	.022	.035	0	.841	0	72	0	0	1705	-10.5	7.0	-19.0
.250	.975	.085	0	.002	.021	.033	0	.825	0	76	0	0	1700	-15.0	0	-14.5
.250	1.000	.091	0	.003	.020	.028	0	.852	0	79	0	0	1700	-24.5	-7.5	-0.5
.250	1.025	.089	0	.002	.020	.029	0	.841	0	80	0	0	1700	-10.5	-14.0	11.7
.250	1.050	.092	0	.003	.021	.028	0	.852	0	79	0	0	1700	-16.0	-19.5	17.0
.250	1.075	.087	0	.002	.023	.032	0	.841	0	76	0	0	1700	-32.5	-23.0	21.5
.250	1.100	.085	0	.002	.025	.036	0	.841	0	69	0	0	1690	-16.0	-26.5	24.0
.250	1.125	.088	0	.002	.022	.042	0	.830	0	61	0	0	1675	28.7	-28.3	24.3
.250	1.150	.065	0	.002	.019	.037	0	.830	0	52	0	0	1655	49.7	-21.5	19.0
.250	1.175	.096	0	.009	0	.023	0	.865	0	41	52	0	1610	59.7	-11.5	12.7
.250	1.200	.097	0	.026	0	.007	0	.865	0	41	66	0	1560	59.8	-0.7	8.0
.250	1.225	.099	0	.037	0	0	0	.875	0	47	77	0	1495	31.0	4.7	1.7
.250	1.250	.099	0	.034	0	0	0	.869	0	65	65	0	1450	15.2	2.7	-0.6
.250	1.300	.109	0	.024	0	0	0	.875	0	96	112	0	1375	0	0	0
.500	.200	.111	0	.021	0	0	0	.875	0	123	136	0	1340	0	0	0
.500	.400	.111	0	.019	0	0	0	.880	0	123	137	0	1350	0	0	0
.500	.600	.111	0	.017	0	0	0	.880	0	117	135	0	1430	1.6	-2.5	-2.8
.500	.700	.109	0	.021	0	0	0	.880	0	105	124	0	1500	14.8	4.2	-7.5
.500	.750	.107	0	.021	0	0	0	.875	0	95	115	0	1550	27.6	6.4	-10.9
.500	.800	.106	0	.021	0	.001	0	.885	0	84	106	0	1605	42.3	6.9	-14.1
.500	.825	.108	0	.015	0	.003	0	.880	0	82	105	0	1645	46.9	5.6	-16.8
.500	.850	.109	0	.012	0	.005	0	.885	0	83	103	0	1670	47.0	4.8	-20.9
.500	.875	.109	0	.009	0	.007	0	.885	0	56	104	0	1700	46.8	4.1	-25.1
.500	.900	.109	0	.006	0	.009	0	.885	0	94	104	0	1720	44.3	4.2	-25.6
.500	.925	.109	0	.005	0	.009	0	.888	0	102	106	0	1725	37.4	5.1	-21.7
.500	.950	.108	0	.004	0	.010	0	.875	0	106	105	0	1725	26.8	9.2	-16.2

FLAME: 119

A.D.	H.P.	CO_2	C_2H_4	O_2	CO	H_2	CH_4	N_2	C_2H_6	NO	NO_x	S	T	V_x	V_y	V_z
m.	m.	Nm^3/Nm^3 dry gas								ppm		solids	^oC	m/s		
.500	.975	.109	0	.004	0	.009	0	.680	0	106	112	0	1725	13.4	12.3	-8.6
.500	1.000	.109	0	.003	0	.008	0	.885	0	102	108	0	1725	16.1	17.4	10.2
.500	1.025	.109	0	.005	0	.007	0	.885	0	105	109	0	1725	22.5	15.2	23.9
.500	1.050	.109	0	.006	0	.007	0	.885	0	100	113	0	1725	29.7	14.8	25.6
.500	1.075	.109	0	.007	0	.006	0	.882	0	95	111	0	1690	31.3	12.6	21.8
.500	1.100	.109	0	.008	0	.005	0	.880	0	91	110	0	1675	38.8	6.9	20.7
.500	1.125	.109	0	.010	0	.005	0	.882	0	87	100	0	1655	40.5	3.2	13.1
.500	1.150	.110	0	.013	0	.004	0	.885	0	85	104	0	1635	38.3	.3	8.8
.500	1.175	.109	0	.017	0	0	0	.922	0	56	105	0	1610	32.3	-1.1	6.9
.500	1.200	.108	0	.021	0	0	0	.960	0	87	109	0	1575	27.9	-2.0	3.1
.500	1.250	.108	0	.022	0	0	0	.880	0	93	103	0	1510	12.8	-1.9	-2.1
.500	1.300	.109	0	.021	0	0	0	.885	0	100	118	0	1445	4.2	-1.1	-2.6
.500	1.395	0	0	.209	0	0	0	.791	0	109	125	0	0	0	0	0
.750	.200	.112	0	.016	0	0	0	.880	0	117	134	0	1340	0	0	0
.750	.400	.111	0	.017	0	0	0	.880	0	118	135	0	1365	0	0	0
.750	.600	.111	0	.017	0	0	0	.880	0	108	128	0	1450	10.3	1.5	-7.6
.750	.700	.110	0	.019	0	0	0	.875	0	103	123	0	1540	23.6	4.5	-10.9
.750	.750	.110	0	.017	0	0	0	.875	0	99	119	0	1580	31.0	8.0	-11.2
.750	.800	.111	0	.014	0	.002	0	.875	0	97	117	0	1620	37.7	10.1	-14.5
.750	.850	.112	0	.010	0	.002	0	.880	0	101	120	0	1655	48.2	9.0	-16.1
.750	.900	.113	0	.007	0	.003	0	.885	0	106	124	0	1675	35.0	10.3	-17.1
.750	.925	.113	0	.007	0	.003	0	.887	0	106	126	0	1680	31.8	11.0	-13.0
.750	.950	.114	0	.008	0	.003	0	.890	0	107	127	0	1680	28.2	11.8	-6.7
.750	1.000	.111	0	.010	0	.003	0	.885	0	107	127	0	1680	24.6	14.5	5.2
.750	1.050	.111	0	.012	0	.001	0	.885	0	97	120	0	1665	38.8	10.0	10.0
.750	1.100	.112	0	.015	0	.001	0	.875	0	96	119	0	1645	41.9	3.0	9.9
.750	1.150	.111	0	.016	0	0	0	.880	0	93	112	0	1610	32.0	-1.2	8.4
.750	1.175	.111	0	.018	0	0	0	.882	0	93	112	0	1585	28.8	-2.1	6.2
.750	1.200	.110	0	.021	0	0	0	.885	0	93	112	0	1570	24.8	-8.2	4.4
.750	1.250	.109	0	.019	0	0	0	.880	0	94	115	0	1530	17.5	-2.4	1.3
.750	1.300	.108	0	.021	0	0	0	.885	0	99	120	0	1475	11.1	-2.6	1.7
.750	1.395	0	0	.209	0	0	0	.791	0	107	125	0	0	0	0	0
1.000	.200	.110	0	.016	0	0	0	.865	0	123	138	0	1360	0	0	0
1.000	.400	.111	0	.016	0	0	0	.870	0	116	134	0	1400	0	0	0

FLAME: 119

A.D.	H.P.	CO_2	C_2H_4	O_2	CO	H_2	CH_4	N_2	C_2H_6	NO	NO_x	S	T	V_x	V_y	V_z
m.	m.	Nm^3/Nm^3 dry gas								ppm		solids	°C	m/s		
1.000	.600	.111	0	.016	0	0	0	.860	0	111	130	0	1500	0	0	0
1.000	.700	.111	0	.016	0	0	0	.860	0	108	127	0	1565	0	0	0
1.000	.800	.111	0	.014	0	0	0	.660	0	106	125	0	1600	0	0	0
1.000	.850	.111	0	.011	0	0	0	.865	0	107	127	0	1620	0	0	0
1.000	.900	.111	0	.011	0	0	0	.860	0	107	127	0	1640	0	0	0
1.000	.950	.111	0	.014	0	0	0	.865	0	105	127	0	1650	0	0	0
1.000	1.000	.110	0	.015	0	0	0	.860	0	104	126	0	1650	0	0	0
1.000	1.050	.111	0	.014	0	0	0	.870	0	103	124	0	1640	0	0	0
1.000	1.100	.110	0	.014	0	0	0	.865	0	100	121	0	1620	0	0	0
1.000	1.150	.109	0	.019	0	0	0	.860	0	98	119	0	1600	0	0	0
1.000	1.200	.109	0	.019	0	0	0	.865	0	98	119	0	1570	0	0	0
1.000	1.250	.108	0	.021	0	0	0	.865	0	99	118	0	1530	0	0	0
1.000	1.300	.108	0	.021	0	0	0	.865	0	99	120	0	1490	0	0	0
1.000	1.350	0	0	.209	0	0	0	.791	0	100	120	0	0	0	0	0
1.250	.200	.111	0	.017	0	0	0	.865	0	112	130	0	1380	0	0	0
1.250	.400	.111	0	.016	0	0	0	.870	0	111	131	0	1410	0	0	0
1.250	.600	.111	0	.015	0	0	0	.870	0	110	128	0	1450	13.6	4.3	-2.6
1.250	.700	.111	0	.016	0	0	0	.870	0	108	128	0	1525	22.6	4.6	-3.8
1.250	.750	.111	0	.016	0	0	0	.860	0	108	127	0	1550	22.9	4.7	-5.1
1.250	.800	.111	0	.016	0	0	0	.865	0	108	127	0	1570	24.9	4.9	-6.1
1.250	.850	.110	0	.014	0	0	0	.870	0	107	128	0	1580	29.3	5.4	-6.2
1.250	.900	.111	0	.014	0	0	0	.870	0	107	129	0	1595	29.1	7.3	-3.5
1.250	.950	.110	0	.015	0	0	0	.870	0	105	124	0	1600	30.5	8.7	-0.5
1.250	1.000	.111	0	.016	0	0	0	.870	0	103	122	0	1620	29.9	7.3	3.1
1.250	1.050	.111	0	.014	0	0	0	.870	0	100	122	0	1610	31.8	5.6	4.3
1.250	1.100	.111	0	.015	0	0	0	.870	0	100	122	0	1590	29.4	2.9	5.7
1.250	1.150	.110	0	.017	0	0	0	.880	0	99	121	0	1580	29.6	1.2	6.0
1.250	1.200	.109	0	.020	0	0	0	.865	0	100	119	0	1560	21.4	-0.3	4.8
1.250	1.250	.109	0	.018	0	0	0	.870	0	100	121	0	1530	13.8	-1.6	4.3
1.250	1.300	.109	0	.018	0	0	0	.870	0	100	121	0	1500	12.9	-0.4	3.5
1.250	1.350	0	0	.209	0	0	0	.791	0	102	121	0	0	0	0	0
1.250	1.390	0	0	.209	0	0	0	.791	0	102	121	0	0	0	0	0
1.500	.200	.111	0	.016	0	0	0	.872	0	115	130	0	1370	0	0	0
1.500	.400	.111	0	.015	0	0	0	.878	0	114	130	0	1400	4.9	3.4	-3.1

FLAME: 119

A.D.	H.P.	CO_2	C_2H_4	O_2	CO	H_2	CH_4	N_2	C_2H_6	NO	NO_x	S	T	V_x	V_y	V_z
m.	m.	Nm^3/Nm^3 dry gas								ppm		solids	^oC	m/s		
1.500	.600	.109	0	.016	0	0	0	.868	0	113	130	0	1450	13.4	3.7	-2.5
1.500	.700	.111	0	.015	0	0	0	.865	0	110	129	0	1480	16.1	4.7	-3.9
1.500	.800	.111	0	.015	0	0	0	.865	0	109	130	0	1510	21.5	5.5	-3.3
1.500	.850	.111	0	.015	0	0	0	.865	0	109	130	0	1530	23.2	5.6	-2.4
1.500	.900	.109	0	.016	0	0	0	.870	0	108	129	0	1535	24.8	5.5	-1.4
1.500	.950	.111	0	.015	0	0	0	.865	0	108	129	0	1540	26.5	5.2	-0.2
1.500	1.000	.111	0	.015	0	0	0	.865	0	106	126	0	1540	28.0	4.7	1.0
1.500	1.050	.111	0	.016	0	0	0	.860	0	103	125	0	1535	28.8	3.5	2.2
1.500	1.100	.109	0	.016	0	0	0	.865	0	102	123	0	1530	28.4	2.1	2.7
1.500	1.150	.109	0	.016	0	0	0	.870	0	102	123	0	1520	26.0	1.1	2.6
1.500	1.200	.109	0	.017	0	0	0	.865	0	102	122	0	1500	22.6	0	2.5
1.500	1.250	.109	0	.017	0	0	0	.865	0	101	121	0	1485	18.5	-0.3	2.4
1.500	1.300	.109	0	.018	0	0	0	.870	0	100	121	0	1470	19.4	-0.6	2.3
1.500	1.395	0	0	.209	0	0	0	.791	0	100	121	0	0	0	0	0
2.000	.200	.109	0	.016	0	0	0	.862	0	114	128	0	1405	0	0	0
2.000	.400	.110	0	.015	0	0	0	.869	0	112	125	0	1425	7.8	3.4	-0.2
2.000	.600	.111	0	.016	0	0	0	.878	0	109	122	0	1455	11.1	3.4	-1.5
2.000	.700	.109	0	.015	0	0	0	.867	0	109	122	0	1480	16.5	3.3	-1.0
2.000	.800	.109	0	.016	0	0	0	.867	0	105	120	0	1480	18.5	3.5	-1.4
2.000	.850	.109	0	.016	0	0	0	.867	0	105	121	0	1490	18.3	3.5	-1.2
2.000	.900	.109	0	.016	0	0	0	.867	0	104	119	0	1495	18.0	3.4	-0.7
2.000	.950	.109	0	.016	0	0	0	.867	0	101	121	0	1495	18.1	2.6	-0.2
2.000	1.000	.109	0	.015	0	0	0	.867	0	103	119	0	1495	18.5	1.6	.4
2.000	1.050	.109	0	.016	0	0	0	.872	0	102	117	0	1490	18.8	1.2	1.2
2.000	1.100	.109	0	.016	0	0	0	.872	0	100	116	0	1490	19.1	.8	2.2
2.000	1.150	.109	0	.016	0	0	0	.867	0	99	116	0	1480	18.6	-0.1	1.8
2.000	1.200	.109	0	.016	0	0	0	.869	0	99	115	0	1475	17.0	-1.3	1.6
2.000	1.250	.109	0	.016	0	0	0	.869	0	98	113	0	1465	13.1	-1.5	2.5
2.000	1.300	.110	0	.016	0	0	0	.878	0	98	114	0	1460	0	0	0
2.750	.200	.109	0	.010	0	0	0	.868	0	121	143	0	1380	0	0	0
2.750	.400	.109	0	.012	0	0	0	.872	0	122	139	0	1400	0	0	0
2.750	.600	.109	0	.011	0	0	0	.860	0	119	137	0	1430	0	0	0
2.750	.700	.109	0	.010	0	0	0	.855	0	118	136	0	1430	0	0	0
2.750	.800	.109	0	.010	0	0	0	.858	0	118	136	0	1450	0	0	0

FLAME: 119

A.D.	H.P.	CO_2	C_2H_4	O_2	CO	H_2	CH_4	N_2	C_2H_6	NO	NO_x	S	T	V_x	V_y	V_z
m.	m.	Nm^3/Nm^3 dry gas								ppm		solids	^oC	m/s		
2.750	.850	.109	0	.010	0	0	0	.855	0	117	135	0	1450	0	0	0
2.750	.900	.109	0	.010	0	0	0	.861	0	116	134	0	1455	0	0	0
2.750	.950	.109	0	.011	0	0	0	.867	0	116	134	0	1450	0	0	0
2.750	1.000	.109	0	.011	0	0	0	.872	0	116	134	0	1450	0	0	0
2.750	1.050	.109	0	.011	0	0	0	.872	0	116	134	0	1450	0	0	0
2.750	1.100	.109	0	.011	0	0	0	.872	0	116	134	0	1450	0	0	0
2.750	1.150	.106	0	.011	0	0	0	.872	0	116	134	0	1445	0	0	0
2.750	1.200	.107	0	.012	0	0	0	.872	0	116	134	0	1445	0	0	0
2.750	1.250	.107	0	.012	0	0	0	.861	0	116	134	0	1435	0	0	0
2.750	1.300	.107	0	.013	0	0	0	.850	0	117	134	0	1425	0	0	0
2.750	1.400	0	0	.209	0	0	0	.791	0	118	134	0	0	0	0	0
3.500	.200	.109	0	.011	0	0	0	.872	0	125	145	0	1350	0	0	0
3.500	.400	.108	0	.012	0	0	0	.872	0	125	144	0	1375	0	0	0
3.500	.600	.109	0	.011	0	0	0	.860	0	123	143	0	1390	0	0	0
3.500	.800	.108	0	.011	0	0	0	.860	0	122	140	0	1395	0	0	0
3.500	.900	.109	0	.010	0	0	0	.868	0	121	140	0	1405	0	0	0
3.500	.950	.109	0	.010	0	0	0	.868	0	120	139	0	1405	0	0	0
3.500	1.000	.109	0	.010	0	0	0	.868	0	120	139	0	1405	0	0	0
3.500	1.050	.109	0	.011	0	0	0	.864	0	120	140	0	1405	0	0	0
3.500	1.100	.109	0	.012	0	0	0	.860	0	120	140	0	1405	0	0	0
3.500	1.200	.109	0	.010	0	0	0	.860	0	120	140	0	1400	0	0	0
3.500	1.300	.109	0	.011	0	0	0	.860	0	120	140	0	1345	0	0	0
3.500	1.400	0	0	.209	0	0	0	.791	0	120	140	0	0	0	0	0
4.250	.200	.110	0	.010	0	0	0	.585	0	129	147	0	1295	0	0	0
4.250	.400	.110	0	.012	0	0	0	.885	0	128	146	0	1325	0	0	0
4.250	.600	.110	0	.012	0	0	0	.879	0	126	145	0	1320	0	0	0
4.250	.800	.110	0	.010	0	0	0	.865	0	126	144	0	1330	0	0	0
4.250	.900	.110	0	.010	0	0	0	.878	0	123	142	0	1350	0	0	0
4.250	.925	.110	0	.011	0	0	0	.878	0	123	141	0	1348	0	0	0
4.250	1.000	.110	0	.011	0	0	0	.872	0	122	140	0	1345	0	0	0
4.250	1.100	.110	0	.011	0	0	0	.868	0	123	142	0	1340	0	0	0
4.250	1.200	.110	0	.011	0	0	0	.872	0	126	142	0	1350	0	0	0
4.250	1.300	.110	0	.011	0	0	0	.860	0	125	141	0	1345	0	0	0
4.250	1.400	0	0	.209	0	0	0	.791	0	125	141	0	0	0	0	0

FLAME: 119

A.D.	H.P.	CO_2	C_2H_4	O_2	CO	H_2	CH_4	N_2	C_2H_6	NO	NO_x	S	T	V_x	V_y	V_z
m.	m.	Nm^3/Nm^3 dry gas								ppm		solids	^oC	m/s		
5.000	.200	.110	0	.014	0	0	0	.872	0	132	149	0	1230	0	0	0
5.000	.400	.111	0	.010	0	0	0	.872	0	135	149	0	1240	0	0	0
5.000	.600	.111	0	.011	0	0	0	.897	0	131	150	0	1250	0	0	0
5.000	.800	.110	0	.013	0	0	0	.885	0	132	148	0	1260	0	0	0
5.000	.900	.110	0	.013	0	0	0	.878	0	132	148	0	1260	0	0	0
5.000	1.000	.110	0	.013	0	0	0	.872	0	132	148	0	1270	0	0	0
5.000	1.100	.110	0	.013	0	0	0	.885	0	132	148	0	1260	0	0	0
5.000	1.200	.110	0	.012	0	0	0	.879	0	132	149	0	1260	0	0	0
5.000	1.300	.110	0	.012	0	0	0	.897	0	134	150	0	1260	0	0	0
5.000	1.400	0	0	.209	0	0	0	.791	0	135	150	0	0	0	0	0
5.750	.200	.105	0	.013	0	0	0	.860	0	132	146	0	1200	0	0	0
5.750	.400	.104	0	.014	0	0	0	.855	0	133	147	0	1200	0	0	0
5.750	.600	.105	0	.014	0	0	0	.855	0	132	147	0	1210	0	0	0
5.750	.800	.105	0	.014	0	0	0	.868	0	132	147	0	1220	0	0	0
5.750	.900	.106	0	.013	0	0	0	.868	0	131	146	0	1220	0	0	0
5.750	1.000	.108	0	.012	0	0	0	.868	0	131	148	0	1230	0	0	0
5.750	1.100	.107	0	.013	0	0	0	.868	0	130	147	0	1225	0	0	0
5.750	1.200	.107	0	.013	0	0	0	.855	0	129	146	0	1230	0	0	0
5.750	1.300	.107	0	.013	0	0	0	.860	0	129	146	0	1230	0	0	0
5.750	1.400	0	0	.209	0	0	0	.791	0	129	147	0	0	0	0	0

FLAME: 120

A.D.	H.P.	CO_2	C_2H_4	O_2	CO	H_2	CH_4	N_2	C_2H_6	NO	NO_x	S	T	V_x	V_y	V_z
m.	m.	Nm^3/Nm^3 dry gas								ppm		solids	°C	m/s		
.100	.200	.113	0	.009	0	0	0	.853	.001	521	670	0	1375	0	0	0
.100	.400	.114	0	.011	0	0	0	.867	0	149	166	0	1385	0	0	0
.100	.600	.112	0	.013	0	0	0	.891	0	149	164	0	1395	0	0	0
.100	.700	.112	0	.011	0	0	0	.877	0	147	160	0	1395	0	0	0
.100	.800	.109	0	.024	0	0	0	.864	0	138	145	0	1340	0	0	0
.100	.813	.086	0	.071	0	0	0	.843	0	111	130	0	1210	0	0	0
.100	.825	.054	0	.118	0	0	0	.822	0	84	105	0	1060	0	0	0
.100	.838	.062	0	.094	0	0	0	.827	0	48	70	0	1135	0	0	0
.100	.850	.070	0	.068	.011	.006	0	.832	0	12	33	0	1470	43.6	-22.3	-28.9
.100	.863	.068	0	.035	.036	0	0	.861	0	22	0	0	1620	27.3	-21.8	-41.3
.100	.875	.067	0	.002	.071	.067	.017	.776	0	33	0	0	1580	6.1	-21.4	-12.4
.100	.888	.063	0	.002	.071	.070	.024	.770	0	38	0	0	1525	12.7	-10.4	-3.5
.100	.900	.057	0	.002	.071	.076	.031	.763	0	44	0	0	1480	19.3	-0.4	8.9
.100	.925	.060	0	0	.069	.073	.052	.746	0	40	0	0	1410	17.7	.9	7.9
.100	.950	.059	0	0	.063	.072	.085	.721	0	39	0	0	1360	15.2	-2.6	1.9
.100	.975	.056	0	0	.057	.069	.124	.694	0	37	0	0	1305	8.1	-4.8	-8.6
.100	1.000	.052	0	0	.054	.066	.175	.653	0	36	0	0	1210	27.9	8.8	.7
.100	1.025	.041	0	0	.046	.063	.243	.607	0	29	0	0	1000	74.6	-2.3	.3
.100	1.050	.034	0	0	.043	.054	.308	.561	0	23	0	0	840	81.8	-16.3	4.9
.100	1.075	.032	0	0	.043	.055	.334	.536	0	22	0	0	875	52.5	-20.4	3.4
.100	1.100	.035	0	0	.043	.056	.297	.569	0	24	0	0	985	32.2	-17.4	6.3
.100	1.125	.041	0	0	.043	.059	.260	.592	0	29	0	0	1140	16.3	-11.4	13.2
.100	1.150	.050	0	0	.055	.060	.130	.785	0	33	0	0	1368	32.1	11.6	35.8
.100	1.163	.061	0	0	.045	.045	.087	.762	0	33	0	0	1540	0	0	0
.100	1.175	.072	0	.025	.035	.030	.044	.794	0	33	0	0	1510	0	0	0
.100	1.188	.068	0	.075	.018	0	.025	.822	0	30	0	0	1160	0	0	0
.100	1.200	.047	0	.124	.001	0	.006	.822	0	3	0	0	1120	0	0	0
.100	1.225	.105	0	.023	0	0	0	.872	0	24	0	0	1300	0	0	0
.100	1.250	.112	0	.009	0	0	0	.879	0	102	0	0	1340	0	0	0
.100	1.300	.115	0	.013	0	0	0	.872	0	122	0	0	1380	0	0	0
.100	1.390	.090	0	.013	0	0	0	.897	0	113	0	0	1385	0	0	0
.250	.200	.115	0	.011	0	0	0	.879	0	142	147	0	1395	0	0	0
.250	.400	.114	0	.012	0	0	0	.879	0	146	166	0	1405	0	0	0
.250	.600	.116	0	.013	0	0	0	.859	0	144	163	0	1410	0	0	0

FLAME: 120

A.D.	H.P.	CO_2	C_2H_4	O_2	CO	H_2	CH_4	N_2	C_2H_6	NO	NO_x	S	T	V_x	V_y	V_z
m.	m.	Nm^3/Nm^3 dry gas								ppm		solids	^oC	m/s		
.250	.700	.114	0	.014	0	0	0	.874	0	143	158	0	1410	0	0	0
.250	.750	.104	0	.032	0	0	0	.878	0	133	152	0	1380	0	0	0
.250	.800	.094	0	.051	0	0	0	.865	0	98	118	0	1345	0	0	0
.250	.825	.070	0	.068	0	0	0	.850	0	79	98	0	1330	0	0	0
.250	.850	.082	0	.070	0	0	0	.855	0	67	88	0	1390	54.6	-13.7	-31.0
.250	.875	.088	0	.051	.007	.004	.002	.855	0	62	87	0	1490	49.6	-16.0	-39.5
.250	.900	.090	0	.031	.017	.013	.003	.855	0	59	90	0	1575	27.3	-15.1	-44.6
.250	.925	.083	0	.014	.034	.032	.014	.818	0	47	0	0	1580	16.4	-11.0	-42.9
.250	.950	.074	0	.007	.051	.050	.035	.766	0	48	0	0	1520	7.9	-4.2	-29.4
.250	.975	.067	0	.003	.054	.058	.058	.747	0	49	0	0	1430	7.0	6.2	-5.6
.250	1.000	.064	0	.003	.057	.052	.090	.710	0	54	0	0	1380	20.6	8.7	-1.3
.250	1.025	.062	0	.002	.055	.058	.103	.710	0	52	0	0	1375	33.2	7.2	1.6
.250	1.050	.064	0	.002	.054	.054	.114	.705	0	52	0	0	1385	30.1	9.5	12.1
.250	1.060	.065	0	.002	.051	.054	.114	.712	0	51	0	0	1380	29.8	8.0	17.8
.250	1.075	.066	0	.002	.049	.054	.115	.758	0	51	0	0	1400	28.9	7.4	23.6
.250	1.100	.068	0	.002	.044	.049	.109	.705	0	51	0	0	1360	18.5	5.6	38.4
.250	1.125	.072	0	.007	.042	.041	.091	.725	0	51	0	0	1360	29.2	10.2	34.9
.250	1.150	.075	0	.012	.039	.047	.062	.752	0	48	0	0	1400	46.6	7.0	32.7
.250	1.175	.082	0	.022	.027	.043	.034	.797	0	45	0	0	1440	0	0	0
.250	1.200	.086	0	.041	.017	.035	.015	.807	0	43	0	0	1460	0	0	0
.250	1.225	.091	0	.042	.010	.006	0	.828	0	52	0	0	1445	0	0	0
.250	1.250	.100	0	.033	.004	.024	0	.869	0	65	0	0	1440	0	0	0
.250	1.300	.111	0	.022	0	.013	0	.879	0	109	0	0	1420	0	0	0
.250	1.390	.117	0	.014	0	0	0	.865	0	121	0	0	1390	0	0	0
.500	.200	.118	0	.010	0	0	0	.872	0	145	166	0	1415	0	0	0
.500	.400	.118	0	.015	0	0	0	.867	0	146	164	0	1420	0	0	0
.500	.600	.115	0	.014	0	0	0	.871	0	143	162	0	1420	0	0	0
.500	.700	.116	0	.018	0	0	0	.866	0	133	153	0	1440	4.7	4.8	-8.4
.500	.750	.110	0	.026	0	0	0	.864	0	117	136	0	1450	18.0	8.6	-14.0
.500	.800	.103	0	.034	0	0	0	.863	0	101	120	0	1430	31.6	11.5	-20.5
.500	.850	.100	0	.029	.012	.080	0	.880	0	83	103	0	1540	41.6	11.1	-24.1
.500	.900	.094	0	.010	.030	.024	0	.842	0	63	0	0	1545	30.7	23.5	-21.8
.500	.950	.089	0	.007	.050	.037	.011	.847	0	68	0	0	1550	21.7	18.6	-19.2
.500	1.000	.088	0	.004	.042	.036	.011	.821	0	73	0	0	1555	13.5	11.6	-9.7

FLAME: 120

A.D.	H.P.	CO_2	C_2H_4	O_2	CO	H_2	CH_4	N_2	C_2H_6	NO	NO_x	S	T	V_x	V_y	V_z
m.	m.	Nm^3/Nm^3 dry gas								ppm		solids	^oC	m/s		
.500	1.050	.098	0	.007	.032	.027	0	.844	0	81	0	0	1580	18.1	14.0	2.3
.500	1.100	.101	0	.010	.025	.018	0	.847	0	80	0	0	1695	27.9	17.4	14.6
.500	1.150	.102	0	.018	.019	.010	0	.851	0	79	0	0	1600	41.7	5.5	18.7
.500	1.200	.101	0	.030	.006	.005	0	.868	0	87	109	0	1555	38.0	-9.3	11.9
.500	1.250	.101	0	.038	0	0	0	.861	0	92	111	0	1500	26.1	-4.6	12.5
.500	1.300	.102	0	.026	0	0	0	.872	0	99	120	0	1465	13.6	-4.3	10.6
.500	1.390	.113	0	.023	0	0	0	.864	0	116	134	0	1435	0	0	0
.750	.200	.122	0	.012	0	0	0	.866	0	126	146	0	1430	0	0	0
.750	.400	.121	0	.016	0	0	0	.863	0	128	145	0	1435	0	0	0
.750	.600	.122	0	.013	0	0	0	.865	0	129	143	0	1450	9.8	.4	-0.4
.750	.700	.121	0	.013	0	0	0	.860	0	119	135	0	1490	7.3	6.8	-0.7
.750	.750	.117	0	.016	0	0	0	.862	0	110	124	0	1520	13.4	7.1	-6.6
.750	.800	.114	0	.019	.009	.005	0	.864	0	100	112	0	1550	24.7	5.5	-13.8
.750	.850	.113	0	.014	.113	.009	0	.858	0	97	104	0	1575	28.1	7.4	-16.6
.750	.900	.111	0	.011	.017	.012	0	.841	0	86	83	0	1595	24.8	8.2	-18.6
.750	.950	.113	0	.006	.017	.013	0	.891	0	86	62	0	1605	22.0	10.8	-15.7
.750	1.000	.115	0	.009	.014	.009	0	.852	0	95	97	0	1620	13.5	10.3	-15.9
.750	1.050	.119	0	.011	.010	.006	0	.854	0	96	107	0	1620	25.8	9.0	-2.9
.750	1.100	.117	0	.015	0	0	0	.859	0	95	111	0	1615	21.9	16.9	4.9
.750	1.150	.115	0	.021	0	0	0	.865	0	91	108	0	1685	35.4	8.4	6.5
.750	1.200	.111	0	.025	0	0	0	.864	0	89	108	0	1585	33.5	3.1	9.4
.750	1.250	.110	0	.032	0	0	0	.859	0	88	108	0	1545	29.8	-1.2	8.9
.750	1.300	.110	0	.031	0	0	0	.859	0	92	111	0	1500	28.2	-2.1	7.6
.750	1.390	.111	0	.031	0	0	0	.858	0	97	114	0	1465	0	0	0
1.000	.200	.112	0	.015	0	0	0	.873	0	131	144	0	1440	0	0	0
1.000	.400	.114	0	.013	0	0	0	.872	0	128	147	0	1445	0	0	0
1.000	.600	.115	0	.010	0	0	0	.875	0	129	143	0	1475	18.5	-0.9	-2.2
1.000	.700	.115	0	.010	0	0	0	.876	0	123	136	0	1520	13.9	2.5	-7.7
1.000	.800	.112	0	.007	0	0	0	.881	0	120	132	0	1560	22.7	6.9	-7.5
1.000	.850	.113	0	.007	0	0	0	.882	0	115	127	0	1580	23.8	6.8	-9.9
1.000	.900	.113	0	.007	0	0	0	.876	0	111	126	0	1595	22.8	6.0	-9.9
1.000	.950	.113	0	.012	0	0	0	.875	0	108	125	0	1600	20.9	7.4	-8.9
1.000	1.000	.113	0	.013	0	0	0	.874	0	108	121	0	1595	21.9	9.5	-5.7
1.000	1.050	.114	0	.014	0	0	0	.872	0	105	122	0	1590	23.5	8.8	-3.4

FLAME: 120

A.D.	H.P.	CO_2	C_2H_4	O_2	CO	H_2	CH_4	N_2	C_2H_6	NO	NO_x	S	T	V_x	V_y	V_z
m.	m.	Nm^3/Nm^3 dry gas								ppm		solids	°C	m/s		
1.000	1.100	.111	0	.017	0	0	0	.872	0	102	121	0	1580	14.7	11.1	-8.5
1.000	1.150	.111	0	.017	0	0	0	.872	0	102	119	0	1575	21.6	6.5	2.3
1.000	1.200	.111	0	.015	0	0	0	.874	0	99	118	0	1570	19.8	5.3	4.9
1.000	1.250	.111	0	.017	0	0	0	.871	0	99	115	0	1560	21.6	2.8	3.4
1.000	1.300	.111	0	.018	0	0	0	.871	0	97	115	0	1540	19.2	.7	5.0
1.000	1.390	.113	0	.014	0	0	0	.873	0	98	117	0	1510	0	0	0
1.250	.200	.112	0	.016	0	0	0	.880	0	132	147	0	1470	0	0	0
1.250	.400	.113	0	.013	0	0	0	.887	0	127	145	0	1475	0	0	0
1.250	.600	.112	0	.012	0	0	0	.887	0	124	148	0	1510	12.3	4.1	-4.4
1.250	.700	.113	0	.011	0	0	0	.887	0	122	137	0	1540	14.1	6.5	-4.7
1.250	.800	.114	0	.010	0	0	0	.887	0	120	135	0	1560	19.2	6.2	-5.9
1.250	.850	.112	0	.012	0	0	0	.887	0	119	133	0	1575	18.7	7.3	-5.9
1.250	.900	.112	0	.013	0	0	0	.873	0	117	131	0	1580	21.0	6.3	-5.3
1.250	.950	.112	0	.012	0	0	0	.880	0	116	129	0	1580	19.7	4.8	-4.1
1.250	1.000	.112	0	.014	0	0	0	.887	0	116	127	0	1570	19.5	5.7	-2.9
1.250	1.050	.111	0	.017	0	0	0	.887	0	116	129	0	1560	16.2	4.9	-0.9
1.250	1.100	.111	0	.017	0	0	0	.887	0	115	131	0	1555	17.5	6.0	.1
1.250	1.150	.111	0	.017	0	0	0	.887	0	114	130	0	1540	17.6	5.3	1.7
1.250	1.200	.111	0	.017	0	0	0	.887	0	113	128	0	1540	13.9	3.7	-0.4
1.250	1.250	.111	0	.017	0	0	0	.887	0	113	128	0	1530	11.0	2.6	4.9
1.250	1.300	.111	0	.018	0	0	0	.887	0	113	128	0	1530	13.8	2.2	-0.6
1.250	1.390	.111	0	.017	0	0	0	.887	0	111	127	0	1525	0	0	0
1.500	.200	.111	0	.014	0	0	0	.873	0	131	148	0	1460	0	0	0
1.500	.400	.111	0	.015	0	0	0	.887	0	131	147	0	1470	0	0	0
1.500	.600	.112	0	.017	0	0	0	.880	0	123	140	0	1500	4.6	8.8	-8.1
1.500	.700	.112	0	.014	0	0	0	.873	0	122	138	0	1510	7.5	6.8	-6.4
1.500	.800	.111	0	.016	0	0	0	.873	0	121	136	0	1520	18.0	4.8	-4.3
1.500	.850	.112	0	.016	0	0	0	.873	0	120	136	0	1522	16.6	4.3	-3.0
1.500	.900	.112	0	.015	0	0	0	.873	0	118	135	0	1525	14.8	4.0	-2.8
1.500	.950	.112	0	.015	0	0	0	.860	0	117	133	0	1520	12.2	4.3	-2.7
1.500	1.000	.112	0	.016	0	0	0	.873	0	117	131	0	1515	12.4	3.2	-2.2
1.500	1.050	.112	0	.015	0	0	0	.873	0	116	131	0	1510	8.8	2.9	-1.4
1.500	1.100	.112	0	.015	0	0	0	.873	0	115	131	0	1500	9.2	3.1	-0.1
1.500	1.150	.112	0	.016	0	0	0	.880	0	115	131	0	1500	12.5	2.6	.1

FLAME: 120

A.D.	H.P.	CO_2	C_2H_4	O_2	CO	H_2	CH_4	N_2	C_2H_6	NO	NO_x	S	T	V_x	V_y	V_z
m.	m.	Nm^3/Nm^3 dry gas								ppm		solids	°C	m/s		
1.500	1.200	.112	0	.016	0	0	0	.880	0	115	131	0	1495	9.2	1.8	1.0
1.500	1.250	.112	0	.017	0	0	0	.873	0	115	131	0	1490	0	0	0
1.500	1.300	.112	0	.014	0	0	0	.887	0	115	131	0	1490	0	0	0
1.500	1.390	.112	0	.016	0	0	0	.880	0	114	128	0	1490	0	0	0
2.000	.200	.113	0	.011	0	.006	0	.860	0	128	149	0	1470	0	0	0
2.000	.400	.112	0	.013	0	.005	0	.873	0	131	149	0	1480	0	0	0
2.000	.600	.113	0	.014	0	.004	0	.867	0	130	144	0	1485	8.2	3.1	-1.1
2.000	.800	.112	0	.014	0	.005	0	.873	0	126	141	0	1480	6.8	1.8	-0.7
2.000	.850	.113	0	.013	0	.006	0	.873	0	126	140	0	1475	6.5	1.5	-0.9
2.000	.900	.113	0	.012	0	.006	0	.873	0	126	141	0	1470	11.5	2.1	1.7
2.000	.950	.112	0	.016	0	.002	0	.867	0	126	141	0	1465	1.5	3.8	-3.3
2.000	1.000	.113	0	.012	0	.005	0	.873	0	126	141	0	1455	5.8	.4	-0.7
2.000	1.050	.113	0	.011	0	.004	0	.867	0	126	141	0	1455	1.2	2.7	3.0
2.000	1.100	.112	0	.015	0	.003	0	.873	0	126	141	0	1450	1.5	-0.8	-2.7
2.000	1.150	.112	0	.014	0	.003	0	.860	0	126	137	0	1440	2.8	3.1	-9.9
2.000	1.200	.111	0	.014	0	.005	0	.873	0	122	137	0	1435	5.2	-3.6	-1.4
2.000	1.250	.112	0	.013	0	0	0	.870	0	121	137	0	1430	0	0	0
2.000	1.300	.113	0	.011	0	0	0	.867	0	121	135	0	1435	0	0	0
2.000	1.390	.112	0	.014	0	0	0	.860	0	120	134	0	1435	0	0	0
2.750	.200	.112	0	.012	0	0	0	.869	0	129	140	0	1440	0	0	0
2.750	.400	.112	0	.012	0	0	0	.867	0	135	152	0	1420	0	0	0
2.750	.600	.113	0	.011	0	0	0	.867	0	131	151	0	1410	0	0	0
2.750	.700	.113	0	.011	0	0	0	.867	0	132	151	0	1395	0	0	0
2.750	.800	.113	0	.012	0	.003	0	.867	0	134	151	0	1400	0	0	0
2.750	.850	.112	0	.012	0	.004	0	.860	0	134	150	0	1410	0	0	0
2.750	.900	.113	0	.013	0	.004	0	.867	0	134	148	0	1395	0	0	0
2.750	.950	.113	0	.011	0	.004	0	.860	0	134	149	0	1395	0	0	0
2.750	1.000	.112	0	.012	0	.005	0	.860	0	134	150	0	1395	0	0	0
2.750	1.050	.113	0	.011	0	.003	0	.867	0	133	149	0	1390	0	0	0
2.750	1.100	.114	0	.011	0	.005	0	.867	0	132	147	0	1395	0	0	0
2.750	1.150	.115	0	.011	0	.004	0	.867	0	131	145	0	1390	0	0	0
2.750	1.200	.114	0	.011	0	.001	0	.873	0	131	144	0	1395	0	0	0
2.750	1.225	.113	0	.012	0	.002	0	.873	0	131	143	0	1400	0	0	0
2.750	1.300	.113	0	.013	0	.003	0	.873	0	131	142	0	1400	0	0	0

FLAME: 120

A.D.	H.P.	CO_2	C_2H_4	O_2	CO	H_2	CH_4	N_2	C_2H_6	NO	NO_x	S	T	V_x	V_y	V_z
m.	m.	Nm^3/Nm^3 dry gas								ppm		solids	°C	m/s		
2.750	1.390	.114	0	.013	0	0	0	.873	0	128	141	0	1405	0	0	0
3.500	.200	.113	0	.009	0	0	0	.854	0	130	145	0	1395	0	0	0
3.500	.400	.114	0	.010	0	0	0	.867	0	137	151	0	1382	0	0	0
3.500	.600	.114	0	.012	0	0	0	.867	0	136	149	0	1365	0	0	0
3.500	.700	.113	0	.011	0	0	0	.863	0	136	149	0	1360	0	0	0
3.500	.800	.113	0	.011	0	0	0	.860	0	136	149	0	1350	0	0	0
3.500	.900	.114	0	.010	0	0	0	.873	0	136	149	0	1358	0	0	0
3.500	1.000	.115	0	.012	0	0	0	.873	0	136	146	0	1355	0	0	0
3.500	1.100	.114	0	.009	0	0	0	.873	0	134	144	0	1360	0	0	0
3.500	1.200	.113	0	.010	0	0	0	.867	0	132	143	0	0	0	0	0
3.500	1.390	.115	0	.011	0	0	0	.867	0	131	142	0	0	0	0	0
4.250	.200	.114	0	.009	0	0	0	.867	0	138	150	0	1340	0	0	0
4.250	.400	.113	0	.010	0	0	0	.878	0	138	150	0	1335	0	0	0
4.250	.600	.112	0	.011	0	0	0	.873	0	138	150	0	1330	0	0	0
4.250	.800	.113	0	.009	0	0	0	.367	0	138	150	0	1315	0	0	0
4.250	.900	.113	0	.009	0	0	0	.873	0	138	150	0	1310	0	0	0
4.250	1.000	.113	0	.009	0	0	0	.860	0	138	150	0	1305	0	0	0
4.250	1.100	.114	0	.009	0	0	0	.867	0	137	149	0	1300	0	0	0
4.250	1.200	.113	0	.010	0	0	0	.860	0	136	148	0	1300	0	0	0
4.250	1.390	.113	0	.008	0	0	0	.860	0	136	146	0	1300	0	0	0
5.000	.200	.124	0	.011	0	0	0	.866	0	141	155	0	1292	0	0	0
5.000	.400	.124	0	.011	0	0	0	.866	0	139	153	0	1290	0	0	0
5.000	.600	.124	0	.011	0	0	0	.866	0	141	154	0	1235	0	0	0
5.000	.900	.124	0	.011	0	0	0	.866	0	142	155	0	1288	0	0	0
5.000	1.000	.124	0	.011	0	0	0	.866	0	141	153	0	1275	0	0	0
5.000	1.200	.122	0	.012	0	0	0	.866	0	142	152	0	1280	0	0	0
5.000	1.390	0	0	.209	0	0	0	.791	0	143	154	0	0	0	0	0
5.750	.200	.125	0	.010	0	0	0	.865	0	139	148	0	1240	0	0	0
5.750	.400	.125	0	.011	0	0	0	.865	0	141	149	0	1242	0	0	0
5.750	.600	.124	0	.012	0	0	0	.865	0	144	148	0	1245	0	0	0
5.750	.800	.125	0	.012	0	0	0	.864	0	142	150	0	1247	0	0	0
5.750	.900	.125	0	.011	0	0	0	.864	0	142	150	0	1250	0	0	0
5.750	1.000	.125	0	.011	0	0	0	.864	0	142	150	0	1250	0	0	0
5.750	1.100	.124	0	.011	0	0	0	.863	0	142	150	0	1250	0	0	0

FLAME: 120

A.D.	H.P.	CO_2	C_2H_4	O_2	CO	H_2	CH_4	N_2	C_2H_6	NO	NO_x	S	T	V_x	V_y	V_z
m.	m.	Nm^3/Nm^3 dry gas								ppm		solids	^oC	m/s		
5.750	1.200	.123	0	.012	0	0	0	.867	0	141	149	0	1240	0	0	0
5.750	1.300	.124	0	.012	0	0	0	.865	0	0	150	0	1250	0	0	0

FLAME: 121

A.D.	H.P.	CO_2	C_2H_4	O_2	CO	H_2	CH_4	N_2	NO	S	C	A	T	V_x	V_y	V_z
m.	m.	Nm^3/Nm^3 dry gas							ppm	$\frac{\text{kg solid}}{Nm^3 \text{ dry gas}}$	kg/kg dry solid		^oC	m/s		
.10	.200	.149	0	.042	0	0	0	.811	750	0	1.000	0	1320	0	0	0
.10	.400	.148	0	.040	0	0	0	.815	750	0	1.000	0	1320	0	0	0
.10	.600	.147	0	.050	0	0	0	.811	752	0	1.000	0	1320	0	0	0
.10	.700	.150	0	.045	0	0	0	.815	752	0	1.000	0	1315	0	0	0
.10	.725	.149	0	.045	0	0	0	.813	764	0	1.000	0	1317	0	0	0
.10	.750	.140	0	.045	0	0	0	.811	750	0	1.000	0	1310	0	0	0
.10	.775	.147	0	.047	0	0	0	.816	726	0	1.000	0	1325	0	0	0
.10	.800	.147	0	.049	0	0	0	.820	668	.02137	.535	.465	1340	0	0	0
.10	.825	.147	0	.046	0	0	0	.826	370	.85069	.912	.088	1190	0	0	0
.10	.850	.131	0	.082	0	0	0	.823	100	.91557	.899	.101	850	0	0	0
.10	.875	.010	0	.191	0	0	0	.828	158	.30736	.918	.082	760	0	0	0
.10	.900	.021	0	.186	0	0	0	.810	216	.06201	.905	.095	790	0	0	0
.10	.925	.029	0	.174	0	0	0	.796	231	0	1.000	0	785	0	0	0
.10	.950	.037	0	.165	0	0	0	.810	246	.02736	.799	.291	828	0	0	0
.10	.975	.040	0	.161	0	0	0	.806	253	0	1.000	0	845	0	0	0
.10	1.000	.039	0	.159	0	0	0	.801	260	.02378	.562	.438	845	0	0	0
.10	1.025	.036	0	.167	0	0	0	.801	248	0	1.000	0	865	0	0	0
.10	1.050	.036	0	.157	0	0	0	.797	232	.02578	.776	.224	840	0	0	0
.10	1.075	.023	0	.180	0	0	0	.801	196	0	1.000	0	780	0	0	0
.10	1.100	.029	0	.170	0	0	0	.795	160	.02969	.751	.249	730	0	0	0
.10	1.125	.020	0	.184	0	0	0	.790	126	.07671	.899	.101	690	0	0	0
.10	1.150	.014	0	.191	0	0	0	.790	92	.20948	.914	.886	700	0	0	0
.10	1.175	.011	0	.191	0	0	0	.790	90	.93780	.924	.876	950	0	0	0
.10	1.190	.022	0	.161	0	0	0	.796	340	0	1.000	0	1300	0	0	0
.10	1.200	.023	0	.159	0	0	0	.802	632	2.60121	.931	.069	1310	0	0	0
.10	1.225	.140	0	.052	0	0	0	.808	781	.02773	.538	.462	1365	0	0	0
.10	1.250	.154	0	.037	0	0	0	.815	770	0	1.000	0	1420	0	0	0
.10	1.300	0	0	.209	0	0	0	.791	726	0	1.000	0	1365	0	0	0
.25	.200	.152	0	.034	0	0	0	.882	0	0	1.000	0	1325	0	0	0
.25	.400	.152	0	.032	0	0	0	.786	0	0	1.000	0	1330	0	0	0
.25	.600	.149	0	.036	0	0	0	.786	0	0	1.000	0	1320	0	0	0
.25	.700	.151	0	.035	0	0	0	.700	752	0	1.000	0	1395	0	0	0
.25	.750	.155	0	.021	0	0	0	.802	790	0	1.000	0	1395	0	0	0
.25	.800	.145	0	.032	0	0	0	.811	752	.14252	.799	.281	1460	24.1	-8.9	-7.5

FLAME: 121

A.D.	H.P.	CO_2	C_2H_4	O_2	CO	H_2	CH_4	N_2	NO	S	C	A	T	V_x	V_y	V_z
m.	m.	Nm^3/Nm^3 dry gas							ppm	$\frac{\text{kg solid}}{Nm^3 \text{ dry gas}}$	kg/kg dry solid		^oC	m/s		
.25	.825	.147	0	.014	0	0	0	.797	844	.50337	.831	.169	1420	18.2	-16.8	-8.0
.25	.850	.112	0	.060	0	0	0	.797	536	.40640	.830	.170	1295	10.0	-7.0	1.4
.25	.875	.086	0	.100	0	0	0	.791	444	.38039	.831	.169	1220	9.5	2.5	10.8
.25	.900	.059	0	.127	0	0	0	.758	366	.11524	.647	.353	1130	8.2	1.5	1.7
.25	.925	.054	0	.138	0	0	0	.769	353	0	1.000	0	1075	6.5	1.4	4.7
.25	.950	.053	0	.144	0	0	0	.769	340	.06486	.823	.177	1085	8.9	-4.6	5.8
.25	.975	.056	0	.136	0	0	0	.745	363	0	1.000	0	1100	9.0	1.9	2.6
.25	1.000	.059	0	.137	0	0	0	.758	386	.03891	.743	.257	1100	10.0	-18.0	2.0
.25	1.025	.061	0	.134	0	0	0	.758	400	0	1.000	0	1105	11.0	-19.3	1.4
.25	1.050	.058	0	.140	0	0	0	.769	392	.03229	.741	.259	1075	12.1	-40.6	-0.8
.25	1.075	.056	0	.141	0	0	0	.758	371	0	1.000	0	1065	9.0	-4.3	.1
.25	1.100	.054	0	.143	0	0	0	.797	350	.11873	.831	.169	1075	12.0	-0.2	-1.4
.25	1.125	.058	0	.136	0	0	0	.758	385	.21608	.813	.167	1130	12.3	3.0	2.7
.25	1.150	.145	0	.032	0	0	0	.811	420	.08812	.848	.152	1190	7.6	-0.5	3.5
.25	1.175	.099	0	.076	0	0	0	.780	518	.31068	.816	.104	1310	4.7	7.7	24.4
.25	1.200	.121	0	.061	0	0	0	.881	616	.52583	.836	.164	1410	25.2	10.2	18.4
.25	1.250	.149	0	.044	0	0	0	.801	820	0	1.000	0	1475	0	0	0
.25	1.300	0	0	.209	0	0	0	.791	780	0	1.000	0	1415	0	0	0
.50	.200	.164	0	.046	0	0	0	.827	746	0	1.000	0	1350	0	0	0
.50	.400	.159	0	.048	0	0	0	.827	746	0	1.000	0	1355	0	0	0
.50	.600	.154	0	.051	0	0	0	.799	728	0	1.000	0	1355	0	0	0
.50	.700	.157	0	.057	0	0	0	.798	736	.05107	.657	.343	1385	16.2	2.2	-9.3
.50	.750	.154	0	.059	0	0	0	.798	746	.08527	.680	.328	1405	16.5	2.2	-9.5
.50	.800	.148	0	.059	0	0	0	.810	732	.08627	.727	.273	1395	15.5	.1	-12.4
.50	.825	.149	0	.058	0	0	0	.807	699	0	1.000	0	1405	13.5	1.6	-12.8
.50	.850	.150	0	.057	0	0	0	.804	666	.08101	.643	.357	1365	11.1	2.9	-16.2
.50	.875	.149	0	.057	0	0	0	.797	641	0	1.000	0	1330	15.4	.4	-11.8
.50	.900	.148	0	.050	0	0	0	.790	616	.05800	.542	.458	1310	9.5	6.7	-15.9
.50	.925	.145	0	.064	0	0	0	.884	593	0	1.000	0	1295	7.7	5.5	-13.9
.50	.950	.142	0	.070	0	0	0	.817	570	.03933	.532	.468	1290	6.0	7.4	-10.6
.50	.975	.146	0	.064	0	0	0	.822	570	0	1.000	0	1295	3.5	13.2	-10.3
.50	1.000	.150	0	.058	0	0	0	.827	570	.04556	.563	.437	1300	5.8	10.2	-5.4
.50	1.025	.151	0	.058	0	0	0	.827	578	0	1.000	0	1300	4.2	14.5	-5.0
.50	1.050	.153	0	.059	0	0	0	.827	587	0	1.000	0	1290	3.4	17.4	-4.8

FLAME: 121

A.D.	H.P.	CO_2	C_2H_4	O_2	CO	H_2	CH_4	N_2	NO	S	C	A	T	V_x	V_y	V_z
m.	m.	Nm^3/Nm^3 dry gas							ppm	$\frac{kg\ solid}{Nm^3\ dry\ gas}$	kg/kg dry solid		^oC	m/s		
.50	1.075	.155	0	.058	0	0	0	.827	573	0	1.000	0	1280	5.8	15.7	-2.3
.50	1.100	.157	0	.056	0	0	0	.827	568	.03846	.495	.585	1270	8.4	13.8	-0.1
.50	1.125	.157	0	.055	0	0	0	.827	549	0	1.000	0	1270	3.4	13.9	-3.9
.50	1.150	.157	0	.055	0	0	0	.827	538	0	1.000	0	1290	11.7	12.8	-1.8
.50	1.175	.155	0	.058	0	0	0	.787	566	0	1.000	0	1320	16.3	11.2	-4.9
.50	1.200	.153	0	.062	0	0	0	.780	594	.06289	.656	.344	1365	19.7	7.9	-2.4
.50	1.250	0	0	.209	0	0	0	.791	694	0	1.000	0	1430	23.6	3.1	-0.2
.50	1.300	0	0	.209	0	0	0	.791	0	0	1.000	0	1410	0	0	0
.75	.200	.147	0	.044	0	0	0	.818	752	0	1.000	0	1370	0	0	0
.75	.400	.147	0	.044	0	0	0	.818	752	0	1.000	0	1375	0	0	0
.75	.600	.148	0	.045	0	0	0	.818	742	0	1.000	0	1390	0	0	0
.75	.700	.142	0	.049	0	0	0	.813	720	.04844	.537	.463	1410	0	0	0
.75	.750	.148	0	.050	0	0	0	.881	712	0	1.000	0	1415	0	0	0
.75	.800	.139	0	.051	0	0	0	.789	694	.10883	.646	.354	1410	0	0	0
.75	.850	.137	0	.052	0	0	0	.789	674	.11318	.672	.326	1415	0	0	0
.75	.900	.129	0	.060	0	0	0	.793	666	.09821	.553	.447	1485	0	0	0
.75	.925	.125	0	.068	0	0	0	.793	656	0	1.000	0	1482	0	0	0
.75	.950	.124	0	.071	0	0	0	.793	646	0	1.000	0	1400	0	0	0
.75	1.000	.121	0	.072	0	0	0	.798	638	.09960	.599	.401	1395	0	0	0
.75	1.050	.119	0	.074	0	0	0	.793	626	0	1.000	0	1395	0	0	0
.75	1.100	.118	0	.074	0	0	0	.783	616	0	1.000	0	1370	0	0	0
.75	1.150	.115	0	.076	0	0	0	.783	618	0	1.000	0	1390	0	0	0
.75	1.200	.117	0	.078	0	0	0	.793	620	0	1.000	0	1400	0	0	0
.75	1.250	0	0	.209	0	0	0	.791	634	0	1.000	0	1425	0	0	0
.75	1.300	0	0	.209	0	0	0	.791	670	0	1.000	0	1430	0	0	0
1.00	.200	.150	0	.043	0	0	0	.868	740	0	1.000	0	1415	0	0	0
1.00	.400	.153	0	.045	0	0	0	.858	740	0	1.000	0	1415	0	0	0
1.00	.600	.149	0	.048	0	0	0	.884	730	0	1.000	0	1425	6.3	0	0
1.00	.700	.147	0	.051	0	0	0	.884	780	.84646	.493	.582	1440	12.2	.5	-5.1
1.00	.750	.147	0	.051	0	0	0	.802	689	0	1.000	0	1445	15.6	.4	-4.6
1.00	.800	.148	0	.051	0	0	0	.800	675	.10353	.687	.393	1445	14.4	-1.6	-6.2
1.00	.850	.148	0	.051	0	0	0	.817	675	.11548	.594	.405	1450	21.7	-8.3	-0.2
1.00	.900	.142	0	.056	0	0	0	.808	675	.10445	.585	.415	1470	15.5	-4.7	-7.6
1.00	.950	.136	0	.066	0	0	0	.795	655	.09358	.966	.434	1465	12.7	-2.1	-10.6

FLAME: 121

A.D.	H.P.	CO_2	C_2H_4	O_2	CO	H_2	CH_4	N_2	NO	S	C	A	T	V_x	V_y	V_z
m.	m.	Nm^3/Nm^3 dry gas							ppm	$\frac{kg\ solid}{Nm^3\ dry\ gas}$	kg/kg dry solid		^oC	m/s		
1.00	1.000	.131	0	.069	0	0	0	.800	648	.07906	.586	.434	1465	9.1	-0.2	-11.9
1.00	1.050	.130	0	.070	0	0	0	.795	637	0	1.000	0	1460	10.4	-0.4	-8.8
1.00	1.100	.129	0	.071	0	0	0	.795	635	.08008	.511	.489	1455	10.3	-2.5	4.9
1.00	1.150	.129	0	.071	0	0	0	.795	0	0	1.000	0	1450	17.5	1.0	3.6
1.00	1.200	.131	0	.070	0	0	0	.795	0	.06154	.524	.476	1450	22.3	-0.6	6.0
1.00	1.250	.135	0	.066	0	0	0	.800	0	0	1.000	0	1445	22.6	-6.7	5.4
1.00	1.300	.139	0	.060	0	0	0	.795	0	0	1.000	0	1440	0	0	0
1.00	1.350	0	0	.209	0	0	0	.791	0	0	1.000	0	1430	0	0	0
1.25	.200	.154	0	.048	0	0	0	.816	720	0	1.000	0	1420	0	0	0
1.25	.400	.168	0	.041	0	0	0	.816	720	0	1.000	0	1430	0	0	0
1.25	.600	.155	0	.044	0	0	0	.821	700	0	1.000	0	1445	0	0	0
1.25	.700	.154	0	.046	0	0	0	.820	692	0	1.000	0	1460	6.1	2.0	-4.8
1.25	.750	.153	0	.043	0	0	0	.817	683	0	1.000	0	1460	9.9	.8	-4.1
1.25	.800	.152	0	.050	0	0	0	.816	675	0	1.000	0	1455	14.2	-1.2	-5.7
1.25	.850	.151	0	.048	0	0	0	.816	674	0	1.000	0	1460	13.3	-4.2	-5.2
1.25	.900	.151	0	.051	0	0	0	.816	673	0	1.000	0	1460	17.0	-5.5	-3.8
1.25	.950	.152	0	.050	0	0	0	.814	671	0	1.000	0	1460	18.6	-5.7	-4.6
1.25	1.000	.153	0	.049	0	0	0	.812	670	0	1.000	0	1455	18.2	-6.6	-2.9
1.25	1.050	.152	0	.048	0	0	0	.819	668	0	1.000	0	1455	17.6	-7.6	-0.5
1.25	1.100	.152	0	.048	0	0	0	.826	666	0	1.000	0	1475	16.6	-6.8	2.1
1.25	1.150	.151	0	.049	0	0	0	.826	663	0	1.000	0	1480	18.4	-4.9	3.6
1.25	1.200	.151	0	.049	0	0	0	.826	660	0	1.000	0	1485	28.2	-7.3	5.1
1.25	1.250	.150	0	.048	0	0	0	.821	664	0	1.000	0	1485	21.1	-7.9	6.5
1.25	1.300	.150	0	.048	0	0	0	.816	668	0	1.000	0	1480	0	0	0
1.25	1.350	0	0	.209	0	0	0	.791	670	0	1.000	0	1470	0	0	0
1.25	1.400	0	0	.209	0	0	0	.791	680	0	1.000	0	0	0	0	0
1.50	.200	.156	0	.042	0	0	0	.808	725	0	1.000	0	1450	0	0	0
1.50	.400	.156	0	.047	0	0	0	.816	720	0	1.000	0	1450	0	0	0
1.50	.600	.158	0	.043	0	0	0	.827	690	0	1.000	0	1460	0	0	0
1.50	.700	.157	0	.044	0	0	0	.823	688	.04433	.406	.594	1470	9.5	2.2	-6.8
1.50	.750	.157	0	.044	0	0	0	.820	684	0	1.000	0	1465	12.8	1.4	-3.5
1.50	.800	.157	0	.044	0	0	0	.817	680	.04359	.321	.679	1465	14.7	.1	-3.6
1.50	.850	.156	0	.043	0	0	0	.817	680	0	1.000	0	1470	16.1	-1.6	-3.1
1.50	.900	.155	0	.044	0	0	0	.817	679	.04171	.408	.592	1465	16.2	-2.6	-3.3

FLAME: 121

A.D.	H.P.	CO_2	C_2H_4	O_2	CO	H_2	CH_4	N_2	NO	S	C	A	T	V_x	V_y	V_z
m.	m.	Nm^3/Nm^3 dry gas							ppm	$\frac{kg\ solid}{Nm^3\ dry\ gas}$	kg/kg dry solid		^oC	m/s		
1.50	.950	.155	0	.045	0	0	0	.817	677	0	1.000	0	1465	14.9	-4.1	-4.3
1.50	1.000	.156	0	.045	0	0	0	.817	675	.03956	.407	.593	1460	15.6	-4.7	-5.0
1.50	1.050	.156	0	.045	0	0	0	.822	652	0	1.000	0	1450	14.8	-6.2	-1.9
1.50	1.100	.156	0	.045	0	0	0	.827	670	0	1.000	0	1460	15.4	-5.3	-1.7
1.50	1.150	.156	0	.045	0	0	0	.827	667	0	1.000	0	1470	16.1	-7.3	.2
1.50	1.200	.156	0	.045	0	0	0	.827	665	0	1.000	0	1470	17.1	-5.3	1.4
1.50	1.250	.157	0	.045	0	0	0	.822	0	0	1.000	0	1475	17.8	-4.8	3.4
1.50	1.300	.158	0	.045	0	0	0	.817	0	0	1.000	0	1470	14.5	-8.6	.3
1.50	1.350	0	0	.209	0	0	0	.791	0	0	1.000	0	1470	0	0	0
2.00	.200	.164	0	.041	0	0	0	.776	720	0	1.000	0	1450	0	0	0
2.00	.400	.164	0	.041	0	0	0	.778	710	0	1.000	0	1460	0	0	0
2.00	.600	.164	0	.041	0	0	0	.781	700	0	1.000	0	1465	0	0	0
2.00	.700	.163	0	.041	0	0	0	.888	697	0	1.000	0	1470	6.7	.6	-3.8
2.00	.750	.163	0	.041	0	0	0	.798	694	0	1.000	0	1470	8.0	-1.2	-1.5
2.00	.800	.162	0	.042	0	0	0	.804	690	0	1.000	0	1470	9.9	.1	-1.9
2.00	.850	.163	0	.041	0	0	0	.800	609	0	1.000	0	1470	7.8	-1.1	-2.5
2.00	.900	.164	0	.041	0	0	0	.797	688	0	1.000	0	1465	9.8	-1.5	-2.4
2.00	.950	.165	0	.041	0	0	0	.794	687	0	1.000	0	1465	13.2	-1.5	-2.8
2.00	1.000	.166	0	.041	0	0	0	.791	685	0	1.000	0	1475	7.6	1.3	-2.7
2.00	1.050	.166	0	.041	0	0	0	.793	680	0	1.000	0	1475	13.9	-2.6	-0.9
2.00	1.100	.166	0	.041	0	0	0	.796	672	0	1.000	0	1480	12.6	-4.1	-1.3
2.00	1.150	.167	0	.042	0	0	0	.799	666	0	1.000	0	1475	12.2	.2	-4.3
2.00	1.200	.168	0	.043	0	0	0	.881	660	0	1.000	0	1480	14.1	-3.9	-0.1
2.00	1.250	.169	0	.043	0	0	0	.800	0	0	1.000	0	1475	12.4	-4.1	.5
2.00	1.300	.170	0	.043	0	0	0	.796	0	0	1.000	0	1480	0	0	0
2.00	1.350	0	0	.209	0	0	0	.791	0	0	1.000	0	1480	0	0	0
2.75	.200	0	0	.209	0	0	0	.791	725	0	1.000	0	1445	0	0	0
2.75	.250	.147	0	.048	0	0	0	.802	725	0	1.000	0	1450	0	0	0
2.75	.400	.150	0	.047	0	0	0	.802	725	0	1.000	0	1455	0	0	0
2.75	.600	.152	0	.045	0	0	0	.802	720	.02724	.043	.957	1465	0	0	0
2.75	.800	.153	0	.044	0	0	0	.802	720	.03024	.032	.968	1465	0	0	0
2.75	1.000	.152	0	.045	0	0	0	.798	720	.02896	.041	.959	1455	0	0	0
2.75	1.200	.153	0	.045	0	0	0	.802	728	.02806	.045	.955	1445	0	0	0
2.75	1.350	0	0	.209	0	0	0	.791	0	0	1.000	0	1430	0	0	0

FLAME: 121

A.D.	H.P.	CO_2	C_2H_4	O_2	CO	H_2	CH_4	N_2	NO	S	C	A	T	V_x	V_y	V_z
m.	m.	Nm^3/Nm^3 dry gas							ppm	$\frac{kg\ solid}{Nm^3\ dry\ gas}$	kg/kg dry solid		^oC	m/s		
3.50	.200	0	0	.209	0	0	0	.791	0	0	1.000	0	1395	0	0	0
3.50	.600	0	0	.209	0	0	0	.791	0	0	1.000	0	1395	0	0	0
3.50	.800	0	0	.209	0	0	0	.791	0	0	1.000	0	1395	0	0	0
3.50	1.000	0	0	.209	0	0	0	.791	0	0	1.000	0	1405	0	0	0
3.50	1.200	0	0	.209	0	0	0	.791	0	0	1.000	0	1395	0	0	0
3.50	1.350	0	0	.209	0	0	0	.791	0	0	1.000	0	1395	0	0	0
4.25	.200	.148	0	.047	0	0	0	.825	740	0	1.000	0	1350	0	0	0
4.25	.400	.148	0	.046	0	0	0	.825	740	0	1.000	0	1350	0	0	0
4.25	.600	.149	0	.045	0	0	0	.825	745	0	1.000	0	1350	0	0	0
4.25	.800	.150	0	.045	0	0	0	.825	745	.02944	.022	.976	1320	0	0	0
4.25	1.000	.145	0	.053	0	0	0	.820	748	0	1.000	0	1315	0	0	0
4.25	1.200	.146	0	.053	0	0	0	.818	748	0	1.000	0	1320	0	0	0
4.25	1.350	0	0	.209	0	0	0	.791	0	0	1.000	0	1325	0	0	0
5.00	.200	0	0	.209	0	0	0	.791	0	0	1.000	0	1305	0	0	0
5.00	.600	0	0	.209	0	0	0	.791	0	0	1.000	0	1315	0	0	0
5.00	.800	0	0	.209	0	0	0	.791	0	0	1.000	0	1320	0	0	0
5.00	1.000	0	0	.209	0	0	0	.791	0	.02893	.017	.983	1315	0	0	0
5.00	1.200	0	0	.209	0	0	0	.791	0	0	1.000	0	1320	0	0	0
5.00	1.350	0	0	.209	0	0	0	.791	0	0	1.000	0	1325	0	0	0
5.75	.200	0	0	.209	0	0	0	.791	745	0	1.000	0	1250	0	0	0
5.75	.400	.151	0	.042	0	0	0	.807	740	0	1.000	0	1270	0	0	0
5.75	.600	.151	0	.045	0	0	0	.804	740	.03340	.008	.992	1285	0	0	0
5.75	.800	.151	0	.047	0	0	0	.802	740	.03209	.017	.983	1295	0	0	0
5.75	1.000	.151	0	.042	0	0	0	.807	740	.03136	.014	.986	1305	0	0	0
5.75	1.200	.151	0	.047	0	0	0	.802	735	0	1.000	0	1290	0	0	0
5.75	1.350	0	0	.209	0	0	0	.791	0	0	1.000	0	1295	0	0	0

FLAME: 122

A.D.	H.P.	CO_2	C_2H_4	O_2	CO	H_2	CH_4	N_2	NO	S	C	A	T	V_x	V_y	V_z
m.	m.	Nm^3/Nm^3 dry gas							ppm	$\frac{kg\ solid}{Nm^3\ dry\ gas}$	kg/kg dry solid		^oC	m/s		
.10	.200	.072	0	.124	0	0	0	.780	240	0	1.000	0	1370	-0.6	-11.2	11.2
.10	.400	.074	0	.123	0	0	0	.780	240	0	1.000	0	1375	1.2	.8	-3.2
.10	.600	.075	0	.122	0	0	0	.785	225	0	1.000	0	1370	2.3	2.3	1.0
.10	.700	.072	0	.125	0	0	0	.785	210	0	1.000	0	1370	2.3	-1.3	-2.9
.10	.750	.068	0	.128	0	0	0	.785	202	0	1.000	0	1360	2.4	-6.0	-3.4
.10	.800	.037	0	.166	0	0	0	.785	120	0	1.000	0	1275	3.9	2.9	-17.5
.10	.825	.016	0	.189	0	0	0	.700	100	0	1.000	0	1003	39.9	14.8	-34.9
.10	.850	.017	0	.189	0	0	0	.705	126	0	1.000	0	730	64.9	-4.5	-24.8
.10	.875	.026	0	.177	0	0	0	.700	102	0	1.000	0	690	41.7	-9.9	-29.1
.10	.900	.049	0	.151	0	0	0	.789	254	0	1.000	0	730	3.3	0	-17.8
.10	.925	.083	0	.113	0	0	0	.793	326	0	1.000	0	860	18.9	1.0	3.9
.10	.950	.109	0	.085	0	0	0	.797	556	0	1.000	0	1120	7.3	-0.1	7.1
.10	.952	.110	0	.084	0	0	0	.799	644	0	1.000	0	1120	0	0	0
.10	.975	.127	0	.026	.032	.005	0	.800	474	.24450	.845	.155	1380	0	0	0
.10	1.000	.154	0	.017	.027	.004	0	.820	32	1.76010	.924	.076	1575	0	0	0
.10	1.021	.157	0	.013	.029	.005	0	.820	564	0	1.000	0	1590	0	0	0
.10	1.025	.159	0	.009	.032	.006	0	.820	542	1.57940	.918	.882	1600	0	0	0
.10	1.050	.158	0	.022	.011	0	0	.810	542	0	1.000	0	1650	0	0	0
.10	1.075	.143	0	.044	0	0	0	.820	556	0	1.000	0	1090	5.7	2.6	6.3
.10	1.100	.082	0	.118	0	0	0	.818	556	0	1.000	0	790	11.3	-0.5	-4.3
.10	1.125	.047	0	.160	0	0	0	.818	0	0	1.000	0	650	2.6	-7.3	-12.4
.10	1.150	.030	0	.171	0	0	0	.805	0	0	1.000	0	570	18.3	10.7	32.4
.10	1.175	.030	0	.175	0	0	0	.800	0	0	1.000	0	560	33.0	4.1	35.3
.10	1.200	.076	0	.128	0	0	0	.810	0	0	1.000	0	750	41.1	-14.4	36.3
.10	1.225	.090	0	.102	0	0	0	.810	0	0	1.000	0	1110	5.9	6.8	-2.6
.10	1.300	.123	0	.070	0	0	0	.810	0	0	1.000	0	1330	2.3	3.4	.1
.25	.200	.121	0	.083	0	0	0	.807	256	0	1.000	0	1370	2.9	-0.5	.1
.25	.200	.121	0	.083	0	0	0	.807	256	0	1.000	0	1370	2.9	-0.5	.1
.25	.600	.123	0	.081	0	0	0	.807	250	0	1.000	0	1370	2.1	.5	-2.8
.25	.675	.122	0	.086	0	0	0	.807	225	0	1.000	0	1355	1.4	-2.6	-2.6
.25	.700	.110	0	.096	0	0	0	.807	200	0	1.000	0	1345	1.4	-2.8	-2.4
.25	.750	.087	0	.118	0	0	0	.800	160	0	1.000	0	1280	2.8	1.5	-11.1
.25	.800	.059	0	.149	0	0	0	.800	136	0	1.000	0	1170	12.8	4.6	-13.7
.25	.825	.049	0	.159	0	0	0	.796	136	0	1.000	0	1060	17.0	7.9	-22.6

FLAME: 122

A.D.	H.P.	CO_2	C_2H_4	O_2	CO	H_2	CH_4	N_2	NO	S	C	A	T	V_x	V_y	V_z
m.	m.	Nm^3/Nm^3 dry gas							ppm	$\frac{kg\ solid}{Nm^3\ dry\ gas}$	kg/kg dry solid		°C	m/s		
.25	.850	.045	0	.163	0	0	0	.800	141	0	1.000	0	990	25.8	11.5	-24.9
.25	.875	.043	0	.164	0	0	0	.793	150	0	1.000	0	970	26.9	1.2	-33.1
.25	.900	.046	0	.162	0	0	0	.793	180	0	1.000	0	1015	19.8	-3.0	-34.0
.25	.925	.057	0	.153	0	0	0	.800	256	0	1.000	0	1170	11.3	-6.4	-28.5
.25	.950	.111	0	.088	0	0	0	.807	618	0	1.000	0	1540	8.6	5.5	-11.6
.25	.975	.158	0	.017	.026	.004	0	.807	572	.67700	.855	.145	1710	0	0	0
.25	1.000	.152	0	.005	.056	.014	0	.793	124	.14260	.928	.072	1705	0	0	0
.25	1.025	.166	0	.021	.010	0	0	.821	496	.40110	.716	.284	1630	0	0	0
.25	1.050	.186	0	.008	.013	0	0	.887	438	0	1.000	0	1645	0	0	0
.25	1.075	.110	0	.092	0	0	0	.800	445	0	1.000	0	1390	6.7	-4.8	-5.5
.25	1.100	.050	0	.144	0	0	0	.880	440	0	1.000	0	1135	4.9	-1.6	3.4
.25	1.125	.048	0	.163	0	0	0	.793	0	0	1.000	0	1005	2.6	10.6	17.7
.25	1.150	.046	0	.160	0	0	0	.796	0	0	1.000	0	950	11.7	14.2	29.1
.25	1.175	.046	0	.163	0	0	0	.796	0	0	1.000	0	950	24.7	9.0	30.4
.25	1.200	.048	0	.162	0	0	0	.793	0	0	1.000	0	1000	23.1	6.4	21.8
.25	1.225	.063	0	.146	0	0	0	.797	0	0	1.000	0	1070	34.7	-5.6	22.9
.25	1.250	.078	0	.131	0	0	0	.880	0	0	1.000	0	1170	25.6	-7.7	20.0
.25	1.300	.132	0	.075	0	0	0	.887	0	0	1.000	0	1300	6.9	.3	14.4
.50	.200	.135	0	.068	0	0	0	.883	246	0	1.000	0	1370	1.9	-2.7	.9
.50	.400	.124	0	.073	0	0	0	.810	246	0	1.000	0	1370	1.9	-3.2	1.9
.50	.600	.113	0	.086	0	0	0	.810	214	0	1.000	0	1330	3.2	3.3	-7.7
.50	.700	.097	0	.102	0	0	0	.810	182	0	1.000	0	1260	15.4	10.1	-13.1
.50	.750	.086	0	.117	0	0	0	.810	176	0	1.000	0	1230	21.4	10.1	-17.1
.50	.775	.085	0	.116	0	0	0	.805	184	0	1.000	0	1235	21.8	9.2	-18.6
.50	.800	.085	0	.117	0	0	0	.800	190	0	1.000	0	1240	21.9	8.9	-19.5
.50	.825	.091	0	.109	0	0	0	.810	212	0	1.000	0	1295	21.8	8.2	-19.4
.50	.850	.098	0	.100	0	0	0	.810	250	0	1.000	0	1350	21.3	8.1	-19.1
.50	.875	.115	0	.080	.005	0	0	.810	342	0	1.000	0	1445	13.0	8.1	-18.7
.50	.900	.116	0	.080	.005	.003	0	.810	447	0	1.000	0	1540	10.3	8.4	-17.6
.50	.925	.113	0	.077	0	.003	0	.795	525	.01990	.629	.371	1585	10.4	10.6	-11.2
.50	.950	.110	0	.074	0	.003	0	.781	486	.09080	.793	.287	1570	10.6	13.3	-5.2
.50	.975	.107	0	.077	0	0	0	.816	353	0	1.000	0	1495	0	0	0
.50	1.000	.103	0	.080	0	0	0	.817	294	.19960	.911	.089	1420	0	0	0
.50	1.025	.100	0	.083	0	0	0	.817	281	1.17000	.891	.109	1440	0	0	0

FLAME: 122

A.D.	H.P.	CO_2	C_2H_4	O_2	CO	H_2	CH_4	N_2	NO	S	C	A	T	V_x	V_y	V_z
m.	m.	Nm^3/Nm^3 dry gas							ppm	$\frac{kg\ solid}{Nm^3\ dry\ gas}$	kg/kg dry solid		^oC	m/s		
.50	1.050	.096	0	.086	0	0	0	.818	342	.16910	.854	.146	1460	0	0	0
.50	1.075	.104	0	.087	0	0	0	.809	352	0	1.000	0	1505	0	0	0
.50	1.100	.112	0	.088	0	0	0	.800	358	0	1.000	0	1550	8.6	-3.1	3.5
.50	1.125	.202	0	.101	0	0	0	.697	331	0	1.000	0	1570	8.0	-15.4	-2.0
.50	1.150	.093	0	.115	0	0	0	.800	304	0	1.000	0	1510	6.4	-21.1	-0.4
.50	1.175	.089	0	.117	0	0	0	.800	275	0	1.000	0	1467	4.3	-4.0	.2
.50	1.200	.086	0	.120	0	0	0	.800	248	0	1.000	0	1425	3.4	7.0	1.1
.50	1.250	.088	0	.116	0	0	0	.800	0	0	1.000	0	1270	10.0	1.7	11.0
.50	1.300	.095	0	.110	0	0	0	.795	0	0	1.000	0	1220	19.2	-5.0	14.2
.75	.200	0	0	.209	0	0	0	.791	218	0	1.000	0	1370	0	0	0
.75	.400	.113	0	.077	0	0	0	.806	205	0	1.000	0	1350	0	0	0
.75	.600	.102	0	.093	0	0	0	.802	178	0	1.000	0	1315	0	0	0
.75	.700	.103	0	.088	0	0	0	.806	192	0	1.000	0	1380	0	0	0
.75	.750	.120	0	.064	0	0	0	.808	204	0	1.000	0	1455	0	0	0
.75	.800	.136	0	.040	.019	.003	0	.810	200	.06540	.763	.237	1550	10.8	2.7	-11.8
.75	.850	.139	0	.029	.029	.006	0	.810	345	.09020	.680	.312	1590	8.0	.4	-9.2
.75	.900	.136	0	.041	.013	0	0	.802	422	.61030	.687	.313	1565	2.6	7.5	-6.7
.75	.950	0	0	.209	0	0	0	.791	355	.57830	.647	.153	1480	0	0	0
.75	1.000	0	0	.209	0	0	0	.791	312	.35460	.903	.097	1410	0	0	0
.75	1.050	0	0	.209	0	0	0	.791	0	.70460	.877	.123	1480	9.3	-2.3	-1.3
.75	1.075	0	0	.209	0	0	0	.791	0	0	1.000	0	1510	8.8	-3.0	.5
.75	1.100	.134	0	.061	.012	.002	0	.810	0	.15630	.754	.246	1520	6.9	-3.5	1.3
.75	1.125	.126	0	.074	0	0	0	.802	0	0	1.000	0	1525	2.5	.1	-4.0
.75	1.150	.119	0	.087	0	0	0	.795	0	0	1.000	0	1525	.2	4.4	-5.5
.75	1.200	.115	0	.090	0	0	0	.795	0	0	1.000	0	1495	1.2	1.7	5.9
.75	1.250	.114	0	.091	0	0	0	.790	0	0	1.000	0	1460	4.7	2.9	1.8
.75	1.300	.108	0	.100	0	0	0	.795	0	0	1.000	0	1395	8.7	1.5	3.7
1.00	.200	0	0	.209	0	0	0	.791	210	0	1.000	0	1300	0	0	0
1.00	.400	.127	0	.074	0	0	0	.809	200	0	1.000	0	1380	0	0	0
1.00	.600	.139	0	.058	0	0	0	.817	205	0	1.000	0	1430	0	0	0
1.00	.700	.154	0	.036	.010	.001	0	.817	230	0	1.000	0	1510	10.0	4.5	-8.7
1.00	.750	.154	0	.025	.022	.005	0	.813	246	0	1.000	0	1565	9.5	3.4	-8.8
1.00	.800	.154	0	.013	.034	.008	0	.809	274	.04170	.369	.631	1575	6.0	3.5	-10.8
1.00	.850	.142	0	.088	.056	.023	0	.791	330	.11560	.593	.407	1565	4.5	3.6	-8.8

FLAME: 122

A.D.	H.P.	CO_2	C_2H_4	O_2	CO	H_2	CH_4	N_2	NO	S	C	A	T	V_x	V_y	V_z
m.	m.	Nm^3/Nm^3 dry gas							ppm	$\frac{kg\ solid}{Nm^3\ dry\ gas}$	kg/kg dry solid		^oC	m/s		
1.00	.900	.131	0	.003	.077	.039	0	.774	350	.20520	.779	.221	1530	3.0	4.1	-7.5
1.00	.950	.136	0	.003	.071	.033	0	.774	348	.51840	.857	.143	1490	10.6	5.7	-2.5
1.00	1.000	.142	0	.003	.066	.027	0	.774	350	2.12150	.883	.117	1470	0	0	0
1.00	1.050	.140	0	.044	.008	.002	0	.817	335	1.12660	.866	.134	1500	0	0	0
1.00	1.100	.136	0	.065	0	0	0	.817	0	.43570	.854	.146	1520	14.2	-4.5	.3
1.00	1.150	.133	0	.068	0	0	0	.817	0	0	1.000	0	1530	5.4	-5.9	.5
1.00	1.200	.130	0	.071	0	0	0	.817	0	0	1.000	0	1525	1.5	7.3	-0.7
1.00	1.250	.126	0	.077	0	0	0	.801	0	0	1.000	0	1580	-1.0	-18.5	18.5
1.00	1.300	.121	0	.082	0	0	0	.776	0	0	1.000	0	1490	1.1	-2.6	-3.9
1.25	.200	0	0	.209	0	0	0	.791	210	0	1.000	0	1395	5.7	5.6	-3.2
1.25	.400	.139	0	.054	0	0	0	.800	202	0	1.000	0	1420	7.4	6.7	-4.0
1.25	.600	.158	0	.029	.007	.001	0	.804	220	0	1.000	0	1500	5.0	4.1	-3.3
1.25	.700	.159	0	.018	.014	.003	0	.800	250	0	1.000	0	1545	7.1	5.0	-3.1
1.25	.750	.156	0	.015	.024	.006	0	.796	284	0	1.000	0	1547	7.6	5.7	-2.5
1.25	.800	.153	0	.009	.034	.009	0	.792	312	.09260	.690	.316	1550	7.4	7.2	-2.3
1.25	.850	.153	0	.007	.046	.015	0	.787	335	.25050	.812	.168	1535	11.4	6.0	-1.3
1.25	.900	.144	0	.006	.059	.021	0	.783	335	.12600	.717	.283	1520	15.5	4.6	-1.1
1.25	.950	.147	0	.016	.045	.016	0	.787	335	.26700	.887	.193	1510	17.6	3.3	-0.7
1.25	1.000	.151	0	.017	.030	.010	0	.792	335	.29140	.793	.207	1510	15.4	1.1	-0.5
1.25	1.050	.150	0	.021	0	0	0	.860	302	.11870	.695	.305	1515	6.8	.1	-2.4
1.25	1.100	.149	0	.046	0	0	0	.809	274	0	1.000	0	1510	5.7	-0.9	-0.7
1.25	1.150	.143	0	.052	0	0	0	.809	0	0	1.000	0	1510	5.3	-0.3	-1.6
1.25	1.200	.138	0	.059	0	0	0	.809	0	0	1.000	0	1495	3.2	.8	-2.7
1.25	1.250	.135	0	.063	0	0	0	.809	0	0	1.000	0	1475	4.3	.8	-1.7
1.25	1.300	.133	0	.068	0	0	0	.809	0	0	1.000	0	1470	2.9	1.9	-0.4
1.50	.200	.143	0	.046	0	0	0	.805	207	0	1.000	0	1405	4.2	5.3	.5
1.50	.400	.154	0	.030	0	0	0	.880	222	0	1.000	0	1420	3.1	3.7	-2.8
1.50	.600	.166	0	.017	.009	.002	0	.805	252	0	1.000	0	1475	1.4	5.5	-1.7
1.50	.700	.159	0	.011	.016	.004	0	.789	274	0	1.000	0	1500	6.5	2.6	-1.2
1.50	.800	.151	0	.009	.028	.007	0	.799	304	.03790	.352	.648	1520	7.9	3.0	-0.9
1.50	.900	.152	0	.007	.033	.018	0	.799	305	.17460	.778	.222	1515	11.3	1.9	-0.9
1.50	1.000	.154	0	.016	.016	.005	0	.779	292	.30220	.802	.198	1520	9.4	-0.4	-0.9
1.50	1.100	.152	0	.031	0	0	0	.799	245	.05860	.544	.456	1505	4.9	-1.1	.3
1.50	1.200	.142	0	.043	0	0	0	.796	214	0	1.000	0	1495	3.1	-1.9	-0.5

FLAME: 122

A.D.	H.P.	CO_2	C_2H_4	O_2	CO	H_2	CH_4	N_2	NO	S	C	A	T	V_x	V_y	V_z
m.	m.	Nm^3/Nm^3 dry gas							ppm	$\frac{kg\ solid}{Nm^3\ dry\ gas}$	kg/kg dry solid		^oC	m/s		
1.50	1.300	.136	0	.054	0	0	0	.799	0	0	1.000	0	1470	1.4	1.9	-2.0
2.00	.200	0	0	.209	0	0	0	.791	270	0	1.000	0	1410	0	0	0
2.00	.400	.147	0	.038	.004	.002	0	.803	276	0	1.000	0	1425	0	0	0
2.00	.600	.147	0	.023	.017	.004	0	.800	290	0	1.000	0	1435	0	0	0
2.00	.700	.157	0	.022	.011	.003	0	.800	302	0	1.000	0	1440	1.0	-3.1	.2
2.00	.800	.158	0	.016	.014	.003	0	.793	302	0	.626	.374	1455	.3	-4.4	1.3
2.00	.900	.159	0	.013	.021	.005	0	.800	298	0	.519	.481	1455	-0.3	-9.3	2.8
2.00	1.000	.161	0	.015	.014	.003	0	.800	286	0	.466	.534	1455	1.2	2.4	.5
2.00	1.100	.164	0	.014	.007	.003	0	.800	288	0	1.000	0	1450	.1	-5.1	-3.8
2.00	1.200	.163	0	.018	.011	.002	0	.793	274	0	1.000	0	1445	5.7	-8.8	.8
2.00	1.300	.165	0	.019	.004	0	0	.796	272	0	1.000	0	1445	2.1	-3.2	.2
2.75	.200	0	0	.209	0	0	0	.791	258	0	1.000	0	1380	0	0	0
2.75	.400	0	0	.209	0	0	0	.791	266	0	1.000	0	1385	0	0	0
2.75	.600	0	0	.209	0	0	0	.791	276	.03030	.891	.989	1385	0	0	0
2.75	.700	0	0	.209	0	0	0	.791	270	0	1.000	0	1385	0	0	0
2.75	.800	0	0	.209	0	0	0	.791	276	0	1.000	0	1385	0	0	0
2.75	.900	.138	0	.045	0	0	0	.801	268	.02978	.179	.821	1390	0	0	0
2.75	1.000	.150	0	.030	0	0	0	.801	268	.03038	.198	.802	1395	0	0	0
2.75	1.100	.150	0	.030	0	0	0	.817	254	.03710	.225	.775	1400	0	0	0
2.75	1.200	.157	0	.029	0	0	0	.801	248	.03590	.189	.828	1405	0	0	0
2.75	1.300	0	0	.209	0	0	0	.791	0	0	1.000	0	1485	0	0	0
4.25	.200	0	0	.209	0	0	0	.791	276	0	1.000	0	1340	0	0	0
4.25	.600	.143	0	.046	0	0	0	.817	274	.02820	.015	.985	1330	0	0	0
4.25	.800	.145	0	.047	0	0	0	.809	270	.02790	.017	.983	1330	0	0	0
4.25	1.000	.147	0	.048	0	0	0	.804	260	.02760	1.000	0	1330	0	0	0
4.25	1.200	.147	0	.044	0	0	0	.809	260	.02880	.021	.979	1340	0	0	0
4.25	1.300	0	0	.209	0	0	0	.791	270	0	1.000	0	1340	0	0	0
5.75	.200	0	0	.209	0	0	0	.791	266	0	1.000	0	1251	0	0	0
5.75	.600	.147	0	.044	0	0	0	.801	258	.02690	.018	.982	1260	0	0	0
5.75	.800	.146	0	.043	0	0	0	.801	248	0	1.000	0	1278	0	0	0
5.75	1.000	.146	0	.044	0	0	0	.817	230	.02710	.021	.979	1278	0	0	0
5.75	1.200	.147	0	.042	0	0	0	.801	230	.02550	.045	.955	1262	0	0	0
5.75	1.300	0	0	.209	0	0	0	.791	248	0	1.000	0	0	0	0	0
.10	1.250	.120	0	.068	0	0	0	.818	0	0	1.000	0	1255	4.4	2.8	1.3

FLAME: 123

A.D.	H.P.	CO_2	C_2H_4	O_2	CO	H_2	CH_4	N_2	NO	S	C	A	T	V_x	V_y	V_z
m.	m.	Nm^3/Nm^3 dry gas							ppm	$\frac{kg\ solid}{Nm^3\ dry\ gas}$	kg/kg dry solid		^oC	m/s		
.10	.200	.105	0	.102	0	0	0	.796	365	0	1.000	0	1340	0	0	0
.10	.400	.107	0	.099	0	0	0	.885	365	0	1.000	0	1340	0	0	0
.10	.600	.102	0	.101	0	0	0	.796	370	0	1.000	0	1360	0	0	0
.10	.700	.102	0	.099	0	0	0	.796	370	0	1.000	0	1350	0	0	0
.10	.750	.103	0	.104	0	0	0	.796	340	0	1.000	0	1330	0	0	0
.10	.800	.091	0	.112	0	0	0	.796	250	0	1.000	0	1130	0	0	0
.10	.825	.070	0	.146	0	0	0	.796	185	0	1.000	0	810	0	0	0
.10	.850	.039	0	.180	0	0	0	.796	75	0	1.000	0	620	0	0	0
.10	.863	.031	0	.183	0	0	0	.796	60	0	1.000	0	620	0	0	0
.10	.875	.023	0	.186	0	0	0	.796	55	0	1.000	0	620	0	0	0
.10	.900	.024	0	.188	0	0	0	.796	55	0	1.000	0	685	0	0	0
.10	.925	.031	0	.180	0	0	0	.796	75	0	1.000	0	775	0	0	0
.10	.950	.030	0	.169	0	0	0	.796	105	0	1.000	0	855	0	0	0
.10	.975	.043	0	.167	0	0	0	.796	40	0	.859	.141	1020	0	0	0
.10	1.000	.048	0	.165	0	0	0	.796	5	.96450	.920	.080	1300	0	0	0
.10	1.025	.005	0	.208	0	0	0	.796	0	0	.915	.085	1520	0	0	0
.10	1.050	.009	0	.206	0	0	0	.796	0	0	1.000	0	1510	0	0	0
.10	1.075	.035	0	.171	0	0	0	.796	0	0	1.000	0	1490	0	0	0
.10	1.100	.035	0	.176	0	0	0	.796	0	0	1.000	0	0	0	0	0
.25	.200	.104	0	.096	0	0	0	.794	340	0	1.000	0	1355	0	0	0
.25	.400	.103	0	.095	0	0	0	.794	340	0	1.000	0	1360	0	0	0
.25	.600	.102	0	.096	0	0	0	.794	340	0	1.000	0	1345	0	0	0
.25	.700	.097	0	.104	0	0	0	.794	300	0	1.000	0	1245	.6	-5.8	-7.6
.25	.750	.086	0	.114	0	0	0	.794	255	0	1.000	0	1090	4.9	.6	-5.9
.25	.800	.073	0	.127	0	0	0	.794	190	0	1.000	0	940	10.7	3.7	-12.7
.25	.825	.064	0	.139	0	0	0	.794	155	0	1.000	0	900	12.7	3.8	-16.7
.25	.850	.064	0	.151	0	0	0	.794	135	0	1.000	0	890	19.0	2.6	-19.8
.25	.875	.050	0	.157	0	0	0	.794	135	0	1.000	0	895	19.3	-0.4	-22.0
.25	.900	.041	0	.163	0	0	0	.794	135	0	1.000	0	950	14.4	-2.3	-27.1
.25	.925	.045	0	.156	0	0	0	.794	150	0	1.000	0	1080	7.1	-4.2	-20.5
.25	.950	.050	0	.148	0	0	0	.794	165	0	1.000	0	1250	0	0	0
.25	.975	.019	0	.187	0	0	0	.794	55	0	.905	.095	1400	0	0	0
.25	.988	.013	0	.194	0	0	0	.794	25	0	.915	.085	1490	0	0	0
.25	1.000	.007	0	.201	0	0	0	.794	10	.34960	.906	.094	1230	0	0	0

FLAME: 123

A.D.	H.P.	CO_2	C_2H_4	O_2	CO	H_2	CH_4	N_2	NO	S	C	A	T	V_x	V_y	V_z
m.	m.	Nm^3/Nm^3 dry gas							ppm	$\frac{kg\ solid}{Nm^3\ dry\ gas}$	kg/kg dry solid		^oC	m/s		
.25	1.013	.006	0	.202	0	0	0	.794	10	0	.913	.087	1400	0	0	0
.25	1.025	.006	0	.202	0	0	0	.794	10	0	.914	.086	1610	0	0	0
.25	1.030	.018	0	.186	0	0	0	.794	95	1.24850	.899	.101	1610	0	0	0
.25	1.040	.018	0	.186	0	0	0	.794	775	0	1.000	0	1615	0	0	0
.25	1.050	.030	0	.171	0	0	0	.794	785	0	1.000	0	1620	0	0	0
.25	1.073	.049	0	.145	0	0	0	.794	550	0	1.000	0	1490	0	0	0
.25	1.075	.049	0	.145	0	0	0	.794	530	0	1.000	0	1480	0	0	0
.25	1.100	.068	0	.110	0	0	0	.794	365	0	1.000	0	1390	0	0	0
.25	1.150	.084	0	.109	0	0	0	.794	215	0	1.000	0	0	0	0	0
.50	.200	.181	0	.100	0	0	0	.790	360	0	1.000	0	1355	0	0	0
.50	.400	.098	0	.101	0	0	0	.794	365	0	1.000	0	1355	0	0	0
.50	.600	.092	0	.111	0	0	0	.794	320	0	1.000	0	1285	0	0	0
.50	.700	.078	0	.124	0	0	0	.794	280	0	1.000	0	1210	5.1	6.7	.1
.50	.750	.071	0	.133	0	0	0	.794	250	0	1.000	0	1140	5.5	3.4	-9.8
.50	.800	.069	0	.135	0	0	0	.794	235	0	1.000	0	1120	6.8	1.7	-7.9
.50	.825	.067	0	.136	0	0	0	.794	230	0	1.000	0	1100	6.1	-0.1	-10.1
.50	.850	.066	0	.137	0	0	0	.794	225	0	1.000	0	1140	6.2	2.0	-11.9
.50	.875	.069	0	.134	0	0	0	.794	250	0	1.000	0	1200	3.3	-2.0	-12.9
.50	.900	.073	0	.131	0	0	0	.794	310	0	1.000	0	1350	11.7	.1	-4.2
.50	.925	.099	0	.087	.014	.002	0	.794	430	.10520	.785	.214	1450	5.4	2.2	-7.7
.50	.950	.110	0	.075	.013	.003	0	.794	455	.21190	.863	.137	1555	0	0	0
.50	.975	.076	0	.102	.014	.004	0	.794	275	0	1.000	0	1640	0	0	0
.50	1.000	.038	0	.163	.008	.002	0	.794	165	.49730	.911	.089	1690	0	0	0
.50	1.025	.044	0	.147	.013	.003	0	.794	280	.57710	.826	.174	1700	0	0	0
.50	1.030	.042	0	.148	.012	.003	0	.794	370	0	1.000	0	1700	0	0	0
.50	1.033	.040	0	.159	.011	.002	0	.794	400	0	1.000	0	1700	0	0	0
.50	1.040	.056	0	.087	.028	.005	0	.794	585	0	1.000	0	1710	0	0	0
.50	1.050	.133	0	.015	.044	.012	0	.794	765	.26080	.870	.130	1710	0	0	0
.50	1.075	.150	0	.017	.024	.005	0	.794	805	0	1.000	0	1710	0	0	0
.50	1.100	.160	0	.024	.004	0	0	.794	660	0	1.000	0	1690	0	0	0
.50	1.150	.131	0	.064	0	0	0	.794	435	0	1.000	0	0	0	0	0
.75	.200	.097	0	.100	0	0	0	.809	350	0	1.000	0	1345	0	0	0
.75	.400	.094	0	.105	0	0	0	.809	330	0	1.000	0	1300	0	0	0
.75	.600	.084	0	.115	0	0	0	.800	290	0	1.000	0	1260	0	0	0

FLAME: 123

A.D.	H.P.	CO_2	C_2H_4	O_2	CO	H_2	CH_4	N_2	NO	S	C	A	T	V_x	V_y	V_z
m.	m.	Nm^3/Nm^3 dry gas							ppm	$\frac{kg\ solid}{Nm^3\ dry\ gas}$	kg/kg dry solid		^oC	m/s		
.75	.700	.078	0	.124	0	0	0	.803	265	0	1.000	0	1280	6.4	1.6	-7.0
.75	.750	.074	0	.127	0	0	0	.803	255	0	1.000	0	1300	9.3	-0.3	-5.1
.75	.800	.078	0	.123	0	0	0	.809	260	.02140	.361	.639	1390	11.1	.6	-4.8
.75	.825	.080	0	.121	0	0	0	.809	280	0	1.000	0	1420	3.7	7.7	-3.0
.75	.850	.083	0	.119	0	0	0	.809	310	0	1.000	0	1495	2.9	8.9	-1.0
.75	.875	.088	0	.109	.004	0	0	.797	370	0	1.000	0	1560	5.5	.6	-6.7
.75	.900	.104	0	.089	.005	0	0	.811	505	.09450	.714	.286	1610	10.7	2.3	-4.1
.75	.925	.124	0	.056	.006	.002	0	.809	590	0	1.000	0	1690	14.1	6.2	-1.8
.75	.950	.136	0	.026	.028	.007	0	.809	650	1.11470	.863	.117	1710	0	0	0
.75	.975	.126	0	.013	.059	.016	0	.797	590	0	1.000	0	1720	0	0	0
.75	1.000	.102	0	.005	.100	.049	0	.743	475	1.10440	.926	.874	1650	0	0	0
.75	1.010	.102	0	.005	.100	.047	0	.753	545	0	1.000	0	1655	0	0	0
.75	1.025	.103	0	.005	.101	.043	0	.763	545	0	1.000	0	1660	0	0	0
.75	1.050	.110	0	.024	.085	.029	0	.794	590	0	1.000	0	1690	0	0	0
.75	1.075	.131	0	.005	.059	.017	0	.794	660	0	1.000	0	1660	0	0	0
.75	1.100	.146	0	.012	.023	.007	0	.803	650	0	1.000	0	1650	0	0	0
.75	1.150	.143	0	.037	.006	.002	0	.811	445	0	1.000	0	0	0	0	0
1.00	.200	.093	0	.105	0	0	0	.800	325	0	1.000	0	1340	0	0	0
1.00	.400	.089	0	.112	0	0	0	.803	325	0	1.000	0	1330	0	0	0
1.00	.600	.080	0	.121	0	0	0	.800	290	0	1.000	0	1320	0	0	0
1.00	.650	.080	0	.121	0	0	0	.800	290	0	1.000	0	1340	0	0	0
1.00	.700	.081	0	.122	0	0	0	.800	290	0	1.000	0	1360	7.7	1.4	-3.5
1.00	.750	.082	0	.119	0	0	0	.800	310	0	1.000	0	1410	5.9	1.6	-3.3
1.00	.775	.083	0	.116	0	0	0	.800	320	0	1.000	0	1430	5.4	-0.8	-5.1
1.00	.800	.084	0	.117	0	0	0	.800	335	.02770	.365	.635	1450	8.8	.8	-3.1
1.00	.825	.083	0	.118	0	0	0	.800	350	0	1.000	0	1540	4.8	.5	-4.5
1.00	.850	.087	0	.112	0	0	0	.800	370	.04200	.528	.472	1590	6.6	2.0	-3.2
1.00	.875	.090	0	.100	0	0	0	.809	410	0	1.000	0	1590	9.4	1.5	-3.3
1.00	.900	.103	0	.090	0	0	0	.809	465	.10880	.746	.254	1640	10.5	.2	-3.2
1.00	.925	.121	0	.059	.017	.003	0	.809	550	0	1.000	0	1680	10.9	4.3	-3.4
1.00	.950	.128	0	.037	.023	.007	0	.803	560	.64818	.855	.145	1680	0	0	0
1.00	.975	.127	0	.012	.057	.020	0	.786	560	0	1.000	0	1670	0	0	0
1.00	1.000	.121	0	.008	.071	.028	0	.777	570	2.17620	.879	.121	1645	0	0	0
1.00	1.025	.116	0	.005	.078	.034	0	.763	560	0	1.000	0	1642	0	0	0

FLAME: 123

A.D.	H.P.	CO_2	C_2H_4	O_2	CO	H_2	CH_4	N_2	NO	S	C	A	T	V_x	V_y	V_z
m.	m.	Nm^3/Nm^3 dry gas							ppm	$\frac{kg\ solid}{Nm^3\ dry\ gas}$	kg/kg dry solid		^oC	m/s		
1.00	1.050	.127	0	.007	.063	.023	0	.786	550	1.62880	.878	.122	1640	0	0	0
1.00	1.075	.135	0	.012	.046	.015	0	.795	545	0	1.000	0	1660	0	0	0
1.00	1.100	.143	0	.018	.029	.008	0	.803	545	0	1.000	0	1685	20.3	-3.3	-0.9
1.00	1.150	.141	0	.041	.007	.002	0	.809	490	0	1.000	0	0	0	0	0
1.25	.200	0	0	.209	0	0	0	.791	390	0	1.000	0	1355	0	0	0
1.25	.400	.103	0	.098	0	0	0	.797	380	0	1.000	0	1355	0	0	0
1.25	.600	.098	0	.100	0	0	0	.797	344	0	1.000	0	1370	5.3	-0.2	-1.7
1.25	.700	.101	0	.007	0	0	0	.797	360	0	1.000	0	1410	12.9	.2	-0.8
1.25	.750	.107	0	.091	0	0	0	.800	380	0	1.000	0	1450	4.5	2.5	-2.4
1.25	.800	.112	0	.085	0	0	0	.804	400	.06700	.518	.482	1510	6.1	2.3	-1.9
1.25	.850	.122	0	.067	0	0	0	.803	418	.10910	.707	.293	1570	16.0	.9	-0.9
1.25	.900	.132	0	.048	.011	.002	0	.881	468	.23120	.780	.220	1620	12.8	4.9	-4.3
1.25	.950	.131	0	.040	.021	.006	0	.809	520	.26830	.805	.195	1655	19.6	2.7	-2.5
1.25	1.000	.139	0	.011	.043	.016	0	.777	498	.49810	.827	.173	1665	25.6	-0.8	-1.7
1.25	1.050	.135	0	.024	.036	.010	0	.804	500	.99040	.850	.150	0	20.5	-1.5	-1.4
1.25	1.075	.140	0	.024	.038	.006	0	.804	498	0	1.000	0	0	16.6	-2.4	-1.3
1.25	1.100	.143	0	.029	.020	.005	0	.797	492	0	1.000	0	0	12.8	-2.9	-1.2
1.25	1.150	0	0	.209	0	0	0	.791	475	0	1.000	0	0	0	0	0
1.25	1.200	0	0	.209	0	0	0	.791	460	0	1.000	0	0	0	0	0
1.50	.200	.136	0	.061	0	0	0	.797	380	0	1.000	0	1395	0	0	0
1.50	.400	.127	0	.071	0	0	0	.797	384	0	1.000	0	1395	0	0	0
1.50	.600	.124	0	.075	0	0	0	.786	378	0	1.000	0	1410	4.1	-0.5	1.3
1.50	.700	.119	0	.080	0	0	0	.797	400	.03070	.926	.074	1450	.6	.5	-5.0
1.50	.750	.129	0	.070	0	0	0	.797	405	0	1.000	0	1470	1.0	3.6	-0.5
1.50	.800	.134	0	.059	0	0	0	.797	415	.04620	.512	.488	1500	3.0	1.1	-3.5
1.50	.850	.142	0	.045	0	0	0	.797	440	.06300	.605	.395	1550	9.5	1.9	-2.2
1.50	.900	.149	0	.030	.017	.003	0	.797	458	.06700	.708	.292	1585	12.2	2.2	-1.5
1.50	.950	.150	0	.020	.031	.007	0	.797	462	.17320	.764	.236	1620	17.2	2.3	-3.2
1.50	1.000	.151	0	.020	.039	.006	0	.797	474	.23450	.768	.232	1640	16.8	2.5	-0.7
1.50	1.050	.153	0	.021	.026	.005	0	.797	485	.20580	.713	.287	0	12.7	0	-0.9
1.50	1.100	.142	0	.044	.011	.002	0	.797	482	.23980	.671	.329	0	0.2	-0.5	-1.5
1.50	1.200	0	0	.209	0	0	0	.791	460	0	1.000	0	0	0	0	0
2.00	.200	.142	0	.050	0	0	0	.824	460	0	1.000	0	1400	2.0	-0.5	1.9
2.00	.400	.143	0	.046	0	0	0	.824	472	0	1.000	0	1415	4.1	.5	1.0

FLAME: 123

A.D.	H.P.	CO_2	C_2H_4	O_2	CO	H_2	CH_4	N_2	NO	S	C	A	T	V_x	V_y	V_z
m.	m.	Nm^3/Nm^3 dry gas							ppm	$\frac{kg\ solid}{Nm^3\ dry\ gas}$	kg/kg dry solid		°C	m/s		
2.00	.600	.145	0	.042	0	0	0	.814	480	0	1.000	0	1465	5.8	1.1	-0.3
2.00	.700	.151	0	.037	0	0	0	.814	484	0	1.000	0	1500	3.2	-0.7	-1.2
2.00	.750	.154	0	.033	0	0	0	.814	484	0	1.00	0	1510	4.1	2.4	-1.7
2.00	.800	.156	0	.029	.003	0	0	.814	484	.03130	.921	.079	1520	5.8	.6	-1.2
2.00	.850	.157	0	.028	.003	0	0	.820	452	.02980	.201	.799	1510	11.6	1.1	-3.3
2.00	.900	.158	0	.026	.003	.001	0	.820	445	.03050	.228	.772	1540	4.5	1.7	-1.0
2.00	.950	.157	0	.026	.008	.001	0	.820	460	.03460	.252	.748	1550	7.7	.3	-1.2
2.00	1.000	.154	0	.027	.008	.001	0	.814	452	.03770	.287	.713	1570	3.2	.7	-3.1
2.00	1.050	.151	0	.037	.003	.001	0	.820	440	.03980	.320	.680	0	2.6	6.0	-0.3
2.00	1.100	.149	0	.042	0	0	0	.814	450	.04330	.365	.635	0	3.7	.4	1.3
2.00	1.200	0	0	.209	0	0	0	.791	460	0	1.000	0	0	0	0	0
2.75	.200	0	0	.209	0	0	0	.791	550	0	1.000	0	1435	0	0	0
2.75	.300	.148	0	.044	0	0	0	.820	550	0	1.000	0	1435	0	0	0
2.75	.400	.149	0	.044	0	0	0	.820	550	.03410	.196	.884	1435	0	0	0
2.75	.600	.150	0	.045	0	0	0	.820	550	.02420	.058	.942	1455	0	0	0
2.75	.700	.155	0	.043	0	0	0	.820	550	0	1.000	0	1470	0	0	0
2.75	.800	.159	0	.042	0	0	0	.820	550	.02750	.121	.879	1485	0	0	0
2.75	.900	.157	0	.036	0	0	0	.820	550	0	1.000	0	1490	0	0	0
2.75	1.000	.157	0	.036	0	0	0	.820	550	.03050	.166	.834	1500	0	0	0
2.75	1.100	.155	0	.038	0	0	0	.820	550	0	1.000	0	1495	0	0	0
2.75	1.200	0	0	.209	0	0	0	.791	550	0	1.000	0	1495	0	0	0
2.75	1.300	0	0	.209	0	0	0	.791	575	0	1.000	0	1490	0	0	0
4.25	.200	0	0	.209	0	0	0	.791	600	0	1.000	0	0	0	0	0
4.25	.300	.172	0	.017	0	0	0	.811	600	0	1.000	0	1420	0	0	0
4.25	.400	.170	0	.020	0	0	0	.810	600	.03390	.108	.892	1400	0	0	0
4.25	.600	.166	0	.024	0	0	0	.809	600	.03520	.056	.944	1390	0	0	0
4.25	.800	.172	0	.018	0	0	0	.810	600	.03510	.086	.914	1300	0	0	0
4.25	.900	.175	0	.017	0	0	0	.806	600	0	1.000	0	1380	0	0	0
4.25	1.000	.177	0	.016	0	0	0	.807	600	.03790	.116	.884	1390	0	0	0
4.25	1.100	.172	0	.020	0	0	0	.808	600	0	1.000	0	1380	0	0	0
4.25	1.200	0	0	.209	0	0	0	.791	600	0	1.000	0	1385	0	0	0
4.25	1.300	0	0	.209	0	0	0	.791	610	0	1.000	0	1385	0	0	0
5.75	.200	0	0	.209	0	0	0	.791	620	0	1.000	0	0	0	0	0
5.75	.300	.175	0	.020	0	0	0	.806	620	0	1.000	0	1400	0	0	0

FLAME: 123

A.D.	H.P.	CO_2	C_2H_4	O_2	CO	H_2	CH_4	N_2	NO	S	C	A	T	V_x	V_y	V_z
m.	m.	Nm^3/Nm^3 dry gas							ppm	$\frac{kg\ solid}{Nm^3\ dry\ gas}$	kg/kg dry solid		^oC	m/s		
5.75	.600	.178	0	.018	0	0	0	.805	620	.03420	.049	.951	1385	0	0	0
5.75	.800	.177	0	.020	0	0	0	.804	620	.03430	.057	.943	1400	0	0	0
5.75	.900	.178	0	.020	0	0	0	.804	620	0	1.000	0	1395	0	0	0
5.75	1.000	.180	0	.018	0	0	0	.802	620	.03510	.101	.899	1385	0	0	0
5.75	1.200	0	0	.209	0	0	0	.791	620	0	1.000	0	1380	0	0	0
5.75	1.300	0	0	.209	0	0	0	.791	0	0	1.000	0	1365	0	0	0

FLAME: 124

A.D.	H.P.	CO_2	C_2H_4	O_2	CO	H_2	CH_4	N_2	NO	S	C	A	T	V_x	V_y	V_z
m.	m.	Nm^3/Nm^3 dry gas							ppm	$\frac{kg\ solid}{Nm^3\ dry\ gas}$	kg/kg dry solid		^oC	m/s		
.10	.200	.153	0	.037	0	0	0	.804	280	0	1.000	0	1400	0	0	0
.10	.400	.152	0	.045	0	0	0	.804	289	0	1.000	0	1400	0	0	0
.10	.600	.153	0	.037	0	0	0	.804	285	0	1.000	0	1475	0	0	0
.10	.700	.152	0	.039	0	0	0	.804	290	0	1.000	0	1475	.7	-6.5	-2.3
.10	.750	.148	0	.045	0	0	0	.804	275	0	1.000	0	1415	1.2	-10.7	-4.4
.10	.800	.113	0	.080	0	0	0	.804	240	0	1.000	0	1365	3.3	-10.3	.5
.10	.825	.062	0	.145	0	0	0	.795	148	0	1.000	0	1040	4.4	.8	-19.6
.10	.850	.039	0	.171	0	0	0	.804	92	0	1.000	0	840	53.9	6.6	-12.4
.10	.875	.036	0	.173	0	0	0	.795	100	0	1.000	0	815	33.5	-12.9	-35.6
.10	.900	.044	0	.165	0	0	0	.795	124	0	.727	.273	865	4.8	-16.4	-23.8
.10	.925	.058	0	.148	0	0	0	.799	172	0	.516	.384	995	2.7	4.7	12.6
.10	.950	.073	0	.131	0	0	0	.804	244	0	.661	.339	1235	16.2	-3.0	3.2
.10	.975	.097	0	.100	.004	0	0	.804	168	0	.200	.000	1660	12.0	4.8	-3.6
.10	1.000	.137	0	.015	.048	.012	0	.795	0	0	1.000	0	1580	0	0	0
.10	1.025	.136	0	.028	.036	.011	0	.790	0	0	1.000	0	1575	0	0	0
.10	1.050	.133	0	.017	.049	.016	0	.790	0	0	1.000	0	1605	0	0	0
.10	1.075	0	0	.209	0	0	0	.791	0	0	1.000	0	1500	0	0	0
.25	.200	.155	0	.045	0	0	0	.812	286	0	1.000	0	1490	0	0	0
.25	.400	.156	0	.045	0	0	0	.812	286	0	1.000	0	1490	0	0	0
.25	.600	.150	0	.052	0	0	0	.812	286	0	1.000	0	1480	0	0	0
.25	.700	.135	0	.066	0	0	0	.812	260	0	1.000	0	1445	4.3	-1.2	-1.5
.25	.750	.112	0	.092	0	0	0	.812	220	0	1.000	0	1330	5.4	.2	-7.5
.25	.800	.084	0	.124	0	0	0	.803	172	0	1.000	0	1210	19.2	1.0	-17.4
.25	.825	.075	0	.133	0	0	0	.803	156	0	1.000	0	1147	26.9	6.8	-23.6
.25	.850	.067	0	.142	0	0	0	.803	150	0	1.000	0	1085	32.8	2.5	-28.5
.25	.875	.065	0	.144	0	0	0	.794	152	0	1.000	0	1130	27.7	-2.0	-33.9
.25	.900	.069	0	.136	0	0	0	.803	166	0	.628	.372	1175	15.9	-8.7	-32.7
.25	.925	.086	0	.116	0	0	0	.794	266	0	.751	.249	1361	3.2	-3.7	-27.0
.25	.950	.114	0	.079	0	0	0	.803	402	0	.893	.107	1547	2.9	6.7	-11.2
.25	.975	.045	0	.156	0	0	0	.794	244	0	.938	.062	1700	0	0	0
.25	1.000	.139	0	.022	.044	.011	0	.794	60	0	.944	.056	1562	0	0	0
.25	1.025	.146	0	.014	.044	.011	0	.794	190	0	1.000	0	1685	0	0	0
.25	1.050	.137	0	.049	0	0	0	.803	0	0	1.000	0	1625	0	0	0
.25	1.075	.120	0	.075	0	0	0	.803	0	0	1.000	0	1655	0	0	0

FLAME: 124

A.D.	H.P.	CO_2	C_2H_4	O_2	CO	H_2	CH_4	N_2	NO	S	C	A	T	V_x	V_y	V_z
m.	m.	Nm^3/Nm^3 dry gas							ppm	$\frac{kg\ solid}{Nm^3\ dry\ gas}$	kg/kg dry solid		^oC	m/s		
.25	1.100	.103	0	.100	0	0	0	.803	0	0	1.000	0	1550	0	0	0
.25	1.125	.090	0	.115	0	0	0	.800	0	0	1.000	0	1335	0	0	0
.25	1.150	.078	0	.130	0	0	0	.794	0	0	1.000	0	1230	0	0	0
.25	1.175	.073	0	.135	0	0	0	.794	0	0	1.000	0	1225	0	0	0
.25	1.200	.078	0	.130	0	0	0	.794	0	0	1.000	0	1220	0	0	0
.50	.200	.169	0	.028	0	0	0	.810	255	0	1.000	0	0	0	0	0
.50	.400	.168	0	.030	0	0	0	.810	255	0	1.000	0	1480	0	0	0
.50	.500	.158	0	.042	0	0	0	.800	243	0	1.000	0	1460	0	0	0
.50	.600	.145	0	.057	0	0	0	.810	220	0	1.000	0	1415	0	0	0
.50	.650	.133	0	.068	0	0	0	.805	204	0	1.000	0	1375	0	0	0
.50	.700	.121	0	.080	0	0	0	.800	200	0	1.000	0	1330	8.3	6.0	-10.3
.50	.750	.117	0	.088	0	0	0	.800	204	0	1.000	0	1310	15.7	6.7	-11.7
.50	.800	.116	0	.083	0	0	0	.800	250	0	1.000	0	1370	16.5	4.9	-13.6
.50	.825	.127	0	.060	0	0	0	.800	286	0	1.000	0	1455	17.0	4.5	-15.4
.50	.850	.148	0	.036	.011	0	0	.800	322	0	1.000	0	1540	15.0	2.7	-13.7
.50	.875	.152	0	.028	.010	.003	0	.800	489	0	1.000	0	1640	15.0	1.0	-9.6
.50	.900	.148	0	.010	.043	.014	0	.794	442	0	.835	.165	1650	0	0	0
.50	.925	.122	0	.014	.075	.024	0	.770	460	0	.828	.172	1640	0	0	0
.50	.950	.099	0	.010	.103	.040	0	.736	378	0	.902	.098	1575	0	0	0
.50	.975	.084	0	.043	.098	.059	0	.699	272	0	.913	.087	1510	0	0	0
.50	1.000	.103	0	.011	.099	.055	0	.708	254	0	.955	.045	1450	0	0	0
.50	1.025	.088	0	.026	.088	.052	0	.712	256	0	1.000	0	1380	0	0	0
.50	1.050	.137	0	.021	.045	.014	0	.778	304	0	1.000	0	1435	0	0	0
.50	1.075	.128	0	.050	0	0	0	.785	0	0	1.000	0	1575	0	0	0
.50	1.100	.119	0	.080	0	0	0	.793	0	0	1.000	0	1545	0	0	0
.50	1.125	.113	0	.089	0	0	0	.793	0	0	1.000	0	1565	0	0	0
.50	1.150	.107	0	.098	0	0	0	.793	0	0	1.000	0	1585	0	0	0
.50	1.200	.106	0	.099	0	0	0	.793	0	0	1.000	0	1575	0	0	0
.75	.200	.148	0	.045	0	0	0	.805	310	0	1.000	0	1520	0	0	0
.75	.400	.149	0	.034	0	0	0	.805	300	0	1.000	0	1490	0	0	0
.75	.450	.149	0	.044	0	0	0	.804	285	0	1.000	0	1490	0	0	0
.75	.500	.137	0	.054	0	0	0	.803	288	0	1.000	0	1490	0	0	0
.75	.550	.131	0	.064	0	0	0	.803	286	0	1.000	0	1500	0	0	0
.75	.600	.125	0	.074	0	0	0	.803	280	0	1.000	0	1510	0	0	0

FLAME: 124

A.D.	H.P.	CO_2	C_2H_4	O_2	CO	H_2	CH_4	N_2	NO	S	C	A	T	V_x	V_y	V_z
m.	m.	Nm^3/Nm^3 dry gas							ppm	$\frac{kg\ solid}{Nm^3\ dry\ gas}$	kg/kg dry solid		^oC	m/s		
.75	.700	.120	0	.079	0	0	0	.803	314	0	1.000	0	1685	11.7	3.9	-8.5
.75	.750	.122	0	.072	0	0	0	.802	304	0	1.000	0	1605	11.2	4.5	-9.0
.75	.800	.136	0	.053	.007	0	0	.803	266	0	1.000	0	1590	10.5	2.4	-8.8
.75	.825	.140	0	.040	.016	0	0	.803	263	0	1.000	0	1560	8.4	2.0	-8.3
.75	.850	.145	0	.027	.024	.007	0	.803	260	0	1.000	0	1560	8.8	2.5	-8.0
.75	.875	.138	0	.016	.047	.016	0	.789	259	0	.867	.133	1540	9.3	2.9	-7.6
.75	.900	.131	0	.006	.069	.026	0	.776	258	0	.879	.121	1505	13.4	2.6	-4.6
.75	.925	.118	0	.006	.087	.040	0	.760	260	0	.893	.107	1480	0	0	0
.75	.950	.106	0	.006	.105	.054	0	.750	263	0	.850	.150	1443	0	0	0
.75	.975	.106	0	.006	.108	.053	0	.720	266	0	.799	.201	1400	0	0	0
.75	1.000	.103	0	.006	.111	.059	0	.717	270	0	.886	.112	1378	0	0	0
.75	1.025	.125	0	.005	.092	.040	0	.743	276	0	1.000	0	1403	0	0	0
.75	1.050	.146	0	.004	.074	.031	0	.769	282	0	1.000	0	1428	0	0	0
.75	1.075	.153	0	.005	.050	.020	0	.786	287	0	1.000	0	1453	0	0	0
.75	1.100	.161	0	.007	.027	.088	0	.803	292	0	1.000	0	1470	0	0	0
.75	1.125	.162	0	.012	.021	0	0	.803	0	0	1.000	0	1500	0	0	0
.75	1.150	.164	0	.017	.016	0	0	.803	0	0	1.000	0	1520	0	0	0
.75	1.175	.158	0	.025	.012	0	0	.803	0	0	1.000	0	1550	0	0	0
.75	1.200	.152	0	.034	.008	0	0	.803	0	0	1.000	0	1560	0	0	0
.75	1.300	.134	0	.061	0	0	0	.803	0	0	1.000	0	0	0	0	0
1.00	.200	.144	0	.053	0	0	0	.798	310	0	1.000	0	1490	0	0	0
1.00	.400	.138	0	.058	0	0	0	.801	310	0	1.000	0	1480	0	0	0
1.00	.500	.133	0	.063	0	0	0	.801	320	0	1.000	0	1515	0	0	0
1.00	.600	.133	0	.063	0	0	0	.801	330	0	1.000	0	1550	0	0	0
1.00	.700	.138	0	.053	.003	0	0	.798	340	0	1.000	0	1590	8.7	1.9	-5.8
1.00	.750	.143	0	.039	.010	.003	0	.801	341	0	1.000	0	1588	5.8	2.6	-6.5
1.00	.800	.145	0	.023	.029	.008	0	.793	340	0	1.000	0	1572	5.7	2.7	-5.3
1.00	.825	.140	0	.018	.040	.013	0	.784	333	0	1.000	0	1550	6.2	2.7	-4.8
1.00	.850	.136	0	.013	.050	.010	0	.776	323	0	.806	.194	1540	4.7	3.8	-5.1
1.00	.875	.134	0	.010	.056	.022	0	.774	312	0	1.000	0	1520	9.9	2.6	-3.6
1.00	.900	.133	0	.007	.063	.027	0	.768	302	0	.856	.144	1505	0	0	0
1.00	.925	.129	0	.006	.059	.027	0	.759	297	0	1.000	0	1475	0	0	0
1.00	.950	.125	0	.005	.075	.027	0	.758	293	0	.865	.135	1475	0	0	0
1.00	.975	.123	0	.004	.077	.028	0	.743	291	0	1.000	0	1475	0	0	0

FLAME: 124

A.D.	H.P.	CO_2	C_2H_4	O_2	CO	H_2	CH_4	N_2	NO	S	C	A	T	V_x	V_y	V_z
m.	m.	Nm^3/Nm^3 dry gas							ppm	$Nm^3 \frac{kg\ solid}{dry\ gas}$	kg/kg dry solid		°C	m/s		
1.00	1.000	.135	0	.005	.059	.028	0	.764	286	0	.855	.145	1470	0	0	0
1.00	1.025	.140	0	.012	.045	.020	0	.775	287	0	1.000	0	1470	0	0	0
1.00	1.050	.144	0	.018	.031	.012	0	.785	287	0	1.000	0	1460	0	0	0
1.00	1.075	.145	0	.026	.021	.008	0	.793	287	0	1.000	0	1475	0	0	0
1.00	1.100	.147	0	.034	.011	.004	0	.881	287	0	1.000	0	1490	0	0	0
1.00	1.125	.147	0	.039	.007	0	0	.801	0	0	1.000	0	1510	0	0	0
1.00	1.150	.147	0	.044	.004	0	0	.801	0	0	1.000	0	1515	0	0	0
1.00	1.175	.143	0	.047	0	0	0	.801	0	0	1.000	0	1525	0	0	0
1.00	1.200	.140	0	.053	0	0	0	.801	0	0	1.000	0	1530	0	0	0
1.00	1.300	.132	0	.064	0	0	0	.793	0	0	1.000	0	0	0	0	0
1.25	.200	.147	0	.050	0	0	0	.803	315	0	1.000	0	1540	0	0	0
1.25	.400	.137	0	.062	0	0	0	.803	321	0	1.000	0	1540	0	0	0
1.25	.600	.143	0	.057	0	0	0	.803	335	0	1.000	0	1560	0	0	0
1.25	.700	.147	0	.045	.005	.001	0	.803	330	0	1.000	0	1580	0	0	0
1.25	.750	.149	0	.037	.010	.003	0	.803	319	0	1.000	0	1570	0	0	0
1.25	.800	.151	0	.029	.016	.005	0	.803	310	0	1.000	0	1570	0	0	0
1.25	.850	.150	0	.021	.028	.010	0	.800	310	0	1.000	0	1555	0	0	0
1.25	.900	.149	0	.014	.041	.014	0	.795	313	0	1.000	0	1550	0	0	0
1.25	.950	.146	0	.009	.046	.019	0	.785	316	0	1.000	0	1540	0	0	0
1.25	1.000	.147	0	.010	.040	.016	0	.779	316	0	1.000	0	1550	0	0	0
1.25	1.050	.154	0	.009	.036	.013	0	.785	312	0	1.000	0	1540	0	0	0
1.25	1.100	.161	0	.011	.026	.007	0	.803	306	0	1.000	0	1540	0	0	0
1.25	1.150	.160	0	.012	0	.007	0	.803	0	0	1.000	0	1520	0	0	0
1.25	1.200	.159	0	.014	0	.007	0	.803	0	0	1.000	0	1500	0	0	0
1.25	1.300	.168	0	.023	0	0	0	.803	0	0	1.000	0	0	0	0	0
1.50	.200	.154	0	.040	0	0	0	.803	326	0	1.000	0	1530	0	0	0
1.50	.400	.153	0	.040	0	0	0	.803	326	0	1.000	0	1545	5.0	-0.4	.6
1.50	.600	.152	0	.039	0	0	0	.803	326	0	1.000	0	1555	-0.2	6.2	-5.3
1.50	.700	.154	0	.032	.002	0	0	.803	326	0	1.000	0	1555	5.3	-0.3	-1.2
1.50	.750	.154	0	.030	.005	0	0	.798	326	0	1.000	0	1545	.1	1.6	6.6
1.50	.800	.153	0	.028	.009	.002	0	.793	326	0	1.000	0	1540	4.2	2.9	-6.6
1.50	.850	.156	0	.026	.010	.003	0	.793	326	0	1.000	0	1535	1.6	-1.6	-4.3
1.40	.900	.158	0	.024	.011	.003	0	.793	326	0	1.000	0	1530	3.4	2.7	-0.2
1.50	.950	.154	0	.027	.006	.002	0	.793	326	0	1.000	0	1530	3.3	-3.4	-1.7

FLAME: 124

A.D.	H.P.	CO_2	C_2H_4	O_2	CO	H_2	CH_4	N_2	NO	S	C	A	T	V_x	V_y	V_z
m.	m.	Nm^3/Nm^3 dry gas							ppm	$\frac{\text{kg solid}}{Nm^3 \text{ dry gas}}$	kg/kg dry solid		°C	m/s		
1.50	1.000	.159	0	.022	.008	.003	0	.793	326	0	1.000	0	1535	.1	-3.2	-5.4
1.50	1.050	.159	0	.023	.007	.002	0	.795	326	0	1.000	0	1525	6.1	-0.6	-8.7
1.50	1.100	.159	0	.024	.006	.001	0	.796	326	0	1.000	0	1515	-0.2	.4	6.9
1.50	1.150	.162	0	.026	.004	0	0	.799	0	0	1.000	0	1500	4.4	-0.6	1.5
1.50	1.200	.165	0	.027	.002	0	0	.803	0	0	1.000	0	1490	-0.2	6.4	2.7
1.50	1.300	.161	0	.030	0	0	0	.803	0	0	1.000	0	0	0	0	0
2.00	.200	.159	0	.032	0	0	0	.803	330	0	1.000	0	1545	0	0	0
2.00	.400	.158	0	.033	0	0	0	.803	330	0	1.000	0	1525	1.6	-1.3	-2.6
2.00	.600	.164	0	.027	0	0	0	.799	330	0	1.000	0	1520	.3	-0.4	1.0
2.00	.700	.166	0	.022	0	0	0	.803	330	0	1.000	0	1510	.2	2.9	-2.4
2.00	.750	.167	0	.020	0	0	0	.803	330	0	1.000	0	1510	2.6	.4	-0.3
2.00	.800	.168	0	.021	0	0	0	.803	330	0	1.000	0	1510	4.0	.8	-1.8
2.00	.850	.162	0	.024	0	0	0	.803	330	0	.237	.763	1508	2.2	.6	2.3
2.00	.900	.163	0	.023	0	0	0	.803	330	0	.242	.758	1510	.3	.4	4.6
2.00	.950	.163	0	.024	0	0	0	.803	330	0	.317	.683	1510	1.8	-1.4	-2.0
2.00	1.000	.166	0	.018	0	0	0	.803	330	0	.227	.773	1510	4.8	.7	1.0
2.00	1.050	.166	0	.018	0	0	0	.803	330	0	1.000	0	1500	1.5	-3.3	.9
2.00	1.100	.165	0	.023	0	0	0	.803	330	0	1.000	0	1505	1.0	4.1	.9
2.00	1.150	.166	0	.020	0	0	0	.803	0	0	1.000	0	1500	.2	-1.5	1.5
2.00	1.200	.167	0	.020	0	0	0	.803	0	0	1.000	0	1502	0	-4.1	-4.1
2.00	1.300	.165	0	.023	0	0	0	.803	0	0	1.000	0	0	0	0	0
2.75	.200	.163	0	.027	0	0	0	.803	326	0	1.000	0	1495	0	0	0
2.75	.400	.164	0	.028	0	0	0	.803	326	0	1.000	0	1495	0	0	0
2.75	.600	.167	0	.023	0	0	0	.803	326	0	.060	.940	1490	0	0	0
2.75	.800	.171	0	.021	0	0	0	.803	326	0	.103	.897	1490	0	0	0
2.75	1.000	.171	0	.021	0	0	0	.800	326	0	.116	.884	1490	0	0	0
2.75	1.200	.172	0	.016	0	0	0	.800	326	0	1.000	0	1500	0	0	0
4.25	.200	.169	0	.022	0	0	0	.800	290	0	1.000	0	1445	0	0	0
4.25	.400	.168	0	.023	0	0	0	.806	290	0	1.000	0	1440	0	0	0
4.25	.600	.168	0	.022	0	0	0	.808	290	0	.026	.974	1430	0	0	0
4.25	.800	.174	0	.020	0	0	0	.812	290	0	.024	.976	1432	0	0	0
4.25	1.000	.176	0	.014	0	0	0	.808	290	0	.016	.984	1445	0	0	0
4.25	1.200	.174	0	.016	0	0	0	.808	290	0	1.000	0	1450	0	0	0

FLAME: 124

A.D.	H.P.	CO_2	C_2H_4	O_2	CO	H_2	CH_4	N_2	NO	S	C	A	T	V_x	V_y	V_z
m.	m.	Nm^3/Nm^3 dry gas							ppm	$\frac{\text{kg solid}}{Nm^3 \text{ dry gas}}$	kg/kg dry solid		^oC	m/s		
5.75	.200	.167	0	.024	0	0	0	.812	284	0	1.000	0	1382	0	0	0
5.75	.400	.167	0	.023	0	0	0	.808	284	0	1.000	0	1400	0	0	0
5.75	.600	.169	0	.023	0	0	0	.808	284	0	.046	.954	1415	0	0	0
5.75	.800	.171	0	.018	0	0	0	.803	284	0	.031	.989	1418	0	0	0
5.75	1.000	.171	0	.018	0	0	0	.803	284	0	.030	.970	1402	0	0	0
5.75	1.200	.170	0	.021	0	0	0	.808	284	0	1.000	0	1405	0	0	0